INVESTIGATING THE ROLE OF ACCESSORY CELLS IN THE THYMIC MICROENVIRONMENT FOR CENTRAL TOLERANCE AND THYMUS REGENERATION

By

EMILIE J COSWAY

A thesis submitted to the University of Birmingham

For the Degree of DOCTOR OF PHILOSOPHY

Institute of Immunity and Immunotherapy

College of Medical and Dental Science

University of Birmingham

August 2017

ABSTRACT

Thymic microenvironments act to control T-cell development and selection. While thymic epithelial cells are key regulators of these processes, the thymus also contains multiple accessory cells that influence its function. Considering this, the major aim of this thesis is to examine the roles of dendritic cells and eosinophils in thymus biology. As regulation of thymic DC has previously been correlated to the thymic medulla we focused on the medullary regulator LTβR and generated cell type specific LTβR deficient mice. We found LTβR signalling regulates mTEC in a cell intrinsic manner, independent of thymic DC maintenance. Thymic DC alternatively require LTβR signalling on thymic mesenchyme for their regulation. Additionally, disruption of the medulla in *Ltbr*$^{-/-}$ mice was distinct from tolerance breakdown, which we instead found to correlate to reduced DC and impaired negative selection. Further we found the CCR7 ligand CCL21 was also required to control thymic DC, suggesting a link between these two pathways. Finally, dblGATA mice were used as a model of eosinophil deficiency and we identify a role for eosinophils in thymus recovery following sublethal irradiation damage. Collectively these findings shed new light on accessory cells during key aspects of thymus tolerance and regeneration.

ACKNOWLEDGMENTS

Firstly, I would like to take this opportunity to thank everyone who has supported me during my PhD especially Professor Graham Anderson for his endless help and guidance. I would definitely not have been able to complete my PhD without him and for that I will always be grateful. In addition I would like to thank Dr Will Jenkinson who has also been pivotal during my PhD with his advice and ideas always being well received and appreciated.

Thank you also to every member of the Anderson Lab, as they helped me daily with experiments and offered me endless support and patience as I tried to learn new techniques. For also making my PhD so enjoyable I would like to thank the whole of the fourth floor of the IBR. I have loved all of the laughter and cake.

Finally all of my family and friends deserve a huge thank you for dealing with me during the stressful moments of my PhD and always encouraging me to continue to give my best, which has been more than worth it in the end!

TABLE OF CONTENTS

LIST OF FIGURES

CHAPTER 1

CHAPTER 3

CHAPTER 4

CHAPTER 5

LIST OF TABLES

ABBREVIATIONS

BMSU	Biomedical Services Unit
WT	Wild-Type
DMEM	Dulbecco's Modified Eagle's Medium
VP	Vaginal Plug
E –	Embryonic Day
dGuo	2-deoxyguanosine
FTOC	Fetal Thymic Organ Culture
KCT	Kidney Capsule Transplant
RBC	Red Blood Cell
TEC	Thymic Epithelial Cells
BrdU	Bromodeoxyuridine
OCT	Optimal Cutting Temperature compound
PBS	Phosphate Buffered Saline
BSA	Bovine Serum Albumin
DABCO	1,4 diazabicyclooctane
BMC	Bone Marrow Chimera
H&E	Haemotoxylin and Eosin
PAMPs	Pathogen Associated Molecular Patterns
PRRs	Pattern Recognition Receptors
TLRs	Toll Like Receptors
LPS	Lipopolysaccharide
NOD	Nucleotide binding Oligomerisation Domain
RIG	Retinoic acid Inducible Gene
RAG	Recombinase Activating Gene
Ig	Immunoglobulin
MHC	Major Histocompatibility Complex
APC	Antigen Presenting Cell
nTreg	Natural T Regulatory
Th	T helper
IFN	Interferon
TGFβ	Transforming Growth Factor β
RORγT	RAR-Related Orphan Nuclear Receptor γ
Treg	T regulatory
DC	Dendritic Cells
TAP	Transport Associated with Antigen Processing
CDR	Complementarity Determining Regions
V	Variable
D	Diverse
J	Joining
ITAM	Immunoreceptor Tyrosine based Activation Motifs
ZAP-70	ζ-chain associated protein kinase of 70kDa
LAT	Linker for Activation of T cells
PTK	Protein Tyrosine Kinase
MAP	Mitogen Associated Protein
cTEC	Cortical Thymic Epithelial Cells
mTEC	Medullary Thymic Epithelial Cells

3PP	Third pharyngeal pouch
Fox	Forkhead
GCM2	Glial cells missing 2
BMP-4	Bone-Morphogenic protein 4
TEC	Thymic Epithelial Cells
HSCs	Hematopoietic Stem Cells
MPPs	Multipotent Progenitors
CLPs	Common Lymphoid Progenitors
LSK	Lineage, stem cell antigen 1, cKit
dKO	Double Knock Out
ETP	Early Thymic Progenitors
GPCR	G-protein coupled receptor
VCAM1	Vascular Cell Adhesion Molecule -1
TSP	Thymic settling progenitor
SCZ	Subcapsular zone
iSP8	Intermediate SP8 population
CMJ	Corticomedullary Junction
TNFRs	Tumour Necrosis Factor Receptors
IKK1/2	Inhibitor of κB
CD62L	CD62 Ligand
HSA	Heat Stable Antigen
Sphk1/2	Sphingosine1/2
S_1P_1	Sphingosine 1 phosphate receptor
Cers2	Ceramide synthase 2
SM	Semi mature
M1	Mature 1
M2	Mature 2
IFNαR	Interferon alpha receptor
OPG	Osteoprotegerin
RANK	Receptor Activator for NF-kB
Cld3/4	Claudin 3/4
TSSP	Thymus specific serine proteases
Aire	Autoimmune Regulator
TRA	Tissue Restricted Antigen
APS-1	Autoimmune Polyendocrine Syndrome type 1
Fezf2	FEZ family zinc finger 2
cDC	Conventional Dendritic Cells
Sirpα	Signal regulatory protein α
pDC	Plasmacytoid DC
MDP	Macrophage and Dendritic cell Precursors
CDP	Common Dendritic cell Progenitors
Irf8	Interferon Regulatory Factor 8
Flt-3L	Fms-like tyrosine kinase 3 ligand
MCP-2	Monocyte Chemotactic Protein-2
PSGL-1	P-selectin glycoprotein ligand 1
VLA-4	Very late antigen 4
VCAM-1	Vascular cell adhesion molecule -1
OVA	Ovalbumin

NIK	NFκB inducing kinase
FGF-7	Fibroblast growth factor 7
KGF	Keratinocyte Growth Factor

CHAPTER ONE:

GENERAL INTRODUCTION

1.1 The Immune System Overview

The general function of the immune system is to provide essential protection against foreign pathogens through mechanisms that prevent destruction and damage caused by pathogenic entry into the host. The desperate requirement for a functioning immune system is illustrated in individuals where the immune system has become dysfunctional. This is apparent in immunodeficiency with underactive immune responses leading to disease manifestation or overactive immune activation, in turn assisting the development of autoimmune diseases and allergic responses. Acting in addition to this are the environmental and heritable factors which can further skew the immune system response (Brodin and Davis, 2017). Therefore, regulation of the immune system is pivotal to its correct functioning and host protection.

The immune system has evolved to contain two main arms; the innate and the adaptive. The cells of the innate immune system contains the feature of receptor commonality and as a result, innate immune cells have shared expression of recognition molecules that detect a wide range of common pathogenic molecular identifiers (Brubaker et al., 2015). However, the alternative adaptive arm of the immune system, operates on a far more specific basis with the expression of a unique and diverse range of receptors. These receptors have been acquired through gene rearrangements during adaptive immune cell development and are able to support identification of exclusive pathogenic features thus acting as a far more targeted immune response. Yet despite the diversification in the roles of innate versus adaptive, there is vast interplay between these two arms, with the preliminary activation of the adaptive immune response heavily being reliant upon initial innate triggering.

Upon entry through the primary barrier of the skin by pathogens, surpassing mucosal layers, innate immunity is one of the first lines of defence (Turvey and Broide, 2010). It is poised with a large number of cells that recognise common pathogenic features but most importantly these cells are equipped to initiate a rapid immune response. Innate cells can then become activated to supply the factors required to recruit and support the adaptive response (Gasteiger and Rudensky, 2014). However in the resting state, cells of the adaptive immune system are maintained at a far smaller antigen specific clonal number. As a result, upon activation, these selected adaptive immune cells are required to undergo clonal expansion through the process of proliferation (Burnet, 1959). Clonal expansion obtains sufficient numbers to support an effective response but due to the time taken to increase cell numbers, it results in a delay period in the immune response initiation. Despite this, adaptive immunity is longer lived with the provision of memory cells allowing for immediate responses upon future re-exposure to the same pathogen - providing a vast level of host protection (MacLeod et al., 2010).

1.1.1 The Innate Immune System

The innate immune system is composed of both cellular and humoral factors. Focusing firstly on the cellular aspect, this category includes cells such as neutrophils, eosinophils, dendritic cells (DC), natural killer cells and macrophages. These cells express a plethora of pattern recognition receptors (PRRs) that recognise common pathogenic structures known as Pathogen Associated Molecular Patterns (PAMPs) which include cell wall components, nucleic acids and metabolic products (Janeway and Medzhitov, 2002). The process of PAMP recognition through PRRs ultimately acts to trigger a cascade of responses from the innate immune cells to support the clearance of the pathogenic material that has entered the host.

1.1.1.1 Soluble Pattern Recognition Receptors

PRRs themselves are either categorised as being soluble as they circulate in plasma, or cellular due to receptor expression on the innate cell surface. Soluble PRRs bind to foreign PAMPs, coating their surface in a process known as opsonisation, which allows for these tagged cells to be identified by additional innate immune cells expressing complementary receptors to the PRRs. Subsequently, binding of innate immune cells such as macrophages to opsonised pathogens initiates a process of uptake, removal and destruction termed phagocytosis (Bidula and Schelenz, 2016). Soluble PRRs include collectins (Mannose Binding Lectin), pentraxins (C-reactive protein), antibodies (IgM) and plasma complement (C3b) (Janeway and Medzhitov, 2002).

More specifically, complement adds another layer into the regulation of pathogen destruction by innate immune cells as it has three cascades of activation that all interlink with other soluble PRR mechanisms of pathogen opsonisation. The classical, alternative and mannose binding pathways activate complement through; presence of complexes of antigen and antibodies, spontaneous lysis of plasma complement C3 which binds to pathogen surfaces and presence of mannose binding lectin on bacterial and viral cell walls respectively (Noris and Remuzzi, 2013, Sarma and Ward, 2011). The complement cascade is composed of different complement proteins C1-9, but all pathways act via an intermediate major complement associated molecule C3 convertase which is central to the complement cascade (Carroll, 2004). C3 convertase triggering by the classical, alternative and mannose binding pathways results in production of C3a and b. C3a can initiate localised inflammation supporting recruitment of innate cells whereas C3b binds directly to bacterial cell membranes to induce further opsonisation for internalization by macrophages and neutrophils (Sarma and Ward,

2011, Camous et al., 2011). Furthermore the C3 convertase can become bound to C3b inducing formation of a C5 convertase. C5 convertase allows production of the chemoattractant C5a but also C5b which is necessary, along with C6-9, for formation of a membrane attack complex which punches holes in pathogenic walls upon recruitment, inducing pathogen death and clearance (Parkin and Cohen, 2001).

1.1.1.2 Cellular Pattern Recognition Receptors

Cellular PRRs include families of membrane bound receptors such as Toll-Like Receptors (TLRs) with different TLRs (1-9) recognising various surface expressed common pathogenic features (O'Neill et al., 2013). For example TLR-4 recognises the endotoxin Lipopolysaccharide (LPS) and TLR-5 has an affinity for flagellin on bacterial cells (Akira and Takeda, 2004). In addition, some TLRs are expressed internally within endosomes (TLR 3,7-9) to sense the presence of non-host nucleic acids which would suggest pathogenic invasion of host cells (Beutler, 2009). Alternative PRRs also exist, with different families being cytosolically expressed. These include Nucleotide binding Oligomerisation Domain receptors (NOD- like receptors) that can detect bacterial PAMPs in the cytosol along with Retinoic acid Inducible Gene receptors (RIG-like receptors) that recognise RNA PRRs in the cytosol (Petrilli et al., 2007, Loo and Gale, 2011). Upon activation, all receptors initiate the beginnings of an immune response targeted towards pathogen clearance.

The subsequent binding of PAMPs to PRRs, either soluble or cellular, triggers the activation of downstream signalling pathways associated with the induction of inflammation to support the release of cytokines and chemokines for enhanced cell recruitment to the affected area (Kawai and Akira, 2011). Recruitment of other innate cells is necessary for prolonged

detection of foreign antigens and sustained death of invading microorganisms. Neutrophils are important in this process as they mediate phagocytosis of pathogens. This is possible as antibody or complement opsonised bacteria can bind to neutrophils via FC or complement receptors respectively (Appelberg, 2007). Upon binding, subsequent membrane projections from the neutrophil form a phagosome around the pathogen, this can fuse with cytoplasmic lysosomes to generate a phagolysosome from which cytotoxic granules or reactive oxygen species can then induce pathogenic death (Parkin and Cohen, 2001). Macrophages are also pivotal in supporting the clearance of apoptotic bodies again via phagocytosis (Galli et al., 2011). As a result, the innate immune system is key in initial immune responses to support the clearance of pathogenic material. But importantly one of the main roles of innate immunity is to induce activation of the adaptive arm which can occur through inflammatory cytokine and chemokine release by innate cells but also occurs through dendritic cell (DC) recruitment for subsequent antigen processing and presentation (Kumar et al., 2009). Activated DC trigger the upregulation of their costimulatory molecules CD80 and CD86 which can in turn support increased activation of adaptive immune cells as DC circulate through lymph nodes and spleen (Delves and Roitt, 2000).

1.1.2 The Adaptive Immune System

The defining feature of the adaptive immune system is its ability to express a wide repertoire of receptors each specific for one key pathogenic feature. The adaptive immune system is comprised of T lymphocytes (T-cells) and B lymphocytes (B-cells). T-cells will be discussed in greater detail in 1.1.4.

1.1.2.1 B-cells

B-lymphopoiesis initially occurs from a pool of pluripotent hematopoietic stem cells in the fetal liver. This process then continues in the bone marrow where it subsequently is maintained throughout adult life. During differentiation, B-cells express the endonucleases Recombinase Activating Gene 1/2 (RAG 1/2), which is required to support rearrangement of Variable, Diverse and Joining (VDJ) segments of the surface expressed immunoglobulin genes (Jung and Alt, 2004). It was indeed shown that there was a requirement for Rag1 as well as Rag2 gene expression to support the initial activation of VDJ recombinase activity, with clonal transfection of only Rag1 cDNA to non-lymphoid cells resulting in an apparent inability to confer VDJ recombinase activation which was supported only upon co-transfer of Rag1 and Rag2 (Oettinger et al., 1990). Such rearrangements are required for the reconfiguration of cell surface immunoglobulin (Ig) genes to form a cell surface receptor capable of pathogen recognition (Bassing et al., 2002). This process occurs with the formation of a functional Ig heavy chain, productive rearrangement of the μ chain occurs and the heavy chain can then be expressed on the cell surface with surrogate light chains themselves combining to constitute a pre-B-cell receptor (Tonegawa, 1983, Melchers, 2005). Successfully rearranged light chain variable regions subsequently combine as complete light chains which join with heavy chains to form a IgM molecule inserted onto the cell membrane, bound by the constant region thus leaving the highly specific antigen binding domain exposed (Pieper et al., 2013). If rearrangements are unsuccessful, cells die as they fail to receive key survival signals. During the rearrangement process, developing B-cells are screened against self-antigens. This is absolutely necessary as random gene rearrangement could lead to production of B-cells with a B-cell receptor that is capable of self-recognition and therefore screening against self prevents the release of potentially autoreactive B-cells.

Consequentially, autoreactive B-cells can undergo clonal deletion, receptor editing to try and rearrange the receptor to a non-autoreactive variant or clonal anergy such that the receptor is unable to be triggered peripherally by cognate antigen(Goodnow et al., 2005,Nemazee and Hogquist, 2003).

B-cells expressing IgM leave the bone marrow and migrate to secondary lymphoid organs where they mature and acquire the capacity to produce IgD through alternative mRNA splicing (Loder et al., 1999). B-cells then await activation by successful interaction with cognate pathogenic antigens to in turn be directed down T-cell dependent or T-independent cell fates where they can undergo clonal expansion, further maturing into antibody secreting plasma cells (Liu et al., 1991). Through interaction with activated T-cells, B-cells can enter into germinal centre reactions to begin somatic hypermutation and class switch recombination to become IgG, IgA or IgE and again successful interactions with antigen during this process will allow for selection and emergence of higher affinity B-cell clones (LeBien and Tedder, 2008, Liu et al., 1989, Kranich and Krautler, 2016).

Importantly, it is the process of gene rearrangement in B-cells that helps to support the diversity in the B-cell receptor (BCR) repertoire and peripherally this acts to allow B-cell activation to a wide range of antigens directly. The most important functional feature of B-cells is their ability to go on to provide both long-lived memory cells and plasma cells with the capacity to produce high affinity antibody following germinal centre reactions (Zhang et al., 2016). In addition, more recent evidence has shown production of memory B-cells also from T independent responses – further supporting the important and diverse immune

function of B-cells in host protection upon future reinfections (Obukhanych and Nussenzweig, 2006) (Alugupalli et al., 2004).

1.1.3 T-cells

T-cells develop through similar steps to B-cells with regards to gene rearrangements to produce a surface expressed T-cell receptor (TCR) that forms part of a distinct self-tolerant repertoire. However unlike B-cells, development of T-cells occurs in the thymus from precursors that are recruited from the bone marrow. Due to the thymus centric focus of this thesis, the development of T-cells will be discussed in a latter section 1.2 in greater detail.

1.1.3.1 T-cell Subsets Overview

T-cell populations are themselves either composed of αβ T-cells or γδ T-cells – both of which are generated in the thymus and exit the thymus with a pre-determined lineage commitment. Functions of γδ T-cells are perhaps less well characterised compared to the αβ T-cell population. However what remain clearly apparent are the functional differences between these two populations. αβ T-cells reside in secondary lymphoid organs such as spleen and lymph nodes, whereas the γδ T-cells have been suggested to be mainly localised to epithelial layers of the tissue which include intestinal epithelium and skin (Allison and Havran, 1991). γδ T-cells bear receptors with a tendency to recognise antigens that are more commonly associated with a stressed or diseased state and greatly differ from αβ T-cells in that they can be directly activated and therefore have little dependency on activation through an antigen presenting cell intermediate (Hayday, 2000) (Vantourout and Hayday, 2013). It has been shown in fact that following stress, γδ T-cells can detect signals via TLR triggering to produce substances such as cytotoxic granzymes that directly act to clear pathogens through

lytic molecule release (Dieli et al., 2001, Dudal et al., 2006). This feature causes γδ T-cells to appear to have a phenotype that correlates more directly with that seen in innate immune cells which is supported also by their participation in the early immune response (Xiong and Raulet, 2007).

αβ T-cells are classified as being either $CD4^+$ or $CD8^+$ depending upon their surface expression of these molecules and both have T-cell receptors that tend to recognise pathogenic material that is presented to them in a preprocessed manner rather than directly. Their primary positioning both within and migrating through secondary lymphoid organs allows these αβ T-cells to be localised to regions where they are most likely to come into contact with an antigen presenting cell (APC) for activation. APCs can present antigen to T-cells as it is presented within the context of a major histocompatibility complex (MHC) on the APC surface which can be recognised by cognate αβTCR; differing significantly from γδ T-cells (Haas et al., 1993). Interaction between αβ T-cells and APCs allows αβ T-cells to then differentiate into distinct effector subsets with a helper role being assumed by CD4 T-cells and a cytotoxic role by CD8 T-cells.

Overall it appears that the roles of γδ and αβ T-cells are distinct which in turn is directly reflected by their non-overlapping TCR repertoires and additionally highlights the developmental divergence of these populations, which is postulated to be early in development (Prinz et al., 2006). Going forward; due to the more relevant role of αβ T-cells to the purpose of this thesis, there will only be reference from this point onwards to the αβ T-cell lineage and development.

1.1.3.2 CD4 T-cell Subsets

CD4 T-cells are released from the thymus as naïve conventional cells or natural T-regulatory cells (nTreg). nTreg are fully functional upon exit from the thymus with the capacity to be peripherally activated to suppress autoreactive T-cells that have escaped negative selection. Conventional T-cells are thought to develop intrathymically based upon their medium affinity binding to self-antigens expressed in the medulla which has been illustrated through Nur77GFP models where GFP levels relate to strength of TCR signals. From this, higher TCR signal strengths directly correlated with Treg induction rather than the lower level of GFP and signal strength which was required for T-conventional cells (Moran et al., 2011). Furthermore, generation of nTreg is absolutely dependent upon the medulla, whereas it remains dispensable for T-conventional cells – a finding that appears to directly relate to the requirement for self-antigen exposure to drive nTreg production (Cowan et al., 2013).

There have been two proposed precursors for nTreg development. The conventional two-step process suggests that following binding through the TCR to antigen with a medium affinity, there is upregulation of CD25 (the α chain of the IL-2 receptor) causing cells to become $CD25^{+}Foxp3^{-}$ conventional precursors. These can then mature as IL-2 signaling drives STAT5 to support Foxp3 expression and development into $CD25^{+}Foxp3^{+}$ nTreg (Lio and Hsieh, 2008, Hsieh et al., 2012). Alternatively, Treg have also been proposed to develop from a $Foxp3^{+}CD25^{-}$ Treg precursor. Foxp3 is thought to be acquired initially through the TCR binding causing a consequential increase in phosphorylation of the proapoptotic molecule Bim. From this there is a requirement for common γ cytokine (IL-7, IL-2 and IL-15) exposure to promote Bcl-2 pro-survival factors that in turn rescue cells through CD25 expression as they become $CD25^{+}Foxp3^{+}$ nTreg (Tai et al., 2013). Additional reports supported this

alternative hypothesis through tetracycline inducible Zap-70 models, which indicated high levels of the alternative precursor within the thymus and its requirement for IL-15 to develop whereas IL-2 exposure was subsequently required for efficient maturation of these alternative precursors to $CD25^{+}Foxp3^{+}$ nTreg (Marshall et al., 2014).

Unlike nTreg, naïve CD4 T-cells are required to undergo peripheral maturation to then be able to perform specific functions in immune responses. For this to occur, multiple steps need to be met; this begins with activation of the TCR by APCs such as DC or macrophages, presenting cognate antigen in an MHC class II specific manner. As well as this, there needs to be interaction between CD28 on T-cells and CD80/CD86 on APCs to provide a supportive level of co-stimulation for full T-cell activation. Finally, the determining factor for the destiny of the naïve T-cell, relates to exposure to the lineage inducing cytokines released by the APC (Kaiko et al., 2008, Zhu and Paul, 2010). This will allow the CD4 naïve T-cells to become a specific phenotype of different T helper (Th) subsets.

From this, a Th1 phenotype is assumed if there is exposure to IL-12 and Interferon γ (IFN-γ) as it drives the transcription factor T-bet which defines the Th1 lineage (Szabo et al., 2000). These cells in turn produce IL-2 and IFN-γ to support the destruction of intracellular pathogens (Zhu and Paul, 2008). Exposure of naïve T-cells to IL-4 supports the lineage transcription factor GATA-3, driving a Th2 phenotype with these cells producing IL-4 and IL-5 to support B-cell class switching and in addition the removal of extracellular parasites (Zheng and Flavell, 1997, Kopf et al., 1994). As well as this there is the Th17 phenotype which occurs through exposure to Transforming Growth Factor β (TGFβ) in association with IL-6. These cells use the transcription factor RAR-Related Orphan Nuclear Receptor γ

(RORγt) and produce IL-6 and IL-17 to support extracellular bacteria and fungi destruction (Harrington et al., 2005, Ivanov et al., 2006, Weaver et al., 2006).

All T-cell populations can become dysregulated to some degree and have individually been implicated in destructive responses against self; Th1 and Th17 have been closely linked to autoimmunity and Th2 has been associated with allergy and asthma responses (Zhu and Paul, 2008). Therefore as well as the predetermined nTreg presence peripherally, there are also naïve T-cells which can be induced into a Treg phenotype to assist in regulating this peripheral T-cell pool. Treg induction is driven by exposure of naïve T-cells following TCR triggering to TGFβ alone which turns on Forkhead box P3 (Foxp3) transcription factor (Chen et al., 2003). The requirement for Treg was clearly shown in mice whereby a mutation in the Foxp3 transcription factor resulted in 'scurfy mice' which ultimately died at an early age from lymphoproliferation and multiple organ cellular infiltration (Brunkow et al., 2001). Similarly in man the Immune dysregulation, polyendocrinopathy, enteropathy, X-linked syndrome (IPEX) has been shown to develop whereby mutations in the Foxp3 transcription factor can lead to dysfunctional Treg and resultant multiorgan autoimmune disease (Barzaghi et al., 2012, Oftedal et al., 2015). Therefore the requirement for Treg is significant in the immune system and their expression of Foxp3 drives a plethora of immune regulatory factors that are essential in immune homeostasis, with the suppression of autoreactive T-cell and immune resolution.

Treg can fulfill their regulatory phenotype as they produce inhibitory cytokines such as TGFβ, IL-10 and IL-35. These have been shown to; inhibit proliferation of effector T-cells by the attenuation of cell cycle regulators, inhibit IL-2 production by effector T-cells to cause a

halt in their expansion and generally prevent proliferation of T effector cells (Vignali et al., 2008). In addition Treg produce granzyme B and perforin to induce cytolysis. These molecules are released along microtubules between Treg and effector T-cells upon activation, where perforin supports entry of granzyme B into the cell to disrupt mitochondrial pathways and cause cell death (Lieberman, 2003). This mechanism has also been shown to be used by Treg to control B-cells as well (Zhao et al., 2006). Treg can also additionally induce metabolic disruption by CD39 and CD73, which are involved in pericellular adenosine production binding to the adenosine A2A receptor on effector T-cells to induce suppression (Deaglio et al., 2007, Sitkovsky et al., 2008). Finally expression of CTLA-4 by Treg acts to cause downregulation and further removal of costimulatory molecules CD80/86 on DC, which due to the essential requirement of these molecules in the activation of naïve T-cells, there is a resultant reduction in peripheral naïve T-cell triggering and a halt in the progression of the response (Qureshi et al., 2011).

1.1.3.3 CD8 Cytotoxic T-cells

CD8 T-cells similarly require multiple signals to ensure full activation in the periphery. This includes TCR engagement via antigen, costimulatory molecule exposure and stimulation through inflammatory cytokine receptors (Obar and Lefrançois, 2010). CD8 T-cells however greatly differ to CD4 T-cells in that they recognise antigen being presented in the context of MHC class I. These molecules are expressed on all cells and antigen is processed intracellularly by cellular proteasomes and presented via MHC class I (Blum et al., 2013). Activated CD8 T-cells have a role in removal of viruses and tumours which they are equipped to carry out due to their ability to produce perforin and granzyme molecules and induce cell death via Fas-FasL interactions (Bannard et al., 2009).

1.1.4 Antigen Presentation For T-cell Activation

As previously mentioned, CD4 and CD8 T-cells become activated by antigen presentation in MHCII and MHCI molecules respectively. However the mechanisms that govern the methods of antigen presentation differ between these two populations with presentation of exogenously and endogenously derived peptides respectively.

Expression of MHCII is restricted to the surface of APCs and the MHCII complex itself is produced in the endoplasmic reticulum where it is primarily tethered to an invariant chain to prevent inappropriate activation and instead guide the complex towards the antigen processing compartments through the antigenic motifs that it contains (Blum et al., 2013, Bryant and Ploegh, 2004). Within processing compartments, the invariant chain is degraded leaving a class II associated invariant chain (CLIP) peptide that will support the binding and loading of lysosomally produced peptides (Cresswell, 1996). Peptides for loading are present within these endosomal/lysosomal compartments, as they have been taken up from extracellular sources during immune responses via receptor mediated endocytosis, phagocytosis, autophagy and macropinocytosis (Figure 1.1A) (Roche and Furuta, 2015) (Dengjel et al., 2005). MHCII can then be loaded with peptide and transported in a vesicle to the plasma membrane for presentation to naïve CD4 T-cells.

MHCI is expressed by all cells which therefore have the capability to present endogenous peptides from within the host cell – this process is particularly important during viral infections as host cells become taken over and therefore it supports identification of invasion. Cells can therefore use this mechanism to present viral peptides in MHCI molecules and identify infected cells for destruction by CD8 cytotoxic T-cells (Vyas et al., 2008).

Endogenous peptides are retrieved for MHCI loading through the molecule transport associated with antigen processing (TAP) from the endoplasmic reticulum, following their proteasomal degradation (Figure 1.1B) (Neefjes et al., 2011). TAP forms part of the peptide loading complex containing the transmembrane glycoprotein tapasin and other chaperone proteins which transfer cytosolic peptides from the endoplasmic reticulum to the MHCI molecules (Blum et al., 2013). MHCI molecules can then be expressed on the surface of nucleated cells and if infected, presentation of antigenic peptide will be sufficient to trigger the CD8 cytotoxic lineage and an immune response (Figure 1.1B).

1.1.5 T-cell Receptor Structure and Function

In order for the wide range of antigens being held in MHC molecules to be detectable by the TCRs expressed on the T-cell surface, an equally extensive range of TCRs is required to be present in the host. This is possible due to the variability in the TCR that can be obtained during generation in the thymus. The generation of a functional α and β chain for the TCR requires rearrangement of the variable regions of the gene which are grouped together under the umbrella of complementarity determining regions (CDRs). Within this, recombination of variable (V) diverse (D) and joining (J) elements occurs for the β chain and only V-J for the α chain. This process is similarly driven by the expression of both recombinase activating gene 1/2 (RAG 1/2) as previously discussed with relation to B-cells (Nemazee, 2000, Jung and Alt, 2004, Mombaerts, 1995). Successfully recombined gene regions are subsequently joined to the constant region allowing the ultimate generation of an α or β chain which will come together to form the TCR. As well as this, even greater variation and structural diversity can occur through the incorporation of additional nucleotides, along with the deletion of others, at the joining sections during recombination (Nikolich-Zugich et al., 2004). Due to this process

of random segment selection, each TCR generated will be unique and vitally support sufficient diversity of the TCR repertoire such that an overabundance of foreign antigens can be accommodated for and further recognised, to support a continuously robust immune response.

Equally as important as the dynamic diversity of the TCR repertoire is the ability of the TCR to be functional and responsive with the TCR structure on the cell surface shown in Figure 1.2. The functionality of the TCR is therefore checked prior to release from the thymus into the periphery. The intracellular domain of the αβTCR is short and therefore alone it cannot signal intracellularly following TCR activation, as a result, the TCR is linked non-covalently to the CD3 molecule to connect to a signalling cascade within the cell (Cantrell, 2002). The CD3 complex is composed of CD3εδ, CD3εγ heterodimers, and CD3ζζ homodimers with CD3ε/δ/γ containing a single immunoreceptor tyrosine based activation motif (ITAM) whereas the CD3ζζ homodimers contain three ITAMs (Call et al., 2006, Sun et al., 2001, Arnett et al., 2004). These all exist in an equivalent ratio with one TCRαβ being associated with CD3εγ, CD3εδ, CD3ζζ dimers (Call et al., 2002). As a result, TCR triggering can therefore successfully lead to intracellular signals as it initiates CD3 ITAM phosphorylation by the Src family of tyrosine kinases LCK and FYN (Brownlie and Zamoyska, Samelson, 2002) (Deindl et al., 2007). When there has been phosphorylation, ITAMs are able to recruit the SYK family member ζ-chain associated protein kinase of 70kDa (ZAP-70) through high affinity binding to SH2 domains of ZAP-70 (Au-Yeung et al., 2009, Weiss, 1993). This binding exposes sites on ZAP-70 for its phosphorylation by Lck-mediated mechanisms allowing activated ZAP-70 to target downstream adaptor linker for activation of T-cells (LAT) which in turn enables full TCR signalling including Protein Tyrosine Kinase (PTK)

and Mitogen Associated Protein (MAP) activation (Wang et al., 2010a). Therefore triggering of the TCR in the thymus can allow for functionality checks, with the assessment of downstream signalling cascade activation prior to developmental progression – therefore also acting as a selection mechanism. Additionally, once in the periphery this TCR triggering along with the other necessary accessory signals can functionally activate the T-cell. This will enable it to perform its function and undergo successful gene activation to induce transcription of required genes such as those needed for growth, adhesion and proliferation.

Figure 1.1:

Process of MHC Antigen Presentation

A) Process of MHCII antigen processing with antigens endocytosed and taken into cells in an endocytotic vesicle. This can then be taken into the endoplasmic reticulum with antigenic peptides processed in this compartment. Peptides can then be loaded onto MHCII molecules with the degradation of the invariant chain that is bound to MHCII allowing MHCII to be associated with invariant chain (CLIP) that acts to support peptide loading to MHCII molecule. Loaded MHCII molecules can then be transported to the cell surface.

B) Processing of intracellular antigens for presentation on MHCI surface. Antigens are processed in the proteasome of the cells and then transferred via the transport associated with antigen processing (TAP) molecule into the endoplasmic reticulum for loading onto MHCI molecules. Loaded complexes are then transported onto the cell surface.

A

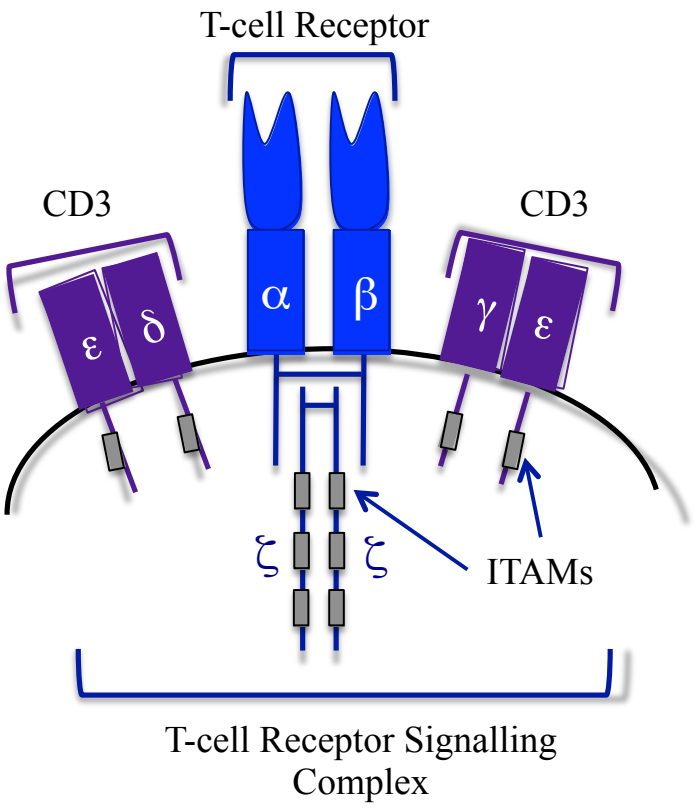
T-cell Receptor
CD3
CD3
ε
δ
α
β
γ
ε
ζ
ζ
ITAMs
T-cell Receptor Signalling Complex

Figure 1.2:
Structure of T-cell Receptor

The T-cell receptor is surface expressed on T-cell surface and is composed of a complex in which α and β TCR chains These are joined and linked intracellularly to immunoreceptor tyrosine based activation motifs (ITAMs). During TCR signalling to support an intracellular signalling cascade, CD3 molecules are required to non-covalently connect to the TCR and allow for the transmission of the TCR signals into the cells. The CD3 complex is composed of different heterodimers themselves linked to ITAMs, necessary to support intracellular signal transmission.

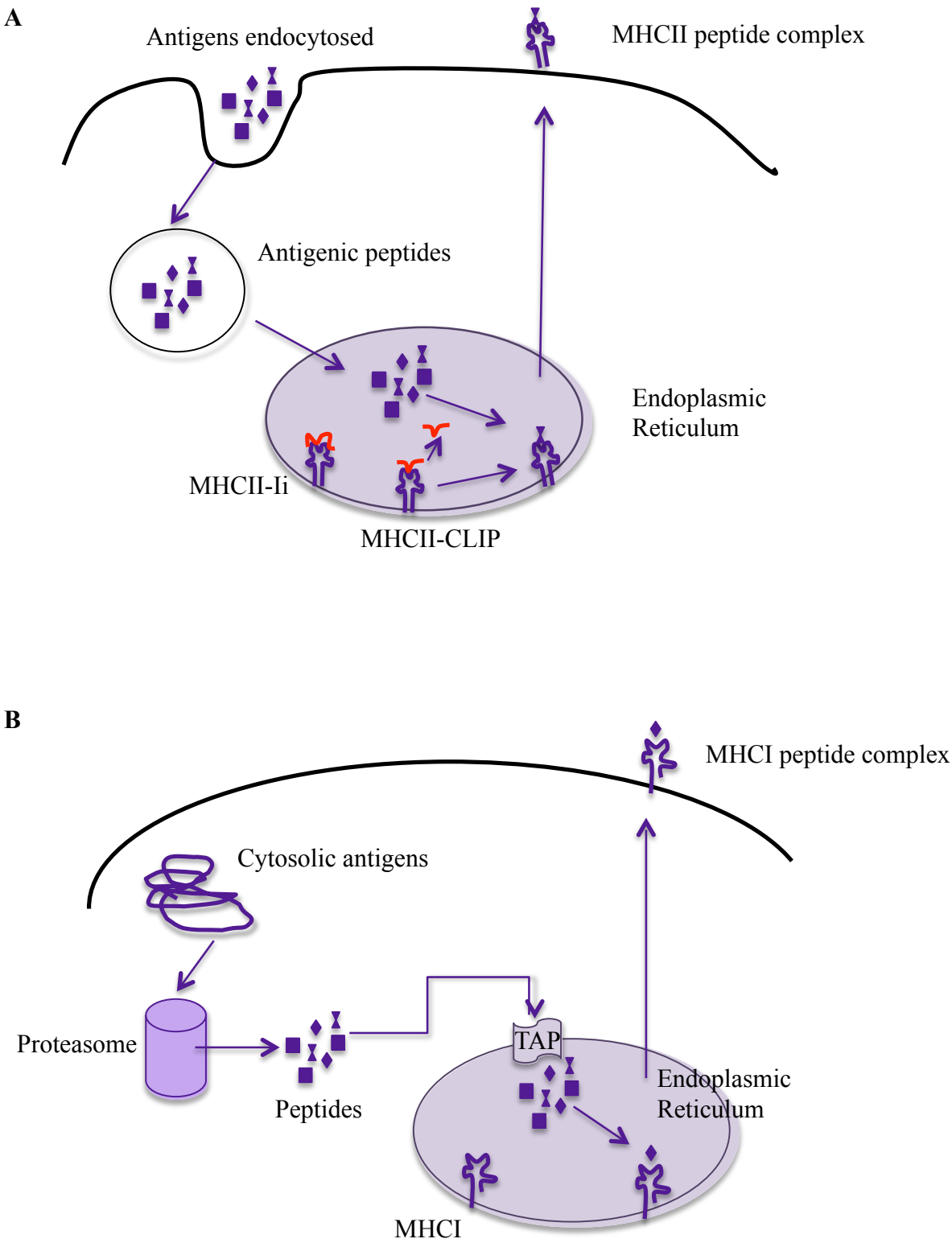
A
Antigens endocytosed
MHCII peptide complex
Antigenic peptides
Endoplasmic
Reticulum
MHCII-Ii
MHCII-CLIP
B
MHCI peptide complex
Cytosolic antigens
Proteasome
Peptides
TAP
Endoplasmic
Reticulum
MHCI

1.2 T-cell Development

The thymus is an organ that is composed of two lobes and is anatomically positioned in the centre of the thoracic cavity above the heart. The thymus provides a unique microenvironment comprised predominately of thymic epithelial cells that act to support the development of T-cells from precursors recruited from the bone marrow. It can be divided into two main areas, the cortex and the medulla, composed of cortical thymic epithelial cells (cTEC) and medullary thymic epithelial cells (mTEC) respectively (Boehm and Swann, 2013). The cortex supports the development of thymocytes until the single positive stage, which occurs following positive selection. Whereas the medulla is mainly concerned with negative selection of potentially autoreactive T-cells and central tolerance induction (Boehm, 2008). This process is summarised in Figure 1.3.

1.2.1 Thymus Organogenesis

During embryogenesis in mice, the thymus arises from the third pharyngeal pouch (3PP) of the endoderm, surrounded by neural crest mesenchyme (Hollander et al., 2006). By E12.5, the thymus begins to physically separate from the parathyroid gland which, until this point, have been closely associated as both develop from the 3PP (Rodewald, 2008) (Vaidya et al., 2016). The thymus additionally separates from the parathyroid gland with regards to functional alterations which are transcription factor mediated. Thymus identity is controlled through expression of the master regulator forkhead (Fox) superfamily of transcription factors containing Foxn1, whereas the parathyroid development remains controlled by Glial cells missing 2 (Gcm2) (Liu et al., 2007). This separation in expression is apparent relatively early as it can be distinguished in the third pharyngeal pouch where Foxn1 expression has been shown to be driven by Bone-Morphogenic protein 4 (BMP-4) and also Wnt4 signalling

Figure 1.3:

T-cell Development In Thymus

The process of T-cell development is illustrated from the progenitor population that enters the thymus at the corticomedullary junction before progressing through the cortex and rearranging TCR genes during various double negative (DN) stages of development. Subsequent to this, a TCR is presented on the cell surface and cells become double positive (DP) expressing both CD4 and CD8. Positive selection can then occur through successful interaction with cTEC allowing cells to become single positive (SP) in phenotype. Upregulation of CCR7 allows SP cells to migrate from the cortex into the medulla to undergo tolerance induction by interacting with tissue restricted antigens (TRAs) expressed by $Aire^{+}$ mTEC and presented by mTEC and dendritic cells. Autoreactive cells are negatively selected and those that are non-responsive can progress through central tolerance induction to mature intrathymically and be able to egress from the thymus as naïve T cells.

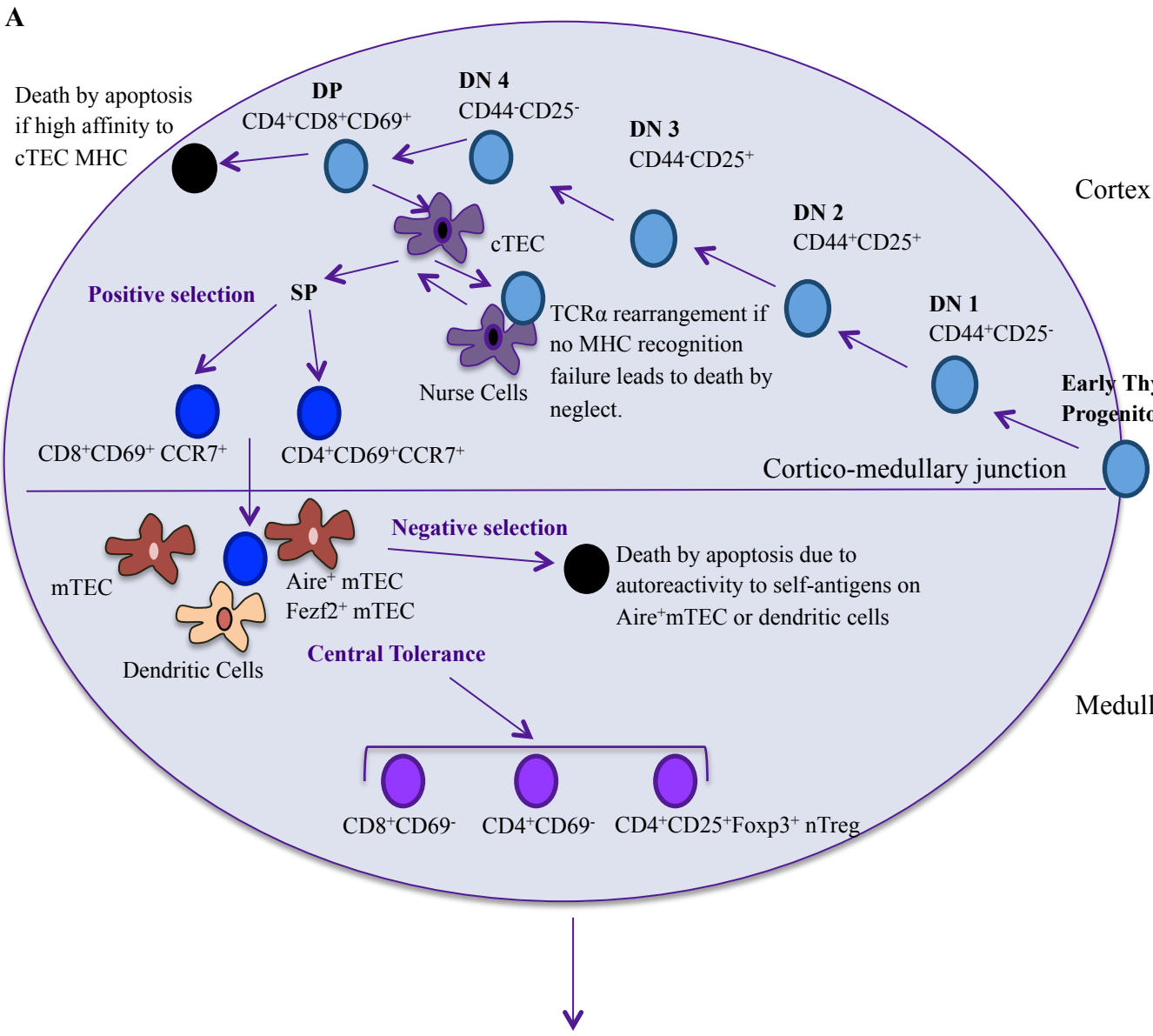

Exit thymus and enter into periphery following S_1P_1 mediated egress.

(Gordon and Manley, 2011). Foxn1 drives the formation of the thymus by supporting the development of the thymic epithelial cell lineage (TEC) which constitutes the basis of the thymic microenvironment required to support T-cell development (Nehls et al., 1994) (Nehls et al., 1996). In the mouse, BMP signalling is required for the sustained maintenance of Foxn1 expression in TEC – with repression of BMP resulting in loss of Foxn1 expression and TEC reverting to a state of pharyngeal epithelium that is subsequently unable to support T-cell development (Soza-Ried et al., 2008). This process of thymus organogenesis further appears to be conserved between mice and humans (Farley et al., 2013).

1.2.2 Thymic Progenitor Colonisation

The thymus requires continuous seeding of progenitor cells from the bone marrow or fetal liver in order to be able to maintain the development of functional naïve T-cells. However the phenotype of the most initial thymus settling progenitor (TSP) that can give rise to a T-cell population has been difficult to determine.

Within the bone marrow, hematopoietic stem cells (HSCs) have the capacity to develop into any blood cell lineage and lie directly upstream of multipotent progenitors (MPPs) whom themselves maintain a broad developmental capacity (Morrison et al., 1997) (Kondo, 2010). MPPs can be identified from HSCs through high levels of fms-like tyrosine kinase receptor-3 (Flt-3) expression and can support the generation of both a lymphoid and myelo-erythroid lineage (Kondo et al., 2000, Akashi et al., 2000). Emergence of lymphoid cells from MPPs is through the intermediate common lymphoid progenitor (CLP), which requires expression of the Ikaros transcription factor (Allman et al., 2003). CLPs also express high levels of IL-7Rα and of Flt-3 and possess the capacity to give rise to both B and T lymphocytes (Sitnicka et al.,

2002). Despite this, the presence of CLPs has not been identified in either the blood or the thymus, suggesting that there may be an additional population downstream of this progenitor which has T-lineage potential following its release from the bone marrow and migration towards the thymus (Scimone et al., 2006).

Nevertheless, ultimately for the successful development of the T-cell lineage, progenitors need to be able to migrate from the bone marrow through the blood and into the thymus (Schwarz and Bhandoola, 2006). For this to occur, there needs to be release of progenitors from the bone marrow niches for them to be able to then travel into the blood – such mobilization requires that there is cleavage of cell adhesions and also removal of chemokine gradients that subsequently were acting to retain the cells in the bone marrow (Schwarz and Bhandoola, 2004). Within the blood, identification of a T-cell progenitor has also been difficult to detect, with the Lineage negative, stem cell antigen 1 and cKit positive (LSK) population, which contains HSCs and MPPs, ultimately being shown to be the only known primary progenitor that is present within the circulation and able to possess T-lineage potential (Schwarz and Bhandoola, 2004).

Despite this, the mechanisms of progenitor recruitment have been determined through various experimental approaches – most utilising techniques of molecular blockade causing reduced T-cell development as a consequence. Circulating TSPs appear to enter the thymus in narrow zones close to the corticomedullary junction through the process of the multi-step adhesion cascade (Scimone et al., 2006). To initiate extravasation into the thymus, tethering/rolling along endothelium occurs by expression of platelet selectin (P-selectin) and P-selectin glycoprotein ligand 1 (PSGL1) on the vasculature and progenitors respectively (Rossi et al.,

2005) (Gossens et al., 2009). Expression of CD44 also appears to be important towards the support of progenitor recruitment with antibody mediated blockade of this fully preventing entry by thymus colonizing progenitors (Bhandoola and Sambandam, 2006).

Subsequent exposure of progenitors to chemokines and consequential signalling through G-protein coupled receptors (GPCR) on the progenitor surface, acts to rapidly activate integrins that are loosely tethered such as through α4β1 and Vascular Cell Adhesion Molecule -1 (VCAM1) expression on progenitor and endothelial surfaces respectively to support firm adhesion and extravasation (Scimone et al., 2006). In particular it appears that CCR7 and CCR9 play key roles in this process with the expression of their ligands CCL19/CCL21 and CCL25 being shown to be by thymic stroma (Takahama, 2006). An important study, highlighted that in adult mice there is upregulated CCR7 expression on progenitors that lie downstream of HSCs and MPPs, linking them to recruitment to the thymus (Zlotoff et al., 2010). This requirement for such chemokines was further supported in this study through generation of CCR7/CCR9 double knock out (dKO) mice whereby under competition with wildtype counterparts in mixed bone marrow chimeras, dKO failed to compete with regards to their ability to seed the thymus.

Interestingly, it is thought that the same chemokines may play a role in early embryonic thymic progenitor settling with progenitors at this stage developing in the fetal liver between E10.5-12.5 in mice gestation and then migrating into the thymic anlage from surrounding mesenchymal areas (Masuda et al., 2005) (Liu et al., 2006) (Bleul and Boehm, 2000) (Foster et al., 2008). As this early process occurs prior to the development of vascularisation it

remains to be dependent upon chemokine gradients – being attracted to thymic epithelial sources of CCL21 and CCL25 expression (Takahama, 2006).

1.2.3 Commitment To The T-cell Lineage

Initial TSPs are thought to give rise to the early thymic progenitor (ETP) population, which is the earliest identifiable T-cell progenitor currently available to study in the thymus so is therefore commonly used as a read out of thymus settling and progenitor recruitment (Benz et al., 2008, Ramond et al., 2015). However for ETP to obtain a committed phenotype to the T-cell lineage, the preceding TSP must have been exposed to Notch signalling (Radtke et al., 2010). This signalling via Delta-Like ligand 4 which is itself expressed by cTEC, occurs through the Notch 1 receptor on lymphocyte progenitors and suppresses the ability of these TSPs to develop into B-cells and rather supports only a T-lineage commitment (Radtke et al., 2013, Yuan et al., 2010). ETP have been shown to fail to develop under absence of functional Notch1 signalling, highlighting its requirement to support the stage between TSP and ETP (Sambandam et al., 2005, Tan et al., 2005).

ETP themselves reside within a double-negative 1 (DN1) population. The DN stage has subdivisions which relate to the expression of CD25 and CD44; DN1 $CD25^{-}CD44^{+}$ to DN2 $CD25^{+}CD44^{+}$ to DN3 $CD25^{+}CD44^{-}$ and finally DN4 $CD25^{-}CD44^{-}$ (Shah and Zuniga-Pflucker, 2014). The DN1 population itself is made up of subpopulations DN1a-e based again on expression of surface markers CD117 and CD24 with the DN1a-b population being shown to be where ETP are positioned and provide the most potent subclass able to give rise to T-cell lineage (Porritt et al., 2004). ETP can then undergo sequential stages in order to develop into

thymocytes progressing from DN stage being $CD4^-CD8^-$ through to double positive (DP) $CD4^+CD8^+$ and finally single positive (SP) $CD4^+$ or $CD8^+$.

1.2.4 Development Of Thymocytes Through The Cortex

DN1 cells are positioned near the site of progenitor entry at the corticomedullary junction (CMJ) and have the capacity to proliferate extensively through expression of IL-7 by cTEC upon entry into the thymus (Porritt et al., 2003). In addition it is the process of Notch signalling, as previously mentioned, that is required to drive these ETP populations down the thymocyte developmental pathway (Schmitt et al., 2004). DN1 cells transition to DN2 cells as they begin to undergo expression of RAG 1/2 genes and CD25 (Di Santo et al., 2000). DN2 cells mature as they migrate towards the subcapsular zone (SCZ), which is thought to be supported by their expression of CXCR4 and subsequent exposure to the corresponding ligand CXCL12, by both occasional cTEC and presence within the SCZ (Takahama, 2006). This chemokine-ligand interaction was shown to be key to support SCZ migration through the generation of $p56lck^{Cre}/CXCR4^{loxP/loxP}$ chimeras, where DN thymocytes lacked CXCR4 expression (Janas et al., 2010, Trampont et al., 2010, Plotkin et al., 2003). Analysis showed that such thymocytes were arrested at DN1 and immunofluorescent localisation reflected accumulation in the cortex near the CMJ where they had initially entered the thymus. As a result this demonstrates the requirement for CXCR4 expression on thymocytes to support migration from the CMJ to the SCZ.

By the time cells reach the SCZ they are DN2 in phenotype and can begin rearrangement of the TCRβ and pre-TCRα genes supported by their RAG expression. Rearrangement of the TCR genes ultimately lends itself to the association of the randomly rearranged TCRβ chain

and CD3 signalling molecules with a pre-TCRα chain to form a pre-TCR complex – from which point cells are confirmed to be DN3 in phenotype (von Boehmer and Fehling, 1997). The DN2 to DN3 transition period acts as a key checkpoint to ensure that only DN2 cells, which have undergone TCRβ chain selection, are allowed to continue differentiation beyond DN3. This is possible due to the requirement for signals at this point through the pre-TCR complex which are thought to be cell-autonomous and occurring in a ligand independent manner but necessary to enable continued development (Yamasaki et al., 2006). Ultimately these signals prevent cells from undergoing apoptosis and cause the cessation of further rearrangements of TCRβ genes with successful β–selection acting to drive the downregulation of CD25 and as a result further support final progression towards the DN4 phenotype (Dudley et al., 1994). Cells which fail to successfully rearrange their TCRβ genes will be triggered to undergo apoptosis as they will be unable to receive the required survival signals. The successfully generated DN4 cells will however continue in development and upregulate CD8, producing an intermediate SP8 population (iSP8), before upregulating CD4 to become DP in phenotype (Ciofani and Zuniga-Pflucker, 2007, MacDonald et al., 1988).

DP thymocytes are then required to successfully rearrange their TCRα chains to express a complete αβ TCR on their surface and become positively selected through cTEC interaction. Reversing upon the initial movement of the DN progenitors towards the SCZ, the DP progenitors begin to relocate back towards the cortex region where they randomly migrate (Dzhagalov and Phee, 2012). DP thymocytes were shown to be highly motile within the cortex, with cells seen to only pause upon interaction with cTEC (Witt et al., 2005) (Bousso et al., 2002). This interaction is necessary for cells to undergo a process known as positive selection, which is itself designed to test the functionality of the newly generated TCR against

the peptide:MHC complex on the cTEC (Werlen et al., 2003). Cells that can interact with a low-affinity can then be directed towards either a CD4 or CD8 single positive phenotype depending upon which MHC molecule class the developing DP thymocyte tends to respond to (detailed in section 1.1.6) (Takahama, 2006, Klein et al., 2009, Takada et al., 2017). Additionally in this selection process, the downstream TCR signalling molecule Zap-70 has been shown to be necessary along with sustained TCR signalling to generate a positive feedback loop that in turn supports differentiation into CD4 SP thymocytes under MHCII selecting ligands or CD8 SP under MHCI interaction during positive selection (Sinclair et al., 2015).

The process of positive selection aims to select cells that would be useful peripherally in being responsive to foreign antigens. As a result, failure of the DP thymocytes to interact will also result in death of the thymocytes by neglect through a programmed cell death mechanism (Palmer, 2003). On the other hand, cells which bind strongly via their TCR to ubiquitously expressed self-antigens in the cortex, are triggered to undergo a process known as negative selection which involves programmed cell death (Stritesky et al., 2013, McCaughtry et al., 2008, Goldman et al., 2005). This process of negative selection was particularly assessed in one study that was able to identify distinct populations of apoptotic cells based upon their expression of Caspase-3 and subsequently whether these cells were undergoing either death by neglect or death as a result of negative selection (Stritesky et al., 2013). Caspase-3 was used to define apoptotic cells due to its involvement in both the extrinsic death ligand and intrinsic mitochondrial associated apoptotic death pathways. Here Caspase-3 is cleaved within the cell by initiator caspases, themselves triggered through apoptosis signalling events. T-cells undergoing apoptosis specifically through negative selection or via death by neglect could be

discriminated in this study by the segregation of Caspase-3 positive cells between CD5 and CD69 expression – double positive ($CD5^{+}CD69^{+}$) cells represented those having been triggered through their TCR as both molecules become upregulated during this process; CD5 acting as a negative regulator of TCR signalling and CD69 acting as a maturation marker. Alternatively, cells that were Caspase-3 expressing but $CD5^{-}CD69^{-}$ were identified as undergoing death by neglect following no TCR signal. Due to this rigorous selection process, it is proposed that only three to five percent of developing thymocytes actually survive past this positive selection stage (Goldrath and Bevan, 1999).

1.2.5 Commitment To CD4 or CD8 T-cell Lineage

The process of commitment to either CD4 or CD8 T-cell lineage appears to depend upon binding of the DP thymocyte to MHCII or MHCI respectively. Various models have then been proposed as to how this interaction leads to the commitment to either the CD4 or CD8 lineage and all appear to involve ideas surrounding length of interaction time, strength of signalling and additional cytokine involvements. One classical model that has long been proposed is known as the 'strength of signal instructional model' and suggests CD4 and TCR co-engagement induces stronger signals from increased intracellular Lck kinase binding on the cytosolic tail of CD4 compared to that of CD8 which induces lower strength signals. This difference in signal strength therefore links to the designated phenotype adopted by the DP cell (Hernandez-Hoyos et al., 2000, Sohn et al., 2001) (Singer et al., 2008).

Alternative models have however been suggested with duration also being thought to be as important as signal strength (Yasutomo et al., 2000, Brugnera et al., 2000). Additionally the stochastic selection model suggests systematic coreceptor downregulation following TCR

involvement, with intermediate cells then requiring rescue through a second TCR signal and selection if the TCR and the downregulated co-receptors were correctly matched (Chan et al., 1993, Davis et al., 1993, Robey et al., 1994). Finally, the 'Kinetic signalling model' proposes that following TCR interaction CD8 becomes downregulated and if signals continue through the TCR then cells adopt a $CD4^+$ phenotype or if signals cease they re-express CD8 and become $CD8^+$ through supportive presence of IL-7 and other common gamma chain cytokines (Singer, 2002, Singer and Bosselut, 2004, Brugnera et al., 2000). However following the proposal of so many different models, the defining signalling pathway that determines cell fate will remain to be of considerable interest.

Yet despite the exact mechanism of cell signalling being debated, what is clear is the involvement of Tumour Necrosis Factor (TNF) signalling and activation of the NFκB signalling pathway in the acquisition of a single positive phenotype (Webb et al., 2016). This study investigated mice that failed to express both subunits of the complex inhibitor of κB (IKK 1/2), within the early thymic progenitor populations, which are required as part of the NFκB signalling cascade. From this it was shown that there was a lack of CD4 and CD8 maturation in the single positive phase which could only be rescued upon TNF blockade as this prevented TNF induced cell death under absence of IKK1/2. Therefore further suggesting that TNF activation of the NFκB pathway is necessary for thymocyte survival and SP progression with CD8 cells being particularly receptive to this process.

Despite continuous dispute as to which model fundamentally is correct in the guidance of DP cells into a SP phenotype, what remains clear is that for full lineage commitment there is involvement of several transcription factors. For CD4 single positive thymocytes there is a

role for ThPOK, TOX and GATA-3 and rather RUNX proteins are necessary for CD8 lineage development.

ThPOK was shown to be important for CD4 lineage commitment but not CD8 cells through the identification of a mutation in ThPOK which resulted in mice that failed to develop CD4 T-cells (He et al., 2005, Sun et al., 2005, Keefe et al., 1999). Additional experiments driving overexpression of ThPOK found that MHCI selected T-cells could be redirected towards a CD4 SP lineage (He et al., 2005). TOX was also identified as being upregulated following TCR signalling in DP thymocytes and therefore was another possible regulator in lineage commitment. This was investigated as TOX deficiency showed that DP thymocytes failed to differentiate into CD4 SP cells but CD8 T-cells remained unperturbed; rather it was seen that reversal of this deficiency through transgene insertion was able to promote differentiation into CD4 lineage (Aliahmad and Kaye, 2008). GATA-3 is a zinc finger protein and was suggested to be expressed in a preferential manner by CD4 SP cells (Hendriks et al., 1999). Clonal deletion of GATA-3 in the DP population supported this, as it led to reduced CD4 T-cell generation but again CD8 development was not affected (Pai et al., 2003). RUNX proteins, especially one and three, have been linked to a CD8 SP phenotype as they were illustrated to bind to CD4 silencer elements and therefore suppress CD4 expression; with experimental systems of RUNX deficiency leading to CD4 gene transcription (Grueter et al., 2005, Kohu et al., 2005, Taniuchi et al., 2002). As a result, the vital role for transcription factors in lineage determination of DP thymocytes is clearly apparent.

Following positive selection, CD4/CD8 SP cells can relocate to the medulla from the cortex. This process is thought to be driven by the expression of the chemokine receptor CCR7 as

developing thymocytes have been shown to upregulate expression following successful positive selection (Kim et al., 1998) (Campbell et al., 1999). The mTEC population expresses CCR7 ligands and therefore it acts to provide a gradient for recruitment of single positive thymocytes from the cortex to the medulla (Kwan and Killeen, 2004). In addition, mice that are deficient for CCR7 are found to undergo maturation post positive selection within the cortex as they fail to be able to migrate into the medullary areas (Ueno et al., 2004).

1.2.6 Medullary Regulation of Developing Thymocytes

Positively selected thymocytes have been able to progress in their development and enter into the medulla of the thymus solely due to their ability to bear a TCR that can recognise MHC/peptide complexes. However due to the process of TCR generation itself (detailed in 1.2.4) requiring the random rearrangement of TCR genes, there is ultimately the possibility that a TCR could be generated with potential self autoreactivity. Upon entry into the medulla, thymocytes therefore undergo tolerance induction, which when taking place in the thymus itself, is generally known as central tolerance and predominantly involves TCR screening (Klein et al., 2014).

1.2.6.1 Negative Selection Of Autoreactive Thymocytes

Screening occurs by medullary thymic epithelial cells and also other antigen presenting cell populations such as DC, which play a major role in tolerance and will therefore be discussed in more detail within section 1.3 (Oh and Shin, 2015). Migrating thymocytes can come into contact with self antigens expressed by both medullary APCs and mTEC and bind with differing affinities depending upon responsiveness of their TCR to particular self peptides. Presentation of self-antigens is possible due to the expression of transcriptional regulators;

Autoimmune Regulator (Aire) and Fez family zinc finger 2 (Fezf2), which both drive tissue restricted antigen expression on thymic epithelial cells (Takaba et al., 2015, Anderson et al., 2002). Both studies into these transcription factors showed that under their absence there were resultant autoimmune manifestations that remained distinct from one another but highly tissue specific.

For a decision to be made as to the fate of the cell, interacting thymocytes have been reported to undergo calcium flux that triggers rapid migratory arrest upon encounter with cognate antigen, holding cells stationary for a subsequent thymocyte fate decision to be determined through TCR signals and cell signalling pathway activation (Dzhagalov et al., 2013). The main determinant of developing thymocyte fate relates overwhelmingly to how strongly their TCR recognises self antigens presented within the medulla with weak interactions correlating to successful development (Morris and Allen, 2012). Dendritic cells and mTEC coordinate this process of self-antigen presentation but also play pivotal roles in Treg generation, which relates to more of an intermediate strength affinity binding of the TCR to the cognate self-antigens (Klein et al., 2011). Strong interactions with self-antigen on the other hand, leads to the initiation of a death pathway to remove the autoreactive cells from the repertoire, which requires activation of various downstream signalling molecules. Within the medulla, the high concentrations of DCs support more efficient negative selection upon interaction with autoreactive cells due to their particularly high expression of costimulatory molecules CD80 and CD86 which can interact with CD28 on thymocytes and support signalling into the thymocyte and fate decisions therefore acting additionally alongside the primary TCR MHC/peptide interaction (Walunas et al., 1996).

There have previously been two suggestions for the pathways responsible for negative selection of autoreactive T-cells; death receptors and Tumour Necrosis Factor Receptors (TNFRs) or Bcl-2 proteins (Palmer, 2003, Hernandez et al., 2010). Death receptors include Fas which is activated by Fas Ligand on stromal cells, however despite the likelihood that Fas could be important in supporting negative selection, experiments infact proved that it is not solely required and may act more in a supportive manner to improve negative selection efficiency rather than be the initial instigator (Newton et al., 1998) (Villunger et al., 2004). Additional work from this study went on to show no clear role for Fas associated death domain containing receptors such as TNFRs either in negative selection.

As a result, the role of Bcl-2 protein members in negative selection was considered and subsequently it was shown that high avidity binding of TCRs to self antigens leads to the engagement of the intrinsic mitochondrial pathway of apoptosis that is itself regulated by the Bcl-2 protein family (Strasser, 2005) (Dzhagalov et al., 2013). Deletion of the BH3-only member of Bcl-2 family Bim, (Bcl-2 interacting mediator of cell death), caused a subsequent inability of cells to undergo any form of negative selection (Bouillet et al., 2002) (Enders et al., 2003). As a result Bim plays a vital role in the regulation of negative selection through apoptosis induction. Additional work identified the requirement for Bak - a Bcl-2 antagonist and Bax - a Bcl-2 associated X protein, in the support of Bim and cell mediated death (Zong et al., 2001). Activation of these molecules through strong TCR/MHCI interaction, supports apoptosis through disruption of the mitochondrial outer membrane and cytochrome c release into the cytosol causing apoptosome formation and caspase activation which in turn leads to protein cleavage and cell destruction (Strasser et al., 2011) (Starr et al., 2003).

More recent work has added to these initial observations and suggested that as well as Bim playing an important role in prevention of autoimmunity by promoting negative selection following strong TCR signals, absence of Bim alone was insufficient to cause peripheral widespread autoimmunity. This suggested the presence of additional supporting factors that cooperatively regulate negative selection in the thymus. It was then shown that only under the absence of the BH3-only protein Puma in conjunction with Bim, was it sufficient to cause spontaneous peripheral autoimmunity further indicating that negative selection is controlled through cooperation between Puma and Bim BH3-only proteins (Gray et al., 2012).

For activation of these death inducing molecules, intracellular signals are involved and tend to specifically map to the mitogen activated protein kinase (MAP kinase) pathway which itself contains extracellular signal regulated kinases (ERK) along with Jun amino terminal kinase (JNK) (Bettini and Kersh, 2007). These pathways have been associated with the regulation of both positive and negative selection but these differing cell fates can be distinguished simply by the level of binding between the TCR and MHC peptide complex and the subsequent signal strength that ensues. The high affinity binding that results in negative selection, causes quick recruitment of ERK, combining with the activation of p38 and JNK to lead to cell death, whereas the positive selection outcome is supported by lower level binding causing reduced signal strength and prolonged activation of intracellular mediators - critical for the differentiation between positive and negative selection (Daniels et al., 2006).

Negatively selected cells can be cleared from the thymus due to a small proportion of thymus resident macrophages which are primed to clear the apoptotic matter (Dzhagalov et al., 2013). In addition, cells that have been screened against self and are tolerant, are able to mature

within the medulla although the period of residence is controversial (Egerton et al., 1990, McCaughtry et al., 2007). During this time they can undergo maturation where they are primed to be able to leave the thymus and contribute towards the naïve T-cell pool.

1.2.7 Maturation Of Developing Thymocytes And Egress

In order for thymocytes to be able to survive once they leave the thymus, there is a need for them to acquire the correct developmental phenotype prior to their egress. This relates to alterations in expression of maturation markers such as CD62 ligand (CD62L) which is a lymphocyte specific L-selectin linked to the ability of cells to egress from the thymus and enter into peripheral lymph nodes (Takahama, 2006). CD69 as an alternative marker, is used often in conjunction with CD62L as during maturation these two markers are alternatively regulated allowing clear population segregation - as CD62L expression increases with maturation whereas CD69 is downregulated; cells therefore progress from $CD69^{+}CD62L^{-}$ to a phenotype of $CD69^{-}CD62L^{+}$ as a mature SP thymocyte population (Reichert et al., 1986) (Sancho et al., 2005). Alternatively the maturation of naïve T-cells can be detected based on their expression of heat stable antigen (HSA) and Qa-2 with cells progressing again from $HSA^{hi}Qa\text{-}2^{low}$ semi mature to $HSA^{low}Qa\text{-}2^{hi}$ mature phenotype (McCaughtry et al., 2007) (Bendelac et al., 1992) (Ramsdell et al., 1991). Semi mature thymocytes are thought to be vulnerable to apoptosis whereas those which are fully mature lose that susceptibility, regulating the release of only mature cells into the periphery (Kishimoto and Sprent, 1997).

Despite this, a recent study has built on previous knowledge to redefine how mature T-cells can be separated and identified. In this study, SP populations were divided into three subpopulations based upon CD69 and MHCI expression progressing from semi mature - SM

($CD69^{+}MHCI^{-}$) to mature 1 - M1 ($CD69^{+}MHCI^{+}$) and finally mature 2 - M2 ($CD69^{-}MHCI^{+}$) (Xing et al., 2016). With increased maturation it was proven that there were also increases in proliferation ability, emigration competency and cytokine responsiveness which are all hallmarks of greater maturational capacity. Signalling through the NFκB pathway was shown to be absolutely necessary for late stage development involving both functional maturation and proliferation with it further protecting cells from TNFR mediated cell death (Webb et al., 2016). Additionally independent of NFκB, constitutively produced interferons within medullary areas and subsequent signalling through interferon alpha receptor (IFNαR) were shown to support maturation by priming T-cells with the capacity to respond to cytokines (Otero et al., 2013, Lienenklaus et al., 2009, Xing et al., 2016).

In addition to this, models can be used to actively track maturation of thymocytes and these are predominately based upon RAG1/2 expression, which is triggered to be expressed during TCR recombination (McCaughtry et al., 2007, Boursalian et al., 2004). This has come about through the generation of transgenic mice with the insertion of a bacterial artificial chromosome encoding for a green fluorescent reporter protein in the place of RAG2 which acts to map levels of RAG2 expression (RAG2p-GFP reporter mice) such that the stage of thymocyte development can be tracked (Yu et al., 1999). The level of fluorescence degrades with time and therefore newly generated SP thymocytes will have high RAG2p-GFP levels whereas those that are negative for GFP represent mature and possibly peripheral recirculating cells. With increasing evidence for the capacity of T-cells, including both conventional and T Regulatory, to recirculate to the thymus, this molecular timer has grown in importance as a tool to discriminate most mature naïve T-cells that are about to leave the

thymus and will be RAG2p-GFP positive, from those which are peripheral recirculants and have lost RAG2p-GFP expression (Cowan et al., 2016) (McCarthy et al., 2015).

Prior to egress, as previously suggested, it has been shown that thymocytes undergo programmed proliferation and cellular expansion (Xing et al., 2016). This proliferative step is cytokine regulated and more specifically occurs due to IL-7 production by epithelial cells, identified as being key to this process for the provision of survival signals through IL-7Rα expression on thymocytes. IL-7Rα is indeed upregulated following positive selection and this expression is an active process dependent upon TCR signalling and as a result this regulates proliferation of only selected cells that have received all of the correct developmental cues prior to their release into the periphery (Hare et al., 2000). This upregulation of IL-7Rα has however itself been shown to be dependent upon NFκB signalling which was necessary for initial expression of IL-7Rα but not for this receptor maintenance post maturation. This was indeed illustrated through IKK2 deletional models, a key complex in the NFκB signalling cascade, at different T cell maturational stages (Silva et al., 2014).

For thymocytes to leave the thymus there is also a requirement for them to express the G-protein coupled receptor sphingosine 1 phosphate receptor (S_1P_1), with expression being upregulated as the marker CD69 becomes downregulated through maturation (Shiow et al., 2006) (Alfonso et al., 2006). Thymocytes express S_1P_1 and require signalling in a cell intrinsic manner for egress along the corresponding chemotaxis gradient of the bioactive sphingolipid, and S_1P_1 ligand, S1P (Takeda et al., 2016). S1P formation is regulated by phosphorylation of kinases sphingosine1/2 (Sphk1/2) and a gradient is maintained between the thymus and blood with levels of ligand expression being low and high respectively to

support emigration (Matloubian et al., 2004, Allende et al., 2004) (Pappu et al., 2007). S1P has recently been suggested to be maintained at low levels in the thymus through ceramide synthase 2 (Cers2), which converts the S1P abundant precursor sphingosine to long chain ceramides in thymic stromal cells as well as hematopoietic populations (Rieck et al., 2017). Considering this, research has shown that there is a role for Cers2 in the thymic regulation of S1P through knockout models which indicated selective accumulation of the most mature thymocytes, further highlighting a role for Cers2 in limiting thymic levels of S1P and maintaining the gradients between thymus and blood (Rieck et al., 2017).

S1P degradation in the thymus has also been suggested to occur via the production of a S1P lyase with blockade of this enzyme leading to retention of thymocytes (Schwab et al., 2005). It was suggested that S1P lyase was mainly expressed by vascular endothelial cells, pericytes and reticular fibroblasts with a more recent emphasis on neural crest derived pericytes which ensheath thymic blood vessels being implicated in thymic egress (Maeda et al., 2014) (Zachariah and Cyster, 2010). Additionally there has been suggestion through deletion of S1P lyase in different thymic populations, that thymic dendritic cells were shown to play a more pivotal role in mediating egress over and above stromal or epithelial mediated expression (Zamora-Pineda et al., 2016). However despite conflicting results, the localisation near the site of exit of these S1P lyase expressing cells appears to allow for the maintenance of S1P degradation at points of exit which is necessary to generate the gradient for egress of mature thymocytes.

Additionally, under an absence of LTβR an accumulation of mature SP thymocytes was previously reported, similar to the phenotype reported under FTY720 treatment, an S_1P_1

agonist resulting in receptor internalization and inability of mature thymocytes to egress (Boehm et al., 2003, Cyster, 2005) (Yagi et al., 2000). However whether mechanisms of LTβR signalling and the S1P axis are linked or remained to be distinct is yet to be determined and how in turn LTβR may impact on the new role of Cers2 also is unknown.

Nevertheless, this mechanism of emigration differs in adult to embryo where embryonic thymocyte emigration is determined by expression of CCR7 and CCL19 mediated signalling; differing from the adult whereby there is thought to possibly be a switch to this S_1P axis (Ueno et al., 2002). Egress of thymocytes and the phenotype that they possess at this stage, allows them to enter into the periphery and further become recruited into lymph nodes where they can await further maturation and later priming by cognate antigen to initiate effective immune responses.

1.3 Cellular Regulators of Central Tolerance

1.3.1 Thymic Epithelial Cells

1.3.1.1 Development of Thymic Epithelial Cells

For the development of the thymus to support T-cell production, there is an overarching dependency on the development of the core thymic structure, which is composed predominately of thymic epithelial cells although mesenchymal cells, fibroblasts and endothelial cells also support this structure (Abramson and Anderson, 2017, Takahama et al., 2017).

It is widely accepted that the development of both the medullary and cortical areas occurs through the presence within the thymus of a common endodermal bipotent progenitor (Gordon et al., 2004, Rossi et al., 2006, Bleul et al., 2006). Recently this concept was confirmed in the adult thymus through the presence of bipotent epithelial cell progenitors with the capacity to give rise to both cortical and medullary areas whilst still remaining persistent throughout adulthood (Ucar et al., 2014, Ulyanchenko et al., 2016, Hamazaki, 2015). Further adult analysis showed that there was indeed the presence of a stem-cell like TEC progenitor with the potential to form colonies in in vitro culture systems and differentiate into mTEC and cTEC both in vivo and in vitro (Wong et al., 2014). Additionally this stem cell population appeared to differ in gene expression analysis from that identified in embryo and therefore highlights the likelihood of different mechanisms being necessary for tissue homeostasis that is required in adult, compared to whole generation of the thymus itself during embryogenesis (Ucar et al., 2016).

From this, embryonic work into the formation of the thymus investigated this potential bipotency at the level of the embryo. At the stage of E12, the ability of early TEC progenitors to give rise to both mTEC and cTEC was investigated with the transfer of E12 TEC into host thymus in in vitro cultures. Subsequently, analysis for corresponding progeny clearly confirmed bipotency potential - yet despite this the mechanisms that directly controlled this process still remained to be completely resolved (Rossi et al., 2006). Further analysis of early embryonic thymus, confirmed bipotency through the presence of key markers specifically related to the cTEC lineage such as the endocytic receptor CD205 and the proteasomal marker β5t that could be detected on stromal populations as early as E11, therefore already appearing to define cells with a cTEC lineage propensity (Baik et al., 2013). However upon isolation and transfer of these cells it was surprisingly shown that as well as cTEC progeny developing, as was somewhat expected, there was also mTEC progeny. This mTEC population was identified through expression of mTEC related markers such as MHCII, Aire and Osteoprotegerin (OPG) which are indicative of mTEC function. Yet moreover, these cells possessed a distinct ability to respond to stimulation of the TNF-Receptor superfamily member, receptor activator for NF-κB (RANK) stimulation; with RANK expression and responsiveness further being a hallmark of mTEC, thus confirming their mTEC phenotype (Baik et al., 2013). This process is summarised in Figure 1.4.

Additionally, this concept remains supported by the work of many others, which suggest the presence of a cTEC associated progenitor in the thymus that remained to be somewhat transient and allow for additional development into mTEC through a sequential developmental pattern (Ohigashi et al., 2015, Mayer et al., 2016, Meireles et al., 2017, Alves et al., 2014). This was further proposed to be possible also at the postnatal stage of

development, highlighting one study that investigated this through the use of $IL7^{YFP}CCRL1^{GFP}$ mice, with IL-7 expression being related to cTEC and CCRL1 being a late cTEC associated marker (Ribeiro et al., 2014). In this study, it was shown that the $CCRL1^{int}$ phenotype, through stimulatory culture conditions in FTOC and also in vivo in reaggregate thymic organ cultures (RTOC), indeed could give rise to a subpopulation of cells with mTEC potential further being $UEA^{+}CD80^{+}$, despite possessing previous cTEC associated traits.

The mTEC population itself is highly heterogeneous but remains predominately composed of two main populations; $MHCII^{lo}CD80^{lo}$ populations known as $mTEC^{lo}$ and $MHCII^{hi}CD80^{hi}$ $mTEC^{hi}$ populations. Within these populations there is a further breakdown with a proportion of $mTEC^{lo}$ expressing CCL21 and a proportion of $mTEC^{hi}$ expressing the transcription factor Aire (Hubert et al., 2008, Ueno et al., 2004). It further appears that development of these populations may also be diverse with development of the $mTEC^{hi}$ population from cells within the $mTEC^{lo}$ compartment through RANK exposure; shown in reaggregate thymic organ cultures (Rossi et al., 2007). However in turn it has also been revealed that $mTEC^{hi}$ populations can give rise to an $mTEC^{lo}$ phenotype that can express CCL21 through LTβR stimulation (Lkhagvasuren et al., 2013).

Due to such apparent developmental and population based diversity, it appears unsurprising for research to have identified that as well as mTEC potentially developing from a cTEC progenitor as previously described, there remains the opportunity for mTEC to develop from a cTEC-independent progenitor. Further from this, evidence has grown to suggest mTEC development independent of cTEC associated progenitors and thus it was suggested that there was the presence of mTEC committed progenitors in the embryo (Figure 1.4). These were

Figure 1.4:

Thymic Epithelial Cell Development In Thymus

TEC develop from a stem cell population expressing the transcription factor Foxn1. These can give rise to bipotent progenitors with the ability to produce both mTEC and cTEC via a cTEC associated progenitor population. mTEC can then go through a maturational series and produce both $mTEC^{lo}$ and $mTEC^{hi}$ populations driven by RelB transcription factor expression and RANK receptor expression dependency respectively. Mature cTEC can also arise. mTEC can also develop independently of a cTEC associated population with stem cells directly giving rise to mTEC through a serial developmental progression model.

A

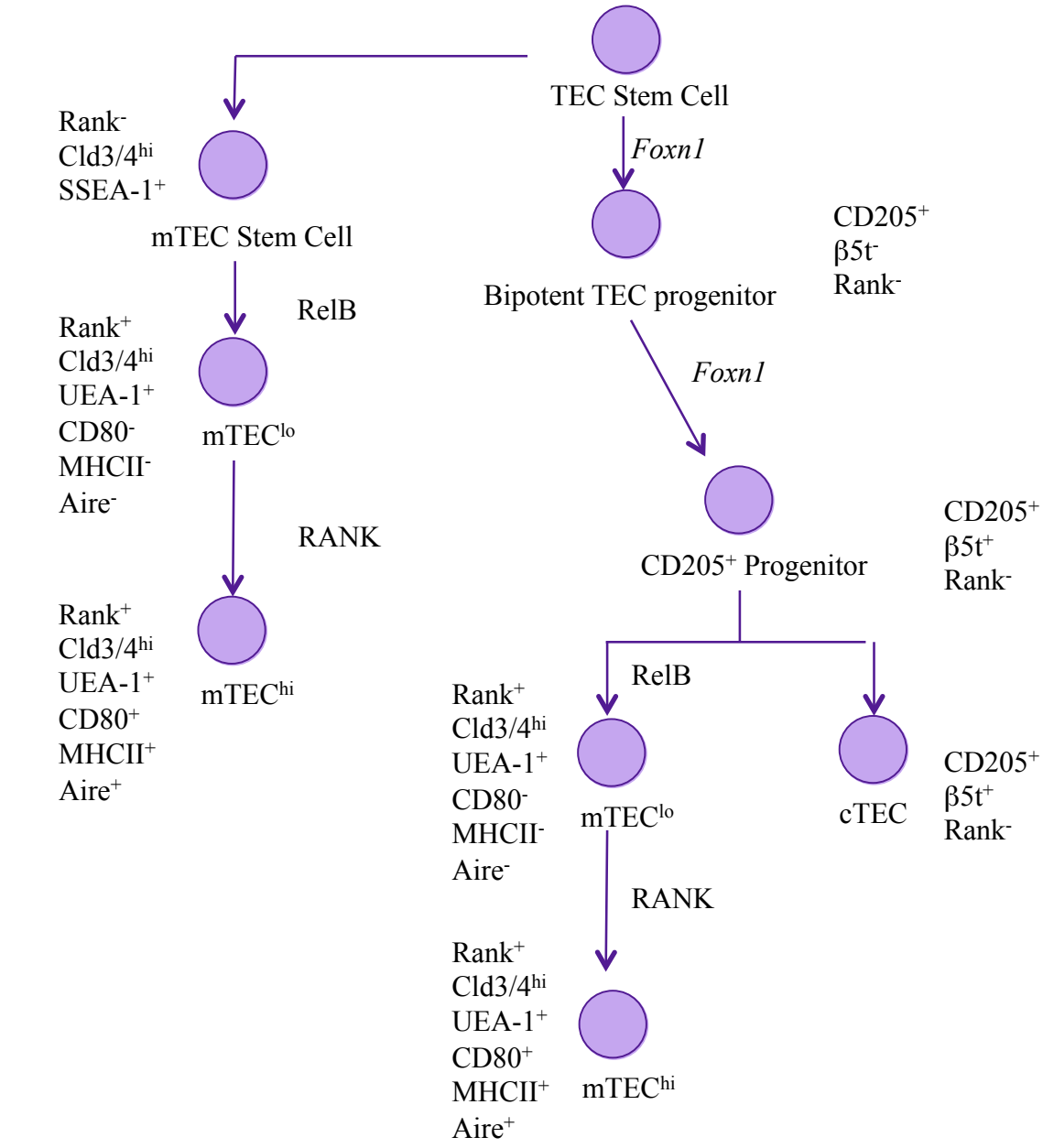
TEC Stem Cell
Foxn1
Bipotent TEC progenitor
CD205+
β5t-
Rank-
Foxn1
CD205+ Progenitor
CD205+
β5t+
Rank-
RelB
Rank+
Cld3/4hi
UEA-1+
CD80-
MHCII-
Aire-
mTEClo
cTEC
CD205+
β5t+
Rank-
RANK
Rank+
Cld3/4hi
UEA-1+
CD80+
MHCII+
Aire+
mTEChi
Rank-
Cld3/4hi
SSEA-1+
mTEC Stem Cell
RelB
Rank+
Cld3/4hi
UEA-1+
CD80-
MHCII-
Aire-
mTEClo
RANK
Rank+
Cld3/4hi
UEA-1+
CD80+
MHCII+
Aire+
mTEChi

indeed identified through the known expression of the tight junction components, Claudin3/4 (Cld3/4^{hi}) in Aire positive mTEC populations and subsequently expression of Cld3/4 was found in embryonic thymus. Isolation of this population at E13.5 and reaggregation in thymic organ cultures prior to kidney capsule transfer showed, through analysis at a later time point, that the Cld3/4 population was a direct mTEC progenitor with the subsequent presence of Aire^{+} mTEC (Hamazaki et al., 2007). Most recently this was expanded by (Sekai et al., 2014) showing that these Cld3/4 cells were able to produce and maintain the mTEC population long term and actually correct for any dysfunctions in central tolerance when transferred into mTEC deficient hosts. However further to this, it was shown that a subpopulation of Cld3/4 expressing cells actually co-expressed the embryonic stem cell marker SSEA-1 and following sorting and reaggregate generation, these also had the capacity to produce mature mTEC populations demonstrating a clonogenic nature which remains to be indicative of a stem cell phenotype. This was further seen to be traceable to the adult mouse with this Cld3/4^{hi}SSEA1^{+} population remaining to be present and mTEC committed.

Additionally later work showed that there was a dependency on NFκB signalling through RelB for progressional development of SSEA1^{+} mTEC stem cells to express the mTEC defining RANK receptor (Baik et al., 2016). Additional research showed that tumor necrosis factor receptor-associated factor 6 (TRAF6) dependent RANK signalling was required to acquire the Aire^{+} mTEC phenotype from mTEC progenitor associated populations (Akiyama et al., 2016). However, the mechanism directly regulating this expression of RANK and commitment to the mTEC lineage is still unclear – yet it is anticipated that there may be a role for LTβR signalling at this point as it has been postulated to play a pivotal role in RANK upregulation and mTEC development in embryonic analysis (Mouri et al., 2011).

Additionally, evidence has been acquired over the possible role of LTβR in mTEC development as it previously had been reported that loss of LTβR signalling on thymic stroma led to a phenotype of reduced mTEC populations, suggesting a role for LTβR in mTEC development within the thymus (Boehm et al., 2003). This remained relatively unexplored until a recent study which used $K14^{Cre}xLtbr^{fl/fl}$ mice to conditionally remove LTβR expression from TEC and infact recapitulated the phenotype seen in the germline knockout with reduced mTEC numbers, highlighting a cell intrinsic requirement for LTβR signalling to support mTEC development but through a mechanism that remained independent of proliferation or survival (Wu et al., 2017). Importantly, the number of Cld3/4^{hi}SSEA1^{+} mTEC progenitors were analysed in these mice and were also significantly reduced at the neonatal stage suggesting LTβR signalling may be necessary for the development of mTEC and possibly in the maintenance of these mTEC progenitors; however how this finding in turn alters the developmental pathway of mTEC and at what specific stage LTβR may be acting is yet to be determined.

As a direct result, it is clearly apparent that developmentally there are a lot of questions, which remain to be answered with regards to TEC development, and potentially this could be crucial research to influence thymus regeneration post injury and following thymic involution with age.

1.3.1.2 cTEC Function

cTEC support the process of positive selection which is necessary to allow DP thymocytes to progress to either a CD4 or a CD8 SP phenotype. cTEC are functionally able to drive positive selection as they present endogenous antigens on their cell surface in the context of an MHC

molecule for developing thymocytes to interact with (Ohigashi et al., 2016). cTEC present antigen within MHCI and MHCII complexes with recent research unveiling a novel mechanism by which cTEC are able to stabilise MHCII expression on their cell surface, to support $CD4^+$ positive selection. Previously, the molecule CD83 has been associated with activation of dendritic cells and was recently shown to stabilise MHCII expression on DC by preventing ubiquitination and MHCII ligation which results in MHCII downregulation (Tze et al., 2011). Considering this along with knowledge that CD83 deficient mice were shown to have defective CD4 selection, the impact of this mechanism on cTEC was examined (Fujimoto et al., 2002). Further investigations identified that CD83 was infact strongly expressed by cTEC and indeed necessary to stabilise MHCII expression through antagonism of March8, an E3 ligase, therefore preventing the loss of MHCII from cTEC surface and the subsequent reduction in positive selection (von Rohrscheidt et al., 2016, Liu et al., 2016). As a result, it appears that cTEC additionally contain molecular mechanisms that allow them to be primed to sustain high levels of positive selection as well as also having unique antigen processing capacities.

cTEC contain a variety of cell specific, unique features that allow for a different range of self-antigens to be expressed within the cortex compared to that seen within the medulla, preventing all positively selected cells being negatively selected under presentation of the same peptide repertoire (Kincaid et al., 2016). One of the ways cTEC are specialised is their ability to perform autophagy – a process which is usually restricted to conditions of starvation (Levine and Klionsky, 2004). Autophagy occurs as cTEC form autophagosomes that contain intracellular proteins. These can fuse to lysosomes for proteolysis producing peptides that can be presented by MHCII molecules for CD4 SP T-cell selection (Nedjic et al., 2008). As a

result, in this study deficiency in *Atg5*, necessary for the formation of autophagosomes, led to altered positive selection of MHCII restricted TCR transgenic CD4 thymocytes.

Furthermore, unlike other antigen presenting cells that express the lysosomal endopeptidase Cathepsin-S, cTEC express Cathepsin–L and thymus specific serine proteases (TSSP) which both function to support CD4 T-cell selection through production of MHCII restricted self-peptides (Nakagawa et al., 1998, Honey et al., 2002, Klein et al., 2009). Considering this, alterations in the expression of TSSP, itself encoded by *Prss16,* especially under situations of TSSP deletion, were shown in transgenic OT-II models to significantly impair positive selection of $CD4^+$ thymocytes (Gommeaux et al., 2009, Viret et al., 2011).

In addition to the unique features of cTEC for $CD4^+$ selection, there are also features to support $CD8^+$ positive selection in the cortex. Mainly this relates to the presence of *Psmb11,* which is required to encode for the proteasomal subunit β5t that forms part of the thymoproteasome found in cTEC (Murata et al., 2007). The expression of this subunit supports presentation of a unique set of MHCI restricted peptides that are alternatively cleaved to reveal unique motifs associated with lower affinity binding of the TCR, in turn providing ideal conditions to select fully competent $CD8^+$ thymocytes in the cortex (Sasaki et al., 2015, Xing et al., 2013). As a result, investigations using mice deficient in *Psmb11* were shown to have a limited and defective $CD8^+$ repertoire (Nitta et al., 2010, Takada et al., 2015). Positive selection in the cortex to a diverse range of antigens is fundamental for the stability of thymocyte development as it selects for a wide array of thymocytes that can then progress into the medulla for tolerance induction.

In addition, cTEC contain a subpopulation of thymic nurse cells, which remain somewhat functionally distinct whilst still maintaining a role in the support of positive selection. Thymic nurse cells are indeed large epithelial cells that form multicellular complexes and are thought to hold developing thymocytes (Takahama et al., 2017). Initial research into these cells suggested that their main role was to infact support proliferation and differentiation of developing thymocytes and possibly impact upon positive selection in the cortex (Li et al., 2005, Shortman et al., 1986, Wick et al., 1991). However subsequent research has proposed that nurse cells encompass $CD4^{+}CD8^{+}$ thymocytes and encourage them to undergo secondary rearrangements of their TCR-Vα genes, in turn ultimately providing another chance for successful positive selection without being directly involved in positive selection (Nakagawa et al., 2012).

1.3.1.3 mTEC Function

The medulla is predominately associated with the role of negative selection of autoreactive thymocytes and central tolerance induction. In order for this to be possible, mTEC are required to express self-antigens on their surface that peripherally could activate thymocytes and induce autoimmunity. mTEC are able to support negative selection due to a proportion of $mTEC^{hi}$ cells expressing the transcription factor Autoimmune Regulator (Aire) (Anderson et al., 2002). This expression is driven by RANK signalling in $mTEC^{lo}$ populations, unlike initial studies that proposed LTβR mediated regulation of Aire expression, further analysis showed that expression of Aire per cell under the absence of LTβR remained unchanged and there was no role for LTβR in Aire expression in mTEC (Rossi et al., 2007, Venanzi et al., 2007, Martins et al., 2008). Aire expression drives the presentation of tissue-restricted antigens (TRAs) onto the mTEC cell surface via MHCI and MHCII to screen the TCR of

developing thymocytes against self for selection (Anderson et al., 2002). Conditions where there are mutations in the Aire gene are sufficient to result in autoimmune related diseases and can be seen in man through an autosomal recessive disease known as autoimmune polyendocrine syndrome type 1 (APS-1) and further less severe mutations such as those in the plant homeodomain zinc finger of Aire have also been associated with suppressed expression of Aire related genes and autoimmunity (Oftedal et al., 2015, Husebye et al., 2009).

The molecular mechanisms that appear to underlie the ability of Aire to drive TRA expression have been more recently explored with growing interest into this regulation and many ideas proposed as a consequence (Bansal et al., 2017, Mathis and Benoist, 2009). Some studies suggested that Aire functions through its recruitment to target genes where it can then induce localised histone modifications via either histone acetylation or methylation to cause relaxation of chromatin and allow for subsequent TRA transcription (Org et al., 2009). It has further been discovered that in mature Aire expressing mTEC, the protein deacetylase Sirtuin-1 or Sirt1 was highly expressed and remained closely associated with Aire causing its deacetylation which in turn is necessary for Aire's transcriptional activity. Furthermore, removal of Sirt1 created a gene expression profile mirroring that under Aire absence (Chuprin et al., 2015).

In addition to Aire expression, a proportion of mTEC have further been proposed to express another transcription factor FEZ family zinc finger 2 (Fezf2), to drive the presentation of an additional array of Aire independent TRAs (Takaba et al., 2015). This was the first study to indicate the possibility of an alternative TRA regulator and showed that under an absence of Fezf2, there was a subsequent autoimmune phenotype with inflammatory infiltrates and

autoantibodies detected in and against multiple organs. Gene analysis of the expression of different TRA associated genes under the presence or absence of Fezf2 indicated no reduction in Aire regulated TRAs; similarly Fezf2 related genes were not reduced in Aire deficient mice further segregating the regulation of these two independent TRA gene sets. Specifically Fezf2 removal from thymic epithelial cells using a Foxn1Cre^{+}x*Fezf2*$^{fl/-}$ system, resulted in disrupted mTEC and peripheral autoimmunity whilst maintaining normal Aire expression. This phenotype was further shown at a regulatory level to only occur under the absence of LTβR and not RANK; again providing more evidence for the differential regulation of the transcription factors Fezf2 and Aire which both act independently to drive distinct TRA expression in the thymus for tolerance.

1.3.2 Dendritic Cells

As well as the documented function of mTEC in central tolerance, the requirement for DC in supporting this process is very clearly apparent. Mouse models lacking thymic DC, such as the CD11c-Cre/R-DTR mice whereby dendritic cells express the diphtheria toxin and treatment with diphtheria toxin results in the ablation of the DC population, have been shown to have widespread peripheral autoimmunity due to the escape of autoreactive T-cells from central tolerance induction (Ohnmacht et al., 2009, Birnberg et al., 2008, Ganguly et al., 2013).

DC populations can be found in the thymus from the late stages of embryogenesis, predominately located in the thymic medulla where their overarching function is to increase the thymic pool of self-antigens in both repertoire and frequency thus supporting central tolerance induction (Klein et al., 2001, Dakic et al., 2004). There is significant heterogeneity within the thymic DC pool with the presence of conventional and plasmacytoid subsets (Li et

al., 2009, Donskoy and Goldschneider, 2003). The conventional dendritic cells (cDC) can be identified based upon expression of CD11c and when subsequently split upon Signal regulatory protein α (Sirpα) expression, the conventional population can be segregated into a Sirpα positive population known as cDC2 and a negative population known as cDC1 (Wu and Shortman, 2005, Proietto et al., 2008a, Lahoud et al., 2006). Furthermore, this cDC population can be alternatively segregated using CD8α and CD11b expression with cDC1 being $CD8\alpha^{+}CD11b^{-}$ and cDC2 being $CD8\alpha^{-}CD11b^{+}$. This phenotyping is consistent with the identification method that we are using (CD11c and Sirpα), causing these markers to not be included in staining for DC populations. In addition there is a third DC population that is $CD11c^{int}$ and expresses the plasmacytoid marker PDCA-1, known as plasmacytoid DC (pDC) (Hadeiba et al., 2012).

Dendritic cell development takes place in the bone marrow, with DC being of myeloid origin with Macrophage and Dendritic cell Precursors (MDP) giving rise to Common Dendritic cell Progenitors (CDP) (Figure 1.5). CDP can directly generate pDC through a stepwise developmental programme which can be traced through a pre-pDC stage that is $CD11c^{+}SiglecH^{-}$ to a $SiglecH^{+}CCR9^{lo}$ intermediate before giving rise to $CCR9^{+}$ differentiated pDC (Dursun et al., 2016). Additionally, CDP also give rise to pre-cDC with all stages requiring exposure to fms-like tyrosine kinase 3 ligand (Flt3L) (Liu and Nussenzweig, 2010). Pre-cDC are able to migrate out of the bone marrow and enter the periphery where they can then give rise to cDC1 and cDC2 (Liu et al., 2009) (Figure 1.5). Further it has been suggested that there may be priming that occurs in the bone marrow skewing the cDC precursors towards either the cDC1 or cDC2 lineage prior to their release (Schlitzer et al., 2015). Additionally it appears possible that lineage skewing may relate to the expression of the

transcription factor Zeb2 which was shown to be required for the development of the cDC2 population as well as pDC with $CD11c^{Cre}xZeb2^{fl/fl}$ mice having significant skewing towards cDC1 to the detriment of cDC2 (Scott et al., 2016).

1.3.2.1 Intrathymic cDC1

The exact origin of the cDC1 that develop within the thymus has been an issue that has long been debated in the literature. Early reports were suggestive of thymic DC development from a common T/DC associated progenitor with evidence for this stemming from the presence of D_HJ_H immunoglobulin rearrangements, common to both intrathymic DC and developing thymocytes with further intrathymic transfers of $CD4^{low}$ precursors developing into both thymocytes and intrathymic cDC populations (Corcoran et al., 2003, Ardavin et al., 1993, Wu et al., 1996).

However a more recent proposal suggests that pre-cDC migrate into the thymus from the bone marrow and contribute towards the DN1c subpopulation of early thymic settling progenitors which is associated with cDC1 development (Luche et al., 2011). There was further confirmation in this study of thymocyte dependent cDC1 development, as depletion of the cDC1 population through Interferon Regulatory Factor 8 $(Irf8)^{-/-}$ models saw that the cDC1 population was not reconstituted by DN1a/b thymocyte associated progenitors but rather an independent population. Supporting this study was additional work showing that through the mapping of the lymphocyte associated IL-7 receptor in a reporter model, IL-7R was only ever associated with thymocytes and that intrathymic cDC1 populations remained again to be a distinct subset that had never expressed IL-7R (Schlenner et al., 2010).

Figure 1.5:

Dendritic Cell Development

Dendritic Cell development begins in the bone marrow with Macrophage and Dendritic cell Precursors (MDP) giving rise to monocytes which develop into macrophages in the tissues. But MDP can also give rise to Common Dendritic cell Progenitors (CDP) through Flt3L exposure. CDP then are able to reconstitute the dendritic cell lineage with production of pre-cDC, which egress from the bone marrow into tissue to develop into conventional dendritic cell populations of cDC1 and cDC2. CDP can also produce pre-pDC, which develop into pDC the bone marrow providing a pre-determined phenotype prior to their release into the periphery. They can then similarly migrate and reside in secondary lymphoid organs awaiting activation.

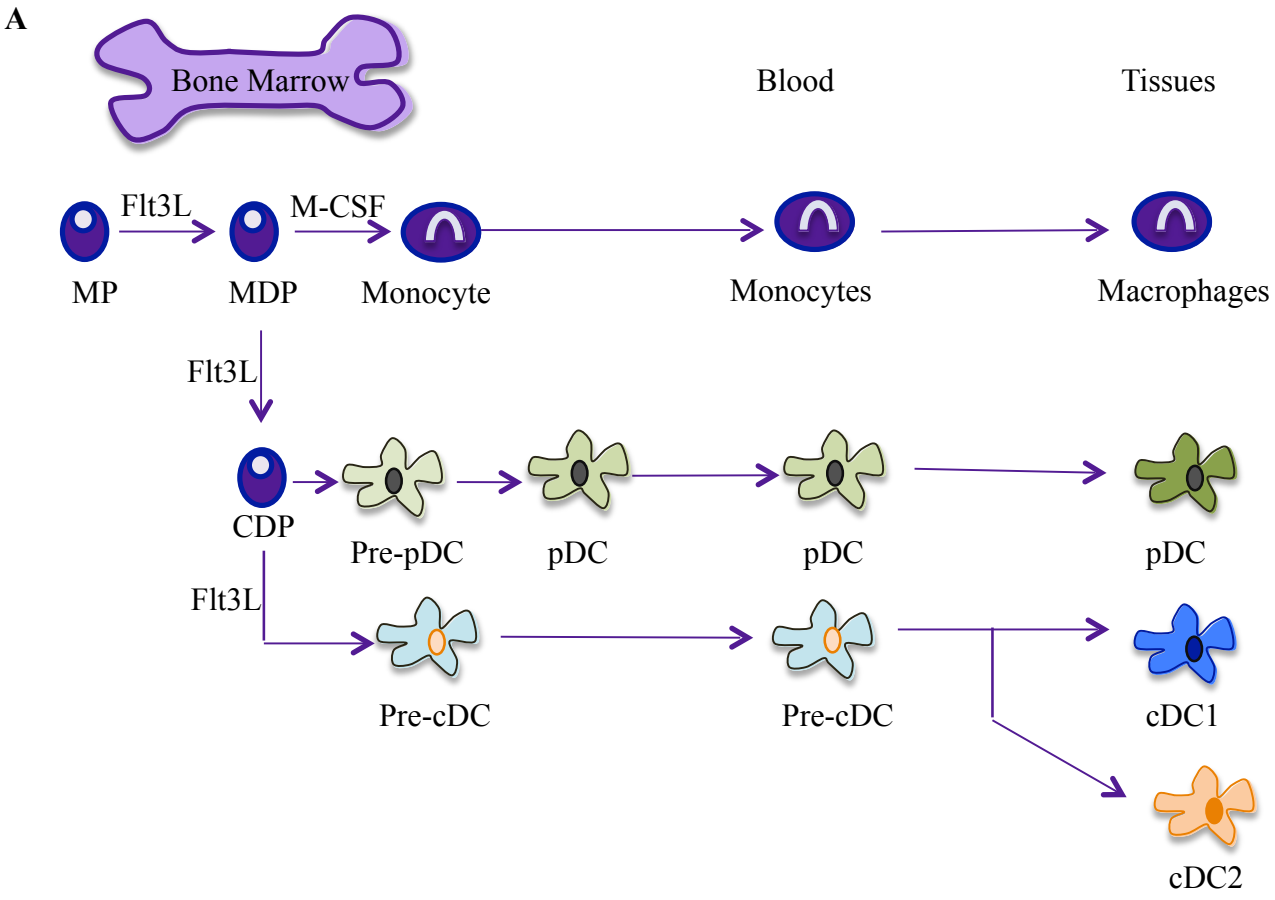
A
Bone Marrow
Blood
Tissues
Flt3L
M-CSF
MP
MDP
Monocyte
Monocytes
Macrophages
Flt3L
CDP
Pre-pDC
pDC
pDC
pDC
Flt3L
Pre-cDC
Pre-cDC
cDC1
cDC2

The potential for crossover between lineages however was later shown with a subpopulation of DN1a/b being identified that were able to express CX3CR1. Further, under the conditions of an empty dendritic cell niche within the thymus, it was seen that this $CX3CR1^{+}$ population has the potential to give rise to cDC1 (Lyszkiewicz et al., 2015). However despite this, the use of barcoding in this study later highlighted that when looking at thymic DC, splenic DC and T-cells there was indeed a closer association of thymic and splenic DC than that between thymic DC and T-cells suggesting again a myeloid developmental origin for cDC1 that remained to be distinct from that of the lymphoid lineage under normal developmental conditions. As a result, research has been varied concerning the origin of thymic cDC1 however it appears to be clear from more recent findings that under normal developmental conditions, cDC1 develop from a pre-cDC progenitor that is distinct from the lymphoid lineage (Luche et al., 2011).

Intrathymic cDC1 are typically localised to the thymic medulla which is mainly due to their expression of the C-subfamily of chemokine receptors XCR1 and the production of its ligand XCL1 in an Aire-dependent manner by mTEC (Lei et al., 2011). Their localisation is however important in their function as they have been suggested to assist central tolerance predominately by cross-presenting antigen from Aire expressing mTEC through the uptake of self-antigens via apoptotic material release or trogocytosis (Viret et al., 1999, Kyewski and Feuerer, 2014).

1.3.2.2 Migratory Thymic cDC2 and pDC

As pre-cDC enter the periphery such as the spleen from the bone marrow, they can also give rise to cDC2 and extrathymic cDC1. Peripherally, cDC2 along with pDC, reside in the spleen

and circulate in the periphery accessing lymph nodes through the blood via high endothelial venules where they can integrate within the dendritic cell network to subsequently mature and await antigen activation in an immune response (Geissmann et al., 2010).

Further common to both cDC2 and pDC is their ability to migrate and reside within the thymus. Following peripheral maturation, these populations of DC can home to the thymus at a general level through cell adhesion molecule expression (Bonasio et al., 2006). In this study, interaction between P-selectin and P-selectin glycoprotein ligand 1 (PSGL-1) was shown to be necessary for DC rolling on the endothelial surface. Additionally there was involvement of α4 integrin which constitutes the molecule very late antigen 4 (VLA-4) on DC and binds to vascular cell adhesion molecule -1 (VCAM-1) on endothelium, to support extravasation into the thymus with blockade causing a subsequent reduction in homing ability of these DC populations.

cDC2 are specifically thought to be recruited to the thymus through their expression of CCR2 with the corresponding ligand Monocyte Chemotactic Protein-2 (MCP-2) being mainly expressed on cortical keratin-8 positive stromal cells (Baba et al., 2009). This study went on to show that cDC2 tend to be localised around blood vessels through MCP-2 expression in perivascular regions. pDC on the other hand migrate towards the thymus via CCR9 expression, attracted to cTEC producing CCL25 (Hadeiba et al., 2012). This study used multiple different knockout models such as $CCR9^{-/-}$ which highlighted the requirement for pDC to express CCR9 to gain entry into the thymus, as absence of CCR9 led to abrogation of pDC thymic entry. Additionally, whether pDC may possibly be recruited to the thymus through CCR7 ligands is still a contentious issue as it was shown that despite low receptor

expression by pDC, they still appeared receptive to the ligands when present in transwell migration assays in lymph node studies (Seth et al., 2011).

Furthermore, this migratory potential of cDC2 and pDC was shown in a study by Hadeiba et al., 2012, where it was illustrated through intravenous flurosphere injections, that cDC2 and pDC could both capture flurospheres and migrate to the thymus transporting the flurospheres with them for intrathymic presentation. In addition painting of flurospheres on the skin also led to DC within the thymus that were flurosphere positive –highlighting the widespread ability of DC to capture, process antigen and migrate to thymus (Bonasio et al., 2006).

1.3.2.3 Dendritic Cells and Negative Selection

cDC2 and pDC populations have been shown to be able to support the process of negative selection following migration into the thymus carrying peripheral self-antigens. At a phenotypic level, the capacity of migratory DC populations to potentially support negative selection became apparent when thymic DC were compared with splenic counterparts and it was shown that cDC2 undergo extensive proliferation upon entry into the thymus with upregulation of MHCII, CD11c and CD86 expression. Similarly pDC were shown to enlarge and upregulate MHCII when entering the thymus along with their expression of CD86 whilst still maintaining a plasmacytoid morphology, making both populations primed to interact with developing thymocytes and support tolerance induction (Li et al., 2009). Their ability to physically induce negative selection was suggested using Ovalbumin (OVA) models whereby OVA-pulsed DC were transferred into transgenic OT-II $Rag^{-/-}$ expressing mice and consequentially there was a resultant peripheral reduction in OT-II T-cells compared to

controls, due to the interaction of developing cognate thymocytes with OVA expressing DC and the induction of negative selection (Bonasio et al., 2006).

In addition cDC2 were further shown to capture and present blood-borne antigen for negative selection within the thymus as they lay situated around blood vessels (Atibalentja et al., 2009, Atibalentja et al., 2011). This was shown through injection of serum IgG and Ovalbumin (OVA) that was later seen captured by cDC2 within the thymus (Baba et al., 2009). Furthermore an interesting study suggested that there may be temporal variations in the ability of the different DC populations to support central tolerance through the monitoring of negative selection during ontogeny. This study illustrated in mice that there was inefficiency in negative selection at newborn stages of ontogeny but that this capacity increased by 4 weeks and appeared to directly correlate with greater levels of cDC2 migrating into the thymus, with increased antigen processing and presentation ability compared to cDC1 or pDC at 4 weeks of age (Kroger et al., 2016). Therefore this suggests that there is a vast requirement for cDC2 at early stages of development to support central tolerance within the thymus.

Additionally, supporting migratory DC, cDC1 have been long associated with the acquisition of antigen directly from mTEC and using this process to in turn cooperatively support tolerance. This was shown to be important particularly regarding CD4 T-cell deletion in a study where the RIP-mOVA model was used to address deletion of OT-II CD4 SP T-cells (Gallegos and Bevan, 2004). It was seen that when OT-II bone marrow (BM) was transferred into a RIP-mOVA model there was efficient deletion of OT-II T-cells. However when OT-II $MHCII^{-/-}$ BM was transferred into RIP-mOVA mice there was reduced deletion. Therefore there was a requirement for hematopoietic expression of MHCII for cross-presentation of

OVA from mTEC, later shown specifically to map to DC for the effective deletion. Additionally in a recent study, combined depletion of mTEC along with cDC1 led to the induction of organ specific autoimmunity that was not seen when either mTEC or cDC1 were singularly reduced– again highlighting the cooperation between these two populations in negative selection (Herbin et al., 2016). Similarly in *aly/aly* mice that have a point mutation in the NFκB inducing kinase (NIK) gene, mTEC and cDC1 numbers were disrupted and consequentially autoimmunity was seen in these mice as it was again suggested that there is a requirement for cross-talk between cDC1 and mTEC for correct negative selection which in this study was shown to be dependent upon normal NIK presence (Mouri et al., 2014).

Furthermore, it was recently shown that thymic DC can actively acquire EpCAM-1 from TEC which increases DC ability to bind to TEC and as a result support increased peptide MHC complex transfer between TEC and DC (Kroger et al., 2017). cDC1 appeared to be by far the most efficient at this process, however there was some small contribution also from cDC2. This transfer was cell-cell contact dependent and restricted completely to thymic cDC – reinforcing the ability of thymic DC to support self-antigen presentation within the thymus to ensure central tolerance.

1.3.2.4 Dendritic Cells and T Regulatory Cell Induction

As well as DC being strongly associated with a role for negative selection, they are also suggested to support central tolerance through induction of T Regulatory cells within the thymus (Proietto et al., 2008b). However this idea was originally controversial as it was shown that ablation of DCs led to comparable Treg numbers as seen in WT (Ohnmacht et al., 2009) (Darrasse-Jeze et al., 2009). However as general transgenic models indicated that

cognate antigen presented by DC could promote Treg development, the role of DC in Treg induction gained support. Further work has suggested that different DC populations may be more effective at this process than others, whilst some arguments remain as to whether DC are actually more important than mTEC at Treg induction or not, or alternatively if there is a synergy between both DC and mTEC in this process (Herbin et al., 2016).

Importantly, the capacity of APCs to support thymic Treg induction was confirmed through analysis of Treg TCR clones utilising various transfer models (Perry et al., 2014). Transfer of $MHCII^{-/-}$ BM resulted in a marked reduction in enrichment of Treg and specifically saw reduced Aire dependent TRA expression as a consequence, further supporting a role for Aire specific antigen cross-presentation by thymic APCs in Treg generation. Importantly using a CIITA knockdown model, which reduces the MHCII expression on mTEC, only a modest alteration was seen in the frequency of Treg which were reduced to far less of an extent than when MHCII deficient BM – suggestive that BM APCs supported selection of more frequent Treg TCRs. Further work showed that DC were responsible and additionally using $CD8\alpha^{+}$ $Batf3^{-/-}$ hosts that indeed suffer cDC1 loss, the same phenotype was recapitulated with regards to Treg population selection. As a result this study highlights further that the cross-presentation of antigen from mTEC via cDC1 is not only pivotal for negative selection but also the induction of nTreg.

Additionally cDC2 have been implicated in Treg studies through in vitro co-culture assays using cDC2 and Treg precursor cells that were $CD4^{+}CD25^{-}CD8^{-}$ in phenotype. This showed that there was clear induction of precursors into a Treg phenotype and that furthermore this

was far greater by thymus specific cDC2 than it was when completed with cDC1 (Proietto et al., 2008b).

As a result, combining all of this previous research, it is becoming more apparent that whilst still considering the necessary requirement for mTEC in tolerance, there is an overwhelming necessity for the presence of DC populations within the thymus for full induction of central tolerance and autoimmune prevention. This lies not only with the process of negative selection of autoreactive T-cells, for which all thymic DC populations appear to be effectively skilled, but also through their individual abilities to drive the production of Treg within the thymus which peripherally remain vital to maintain tolerance.

1.4 General Aims

The thymus is the site of central tolerance, acting to prevent the escape of autoreactive thymocytes into the periphery where they have the ability to initiate an autoimmune response, causing damage to the host. As a result, the factors regulating the maintenance of the cellular mediators of this process are important to determine. Furthermore, the cooperation between dendritic cells and mTEC in this process, lends itself to question whether these populations are somewhat dependent upon one another for successful negative selection. Furthermore, despite information concerning how pDC and cDC2 are recruited to the thymus, how intrathymic cDC1 progenitors are recruited to support persistence of the cDC1 population in the thymus has been little described.

As a result chapter one and two aim to address:

1) What the involvement of the factors regulating the medulla are in the maintenance of thymic DC? There will also be consideration of the subsequent impact of any alterations in tolerance regulators on the peripheral development of autoimmunity.

2) How are the progenitors to the intrathymic cDC1 population regulated by the thymus?

Finally, given that dendritic cells in the thymus have had their function well defined, the third chapter will consider the alternative accessory cell - thymic eosinophils, by addressing:

3) What is the requirement for thymic eosinophils? Are they implicated in thymus development or potentially recovery post-damage?

CHAPTER TWO:

MATERIALS AND METHODS

2.1 Mice

All mice used for experimental work were bred within the Biomedical Services Unit (Birmingham, UK). All breeding was conducted under specified regulations as stated by the Home Office. For experimental purposes, all mice were sacrificed and culled under Schedule 1 procedure, with adult mice being between the ages of 8-12 weeks and of mixed gender unless otherwise stated (Table 2.1). For analysis of transgenic mouse strains, depending upon the background, wild-type (WT) C57/BL6 or Balb/c controls were taken alongside for unmanipulated comparison. For thymic analysis at the embryonic level, timed matings were arranged and the presence of a Vaginal Plug (VP) in the female was used to identify the start of the gestation period (D0) which usually lasts between 18 and 21 days. Pregnant females were harvested when embryos were at Embryonic Day 15-18 (E15-E18) for thymic analysis.

2.2 Media For Cell Preparations and Cell Cultures

For cells to be analysed by either disaggregation or tissue enzymatic digestion, tissues were prepared for both methods in RF10 medium – detailed in Table 2.2. All enzymes used in this process have been listed (Table 2.3) For analysis of samples following the digestion process however, RF10 was no longer used and MACs Buffer (Table 2.4) was used instead due to the presence of EDTA in the medium in turn acting to prevent the clumping of the more sticky digested material. For culturing of cells Dulbecco's Modified Eagle's Medium (DMEM) (Table 2.5) was used. All media were stored in the fridge at 4°C until use and all reagents were obtained from Sigma Aldrich (Poole, UK). For culturing of embryonic tissue in Fetal Thymic Organ Culture (FTOC) (section 2.3.4), DMEM was again used but sometimes in order to remove all haematopoietic cells and maintain the core thymic epithelial structure as an empty niche - 2-deoxyguanosine (dGuo, Sigma) was added at a final concentration of

1.35mM from the stock (9mM) and stored in aliquots at -20°C. This method was necessary for FTOC preparation prior to Kidney Capsule Transplant (KCT) to explore the colonisation of populations of interest into this 'empty' thymus (section 2.3.4).

Table 2.1 Wildtype and Genetically Altered Mouse Strains Used

Strain	Phenotype	Source
C57Bl/6	Wildtype	BMSU
Balb/c	Wildtype	BMSU or externally
BoyJ	Wildtype	BMSU
CD45.1xCD45.2	Wildtype	BMSU
Ltbr$^{-/-}$	Mice suffer from alterations in secondary lymphoid organs with; disrupted splenic architecture, an absence of Peyers Patches and all lymph nodes (Futterer et al., 1998).	Klaus Pfeffer University of Düsseldorf
Ltbr$^{fl/fl}$	Mice were generated through cre/loxP technology with targeting of the *Ltbr* allele with loxP flanking (Wang et al., 2010b).	Alexei V. Tumanov University of Chicago
Foxn1^{Cre}	Mice are heterozygous for Cre with insertion next to the Foxn1 gene. Mice were used for control purposes so did not have any detrimental phenotype (Gordon et al., 2007).	The Jackson Laboratory
Foxn1^{Cre}*x Ltbr*$^{fl/fl}$	Crossing of *Foxn1*^{Cre} mice with homozygous *Ltbr*$^{fl/fl}$ mice; mice were generated whereby LTβR was absent from Foxn1 expressing cells. Mice had no aberrant autoimmune phenotype. Lymph nodes were present.	Generated in house
PDGFRβ^{Cre}	Mice are heterozygous for Cre with insertion next to the PDGFRβ gene. Mice were used for controls so did not have a detrimental phenotype (Foo et al., 2006).	Cancer Research Technologies, London
PDGFRβ^{Cre}*xLtbr* $^{fl\fl}$	Mice were generated by crossing heterozygous *PDGFRβ*^{Cre} mice with homozygous *Ltbr*$^{fl/fl}$ mice. Mice had a normal phenotype.	Generated in house
Tie2^{Cre}	Mice are heterozygous for Cre which is driven by expression of the endothelial specific promoter Tie 2. Mice were used for control purposes so did not have any detrimental phenotype (Kisanuki et al., 2001).	The Jackson Laboratory
Tie2^{Cre} *x Ltbr*$^{fl/fl}$	Generation of mice by crossing *Tie2*^{Cre} with homozygous *Ltbr*$^{fl/fl}$ mice. Mice had a deletion of LTβR from Tie2 expressing endothelial cells. No detrimental phenotype was detected.	Generated in house
Wnt1^{Cre}	Generation of mice that express the Cre recombinase under control of *Wnt1* promoter in a	The Jackson Laboratory

	heterozygous manner. These mice have no detrimental phenotype and were used as controls for *Wnt1^{Cre}xLtbr$^{fl/fl}$* mice (Lewis et al., 2013).	
Wnt1^{Cre}xLtbr$^{fl/fl}$	Mice were generated by crossing *Ltbr$^{fl/fl}$* and *Wnt1^{Cre}* mice. This targeted deletion of LTβR from *Wnt1^{Cre}* expressing mice.	Generated in house
Flk1^{Cre}	Generation of Cre recombinase gene insertion into exon 1 of the Flk1 promoter, with mice being heterozygous for Cre. Mice have no detrimental phenotype and were used as *Flk1^{Cre}xLtbr$^{fl\fl}$* controls (Motoike et al., 2003).	The Jackson Laboratory
Flk1^{Cre}xLtbr$^{fl\fl}$	Generated through the crossing of *Flk1^{Cre}* and *Ltbr$^{fl\fl}$* mice to result in the deletion of LTβR from *Flk1^{Cre}* expressing cells.	Generated in house
TCRα$^{-/-}$	Mice have a targeted mutation leading to the loss of the αβ T-cell receptor expression. As a result, mice suffer from a loss of $CD4^+$ or $CD8^+$ T-cells.	The Jackson Laboratory
Ccr7$^{-/-}$	Mice have loss of the CCR7 receptor expression and so are unresponsive to CCR7 ligands.	Antal Rot University of York
plt/plt	Mice contain a spontaneous deletion on chromosome 4 of the *Ccl21/Ccl19* loci. Ultimately this leads to removal and loss of the production of these ligands.	Antal Rot University of York
Ccl19$^{-/-}$	Mice have no clear detrimental phenotype with maintenance of lymph nodes and splenic architecture, but simply carry a homozygous deletion of *Ccl19* gene (Link et al., 2007).	Sanjiv Luther University of Lausanne
Ccl21$^{-/-}$	Mice were generated to lack *Ccl21* expression by a knock-in system using a targeting vector containing *Ccl21a* genomic BAC fragments and tdTomato-encoding cDNA. When both alleles were targeted there was loss of *Ccl21* expression. Deficient mice were found to develop some peripheral autoimmunity (Kozai et al., 2017).	Yousuke Takahama University of Tokushima
dblGATA	Mice have an x -linked deletion of a high affinity double Gata-binding site in the Gata1 promoter. As a result there is selective loss of eosinophils (Yu et al., 2002).	The Jackson Laboratory
Il4rα$^{-/-}$	Homozygous absence of *Il4ra* in these mice generated by homologous recombination using Cre\loxP method (Mohrs et al., 1999).	Frank Brombacher University of Cape Town

Table 2.2: Constituents of RPMI-1640 Hepes Medium (RF10-H)

Stock Substance	Volume	Final Concentration	Company Source
RPMI-1640 including 20mM Hepes, L-glutamine and w/o bicarbonate	20ml	-	Sigma, Poole, UK
Fetal Calf Serum (FCS) – Heat Inactivated	2ml	10%	Sigma, Poole, UK
200mM L-Glutamine	200µl	2mM	Sigma, Poole, UK
5000IU/ml Penicillin and Streptomycin	400µl	100 IU/ml	Sigma, Poole, UK

Table 2.3: Enzymes Used During Tissue Digestion

Stock Substance	Volume	Final Concentration	Company Source
RF10 composed as in table 2.2	1ml sample	-	Sigma, Poole, UK
Collagenase D or Collagenase Dispase 10mg/ml	25µl	2.5mg/ml	Sigma, Poole, UK
Deoxyribonuclease 1 100mg/ml	40µl	0.4mg/ml	Sigma, Poole, UK

Table 2.4: Constituents of MACs Buffer

Stock Substance	Volume	Final Concentration	Company Source
Dulbeccos phosphate buffered saline without calcium or magnesium	500ml	-	Sigma, Poole, UK
Fetal Calf Serum (FCS) Heat Inactivated	2.5ml	5%	Sigma, Poole, UK
EDTA 0.05M	2ml	0.02M	Sigma, Poole, UK

Table 2.5: Constituents of Dulbecco's Modified Eagle's Medium (DMEM)

Stock Substance	Volume	Final Concentration	Company Source
Dulbecco's medium with 3.7g/l bicarbonate and w/o glutamine	20ml	-	Sigma, Poole, UK
Fetal Calf Serum (FCS) Heat Inactivated	2ml	10%	Sigma, Poole, UK
5000 IU/ml Penicillin and Streptomycin	400µl	100IU/ml	Sigma, Poole, UK
200mM L-Glutamine	400µl	4mM	Sigma, Poole, UK
1M Hepes	200µl	10mM	Sigma, Poole, UK
5000 M2 Mercaptoethanol	200µl	-	Sigma, Poole, UK
100x Non-essential amino acids	200µl	-	Sigma, Poole, UK

2.3 Isolation of Mouse Tissue For Analysis

Sacrificed adult mice were dissected within the BMSU facility to remove thymus and often spleen. These organs were removed using scissors and forceps before being placed into RF10 medium. In the laboratory, organs were cleaned under a microscope to ensure the removal of any fat or blood that remained on the tissue. Depending upon the cell type being analysed, preparation of tissues differed and are detailed according to target cell type in the subsections of 2.3 below. For the isolation of embryonic thymi, within a laminar flow hood, embryos were removed from the amniotic sac and placed under a dissection microscope. There was then subsequent identification and careful removal of the embryonic thymic lobes. Embryonic thymi were then stored in RF10 for immediate analysis or transferred into culture medium, DMEM, for further study in an FTOC or KCT system.

2.3.1 Preparation of Mouse Tissue For Dendritic Cell and Eosinophil Analysis

Thymus and spleen, once isolated and cleaned, were placed into the enzyme mix containing Collagenase D and DNAse I (Sigma) diluted in RF10 for digestion – detailed in table 2.3. Tissue was then cut into small pieces of around 2mm using scissors in an eppendorf before being transferred into 5ml Polypropylene round-bottomed tubes for digestion (Falcon, Thermo Fisher Scientific). Digestion occurred at 37°C on a Thermoblock (Eppendorf Thermomixer C) which shook at 650rpm. This digestion process occurred for approximately 20-30 minutes or until all of the tissue appeared to have been digested. Regular pipetting during this time was employed to help to encourage the fragmentation and disaggregation of tissue. Once digested, tissue was removed from the thermoblock and enzyme activity was stopped through the addition of 30µl of 0.5M EDTA (Sigma Aldrich), which chelated magnesium and calcium ions and therefore prevented sustained enzyme action. Samples were

then washed with MACs Buffer before being filtered through membrane-mesh into a 15ml Falcon (Corning Centistar, RNAse/DNAse free) and spun in the centrifuge for 4mins 1400rpm at 4°C – these are the typical conditions always used for centrifugation unless stated otherwise. Supernatant was removed and thymus samples were resuspended in 2ml of MACs buffer. Splenic samples were resuspended in Red Blood Cell (RBC) lysis buffer Hybri-max (Sigma Aldrich) for 10 minutes at room temperature before being neutralized with an equivalent volume of MACs buffer – spun down in the centrifuge and resuspended in 2ml MACs. When samples were not being used, tubes containing cells were always kept on ice. Following resuspension, cells were counted using AccuCount Blank Beads (Spherotech Inc) whereby a known number of beads could be added to a known volume of cells from the 2ml total sample suspension. By running samples for counting on the LSR Fortessa Machine (BD), the beads and total cells could be distinguished and gated for counting due to different granularity and sizing of the cells. A known number of beads could be collected and compared to the subsequent number of cells obtained and a calculation then allowed the generation of the cell counts per thymus or spleen. This technique for cell counts was maintained throughout the entire study.

2.3.2 Preparation of Mouse Tissue For T-cell Analysis

To allow for T-cell analysis of thymic and splenic tissue, cleaned tissue was disaggregated using cut edge frosted end glass slides (Thermo Scientific) to release the cells into a petri-dish containing RF10 medium. The slides were then washed in RF10 and discarded, leaving cells suspended in medium. This was then filtered through a membrane-mesh filter into 15ml Falcon tubes (Corning Centistar RNAse/DNase free) to allow any remaining clumps to be removed prior to analysis. Centrifugation then occurred and supernatants were removed

before pellets were resuspended in 2mls RF10 for thymic tissue and placed on ice whereas splenic tissue was resuspended in RBC lysis buffer Hybri-max (Sigma Aldrich) and left at room temperature for 10 minutes. Following successful lysis, samples were neutralized with an equivalent volume of RF10 before being centrifuged and resuspended in 2mls RF10. Samples were then ready to be counted as specified in 2.3.1.

2.3.3 Preparation of Mouse Tissue For Thymic Epithelial Cell Analysis

To enable the isolation of thymic epithelial cells (TEC) a different variation of enzyme mix was used compared to that previously described for eosinophil and dendritic cell populations. For TEC, Collagenase Dispase and DNAse I were used and diluted in RF10 medium as listed in table 2.3. Thymus samples were placed into the digestion mix and cut into small pieces approximately 2mm in size, in eppendorfs before being transferred into 5ml Polypropylene round bottom Digestion tubes (Falcon, Thermo Fisher Scientific). Digestion on the Thermoblock (Eppendorf Thermomixer C) was at 37°C with it continuously rotating at 650rpm. This digestion process was maintained for up to 30 minutes or until tissue was disaggregated fully. Samples were then removed from the thermoblock and enzymes neutralized with the addition of EDTA (0.5M, Sigma Aldrich). Samples were then washed with MACs buffer and transferred through filters of membrane-mesh into 15ml Falcon tubes (Corning Centristar). Centrifugation of samples then allowed supernatant to be removed and resuspension in 2mls MACs to prepare the cells ready for counting (as in section 2.3.1). For TEC analysis, an additional step was required post counting and prior to antibody staining such that there could be depletion of $CD45^+$ cells to enrich the TEC populations ($CD45^-$). This was possible as counted cells were then incubated in the fridge at 4°C with anti-CD45 beads (Miltenyi Biotech) in MACs buffer for 20 minutes. Cells could then be passed through a LS

Column (Miltenyi Biotech) on a MACs Magnet to allow for the magnetic separation of CD45 labelled cells. This system acted to pull the $CD45^+$ cells from the cell suspension and as a result, allowed the relative enrichment of the TEC population within the thymus. Cells were collected in 15ml Falcon tubes (Corning Centristar) and then centrifuged and resuspended prior to cell staining.

2.3.4 Fetal Thymic Organ Culture System

Upon isolation of thymic lobes from embryos, lobes could be cultured in an FTOC system, which provided a supportive growth environment to encourage survival of FTOC at this early stage. Often, dGuo was added to cultures (mentioned in section 2.2) in order to remove hematopoietic cells from thymic lobes which was necessary in experiments utilising engraftment under the kidney capsule; possible 5-7days after dGuo culture. This approach was required to study the colonisation of these grafted thymic lobes by host progenitor cells as it provided an empty thymic niche within an in vivo system. For culture set-up, DMEM medium was either supplemented with dGuo or left as DMEM alone and placed in either 35mm or 90mm petri-dishes (Sterilin). These held 2mls DMEM (+300µl dGuo) or 4mls DMEM (+600µl dGuo). In these dishes sterile artiwrap sponge supports (Medipost Ltd) around $1cm^2$ in size were placed. On top of this, 0.8µm sterile nucleopore filters were positioned. Using a mouth pipette with a sterile glass pipette attached, lobes were transferred onto filters. Up to six lobes could be placed onto one individual filter. Following this, petri dishes were put in a humidified chamber at 37°C 10% CO_2 for 10 minutes to normalise pH to between 7.2 and 7.4. Culture boxes containing the petri dishes were then sealed and left in the incubator for 5-7 days prior to experimental transfer (section 2.8).

2.4 Flow Cytometric Analysis of Target Populations

2.4.1 Cell Surface Antibody Staining

Antibodies used to stain markers to identify target cell populations for analysis were, for the most part, primary and directly conjugated antibodies. These have been listed in Table 2.6 along with any secondary antibodies used to identify any unconjugated or biotin tagged primary antibodies. For staining, samples were loaded into a 96 well-plate (Thermo Scientific). For all analysis, 5 million cells were stained – unless there were fewer to begin with due to irradiation damage or depletion techniques. If this occurred, then the entire sample would be stained. 100µl of antibody was always used per sample. Staining was completed on ice in a covered box for 20 minutes. The only exception being detection of CCR7 expression whereby the plate was covered with foil and incubated at 37°C for 20 minutes when this antibody was added. Primary antibodies were added initially, then samples were washed twice with 100µl of MACs buffer (Table 2.4) and centrifuged at 1400rpm, 4°C for 2 minutes before the supernatant was flicked off. Pellets were then resuspended in the secondary or subsequently additional tertiary antibodies and the same incubation on ice for 20 minutes took place. Within staining combinations it was imperative to include samples as controls within the combination whereby there were samples without the primary step, or isotype controls were used as well as possibly fluorescence minus one samples. All controls were used to set the fluorochrome level for negative staining such that positive populations could then be easily identified as levels of fluorescence above this negative gate. Once staining was completed, cells were washed again, resuspended in fresh MACs buffer and transferred into polystyrene 12.5ml FACS tubes (Falcon) to be run on the LSR fortessa (BD).

Table 2.6: Antibodies For Flow Cytometric Analysis

Antibody Specificity	Clone	Flurochrome	Dilution Factor	Company
Aire	5H12	FITC		eBioscience
B220	RA3-6B2	FITC APCCy7	1:200 1:200	eBioscience
BrdU	MoBU-1	APC	1:100	BD
CCL21	Polyclonal rabbit	-	1:100	Lifespan Biosciences
CCR7	4B12	PE	1:50	eBioscience
CD115	AFS98	APC	1:100	eBioscience
CD11b	M1/70	BV711	1:200	Biolegend
CD11c	N418	APC PeCy7	1:200 1:200	eBioscience eBioscience
CD19	eBio1D3	FITC APCCy7	1:200 1:200	eBioscience eBioscience
CD25	PC61.5	APC A700	1:200 1:200	eBioscience eBioscience
CD3	145-2C11	FITC APCCy7	1:200 1:200	eBioscience eBioscience
CD31	390	FITC	1:200	eBioscience
CD4	RM4-5 GK1.5	BV711 Pacific Blue	1:50 1:100	Biolegend eBioscience
CD40	323	PE	1:100	BD Pharmingen
CD45	30-F11	APCCy7	1:800	eBioscience
CD45.1	A20	APCCy7	1:200	eBioscience
CD45.2	30-F11	BV786	1:400	Biolegend
CD5	53-7.3	Biotin	1:100	eBioscience
CD62L	MEL-14	APC	1:3000	eBioscience
CD69	H1.2F3	PerCpCy5.5	1:200	eBioscience
CD8	53-6.7	BV510	1:200	Biolegend
CD80	16-10A1	BV605	1:400	Biolegend
CD86	GL-1	BV650	1:400	Biolegend
cKit	2B8	PerCpCy5.5	1:50	eBioscience
Cleaved Caspase-3	5A1E	PE	1:50	Cell Signalling Technology
EpCAM-1	G8.8	PerCpCy5.5	1:800	eBioscience
Fezf1/2	F441 Polyclonal Rabbit	-	1:200	IBL
Flt-3	A2F10	Biotin PE	1:100 1:100	eBioscience eBioscience
Foxp3	FJK-16s	FITC PE	1:100 1:100	eBioscience eBioscience
Goat-anti Rabbit	IgG	Alexa Fluor 647	1:200	Molecular Probes

gp38	eBio8.1.1	PE	1:800	eBioscience
Gr1	RB6-8C5	FITC	1:200	Biolegend
LTβR	eBio3C8	Biotin	1:100	eBioscience
LTβR Isotype	IgG1κ	Biotin	1:100	eBioscience
Ly51	BP-1	PE	1:800	BD Pharmingen
MHCII	M5/114.15.2	A700 Pacific Blue	1:200 1:2000	eBioscience Biolegend
PDCA-1	927	Pacific Blue	1:200	Biolegend
Siglec-F	ES22-10D8	APC Biotin	1:100 1:100	Miltenyi Biotec Miltenyi Biotec
Sirpα	P84	PE PerCpCy5.5	1:100 1:100	eBioscience eBioscience
Streptavidin	-	PeCy7	1:1500	eBioscience
TCRβ	H57-597	APCCy7	1:200	eBioscience
Ter119	TER-119	A700	1:200	Biolegend
UEA-1	-	Biotin	1:10,000	Vector Labs

2.4.2 Intracellular Antibody Staining

Intracellular staining was occasionally required additionally after surface staining (section 2.4.1), to identify transcription factors such as Foxp3 or Aire as well as apoptotic markers such as Cleaved Caspase-3. All staining for this was maintained in a 96 well-plate subsequent to initial primary antibody staining, with washes being in a 100µl volume and centrifugation being completed at 1400rpm, 4°C for 2 minutes.

For the analysis of Foxp3, Aire and Caspase-3, all required a Transcription Factor Staining Buffer Set (eBioscience). For this technique, cells were surface stained and then incubated with the eBioscience Fixation/Permeabilisation Solution; composed of 1 part fixative concentrate to 3 parts diluent with a volume of 200µl added per well per sample. Foxp3 and Aire staining required that cells were fixed for 40 minutes on ice, however for the Caspase-3, cells were fixed for only 10 minutes. Following this, cells were then all washed with the permeabilisation buffer in the kit which required diluting from the 10x stock provided, to a workable 1x diluted solution made using distilled water. This wash was completed twice. Following this, cells were then stained for Foxp3, Aire or Caspase-3 and again staining occurred on ice for 20 minutes. These intracellular antibodies were further diluted in the 1x permeabilisation buffer. All subsequent washes were also completed with the permeabilisation buffer but prior to FACs analysis (LSR Fortessa) of samples, they were all ultimately resuspended in MACs buffer.

2.4.3 Bromodeoxyuridine Proliferation Analysis

To support the detection of proliferating cells, the technique of Bromodeoxyuridine (BrdU) incorporation was used. For this process, 1.5mg BrdU was injected into mice intraperitoneally

18hours prior to sacrifice. For analysis, tissues were harvested and digested as appropriate for the cell type being analysed (Section 2.3). Once in a 96 well plate, cells were surface stained as section 2.4.1, for the identification of the desired target. Following washing of the cells after primary staining, samples were resuspended in 100µl BD Fix/Perm for 30 minutes 4°C. Samples were then washed with 1xPerm Buffer made with distilled water from 10x stock bottle, from the APC BrdU Flow Kit (BD Pharmingen). BD Cytoperm buffer plus, contained within the set, could then be added neat to samples for 10 minutes on ice. Washing again with 1x Perm Buffer, cells were resuspended in 100µl BD Fix/Perm for 5 minutes on ice. Cells were washed again with perm buffer and resuspended in 100µl of diluted DNAse as manufacturers instructions and kept at 37°C for 1 hour. Following another perm buffer wash, cells could then be stained for BrdU, with the antibody being made up in 1x Perm Buffer solution and incubated at room temperature for 40 minutes before being washed, samples were resuspended in MACs buffer and then ran on the LSR fortessa.

2.4.4 Flow Cytometric Analysis

All samples that were prepared and stained with antibody were ready to run on the fortessa. The LSR Fortessa (BD) was used for all flow cytometric analysis. This machine used the BD FACS diva software from which data was then exported for additional analysis on FlowJo 8.7.3. Single colours were ran first as they were used to set voltages and compensations against the other colours in the combination. Cells analysed were initially pre-gated on FSC and SSC to only include viable cells. Samples that were controls for the staining such as isotype controls were than ran to set positive gates for the desired populations. This allowed positive staining from fluorochromes in actual samples to be determined and recorded.

2.5 Immunohistochemical Analysis

2.5.1 Preparation of Tissue Sections

Following successful isolation of tissue from adult mice, the thymus was cleaned to ensure removal of blood and excess fat from the lobes before being frozen on dry ice simply within a foil casing. All frozen tissue was mounted using Optimal Cutting Temperature compound (OCT) onto the microtome. Sections could then be cut on the cryostat machine which were 7μm in depth and collected sections were placed onto multisport glass slides (Hendley-Essex). Slides were then allowed to air dry for around an hour at room temperature before being fixed in acetone (Baker) for 20 minutes at 4°C. Slides were then air-dried again before being stored in the freezer at -20°C, ready to be antibody labelled for immunofluorescence.

2.5.2 Staining of Tissue Sections For Immunofluorescence

Stored sections were removed from the freezer and allowed to dry at room temperature for 30 minutes before being rehydrated in Phosphate Buffered Saline (PBS, Sigma Aldrich) for 15 minutes. During this time, antibodies were prepared and made up in 1% Bovine Serum Albumin (BSA) diluted in PBS (Sigma Aldrich). Rehydrated sections were then stained with primary antibodies (listed in Table 2.7). All antibody steps occurred in a humidified chamber at room temperature for 30 minutes. Slides were then washed in a PBS bath for 5 minutes before the next step could be added if necessary. Following all antibody staining steps, sections were covered with 4',6-diamidino-2-phenylindole (DAPI) which is a nuclear stain and assists with cellular visualisation during immunofluorescence. After another wash in PBS, sections were covered using a coverslip (Sigma Aldrich) and sealed using 1,4 diazabicyclooctane (DABCO) in glycerol pH 7 to support the vital preservation of the

fluorochromes. Coverslips were then sealed using clear nail varnish around the edges and once dry, stored at -20°C. Confocal imaging was conducted using the Zeiss 780 Zen microscope. Various magnifications were used (x10, x25, x40).

Table 2.7 Antibodies Used For Immunohistology Analysis

Antibody Specificity	**Host/Clone**	**Fluorochrome**	**Dilution Factor**	**Company**
Aire	Rat/ IgG1κ 5H12	Alexa Fluor 488	1:100	eBioscience, ThermoFisher Scientific
Fezf1/2	Rabbit/F441	-	1:200	IBL
ERTR5	Rat/IgM	-	1:5	W.van Ewijk Leiden University
CD11c	Armenian Hamster/ IgG HL3	Biotin	1:200	BD
CD8	Rat/ IgG2b 53-6.7	Biotin	1:200	eBioscience, ThermoFisher Scientific
CD4	Rat/GK1.5	Alexa Fluor 647	1:200	Biolegend
IgG(H+L)	Goat	FITC	1:100	Southern Biotech
Anti-rabbit IgG	Donkey/IgG	Alexa Fluor 594	1:1000	ThermoFisher Scientific
Anti-Rat IgM	Goat/IgM	Alexa Fluor 647/488	1:200	Thermofisher, Scientific
Streptavidin	Goat/IgG	Alexa Fluor 555/488	1:1000	Thermofisher, Scientific

2.5.3 Confocal Quantitation

WT, *Ltbr*$^{-/-}$, *Foxn1*^{Cre}, *Ltbr*^{TEC} thymi were obtained, frozen and sectioned as detailed in 2.5.1. For quantitation, 3-4 sections were taken throughout the whole thymus at differing depths. There was staining of these sections for CD11c and ERTR5 (detailed in 2.5.2, Table 2.7) before visualization on the Zeiss 780 Zen microscope. Five pictures were taken per section per mouse of both the medullary and cortex areas of the thymus at a x40 magnification. Within each image, the region of cortex or medulla randomly selected filled the whole image area. From this, the total number of CD11c^{+} cells were then counted and distribution of these within the cortex or medullary area was noted such that the division anatomically regarding dendritic cell positioning could be determined.

2.6 Stimulations of Cell Cultures

Total thymus was obtained and prepared through the teasing method described in section 2.3.2. Cells were then subsequently prepared and counted. If cells were being analysed for activation status of dendritic cells following stimulations, 2x10^{6} cells were placed in each well of a 24 well-plate (Corning Costar) in a volume of 1ml/well of culture medium DMEM. 10µl of 1µg/ul stock solution was added forming a final concentration of 10µg/ml of anti-CD40, anti-LTβR or both were added to single cell containing wells, with some wells being left unstimulated (DMEM alone). These cultures were left at 37°C, 10% CO_2, for two days before being harvested. All cultures upon completion similarly had cells removed from the wells and washed into 15ml Falcon tubes. Wells were washed thoroughly with DMEM before being centrifuged and resuspended in RF10 medium. Cells could then be transferred into a 96 well plate (Thermo Scientific) and re-centrifuged 1400rpm 2mins 4°C. Primary antibodies were

then added in a volume of 100µl and if subsequent steps were necessary, they were completed following washes. Cells were finally washed and resuspended to be analysed on the Fortessa.

2.7 Kidney Capsule Transplant

In order to investigate how alterations in the thymic microenvironment in *Ltbr*$^{-/-}$ mice affected the colonisation of dendritic cell populations in comparison to that of WT controls, the kidney capsule transplant (KCT) system was used. This allowed transfer of E15 FTOC that had been set up 5-7 days prior to surgery in dGuo, depleting haematopoietic cells (detailed in 2.3.4), and leaving a thymic stromal casing that could be inserted under the kidney capsule of mice. After a period of 8 weeks, grafts were harvested and subsequent presence of host cells identified.

For this process, WT host mice were used aged 7-10weeks. Mice had to weigh above 17g to undergo surgery and weights ensured that the correct dose of Buprenorphine (Tamgesic, Animal Care UK) was administered subcutaneously at least 1 hour before surgery. Mice were anaesthetised with 4% Isoflurane (May and Barker, Dagenham UK) using oxygen as carrier fluid. Following induction of the anaesthesia, the change to a breathing pattern to a deeper and slower pace indicated a level of unconsciousness. Mice were then quickly shaved on the back left-hand side of the spine, wiped with Hibitane solution – an antiseptic solution, and transferred to a fitted facemask. In this set up, mice laid on their chest on a heat pad with their face fitted to the mask through which 2% Isoflurane was administered and maintained during surgery. Pedal reflex was checked prior to surgery to ensure no reaction and an unconscious state.

For surgery, all tools used were sterile and had been autoclaved prior to use and were maintained as sterile throughout surgery, with storage on sterile disposable drapes. An incision was made in the shaved region of the mouse on the left hand side in the area of the kidney. This exposed the peritoneum, which was then cut also and widened with blunt scissors. The incision was held open with needle and suture (Vicryl 16mm) attached to needle holders. The kidney was lifted onto the skin surface by forceps that gripped onto kidney fat to avoid any direct damage to the kidney itself. The kidney was kept hydrated when outside of the body cavity by the repeated application of PBS soaked gauze.

Using a dissection microscope, a small incision was made on the kidney capsule using forceps to allow an opening for thymus transfer. E15 FTOC thymic lobes were then carefully placed one at a time under the kidney capsule – a maximum of two lobes were placed under one kidney capsule. After confirmation that the lobes were in place, the kidney was encouraged back into the body cavity before suturing up the peritoneum and skin separately. The skin was then additionally secured with metal clips to ensure it would not open if sutures were to fall or be pulled out. Saline was administered subcutaneously to restore any fluid loss and mice were transferred to a warming box in the recovery room and monitored until they regained consciousness. Checks were regularly completed by BMSU staff following this point.

2.8 Irradiations of Mice

Mice were sometimes required to have treatment of irradiation either in preparation for Bone Marrow Chimera Generation (Section 2.9) or for a sub-lethal irradiation used as a model for damage. Prior to all irradiation models, mice were placed on Baytril for 7 days; this was additionally maintained for 1 week after the irradiation start date. For Bone Marrow Chimeras, mice were given a lethal dosage of irradiation that was split over two days. When

mice were C57/BL6 in background, a single dosage of 500 rads of irradiation (CIS BIO International, Cedex, France) was given at the start of the protocol (day one) and again repeated on the morning of day two. On the afternoon of day two mice were reconstituted with bone marrow with $5x10^6$ cells transferred into each mouse. For sublethal irradiations, mice were Balb/c in background and given a dosage of 1x425 rad on the morning of day one of the protocol.

2.9 Generation of Bone Marrow Chimeras

Bone Marrow Chimeras (BMC) were used to identify which compartment; haematopoietic or stromal, was responsible for any defects in dendritic cell populations seen in knockout mouse models. However in addition, competitive mixed bone marrow chimeras were used to identify a possible cell-intrinsic role for CCR7 in regulating the presence of dendritic cell populations in the thymus by placing CCR7 deficient bone marrow in competition with WT bone marrow.

Chimeras were generated through the removal of the tibia and femur bones from sacrificed donor mice. Bones were then cleaned to remove excess skin and fat before being cut above and below the knee joint in a sterile laminar flow hood to open up the ends of the bone and allow a needle to be able to be used to access bone marrow. A sterile needle 25g (Terumo Agani) and syringe (BD Plastipak) filled with MACs was then used to flush the bone marrow out into a 95mm petri dish (Sterilin). A 1ml pipette containing sterile MACs was used to break up any clumps of bone marrow within the petri dish before being transferred through sterile mesh into 50ml falcon tubes (Corning Centristar). Suspensions were centrifuged at 1400rpm, 4°C for 10 minutes. Supernatants were removed and pellets lysed with 2mls RBC lysis buffer Hybri-max (Sigma Aldrich) for 10 minutes at room temperature before being neutralised by an equivalent volume of sterile MACs and centrifuged. Samples were

resuspended and counted (as in section 2.3.1) before undergoing removal of mature T-cells from the bone marrow to reduce graft vs host disease complications upon transfer. Removal of T-cells used a CD3 based approach with anti-CD3 antibody (Table 2.6) being used to stain the samples, followed by anti-PE microbeads (Miltenyi Biotech) which were incubated with samples at 4°C for 20 minutes having been thoroughly vortexed. Miltenyi MACs column depletion was used with samples being passed through LS columns held in the QuadroMACs magnets, which were then washed several times with MACs buffer. This allowed $CD3^+$ cell removal, which was checked through the proportional presence of CD3 PE positively stained cells in post-depletion samples compared to pre-depletion samples on the LSR fortessa. Counts were also completed post-depletion to allow for the correct numbers of cells to be resuspended in PBS without magnesium or calcium (Sigma Aldrich) for transfer into host mice. Host mice had previously undergone irradiation in accordance with section 2.8. A total of 5 million cells were transferred intravenously into the host mouse in a carrier volume of 200µl. Baytril was maintained for a week post-transfer of bone marrow to minimise any infections until the haematopoietic compartment was reconstituted. Mice were then left for 8 weeks prior to sacrifice and tissue harvest.

2.10 Autoimmunity Analysis

All autoimmunity analysis was completed in collaboration with M. Carvalho-Gaspar, University of Birmingham.

To provide an alternative and direct read-out of autoimmunity in mouse strains (section 2.1), two methods were used – one of cellular infiltrates into tissues and one of autoantibody detection.

2.10.1 Cellular Infiltrates

For analysis of cellular infiltrates, multiple tissues from host mice were examined; liver, stomach, kidney and salivary glands. Upon schedule one, tissues were harvested and washed in PBS (Sigma Aldrich) and slowly frozen down in liquid nitrogen to preserve the tissue. Samples were stored at -80°C prior to use. When required, tissues were removed and kept on dry ice to be cut on the cryostat at -20°C as detailed in 2.6.1. Frozen sections were cut at 6-7µm thickness at 3-5 different layers (30 – 35µm apart) throughout the whole tissue. Sections were left to dry overnight and placed in cold acetone for 10 minutes the next day. After this sections were then left to dry again at room temperature for 2 hours and then stored at -80°C until needed or stained. For this analysis of cellular infiltrates, a simple Haematoxylin and Eosin (H&E) staining was used (PFM Medical). Haematoxylin - a basic dye with a positive charge and therefore reacts with negatively charged nucleic acids staining them blue. Eosin, due to its acidic properties and negative charge reacts with positively charged proteins in the cell and stains the cytoplasm and extracellular matrix of cells a pink colour. The process for staining was composed of a series of steps of PBS washes, Eosin (1%) and Haematoxylin (Harris) stain washes followed by several different alcohol stages at a gradient from 70-100% to dehydrate the tissue. Sections were then placed in Xylene to prepare the tissue for the Xylene based mounting medium. Tissue was then mounted using DPX Mountant (Sigma Aldrich) to preserve the colouring and covered with a glass coverslip.

2.10.2 Autoantibody Detection

Blood was obtained from experimental mice for use in autoantibody detection via cardiac punctures. For this process, mice were anaesthetised using 4% Isoflurane (May and Barker, Dagenham UK) along with the carrier oxygen which fed into a chamber that the mice were

singularly held in until a state of unconsciousness was reached. Mice were then transferred to a facemask on their backs, chest upright, with isoflurane maintained at 4%. Blood was obtained using a sterile needle 25g (Terumo Agani) and syringe (BD Plastipak) then transferred and held in an eppendorf. Mice were then culled by schedule one. Samples were then left at room temperature until blood had sufficiently clotted. Samples were then centrifuged and the remaining serum was removed as the supernatant and stored in eppendorfs at -20°C until required.

To detect autoantibodies, multi-composite slides (INOVA Diagnostics) that contained WT Rat Liver, Kidney and Stomach were used – alternatively stored at -4°C prior to use. Goat serum (10% diluted in PBS, Sigma) was added initially to sections to prevent non-specific binding of the secondary antibody. This was incubated in a humidified chamber in the dark at room temperature for 30 minutes before being tipped off the slides. Each sample serum was serially diluted using PBS (Sigma Aldrich) to generate a range of dilution factors that could be applied to the same slides to determine if autoantibodies could still be detected. The greater the level of autoantibodies, the higher the dilution factor required to dilute them such that the autoantibodies could no longer be detected. Sections were then incubated with the serum of required dilution factor, in a dark humidified chamber for 30 minutes before being washed in PBS. Goat $F(ab')_2$ anti-mouse IgG(H+L) FITC secondary antibody (Southern Biotech) was then added and incubated for 30 minutes in a humidified chamber in the dark. The secondary antibody recognises IgG, IgA, IgM and therefore acted to detect the presence of autoantibodies in the serum sample that bound to the tissue section. Slides were then washed in a PBS bath for 5 minutes before counterstaining with 4',6-diamidino-2-phenylindole (DAPI) stain was applied and left for 10 seconds before slides were again washed in PBS.

Slides were mounted with a coverslip (as in 2.6.2) and ready to be visualised. All images were taken using the Leica DM6000 microscope.

2.11 Statistical Analysis

GraphPad Prism 6.0 software was subsequently used to generate all graphical representation of data. Statistical analysis was also completed using this program whereby unpaired student two-tailed T tests were used for most analysis. However analysis comparing more than two species for one parameter used a one-way ANOVA, which have been noted in figure legends. P values only below 0.05 were noted as being significant. The significance was noted as: *<0.05, **<0.01, ***<0.001, ****<0.0001.

CHAPTER THREE:

LTβR MEDIATED REGULATION OF DC IS NECESSARY TO MAINTAIN CENTRAL TOLERANCE

3.1 Introduction

DC in the thymus have a close association with mTEC, which was originally determined by the identification of MHC expressing hematopoietic cells within thymic medullary areas (Barclay and Mayrhofer, 1981). These were later directly determined as being DC with their medullary positioning shown to be necessary for their functional role in central tolerance (Herbin et al., 2016). mTEC have been reported to support the efficient localisation of DC with a strong influence upon the regulation of the cDC1 population in particular. Studies have shown that Aire expressing mTEC direct cDC1 into medullary areas through XCL1 production, with the corresponding expression of XCR1 by the cDC1 population (Lei et al., 2011).

Functionally, mTEC present tissue restricted antigens (TRAs) on their cell surface due to the expression of Aire and Fezf2, which are necessary to regulate this process. Therefore once in the medulla, DC can support central tolerance through mTEC interactions, which allows them to cross present these TRAs to screen developing thymocytes. This is thought to help optimise the availability of self-antigen in the thymus for both negative selection and T-Regulatory cell generation (Mouri et al., 2014, Herbin et al., 2016, Perry et al., 2014, Bonasio et al., 2006). As a result, the regulation of medullary areas therefore appears to be somewhat vital to ensure that there is the correct provision of an environment with the capacity to support dendritic cell function and localisation.

Regulation of the medulla has previously been linked to lymphotoxin beta receptor (LTβR) as it was shown that mTEC require LTβR signals in thymic stroma for the correct formation of medullary areas (Boehm et al., 2003). Subsequent analysis has also identified a role of LTβR

signalling in the correct development of the mTEC sub-populations (Lkhagvasuren et al., 2013, White et al., 2010). As a result, due to the association between mTEC and DC, it will be questioned if DC may utilise the same mechanisms of regulation as mTEC populations with investigation into the possible control of DC through LTβR. Considering this, the possibility of LTβR mediated regulation of DC has previously been suggested to occur in the periphery. This stemmed from a study that focused on mechanisms regulating the conventional DC2 populations (cDC2) in the spleen and demonstrated that there is a cell intrinsic requirement for signalling through LTβR in the regulation of the homeostatic proliferation of cDC2 (Kabashima et al., 2005, Wang et al., 2005). These studies are important as they show that LTβR signals can directly regulate peripheral DC. Whether this process also occurs in the thymus is unknown, and will be investigated through this chapter.

In addition, analysis of *Ltbr*$^{-/-}$ mice illustrated that an absence of LTβR led to fragmentation of the medulla and disrupted mTEC populations (Boehm et al., 2003). Furthermore this was shown to result in a direct breakdown in central tolerance with the development of T-cell driven autoimmunity (Venanzi et al., 2007, Zhu et al., 2007). In such studies, this defective central tolerance induction was attributed to the disruption of mTEC. In addition a more recent study puts forward the idea that the breakdown in tolerance seen in *Ltbr*$^{-/-}$ mice may also involve dysregulation of the LTβR mediated transcription factor Fezf2 causing a lack of Fezf2 associated TRA presentation in thymus (Takaba et al., 2015). As a result, these ideas combine to suggest that there is a necessity for a fully formed and functioning medulla to maintain central tolerance within the host. However, whether this breakdown in central tolerance is a direct result of medullary disruption, or rather directly attributable to alterations in the closely associated DC populations, was unknown. As a result this chapter will also use

LTβR absence as a tool to dissect the requirement for an intact medulla for effective central tolerance and regulation of the mediators supporting this process including intrathymic DC populations.

3.2 Results

3.2.1 Defining DC Pools In Thymus and Spleen

In order to begin examination of the possible regulators of dendritic cell (DC) populations, DCs were firstly isolated from the thymus. This was done through enzymatic digestion of the thymus to obtain a single cell suspension that could be antibody stained for DC detection via flow cytometric analysis. DC could be identified in the thymus of adult WT mice (Figure 3.1A) with cDC referring to conventional DC including subsets cDC1 and cDC2 as well as the detection of plasmacytoid DC (pDC).

To determine how DC development alters with age, an ontogeny series was subsequently generated in the thymus of WT mice with the isolation of thymi from mice at differing ages and timed matings being set up for the retrieval of E18 WT thymus lobes. This ontogeny showed that with age there was a steady increase in total thymus cellularity (Figure 3.1 B), as would be expected until around seven weeks of age, from which there appeared to be a slow decline in thymus size as involution of the thymus begins. Interestingly total thymic DC followed a similar trend, with increases until seven weeks of age and then a corresponding decline (Figure 3.1 B). Within the DC compartment, at early stages of development, conventional DC (cDC) dominated with pDC only contributing around 20% of the entire DC population (Figure 3.1 C). However with age, there was an influx of pDC until around two weeks at which point pDC were then 60% of the total DC population. This contribution was statistically significant compared to the pDC population at the one week and five week timepoint. After five weeks however, pDC began to decrease again with consequentially increased cDC seen. Eventually at around seven weeks of age, equilibrium develops with a plateau of DC established. Within the thymus, it also was clear that the cDC1 subset was the

Figure 3.1:
Dendritic Cells Can Be Identified In The Thymus and Change With Age

A) The gating strategy used for the identification of dendritic cell populations within thymus. Lineage (Lin) gate included NK1.1, CD19 and CD3, which were all excluded prior to CD11c and PDCA-1 gating. cDC1 refers to conventional dendritic cells 1, cDC2 - conventional dendritic cells 2 and pDC - plasmacytoid dendritic cells.

All data points for the rest of the figure are representative of different numbers of samples; E18 (n=7), d5 (n=14), 1 week (n=6), 2 weeks (n=8), 5 weeks (n=7), 7 weeks (n=6), 9 weeks (n=8), 11 weeks (n=6) whereby all are from at least two independent experiments.

B) Scatter plots illustrating changes in total thymus cellularity (left panel) and total thymic dendritic cells (right panel) with developmental age.

C) Population percentages obtained through absolute number analysis. For the left hand graph, absolute numbers of cDC1 and cDC2 were added to determine the cDC total, this was then added to pDC to obtain the whole DC population per mice. Relative proportions of the cDC and pDC compartment were then calculated from the total absolute number of dendritic cells. Similarly for the right hand graph, cDC1 and cDC2 absolute numbers were added per mouse and proportions that each population contributed to the total cDC compartment was calculated and plotted.

D) Total thymic DC absolute number changes with age are plotted for the breakdown in the dendritic cell populations. cDC1 (black line), cDC2 (blue line) pDC (red line).

All significance was noted as: *<0.05, **<0.01, ***<0.001, ***<0.0001.

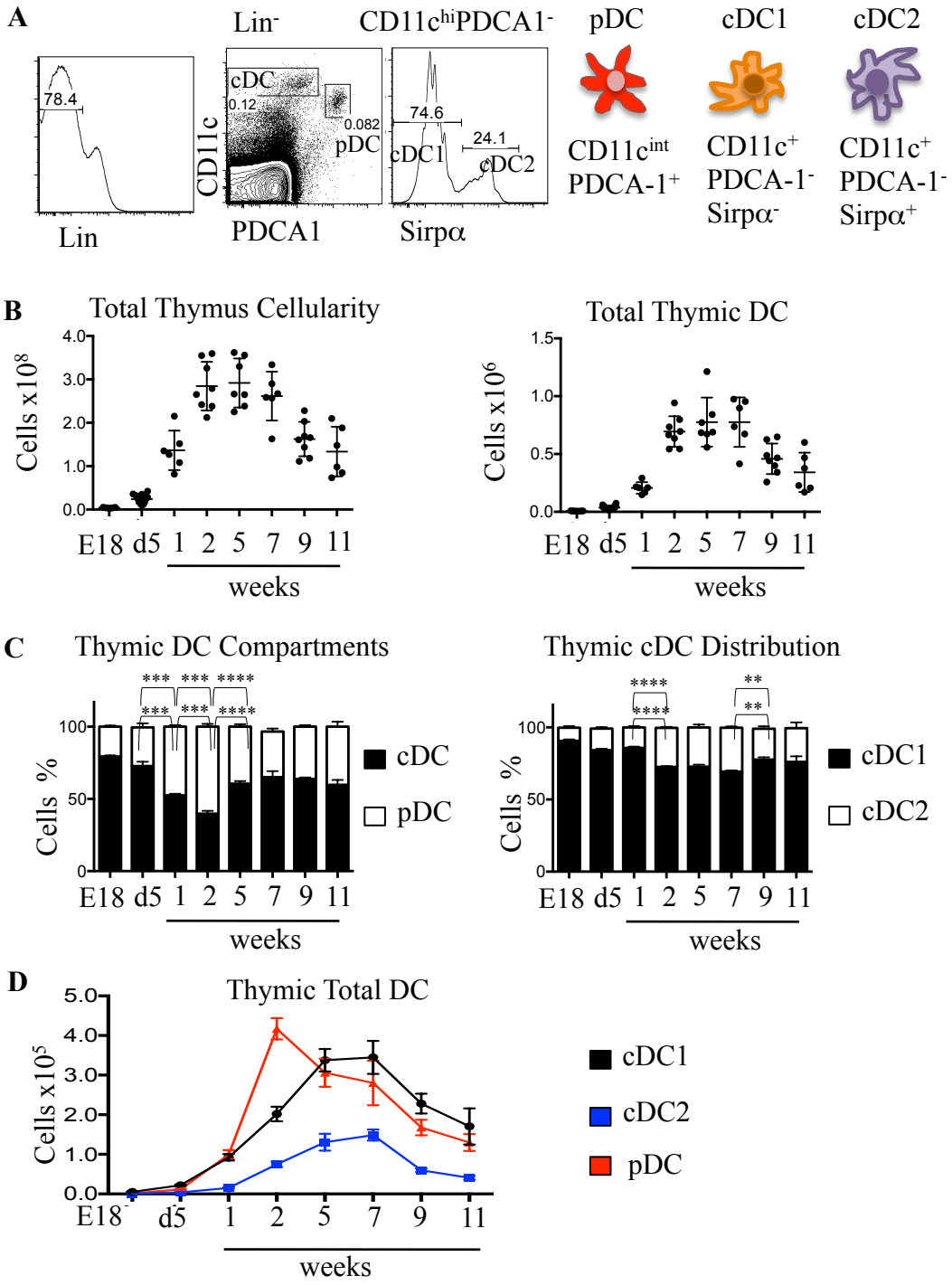
A
Lin-
CD11chiPDCA1-
pDC
cDC1
cDC2
78.4
Lin
cDC
0.12
0.082
pDC
CD11c
PDCA1
74.6
cDC1
24.1
cDC2
Sirpα
CD11cint
PDCA-1+
CD11c+
PDCA-1-
Sirpα-
CD11c+
PDCA-1-
Sirpα+
B
Total Thymus Cellularity
Cells x10^8
4.0
3.0
2.0
1.0
0.0
E18 d5 1 2 5 7 9 11
weeks
Total Thymic DC
Cells x10^6
1.5
1.0
0.5
0.0
E18 d5 1 2 5 7 9 11
weeks
C
Thymic DC Compartments
***
***
***
***
****
****
Cells %
100
50
0
cDC
pDC
E18 d5 1 2 5 7 9 11
weeks
Thymic cDC Distribution
****
****
**
**
Cells %
100
50
0
cDC1
cDC2
E18 d5 1 2 5 7 9 11
weeks
D
Thymic Total DC
Cells x10^5
5.0
4.0
3.0
2.0
1.0
0.0
E18 d5 1 2 5 7 9 11
weeks
cDC1
cDC2
pDC

dominant cDC population with 90% of cDC being cDC1 at E18 which dropped to a lowest level of 70% between five to seven weeks of age; highlighting that this population remained fairly consistent within the thymus during development (Figure 3.1 C). Further this data was plotted to see if proportional trends were supported by absolute number analysis of total DC subsets, which indeed clearly correlated (Figure 3.1 D). This data further confirms that from 5 weeks onwards, cDC1 are the dominant DC subset in the thymus.

Similarly, the DC populations in the spleen were assessed following enzymatic digestion of freshly isolated splenic tissue, cell suspension and surface antibody staining for DC identification (Figure 3.2 A). From this, it was decided to determine how DC populations in the spleen altered with age and therefore a corresponding ontogeny series was generated. The spleen size was shown to change during age with an increase until seven weeks, which then appeared to have variation from that point but generally tended to decrease in size (Figure 3.2 B). Similarly the trend in total DC population numbers mirrored this pattern (Figure 3.2 B) The spleen differed significantly from the thymus in early ontogeny as pDC constituted around 70% of the total DC population (Figure 3.2 C), with cDC only slowly increasing until five weeks of age from which point cDC then contributed towards 80% of total splenic DC. In addition the cDC compartment was predominately cDC1 in early ontogeny (Figure 3.2 C) at around 90% of the total cDC which reduced with increased age as cDC2 increased, plateauing at five weeks to constitute around 70% of cDC. This change was significant between two to five weeks of age. Furthermore it appeared that in absolute number analysis of the DC ontogeny (Figure 3.2 D) there was an increase between two to five weeks of age in cDC2, resembling the trend discussed for proportions of splenic DC (Figure 3.2 C).

Figure 3.2:
Dendritic Cells Within The Spleen Alter With Age

All data points are representative of the following sample numbers; E18 (n=7), d5 (n=14), 1 week (n=6), 2 weeks (n=8), 5 weeks (n=7), 7 weeks (n=6), 9 weeks (n=8), 11 weeks (n=6) whereby all are from at least two independent experiments.

A) The gating strategy used for the identification of dendritic cell populations within Spleen. Lineage (Lin) gate again included NK1.1, CD19 and CD3, which were excluded prior to CD11c and PDCA-1 gating. cDC1 refers to conventional dendritic cells 1, cDC2 - conventional dendritic cells 2 and pDC - plasmacytoid dendritic cells.

B) Proportional bar graphs of the dendritic cell compartment; left graph showing the contribution of the cDC and pDC to the dendritic cell population. These were calculated using absolute numbers of cDC1 and cDC2 for total cDC, combined with pDC for the whole DC pool number. Proportions of cDC and pDC to the whole DC population were then calculated and plotted. Similarly in the right panel contributions of cDC1 and cDC2 to the conventional DC pool were calculated on a per mouse basis through the sum of absolute numbers of cDC1 and cDC2 totaling the whole cDC population and then proportion of cDC1/total cDC and cDC2/total cDC calculated and plotted.

C) Individual changes in the dendritic cell populations absolute numbers through ontogeny is plotted. cDC1 (black line), cDC2 (blue line) and pDC (red line).

All significance was noted as: *<0.05, **<0.01, ***<0.001, ***<0.0001.

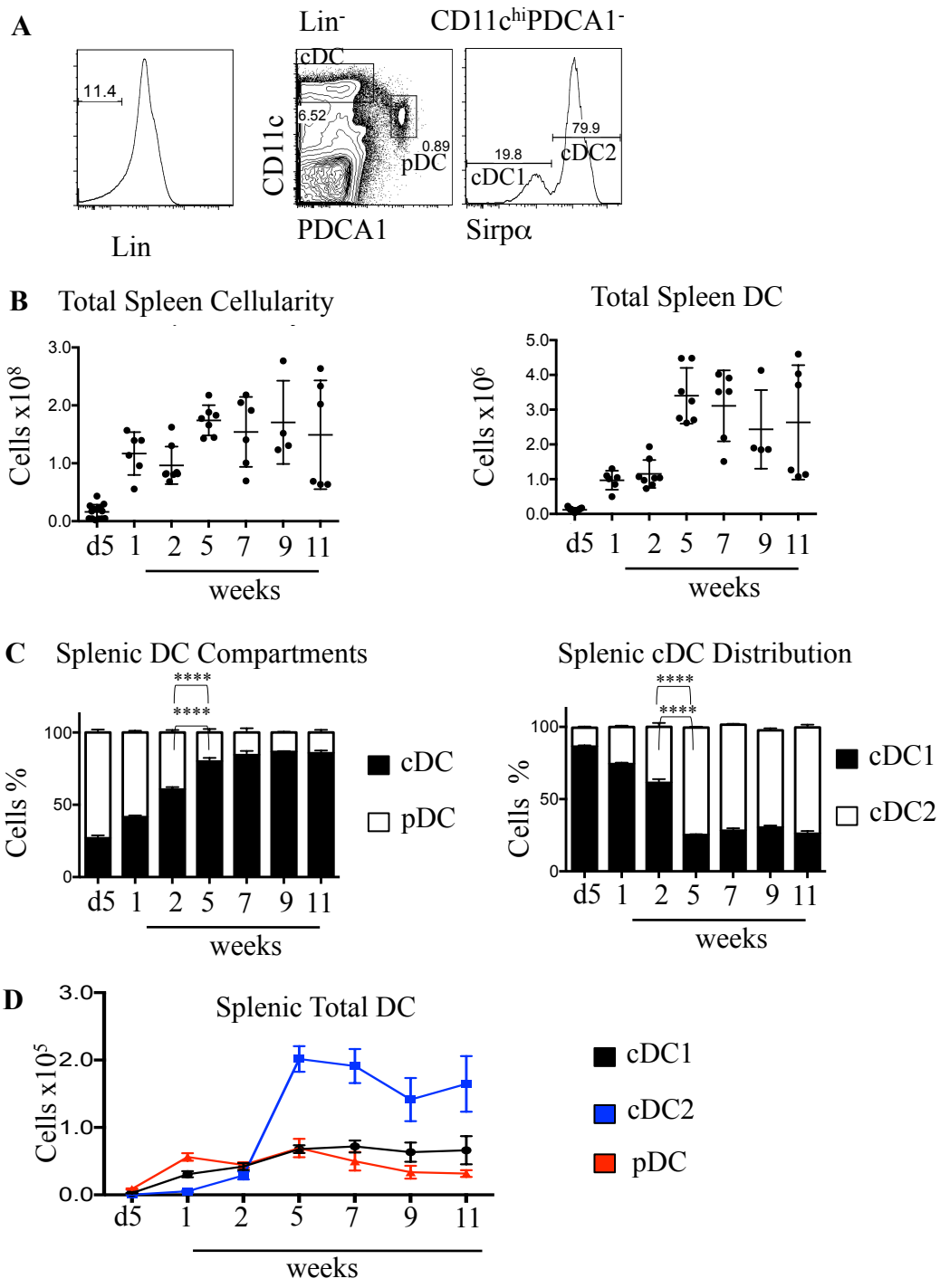
A
Lin-
CD11chiPDCA1-
11.4
Lin
cDC
6.52
0.89
pDC
CD11c
PDCA1
19.8
cDC1
79.9
cDC2
Sirpα
B
Total Spleen Cellularity
Cells x10^8
3.0
2.0
1.0
0.0
d5 1 2 5 7 9 11
weeks
Total Spleen DC
Cells x10^6
5.0
4.0
3.0
2.0
1.0
0.0
d5 1 2 5 7 9 11
weeks
C
Splenic DC Compartments
****
****
Cells %
100
50
0
cDC
pDC
d5 1 2 5 7 9 11
weeks
Splenic cDC Distribution
****
****
Cells %
100
50
0
cDC1
cDC2
d5 1 2 5 7 9 11
weeks
D
Splenic Total DC
Cells x10^5
3.0
2.0
1.0
0.0
d5 1 2 5 7 9 11
weeks
cDC1
cDC2
pDC

As a result, this shows that the spleen differs from the thymus (Figure 3.1 D) with the cDC2 population numerically being the most abundant DC subset maintained throughout adulthood. To determine if phenotypically DCs in the thymus differed from those seen in the spleen, their activation status was compared through flow cytometric analysis (Figure 3.3 A) with activated DCs defined as expressing high levels of CD86 and MHCII. Quantitation of the proportions of $MHCII^{lo}CD86^{lo}$ DC expressing subsets showed significantly higher proportions were present in the spleen for cDC1 and cDC2 than the thymus (Figure 3.3 B) and also in the reciprocal $MHCII^{hi}CD86^{hi}$ proportional analysis, there were increased proportions of cDC1 and cDC2 with an activated phenotype in the thymus compared to the spleen; again of significance. Therefore this data suggests that DCs acquire a greater level of activation in the thymus compared to the spleen.

To assess how DCs acquired this activation in thymus, it was decided to analyse their expression of CD40 and LTβR as previous studies suggest that signalling through these receptors stimulates upregulation of MHC and CD86 (Spidale et al., 2014, Kabashima et al., 2005, De Trez, 2012, Summers-DeLuca et al., 2007). Expression of CD40 and LTβR was determined through flow cytometry with comparisons to fluorescence minus one samples or isotypes, for all DC subsets (Figure 3.4 A). Data showed that all DC subsets had the capacity to express CD40 and LTβR with a shift in the positive staining profile compared to controls. The ability of DC to respond through these receptors was determined through in vitro cultures of total thymus with anti-CD40 or anti-LTβR compared to unstimulated controls (Figure 3.4 B). Samples were obtained following enzymatic digestion and transferred into a culture medium to undergo stimulation for a two-day period at 37°C with 10μg/ml of the stimulant added. Interestingly, culture alone caused some upregulation of DC activation with higher

Figure 3.3:
Dendritic Cells in Thymus Are More Activated Than Those In Spleen

A) Left panel shows summary plots of cDC1, cDC2 and pDC in the thymus when split on the basis of MHCII and CD86 to identify $MHCII^{hi}CD86^{hi}$ and $MHCII^{lo}CD86^{lo}$. Similarly this was done in the spleen in the right panel.

B) Quantitation to show the relative FACs percentages of $MHCII^{hi}CD86^{hi}$ and $MHCII^{lo}CD86^{lo}$ within the different dendritic cell populations. Comparisons are made for each dendritic cell population for the MHC/CD86 phenotype between the thymus (black bar) and the spleen (white bar). Data is from three independent experiments where n=9 for thymus, n=10 spleen.

All significance was noted as: *<0.05, **<0.01, ***<0.001, ***<0.0001.

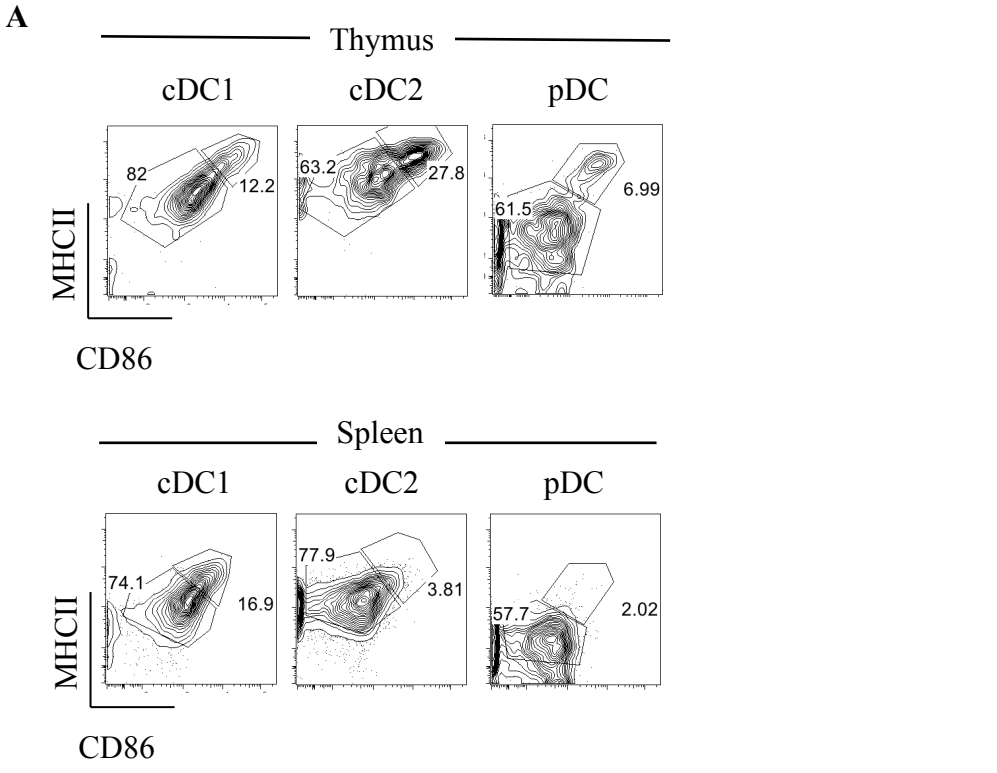
A
Thymus
cDC1
cDC2
pDC
82
12.2
63.2
27.8
61.5
6.99
MHCII
CD86
Spleen
cDC1
cDC2
pDC
74.1
16.9
77.9
3.81
57.7
2.02
MHCII
CD86
B
MHCIIloCD86lo
MHCIIhiCD86hi
Cells %
***
****
****
****
cDC1
cDC2
pDC
Thymus
Spleen

Figure 3.4:

Stimulation Of Dendritic Cells Through CD40 Supports A More Activated Dendritic Cell Phenotype In Thymus

A) Expression of CD40 (blue line) for each DC population in WT adult mice is plotted in the top panel against a sample stained without CD40 (grey plot). The lower panel shows LTβR expression (blue line) in thymic dendritic cells against the isotype control staining (grey plot).

B) Representative FACs plots of DC populations in thymus stained for CD86 and MHCII following total thymus cell suspension that were previously cultured with either culture medium alone (unstimulated), with anti-CD40 (middle panel) or with anti-LTβR (lower panel).

C) Quantitative analysis of the relative proportions of $MHCII^{hi}CD86^{hi}$ following different culture conditions with unstimulated (black bar), anti-CD40 (white bar) anti-LTβR (dark grey bar), or anti-CD40 in combination with anti-LTβR (pale grey bar). Results are representative of three independent experiments n=3.

All significance was noted as: *<0.05, **<0.01, ***<0.001, ***<0.0001.

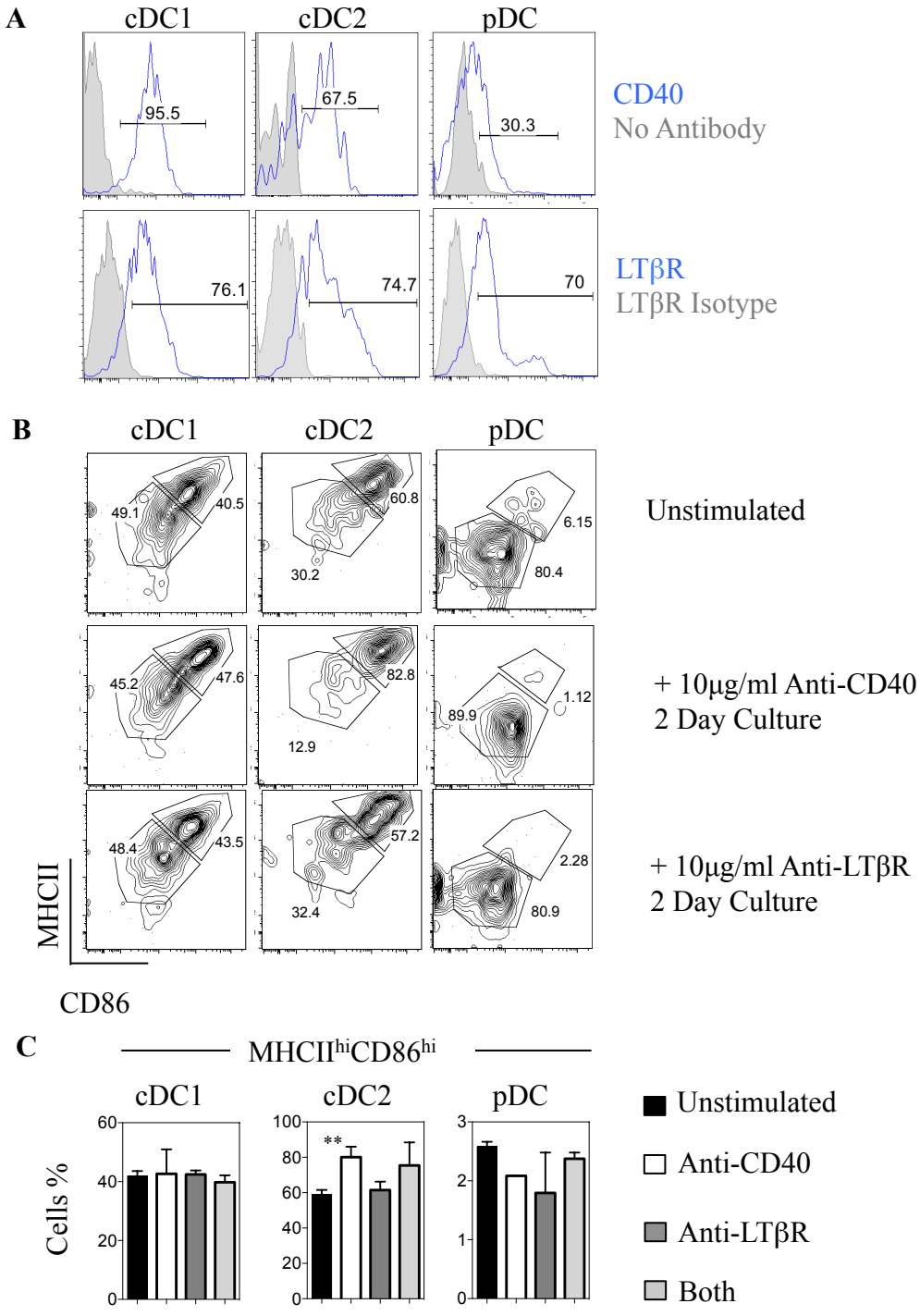
A
cDC1
cDC2
pDC
95.5
67.5
30.3
CD40
No Antibody
76.1
74.7
70
LTβR
LTβR Isotype
B
cDC1
cDC2
pDC
49.1
40.5
60.8
30.2
6.15
80.4
Unstimulated
45.2
47.6
82.8
12.9
89.9
1.12
+ 10µg/ml Anti-CD40
2 Day Culture
48.4
43.5
57.2
32.4
2.28
80.9
+ 10µg/ml Anti-LTβR
2 Day Culture
MHCII
CD86
C
MHCIIhiCD86hi
cDC1
cDC2
pDC
Cells %
60
40
20
0
100
80
60
40
20
0
**
3
2
1
0
Unstimulated
Anti-CD40
Anti-LTβR
Both

proportions of MHCII^{hi}CD86^{hi} cells than is usual in WT adult analysis. Stimulation with anti-CD40 however saw further upregulation of MHCII and CD86 expression for cDC2 activation and an increase was seen in cDC1 MHCII^{hi}CD86^{hi} proportions. However, with anti-LTβR treatment, there was no proportional DC activation increase. Quantitation of the proportions of MHCII^{hi}CD86^{hi} cells under culture stimulations (Figure 3.4 C), mirrored trends that could be seen in FACs analysis, with a significant increase in activation of cDC2 under anti-CD40 stimulation and a trend towards increased activation of cDC1. Additionally anti-LTβR treatment remained comparable to unstimulated controls with no synergistic effect with anti-CD40 and anti-LTβR (Figure 3.4 C).

3.2.2 Requirement For LTβR In The Regulation and Development of Thymic DC Populations

Due to the requirement for LTβR in the development of the medullary areas that are occupied by thymic DC along with the expression of LTβR by thymic DCs and previous reports suggesting a role for LTβR signalling in splenic DC populations (Kabashima et al., 2005, Lkhagvasuren et al., 2013), we explored how DCs in thymus may be affected by an absence of LTβR. To do this, we initially looked at the ontogeny of thymic DC in LTβR heterozygous (*Ltbr*$^{+/-}$) mice compared to LTβR deficient (*Ltbr*$^{-/-}$) mice that were littermate controls (Figure 3.5 A); again taking mice at specified ages following birth to examine dendritic cells. Analysis appeared to highlight that the LTβR heterozygous controls were comparable to the WT mice used in previous ontogeny analysis (Figure 3.1). Thymus cellularities between *Ltbr*$^{+/-}$ and *Ltbr*$^{-/-}$ mice were comparable throughout ontogeny (Figure 3.5 A left panel). However analysis of thymic DCs with age, indicated total numbers of DC were relatively distinct between mice strains from five weeks of age with significant reductions in total DC in

Ltbr$^{-/-}$ mice compared to *Ltbr*$^{+/-}$ control mice, with this maintained further into adulthood with another significant difference still seen at 9 weeks of age (Figure 3.5 A right panel). When this ontogeny variation was broken down more specifically into the DC populations (Figure 3.5 B), the reduced DC population at 5 weeks onwards correlated to reductions in both the cDC1 and pDC populations in adulthood. Plots showed that infact that cDC1 population had slowly increased with age until two weeks where from this point, cDC1 in *Ltbr*$^{-/-}$ mice then failed to continue increasing and instead went into a decline phase with significantly reduced cDC1 numbers seen at five and nine weeks of age. pDC in *Ltbr*$^{-/-}$ mice were similarly greatly increased in absolute numbers, following the trend of *Ltbr*$^{+/-}$ mice until two weeks of age from which point pDC absolute numbers fell greatly and this reduction was maintained at significance even at nine weeks of age. cDC2 on the other hand, had comparable total DC numbers throughout ontogeny to the control *Ltbr*$^{+/-}$ mice. Therefore this ontogeny suggests that LTβR may be regulating the maintenance of thymic DC populations, especially in the adult where cDC1 and pDC populations appear to be subsequently reduced.

Building on from this, we reassessed LTβR expression on DC and thymic stromal populations in adult mice. This was done through digestion of thymi, which differed according to the cell type being identified (specified in Methods), but was necessary to obtain optimal cell suspensions of target populations for surface staining with antibodies and analysis of LTβR expression by flow cytometry. When compared to the anti-LTβR isotype control antibody, there was expression of LTβR by all populations of both DC and thymic stroma with shifts in the expression profile (Figure 3.6 A). As a result, this allowed us to further explore the possible regulation of DCs by LTβR signalling as data suggested regulation could be possible

Figure 3.5:
Dendritic Cell Populations Are Altered During Development In LTβR Deficient Mice

All experimental timepoint analysis corresponds to the following sample numbers; *Ltbr*$^{+/-}$ E18 (n=6), d5 (n=7), 1 week (n=10), 2 weeks (n=7), 5 weeks (n=9), 7 weeks (n=4) *Ltbr*$^{-/-}$ E18 (n=8), d5 (n=13), 1 week (n=5), 2 weeks (n=3), 5 weeks (n=7), 7 weeks (n=6). All data points are from at least two experimental replicates.

A) Changes in total thymus cellularity during ontogeny (left panel). Alterations in absolute numbers of total thymic DC populations during ontogeny (right panel). LTβR$^{+/-}$ (red) compared to LTβR$^{-/-}$ (blue).

B) Breakdown of the total DC population into the cDC1, cDC2 and pDC for changes in absolute numbers across ontogeny analysis. Significant differences between *Ltbr*$^{+/-}$ (red) compared to *Ltbr*$^{-/-}$ (blue) are highlighted.

All significance was noted as: *<0.05, **<0.01, ***<0.001, ***<0.0001.

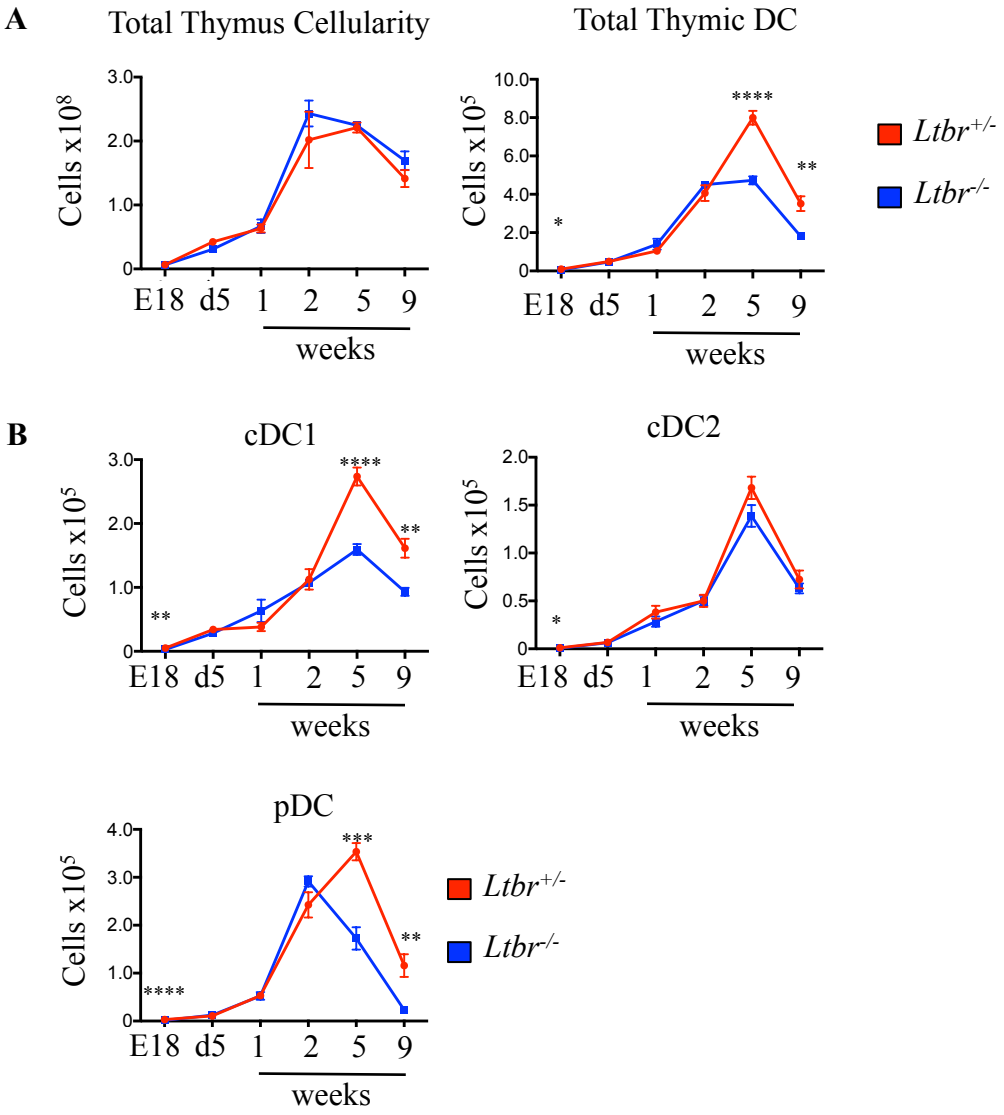
A
Total Thymus Cellularity
Cells x10^8
3.0
2.0
1.0
0
E18 d5 1 2 5 9
weeks
Total Thymic DC
Cells x10^5
10.0
8.0
6.0
4.0
2.0
0
****
**
*
E18 d5 1 2 5 9
weeks
Ltbr+/-
Ltbr-/-
B
cDC1
Cells x10^5
3.0
2.0
1.0
0
****
**
**
E18 d5 1 2 5 9
weeks
cDC2
Cells x10^5
2.0
1.5
1.0
0.5
0
*
E18 d5 1 2 5 9
weeks
pDC
Cells x10^5
4.0
3.0
2.0
1.0
0
***
**
****
E18 d5 1 2 5 9
weeks
Ltbr+/-
Ltbr-/-

Figure 3.6:

LTβR Is Expressed By Dendritic Cells and Stromal Cells In Thymus

A) Expression of LTβR by different dendritic cell populations (top panel) and expression of LTβR by stromal cell populations; total stroma ($CD45^-$), thymic epithelial cells (TEC $CD45^-$ $EpCAM\text{-}1^+$), mesenchymal cells ($CD45^-EpCAM\text{-}1^-Ter119^-PDPN^+CD31^-$), endothelial cells ($CD45^-EpCAM\text{-}1^-Ter119^-PDPN^-CD31^+$). Expression of LTβR by WT (blue line) compared to WT samples stained with LTβR isotype (grey). Results are representative of 3 n=4 across a minimum of 2 independent experiments.

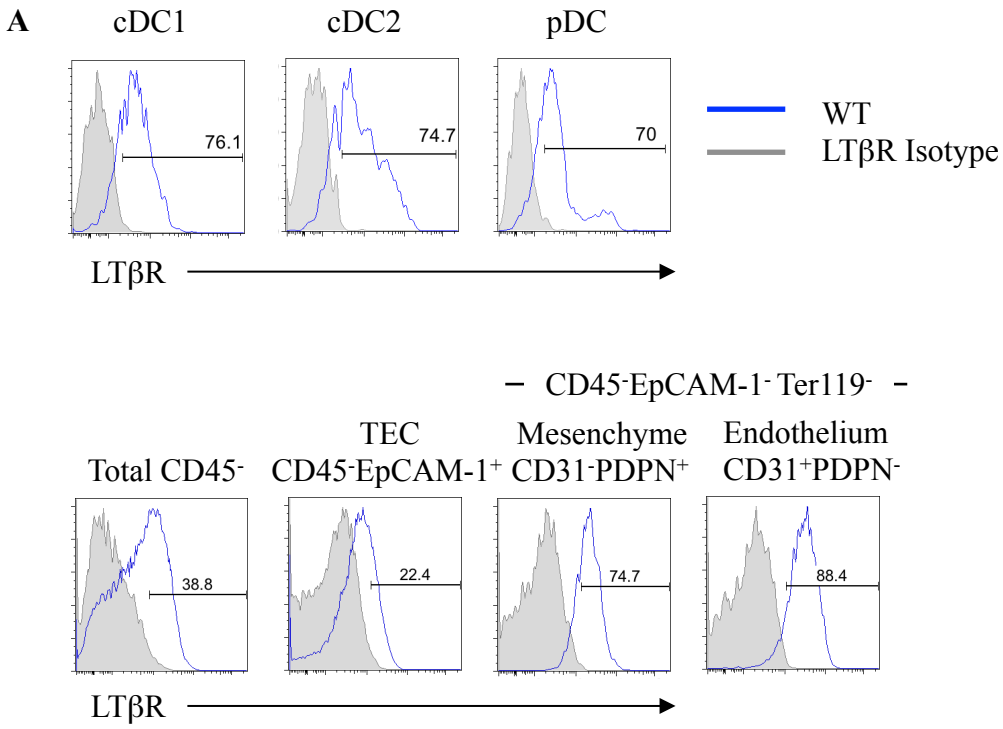
A
cDC1
cDC2
pDC
76.1
74.7
70
WT
LTβR Isotype
LTβR
CD45-EpCAM-1- Ter119-
Total CD45-
TEC
CD45-EpCAM-1+
Mesenchyme
CD31-PDPN+
Endothelium
CD31+PDPN-
38.8
22.4
74.7
88.4
LTβR

within the thymus directly via LTβR on DC cell-intrinsically or alternatively on thymic stromal cell populations in turn potentially regulating DC populations.

As a result, it was decided to focus on 8-12 week old adult mice deficient for LTβR (*Ltbr*$^{-/-}$) as during adulthood there was a marked reduction in thymic cDC1 and pDC seen in the ontogeny series (Figure 3.1). Therefore 8-12 week old *Ltbr*$^{-/-}$ mice were compared to WT controls for differences in thymic DC (Figure 3.7). FACS analysis of antibody stained thymus cell suspensions, showed that in the absence of LTβR there was a loss in total percentage of cDC that specifically mapped to reduced cDC1 proportions with a subsequently increased cDC2 proportion. Additionally pDC were almost absent from the thymus of *Ltbr*$^{-/-}$ mice (Figure 3.7 A). Quantitation in Figure 3.7 B showed no difference in the total thymus cellularity between the two strains, but there was a significant reduction in total pDC and cDC as well as cDC1 in the absence of LTβR. However cDC2 remained unchanged. Splenic analysis was also performed (Figure 3.7 C); highlighting initially that the cellularity of *Ltbr*$^{-/-}$ mice was far greater than WT controls which was attributable to their lack of lymph nodes (Figure 3.7 C). Furthermore, splenic analysis saw a reduction in total cDC that differentially mapped to cDC2 as well as pDC of *Ltbr*$^{-/-}$ mice also being reduced compared to WT controls (Figure 3.7 C). As a result, these findings from the adult mouse highlight a requirement for LTβR in the thymus to support the cDC1 and pDC populations but also that LTβR regulation of DC populations in the spleen is distinct from thymus mediated regulation.

However, whether this reduced DC phenotype was the consequence of reduced proliferation of the DC populations was unknown. As a result, BrdU incorporation was used as a measure of proliferation of thymic DC in WT and *Ltbr*$^{-/-}$ mice (Figure 3.8). For this, BrdU was injected

Figure 3.7:
LTβR Controls The Intrathymic Dendritic Cell Pool

A) Representative FACs plots showing alterations in the distribution of the dendritic cell populations in the thymus under the absence of LTβR (right panel) compared to WT controls (left panel). Lineage discrimination included the exclusion of CD3, CD19 and NK1.1 positively stained cells.

B) Absolute number analysis of total thymic cellularity and dendritic cell populations in thymus with WT (black bar) compared to $LT\beta R^{-/-}$ (white bar) mice. Data was obtained from at least 3 independent experiments with n=11 for WT and 12 for *Ltbr*$^{-/-}$ mice.

C) Splenic absolute number analysis of total cellularity and dendritic cell populations in WT (black bar) compared to *Ltbr*$^{-/-}$ (white bar). Data was again obtained from a minimum of three independent experiments, WT (11) and *Ltbr*$^{-/-}$ (12).

All significance was noted as: *<0.05, **<0.01, ***<0.001, ***<0.0001.

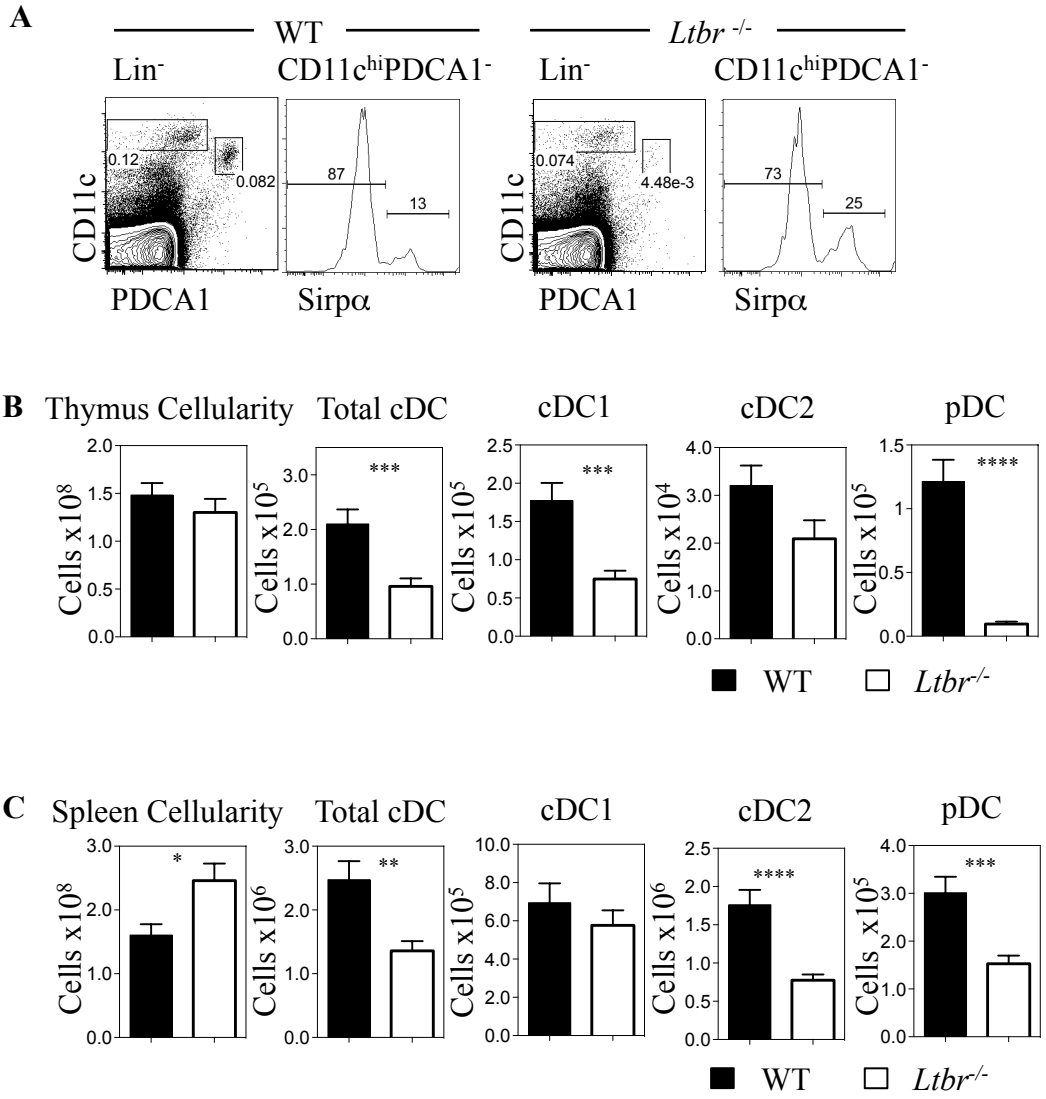
A
WT
Ltbr -/-
Lin-
CD11chiPDCA1-
Lin-
CD11chiPDCA1-
0.12
0.082
87
13
0.074
4.48e-3
73
25
CD11c
PDCA1
Sirpα
CD11c
PDCA1
Sirpα
B
Thymus Cellularity
Total cDC
cDC1
cDC2
pDC
Cells x10^8
Cells x10^5
Cells x10^5
Cells x10^4
Cells x10^5
***
***
****
WT
Ltbr-/-
C
Spleen Cellularity
Total cDC
cDC1
cDC2
pDC
Cells x10^8
Cells x10^6
Cells x10^5
Cells x10^6
Cells x10^5
*
**
****
***
WT
Ltbr-/-

Figure 3.8:

The Proliferation Capacity of Dendritic Cells Is Unaffected Under LTβR absence

A) FACs plots to demonstrate the relative proportions of $BrdU^{+}$ thymic dendritic cell populations in WT (top panel) and *Ltbr*$^{-/-}$ mice (bottom panel).

B) Proportional analysis of the dendritic cell populations in WT (black bar) were compared to *Ltbr*$^{-/-}$ mice (white bar). Data is from two independent experiments, WT (n=5) and *Ltbr*$^{-/-}$ mice (n=4).

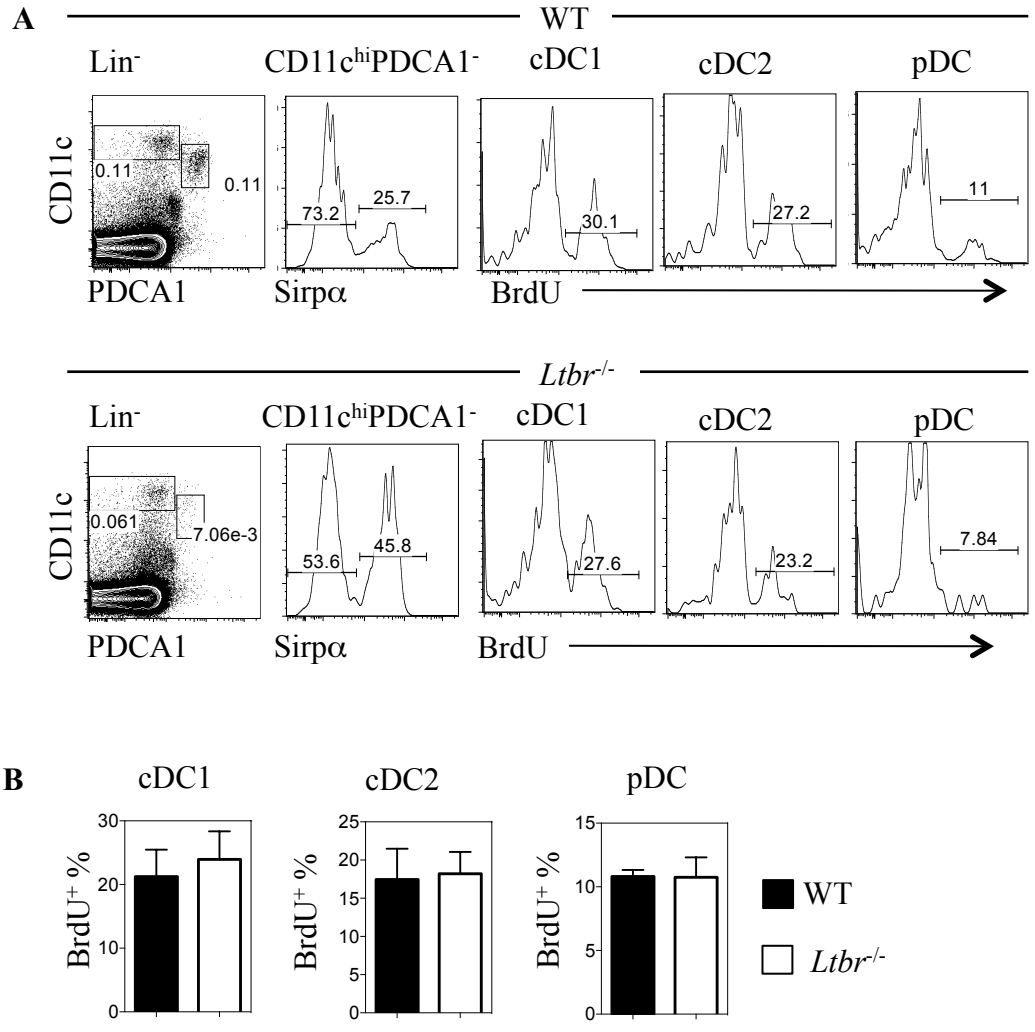
A
WT
Lin-
CD11chiPDCA1-
cDC1
cDC2
pDC
CD11c
0.11
0.11
73.2
25.7
30.1
27.2
11
PDCA1
Sirpα
BrdU
Ltbr-/-
Lin-
CD11chiPDCA1-
cDC1
cDC2
pDC
CD11c
0.061
7.06e-3
53.6
45.8
27.6
23.2
7.84
PDCA1
Sirpα
BrdU

B
cDC1
cDC2
pDC
BrdU+ %
30
20
10
0
25
20
15
10
5
0
15
10
5
0
WT
Ltbr-/-

intraperitoneally into experimental mice and mice were sacrificed 18 hours later for tissue harvest and analysis. Proportions of BrdU positive cells were used for analysis due to *Ltbr*$^{-/-}$ mice having defective numbers of thymic DC. The proliferation of thymic DCs was analysed in WT mice (Figure 3.8 A) with FACs plots showing the relative proportions of proliferating DC subsets. The split in the DC populations that were BrdU positive and therefore undergoing proliferation in WT mice remained at around 30% for WT cDC1 and cDC2 and slightly lower at around 10% for pDC populations. *Ltbr*$^{-/-}$ mice proportionally were shown to have comparable levels of DC proliferation to those recorded for WT (Figure 3.8 A). Quantitation of this confirmed that the proportion of proliferating DCs remained unchanged in *Ltbr*$^{-/-}$ mice compared to WT controls (Figure 3.8 B). Therefore this was suggestive that the defective DC populations seen in *Ltbr*$^{-/-}$ mice was not due to reduced DC proliferative capacity.

To further compartmentalise the effect of LTβR signalling on thymic DC populations, bone marrow chimeras were generated (Figure 3.9). Firstly, *Ltbr*$^{-/-}$ or WT T-cell depleted bone marrow was transferred into lethally irradiated WT host mice. After 8 weeks, the spleen and thymus were harvested for analysis of dendritic cell populations. In this situation, the phenotype seen in the spleen of the germline LTβR deficient mice (Figure 3.7 C) was recapitulated, with reduced total cDC and a significant cDC2 reduction in the spleen of the host post reconstitution. However, in the thymus of these chimeras, there was no significant reduction in any of the DC populations. This suggests that there is no cell intrinsic requirement for LTβR signalling in thymic DCs (Figure 3.9 A), as cDC1 and pDC that were reduced in the germline LTβR deficient mouse remained comparable to controls in this model.

Figure 3.9:

The Defect In Dendritic Cells In *Ltbr*$^{-/-}$ Mice Maps To LTβR Signals on Thymic Stroma

A) Generation of bone marrow chimeras with WT bone marrow reconstituting WT hosts (black bar) and *Ltbr*$^{-/-}$ bone marrow reconstituting WT hosts (white bar). Analysis of total cellularity and then dendritic cell populations in spleen (top panel) and thymus (bottom panel). Data is representative of a minimum of three independent experiments WT bone marrow (n=9) *Ltbr*$^{-/-}$ bone marrow (n=10).

B) Bone marrow chimeras were generated with WT bone marrow into either a WT host (black bar) or an *Ltbr*$^{-/-}$ host (white bar). Subsequent numerical analysis of total cellularity and dendritic cells is shown in spleen (top panel) and thymus (bottom panel). Data represents at least three independent experiments with WT host (n=15) and *Ltbr*$^{-/-}$ host (n=10).

All significance was noted as: *<0.05, **<0.01, ***<0.001, ***<0.0001.

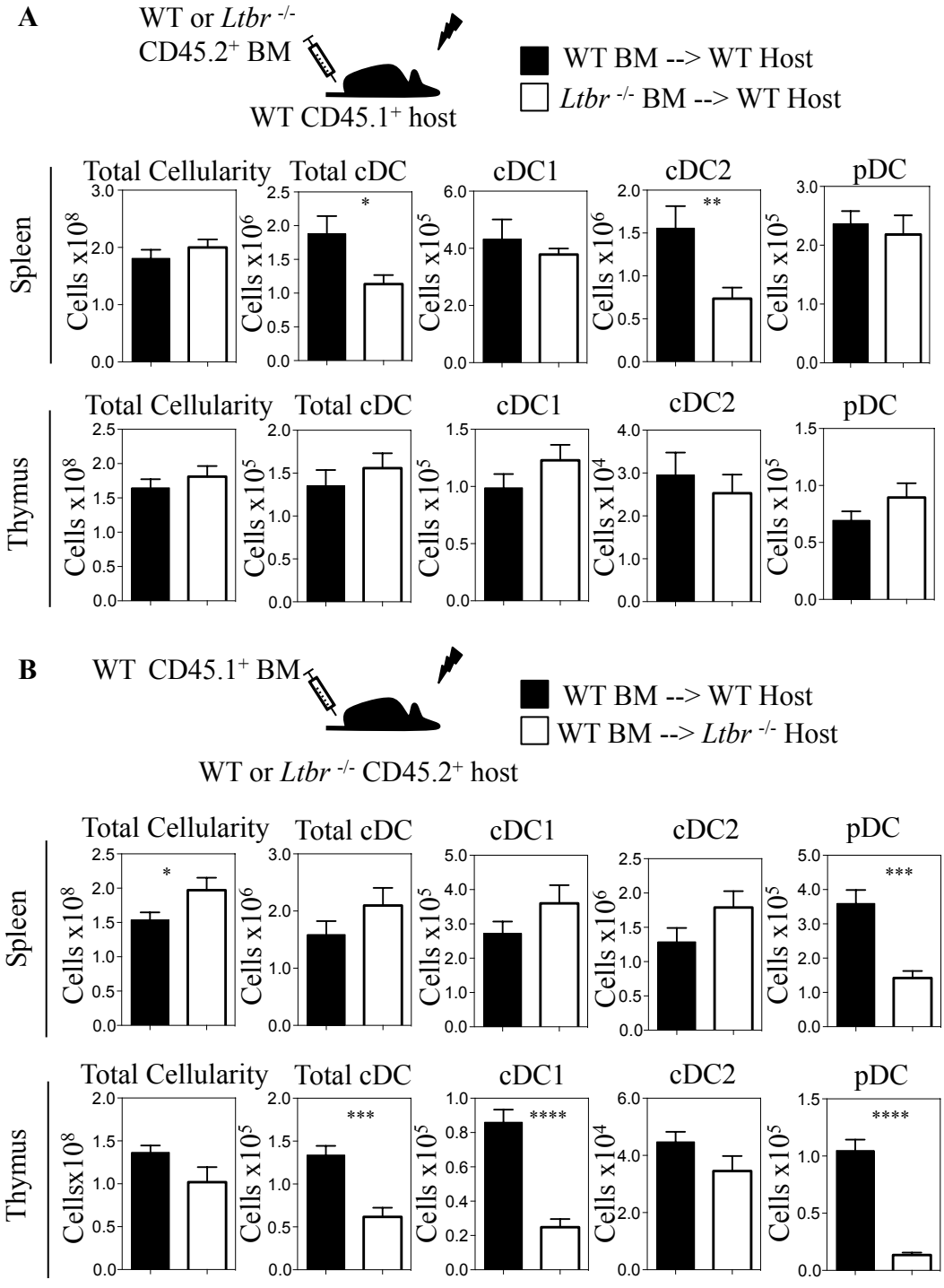
A
WT or Ltbr -/-
CD45.2+ BM
WT CD45.1+ host
WT BM --> WT Host
Ltbr -/- BM --> WT Host
Spleen
Thymus
Total Cellularity
Total cDC
cDC1
cDC2
pDC
Cells x10^8
Cells x10^6
Cells x10^5
Cells x10^4
*
**
B
WT CD45.1+ BM
WT or Ltbr -/- CD45.2+ host
WT BM --> WT Host
WT BM --> Ltbr -/- Host
***
****

The reverse bone marrow chimeras were therefore generated with *Ltbr*$^{-/-}$ or WT host mice being reconstituted with WT bone marrow following lethal irradiation exposure. In these chimeras, the spleen was comparable to control WT transfers, with regards to cDC2 although pDC were reduced (Figure 3.9 B). However the thymus of *Ltbr*$^{-/-}$ host mice reconstituted with WT bone marrow had a severe total cDC, cDC1 and pDC reduction which mirrored the germline mice. As a result this data is suggestive that the maintenance of thymic DC subsets is occurring through an indirect LTβR signalling mechanism on a stromal cell population within the thymus.

To further investigate the role of LTβR in thymic DC development, a kidney capsule transplant model was used. In this model, embryonic thymus lobes were treated with 2-deoxyguanosine to remove all hematopoietic cells (Figure 3.10 A). WT and *Ltbr*$^{-/-}$ cultured thymus lobes were transferred into host mice under the kidney capsule and left for 8 weeks. The corresponding reconstitution of grafted thymi by host cells was determined following this, with quantitation of the DC populations following graft retrieval and digestion for flow cytometric analysis (Figure 3.10 B). Where thymic stroma was *Ltbr*$^{-/-}$, there was a defect in DCs with total cDC, cDC1 and pDC being significantly reduced compared to WT controls. Therefore all of these models highlight the requirement for LTβR on thymic stroma to support the maintenance of thymic cDC1 and pDC.

3.2.3 Targeting of LTβR Deletion In Thymic Epithelial Cells

Due to the close association of thymic DCs with the medulla of the thymus, and their coordinated role in establishing central tolerance, there was questioning as to whether disruption of the medulla, previously reported to occur in the germline *Ltbr*$^{-/-}$ mice, was the

Figure 3.10:

Kidney Capsule Transplants With LTβR Deficient Grafts Highlight Stromal Requirement for LTβR in Intrathymic Dendritic Cell Regulation

A) Illustration of the set up for Kidney Capsule Transplant (KCT) and graft retrieval for analysis.

B) Absolute number analysis of the grafted thymi. WT hosts were grafted with WT grafts (black bar) or *Ltbr*$^{-/-}$ grafts (white bar) which are compared for the total cellularity and absolute numbers of dendritic cells. Data is representative of at least three experimental repeats with WT (n=9) an *Ltbr*$^{-/-}$ mice (n=10).

All significance was noted as: *<0.05, **<0.01, ***<0.001, ***<0.0001.

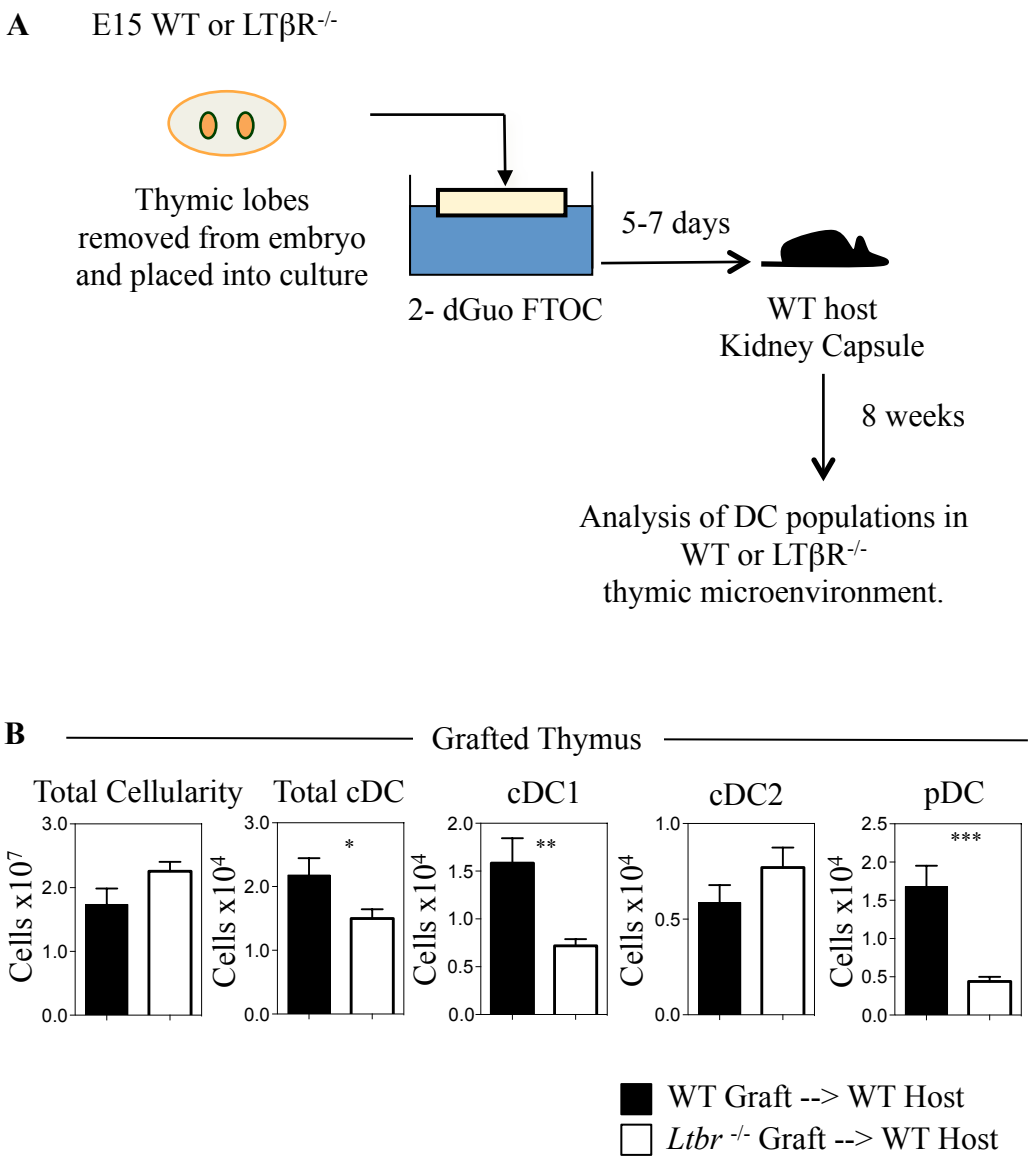
A
E15 WT or LTβR-/-
Thymic lobes
removed from embryo
and placed into culture
2- dGuo FTOC
5-7 days
WT host
Kidney Capsule
8 weeks
Analysis of DC populations in
WT or LTβR-/-
thymic microenvironment.
B
Grafted Thymus
Total Cellularity
Total cDC
cDC1
cDC2
pDC
Cells x10^7
Cells x10^4
*
**
***
WT Graft --> WT Host
Ltbr -/- Graft --> WT Host

reason for the defect in thymic DC (Boehm et al., 2003). To address this directly, mice were generated with LTβR specifically absent from thymic epithelial cells (Figure 3.11 A). These mice were generated by crossing *Foxn1*^{Cre} mice (Gordon et al., 2007) with *Ltbr*$^{fl/fl}$ mice (Wang et al., 2010b), to generate *Foxn1*^{Cre} x *Ltbr*$^{fl/fl}$ mice. In all cases, *Foxn1*^{Cre} mice were used as controls and going forward the resultant *Foxn1*^{Cre} x *Ltbr*$^{fl/fl}$ mice will be known as *Ltbr*^{TEC}. The deletion of LTβR from the thymic epithelial populations in the thymus of the *Ltbr*^{TEC} model was checked (Figure 3.11 B) and *Ltbr*^{TEC} expression of LTβR reflected the germline *Ltbr*$^{-/-}$ mouse; with positive expression shown in the *Foxn1*^{Cre}, used as a positive control. As a result, this proves that this model is functional and therefore can be used to address the impact of LTβR deficiency from thymic epithelial cells on thymic DC maintenance and the process of tolerance.

Further characterisation of these mice was necessary to analyse the impact of LTβR deletion from thymic epithelial cells. For this, visual comparisons were made between the control WT and *Foxn1*^{Cre} mice and the deletional germline *Ltbr*$^{-/-}$ and *Ltbr*^{TEC} mice (Figure 3.12 A). H&E analysis was conducted following freezing and sectioning of thymic tissue from the corresponding mice. Subsequent H&E staining showed that *Ltbr*$^{-/-}$ and *Ltbr*^{TEC} mice had the same structural appearance with disrupted and broken medullary areas spread throughout the cortex, compared to controls. Additional analysis was completed with confocal microscopy using antibodies to CD8 (to highlight the cortex areas) and mTEC specified by ERTR5 positive staining to highlight the medullary areas (Figure 3.12 B). Results suggest that the WT and *Foxn1*^{Cre} mice sections showed normal thymic architecture but in *Ltbr*$^{-/-}$ and *Ltbr*^{TEC} mice, numerous small medullary satellite areas could be seen. This data indicates that the structure of *Ltbr*^{TEC} mice mirrors that seen in *Ltbr*$^{-/-}$ mice and it provides a useful model to

Figure 3.11:

LTβR Deletion from Thymic Epithelial Cells Using Mouse Models Is Effective

A) Model of mouse crosses used to delete LTβR from thymic epithelial cells by generating $Ltbr^{TEC}$ mice.

B) LTβR expression on thymic epithelial cells ($CD45^{-}EpCAM\text{-}1^{+}$) from $Foxn1^{Cre}$ control mice (solid line) with $Ltbr^{-/-}$ mice (grey fill) and $Ltbr^{TEC}$ mice (dashed line). Data is representative of $Foxn1^{Cre}$ mice (n=9) $Ltbr^{-/-}$ and $Ltbr^{TEC}$ mice (n=10) across three independent experiments.

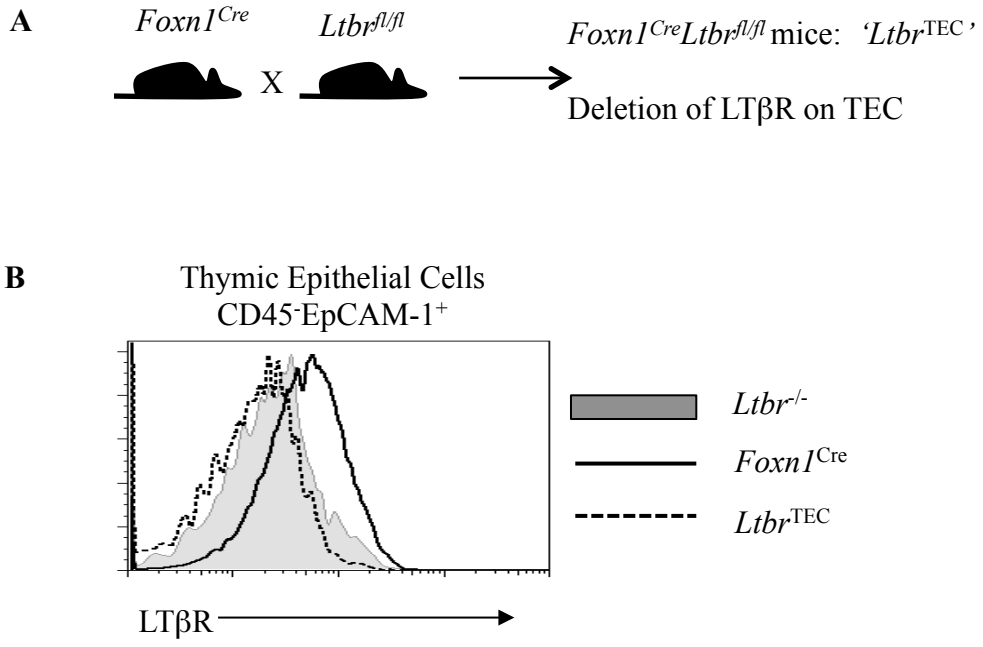
A
Foxn1Cre
Ltbrfl/fl
X
Foxn1CreLtbrfl/fl mice: 'LtbrTEC'
Deletion of LTβR on TEC
B
Thymic Epithelial Cells
CD45-EpCAM-1+
Ltbr-/-
Foxn1Cre
LtbrTEC
LTβR

Figure 3.12:

Absence of LTβR Causes Disruption of Medullary Areas

A) H&E staining of *Foxn1*^{Cre}, *Ltbr*^{TEC}, WT and *Ltbr*$^{-/-}$ thymus sections. Scale bar is equivalent to 500μm.

B) Confocal staining of thymus sections from *Foxn1*^{Cre}, *Ltbr*^{TEC}, WT and *Ltbr*$^{-/-}$ mice. Staining for CD8 (green) highlights cortical areas and ERTR5 (red) highlights mTEC areas. Data is typical of at least n=3 mice per strain for which three individual sections were taken throughout each thymus. Scale bar is equivalent to 500μm.

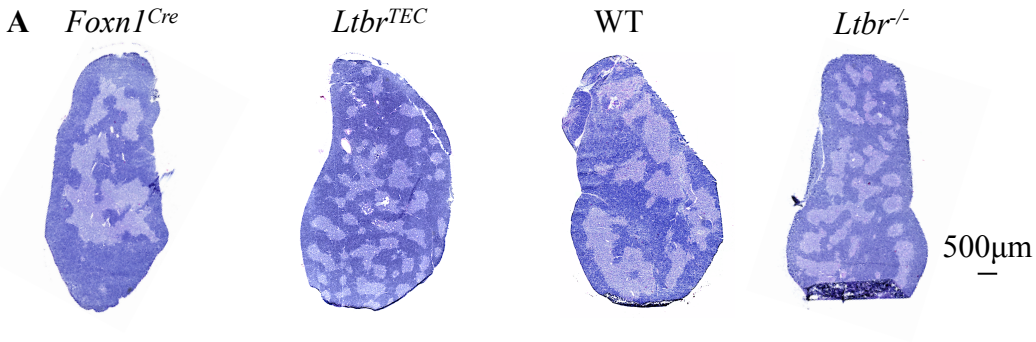
A
Foxn1Cre
LtbrTEC
WT
Ltbr-/-
500μm

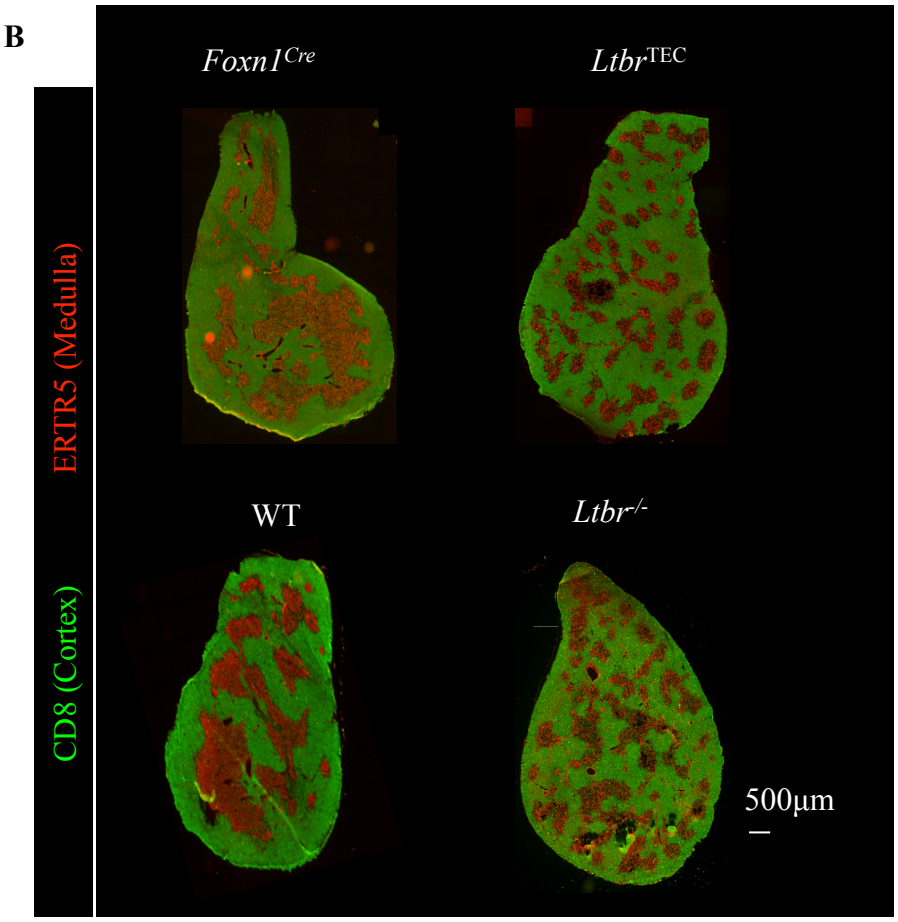
B
Foxn1Cre
LtbrTEC
WT
Ltbr-/-
ERTR5 (Medulla)
CD8 (Cortex)
500μm

study the impact of other cellular regulators of tolerance whereby thymic structure is specifically disorganised through absence of LTβR on TEC.

The disrupted thymic stromal populations in both *Ltbr*$^{-/-}$ and *Ltbr*^{TEC} mice raised the question as to whether and how the whole mTEC compartment was disrupted following TEC specific deletion of LTβR. Therefore *Ltbr*$^{-/-}$ and *Ltbr*^{TEC} adult mice were analysed for TEC populations (Figure 3.13 A). The corresponding proportions of mTEC subdivided on MHCII and CD80 showed that in the absence of LTβR, a shift in these mTEC subpopulations occurred with an increase in mTEC^{hi} to the detriment of the mTEC^{lo} population (Figure 3.13 A). Additionally absolute number analysis of WT and *Ltbr*$^{-/-}$ TEC (Figure 3.13 B) showed total thymus cellularity was unchanged between the WT and *Ltbr*$^{-/-}$ mice; but a reduction was seen in total TEC populations. There was however a reduction in total cortical thymic epithelial cells (cTEC), suggesting a role for LTβR regulation of the TEC compartment as a whole. When mTEC populations were broken down in *Ltbr*$^{-/-}$ mice, all subsets were reduced significantly with the reduction seen in the mTEC^{lo} and in particular the CCL21 expressing mTEC^{lo} population. Further quantitation of the ratio of the mTEC^{lo}:mTEC^{hi} saw that this was reduced in *Ltbr*$^{-/-}$ mice compared to WT control mice; suggesting a large reduction in the mTEC^{lo} with increased mTEC^{hi} compared to corresponding WT controls. Therefore this data highlights that in *Ltbr*$^{-/-}$ mice, disruption of the medulla is accompanied by defects in TEC populations suggesting a role for LTβR in mechanisms that control medullary structure (Figure 3.13 B).

To see whether a similar thymic disruption occurred when LTβR was specifically absent from TEC, FACs analysis was conducted in *Ltbr*^{TEC} thymi (Figure 3.14). Here it was clear that the distribution of the mTEC compartment, again related to an increase in the mTEC^{hi}

MHCII^{hi}CD80^{hi} expressing population in *Ltbr*^{TEC} mice when compared with *Foxn1*^{Cre} control mice (Figure 3.14 A). Interestingly at an absolute number level the same trend could be seen to the germline *Ltbr*$^{-/-}$ mice, with no difference in total thymus cellularity but reduced total TEC, reduced mTEC and mTEC subpopulations (Figure 3.14 B). In *Ltbr*^{TEC} mice mTEC^{lo} and CCL21^{+}mTEC^{lo} populations were predominately reduced against *Foxn1*^{Cre} control mice. The ratio when calculated to compare the mTEC^{lo} to the mTEC^{hi} compartment indicated the loss of the mTEC^{lo} population to the advantage of the mTEC^{hi} population. As a result this data mirrors the main trends in mTEC alteration seen in the germline *Ltbr*$^{-/-}$ mice (Figure 3.13), highlighting a cell intrinsic signalling requirement for LTβR on TEC for mTEC development.

3.2.4 Thymic Absence Of LTβR and Its Impact on Tolerance

Considering the medullary disruption that follows under the absence of LTβR on TEC, (Figure 3.13, 3.14), it remained unknown as to the consequence of this. This is of interest given the DC reduction in the *Ltbr*$^{-/-}$ mice and the role of the medulla in negative selection and T-Regulatory cell generation. To consider this, mice were investigated for autoantibodies and inflammatory infiltrates.

To begin with, infiltrates were investigated in the liver of WT, *Foxn1*^{Cre}, *Ltbr*$^{-/-}$ and *Ltbr*^{TEC} mice with livers being freshly isolated and frozen in liquid nitrogen before being sectioned for analysis. H&E staining was used to identify infiltrates within the tissue through microscope visualization. Infiltrates were determined and clusters of more than 25 cells were counted as a cellular infiltrate (Figure 3.15 A). Quantitation of cellular infiltrates/cm^2 of each section highlighted that there was abundance of cellular infiltrates in *Ltbr*$^{-/-}$ mice. Visually these

Figure 3.13:
Thymic Epithelial Cells Are Reduced Under LTβR Absence

A) Plots to show the distribution of $mTEC^{hi}$ and $mTEC^{lo}$ populations separated based upon MHCII and CD80 expression following previous mTEC gating ($CD45^{-}EpCAM\text{-}1^{+}Ly51^{-}UEA\text{-}1^{+}$).

B) Absolute number analysis of thymus in WT and *Ltbr*$^{-/-}$ mice with total cellularity and TEC populations. Comparing WT mice (black bar) with *Ltbr*$^{-/-}$ mice (white bar). WT mice (n=12) and *Ltbr*$^{-/-}$ mice (n=11) from three experimental repeats. Work for this was completed in collaboration with Kieran James.

All significance was noted as: *<0.05, **<0.01, ***<0.001, ***<0.0001.

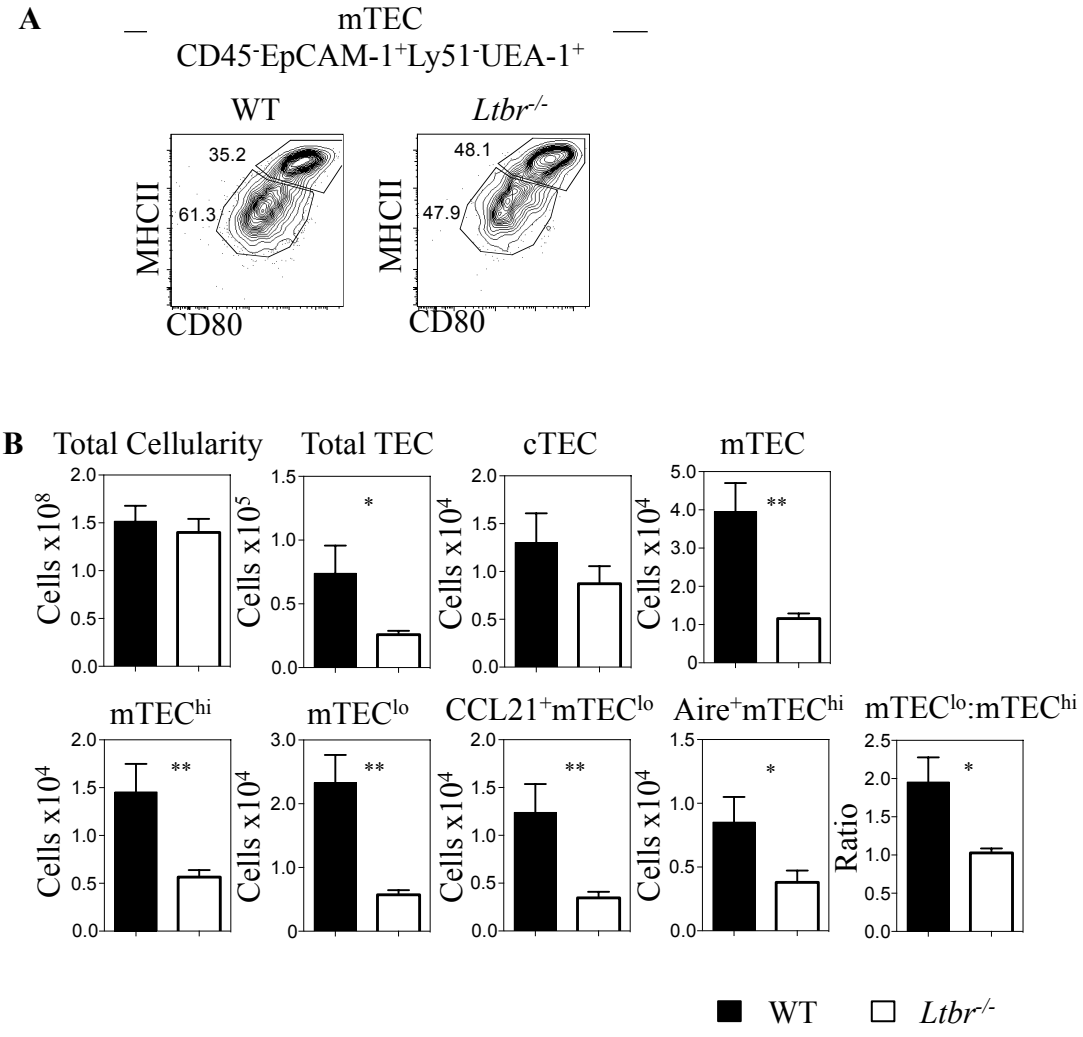
A
mTEC
CD45-EpCAM-1+Ly51-UEA-1+
WT
Ltbr-/-
35.2
61.3
48.1
47.9
MHCII
CD80
B
Total Cellularity
Total TEC
cTEC
mTEC
mTEChi
mTEClo
CCL21+mTEClo
Aire+mTEChi
mTEClo:mTEChi
Cells x10^8
Cells x10^5
Cells x10^4
Ratio
WT
Ltbr-/-

Figure 3.14:
***Ltbr*^{TEC} Mice Have Reduced Thymic Epithelial Cell Populations**

A) FACs plots representative of the mTEC (CD45^{-}EpCAM-1^{+}Ly51^{-}UEA-1^{+}) distribution between mTEC^{hi} (MHCII^{hi}CD80^{hi}) and mTEC^{lo} (MHCII^{lo}CD80^{lo}) compartments in *Foxn1*^{Cre} and *Ltbr*^{TEC} mice.

B) Analysis of thymus total cellularity and absolute numbers of TEC populations in *Foxn1*^{Cre} control mice (black bar) and *Ltbr*^{TEC} mice (white bar); n=12 for both groups performed from a minimum of three independent experiments. Work for this was completed as collaboration with Kieran James.

All significance was noted as: *<0.05, **<0.01, ***<0.001, ***<0.0001.

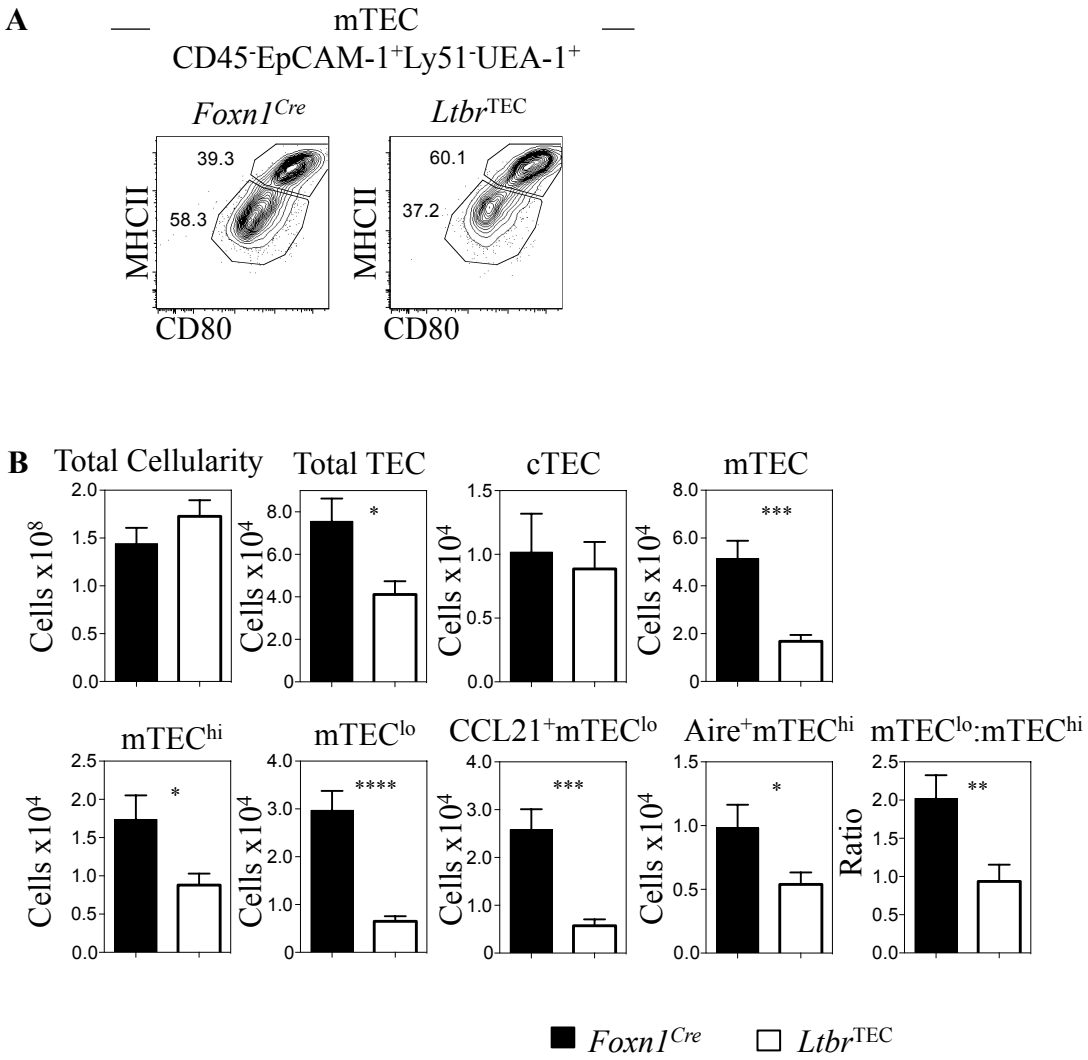
A
mTEC
CD45-EpCAM-1+Ly51-UEA-1+
Foxn1Cre
LtbrTEC
39.3
58.3
60.1
37.2
MHCII
CD80
B
Total Cellularity
Total TEC
cTEC
mTEC
mTEChi
mTEClo
CCL21+mTEClo
Aire+mTEChi
mTEClo:mTEChi
Cells x10^8
Cells x10^4
Ratio
*
***
****
**
Foxn1Cre
LtbrTEC

Figure 3.15:

Absence of LTβR Results In An Autoimmune Phenotype That Doesn't Map To A Thymic Stromal Requirement For LTβR

A) Analysis of cellular infiltrates in the liver of the four mouse groups. Representative infiltrate images (left panel) with quantitation seen in the right panel. This was calculated as mean cellular foci/cm^2 of tissue section with at least 5 sections cut per tissue per mouse; *Ltbr*$^{-/-}$ (black bar), *Ltbr*^{TEC} mice (white bar), *Foxn1*^{Cre} mice (dark grey bar) and WT mice (light grey bar). *Ltbr*$^{-/-}$ (n=4), *Ltbr*^{TEC} (n=3), *Foxn1*^{Cre} (n=3) and WT (n=3).

B) Stomach autoantibody analysis with representative plots at 1:80 dilution (left panel). Arbitrary scores were assigned based on intensity of fluorescence per image, correlating to the level of autoantibodies detected (green staining) with a DAPI counterstain (red). Scores were assigned from 0-6 with 0 being no infiltrates detected and 6 being most infiltrates seen (right panel). *Ltbr*$^{-/-}$ mice (black bar), *Ltbr*^{TEC} mice (white bar), *Foxn1*^{Cre} mice (dark grey bar) and WT mice (light grey bar). *Ltbr*$^{-/-}$ (n=6), *Ltbr*^{TEC} (n=5), *Foxn1*^{Cre} (n=5) and WT (n=5).

C) Segmented plots indicate autoantibody presence in the stomach, liver and kidney of the four mouse groups. A black segment represents autoantibodies detected at a 1:20 dilution factor and a grey segment indicates no autoantibodies; each segment is an individual mouse.

All significance was noted as: *<0.05, **<0.01, ***<0.001, ***<0.0001.

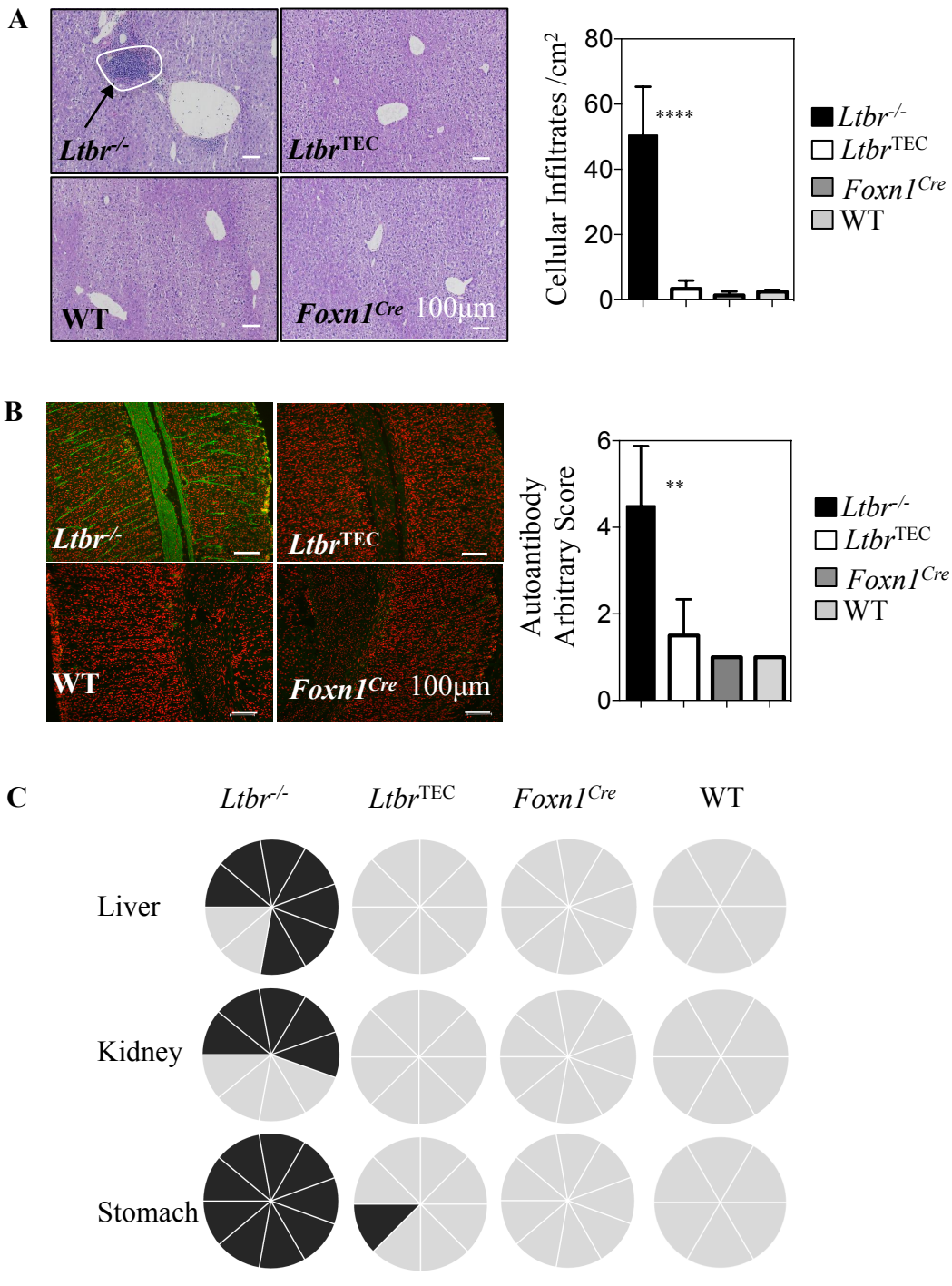
A
Ltbr-/-
LtbrTEC
WT
Foxn1Cre
100µm
Cellular Infiltrates /cm2
80
60
40
20
0
****
Ltbr-/-
LtbrTEC
Foxn1Cre
WT
B
Ltbr-/-
LtbrTEC
WT
Foxn1Cre
100µm
Autoantibody Arbitrary Score
6
4
2
0
**
Ltbr-/-
LtbrTEC
Foxn1Cre
WT
C
Ltbr-/-
LtbrTEC
Foxn1Cre
WT
Liver
Kidney
Stomach

clusters of infiltrates were seen in representative plots shown in Figure 3.15 A in *Ltbr*$^{-/-}$ mice. Furthermore, analysis into the presence of autoantibodies was conducted with serum from these mice obtained prior to sacrifice and applied to tissue sections to determine the level of autoreactive antibodies. This could be visualised through fluorescent tagging of bound autoantibodies to tissue sections with staining against the stomach (shown as green staining), detected in the germline *Ltbr*$^{-/-}$ mouse serum (Figure 3.15 B). This was quantitated through an arbitrary score system (detailed in the methods) with a higher score given to a greater intensity of autoantibody detection, correlating to a higher level of green staining in sections. The presence of autoantibodies in *Ltbr*$^{-/-}$ mice was shown with higher arbitrary scores awarded compared to controls and *Ltbr*^{TEC} mice.

Additional autoantibody analysis was completed at a 1:20 dilution of serum which was added to sections of kidney and liver as well as the stomach as previously shown and analysed in Figure 3.15 C. Here segmental plots have been shown, with each segment representing analysis in one mouse. *Ltbr*$^{-/-}$ mice had autoantibodies detected in all mice (9/9) for the stomach, 5/9 mice for the kidney and 7/9 suffered from autoantibodies in the liver. However, in *Ltbr*^{TEC} mice, one mouse had autoantibodies detected in the stomach, with all other mice analysed failing to show any autoantibodies. As a result this data appears to reveal that there is autoimmune manifestation in mice that are germline knockout for LTβR only. From this, *Ltbr*^{TEC} mice appear to support a normal phenotype with regards to autoimmunity despite the disruption in the medullary compartment, separating the so far identical phenotype between *Ltbr*^{TEC} and *Ltbr*$^{-/-}$ mice.

To address what may be responsible for tolerance breakdown in *Ltbr*$^{-/-}$ mice, it was decided to look at the presence of transcriptional regulators in the thymus of the four mouse strains. This was necessary as the transcriptional regulators Fezf2 and Aire have been shown to be required to drive expression of tissue restricted antigens (TRAs) in the thymus, which in turn are presented on the cell surface of mTEC for the screening of developing thymocytes and central tolerance induction (Takaba et al., 2015, Anderson et al., 2002). Analysis for this was done through confocal microscopy (Figure 3.16) to look at Aire and Fezf2 transcription factor expression on frozen thymus sections. Aire expression was shown as green staining and Fezf2 expression through red staining, both stained along with ERTR5 (blue) to highlight medullary areas of the thymus through mTEC recognition. Analysis appeared to show that expression of Aire and Fezf2 was unperturbed in *Ltbr*$^{-/-}$ and *Ltbr*^{TEC} mice with comparable levels of positive cells seen to WT and *Foxn1*^{Cre} control mice with high magnification (x40) (Figure 4.16 A). Similarly when looking at a low magnification (x10), the distribution of these positive cells appeared to again remain comparable between the strains (Figure 4.16 B). This highlights that the presence of transcriptional regulators of self-antigen expression remain comparable, which is fundamental for central tolerance. It therefore argues against the idea that lack of transcription factor expression under absence of LTβR is the reason for the autoimmunity seen in the germline *Ltbr*$^{-/-}$ mice.

However, the autoimmunity seen in the *Ltbr*$^{-/-}$ but not *Ltbr*^{TEC} mice, despite normal transcriptional regulator expression, still highlights that an additional mechanism remains disrupted to result in autoimmunity in these germline mice. To further consider this, T-Regulatory cells were analysed as they develop intrathymically but act to suppress autoreactive T-cells in the periphery that have escaped negative selection preventing

Figure 3.16:

Absence of LTβR Does Not Cause Alterations In The Presence Of Transcriptional Regulators Fezf2 and Aire

A) Confocal images of thymus from WT, *Ltbr*$^{-/-}$, *Foxn1*^{Cre}, *Ltbr*^{TEC} mice. Staining in the far left panel for Aire (green) and the mTEC marker ERTR5 (blue), middle panel Fezf2 (red) and ETR5 (blue), right panel is a merge of Aire (green), Fezf2 (red) and ERTR5 (blue). Images taken at high magnification x40 with 2.3x zoom (A).

B) Confocal images again from the thymus of the four mice strains, but this time at a high power magnification x40 with a 1x zoom. Comparing Aire (green) and ERTR5 (blue) in the left panel and Fezf2 (red) and ERTR5 (blue) in the right panel.

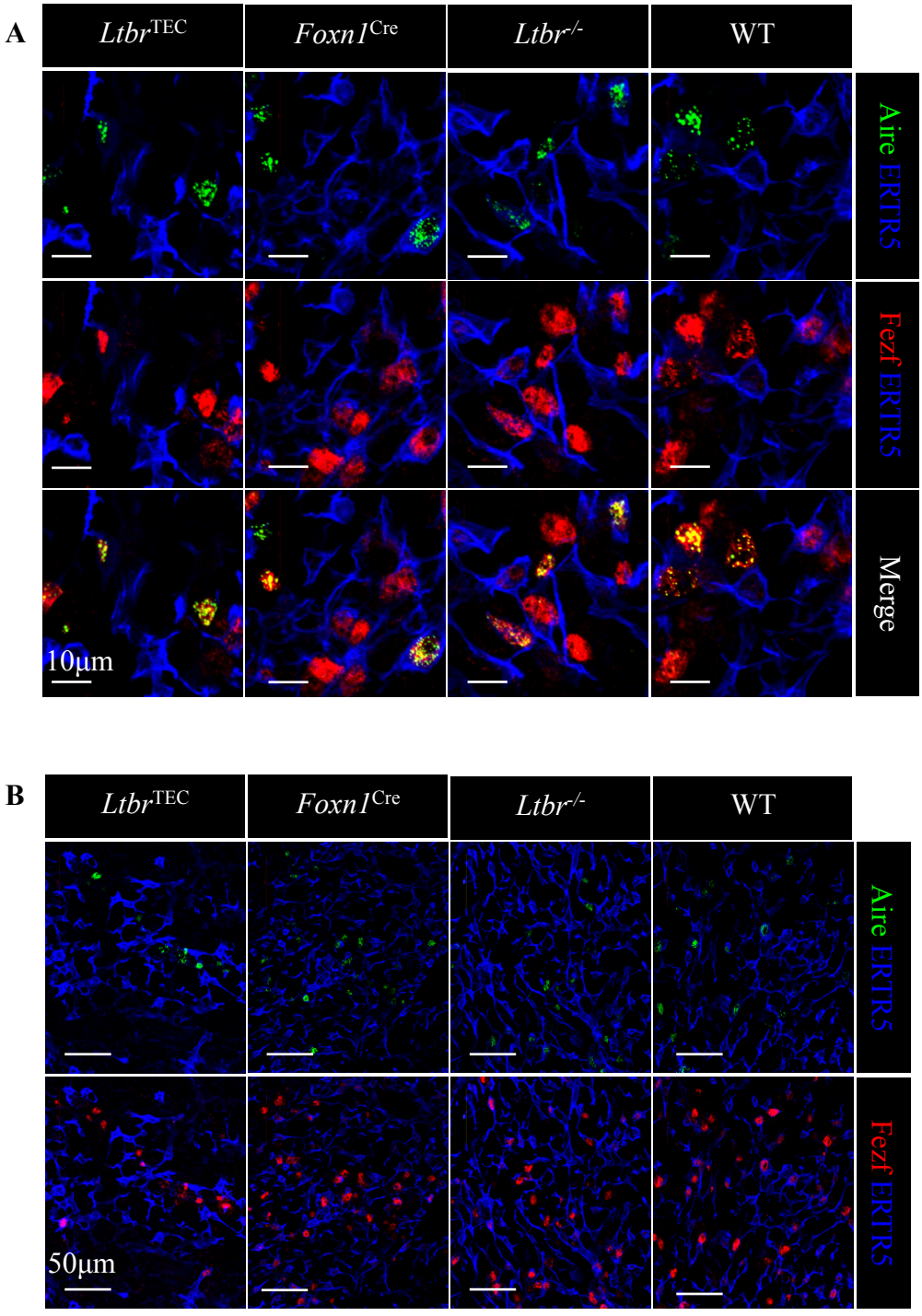
A
Ltbr^TEC
Foxn1^Cre
Ltbr^-/-
WT
Aire ERTR5
Fezf ERTR5
Merge
10μm
B
Ltbr^TEC
Foxn1^Cre
Ltbr^-/-
WT
Aire ERTR5
Fezf ERTR5
50μm

autoimmune manifestations. T-Regulatory populations were identified in the thymus of WT and *Ltbr*$^{-/-}$ mice as thymus tissue was freshly isolated and disaggregated to obtain thymocyte suspensions for analysis by FACs (Figure 3.17 A). T-regulatory populations were further subdivided upon CCR7 expression into newly generated (CCR7^{+}) and those recirculating from the periphery (CCR7^{-}). This was conducted as it has previously been shown that acquisition of CCR7 expression directly correlates to newly generated T-cells through Rag2GFP models and further heterogeneity within the T-regulatory cell pool could be distinguished by CCR7 expression to discount recirculating CCR7^{-} T-regulatory cells (Cowan et al., 2016). The representative FACs distribution of T-Regulatory cells through this division was similar between WT and *Ltbr*$^{-/-}$ mice (Figure 3.17 A). Quantitative analysis confirmed no difference in absolute numbers of T-Regulatory cells between WT and *Ltbr*$^{-/-}$ mice at a total level or under CCR7 subdivision (Figure 3.17 B). Similar analysis in the *Ltbr*^{TEC} mice and *Foxn1*^{Cre} controls showed that proportions of T-Regulatory cells and the breakdown on CCR7 expression were alike between these mice (Figure 3.17 C). When absolute numbers were analysed (Figure 3.17 D), there was no significant difference in total T-Regulatory cells and there was a comparable split based upon CCR7 expression also. As a direct result, there is no requirement for LTβR signalling either totally or specifically on TEC to drive development of T-Regulatory cells in thymus.

3.2.5 Thymic Absence Of LTβR and Consequential Impact on Thymic DC and Negative Selection

Having considered TEC disruption, transcriptional regulators, T-Regulatory populations and showing comparability in these areas between *Ltbr*$^{-/-}$ and *Ltbr*^{TEC} mice, the reasoning for tolerance breakdown in *Ltbr*$^{-/-}$ mice, still remained incompletely addressed. Therefore the

Figure 3.17:

T-Regulatory Cells Develop Intrathymically Independently Of LTβR

A) Representative FACs plots illustrating proportions of Treg (left plot) for both WT and *Ltbr*$^{-/-}$ mice pre-gated on CD4^{+}TCRβ^{hi} expression. Treg are then identified as being CD4^{+}TCRβ^{hi} Foxp3^{+}CD25^{+} then split on expression of CCR7 (right plot).

B) Absolute number analysis of thymus from WT (black bar) and *Ltbr*$^{-/-}$ (white bar) for total Treg, and then subsequently those that were CCR7 expressing or not. Data was obtained from three independent experiments WT mice (n=9) and *Ltbr*$^{-/-}$ mice (n=9).

C) Representative FACs plots as in (A) but looking at *Foxn1*^{Cre} and *Ltbr*^{TEC} mice for Treg populations.

D) Absolute number analysis of the thymus of *Foxn1*^{Cre} (black bar) and *Ltbr*^{TEC} (white bar) mice for total Treg and CCR7$^{+/-}$ subpopulations. All data was from three independent experiments *Foxn1*^{Cre} mice (n=8) and *Ltbr*^{TEC} mice (n=7).

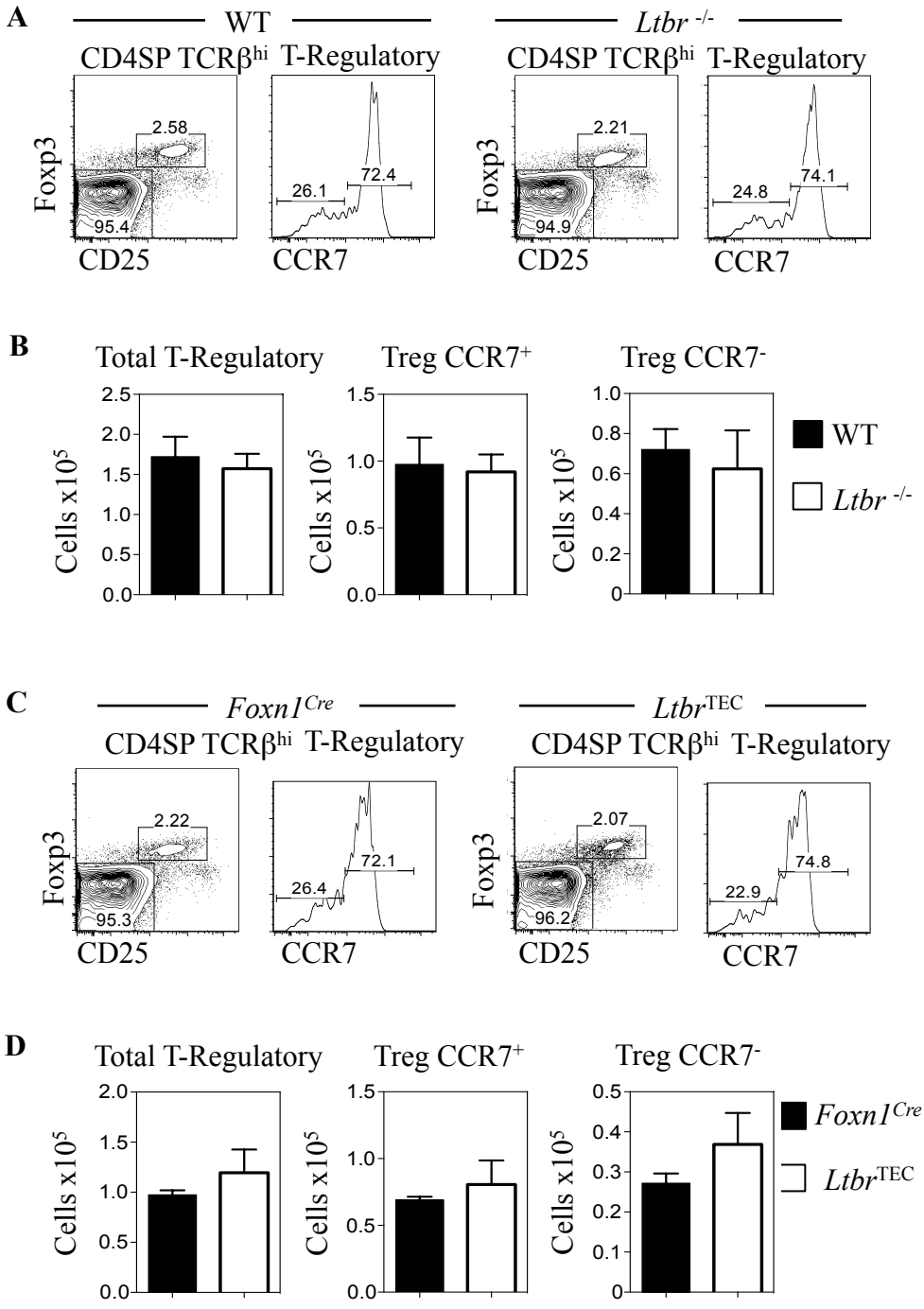
A
WT
Ltbr -/-
CD4SP TCRβhi T-Regulatory
CD4SP TCRβhi T-Regulatory
Foxp3
CD25
2.58
95.4
CCR7
26.1
72.4
2.21
94.9
24.8
74.1
B
Total T-Regulatory
Treg CCR7+
Treg CCR7-
Cells x10^5
WT
Ltbr -/-
C
Foxn1Cre
LtbrTEC
2.22
95.3
26.4
72.1
2.07
96.2
22.9
74.8
D
Foxn1Cre
LtbrTEC

remaining aspect related to central tolerance that was necessary to investigate was thymic DCs. It had already been shown that under the absence of LTβR there was a reduction in cDC1 and pDC (Figure 3.7), and it was in this germline analysis that tolerance appeared to be broken (Figure 3.15). However to correlate these two findings together it was firstly important to rule out that altered DC populations were not seen in $Ltbr^{TEC}$ mice which may contain alternative compensatory mechanisms preventing the break of tolerance in this model (Figure 3.18). For this, freshly isolated thymi were prepared for flow cytometric analysis to identify DC populations. FACs analysis highlighted that all DC populations could be identified in the thymus of $Ltbr^{TEC}$ mice, equivalently to $Foxn1^{Cre}$ controls (Figure 3.18 A). Analysis of absolute numbers from this showed no difference in thymus cellularity or in cDC1 or pDC that had been reported to be altered in the germline $Ltbr^{-/-}$ mice. However there was an increase in cDC2 in the $Ltbr^{TEC}$ mice compared to $Foxn1^{Cre}$ controls. Splenic analysis showed that by FACs the DCs could again be identified and equivalent proportions were seen between the two strains (Figure 3.18 C). Absolute number analysis showed no effect on any peripheral DC populations. This data as a result emphasises that the absence of LTβR from TEC does not disrupt DC populations; despite the obviously altered medullary architecture and reduced mTEC numbers which appear to be distinct from DC regulation in this analysis (Figure 3.14). However despite the lack of any DC numerical reductions in $Ltbr^{TEC}$ mice, we questioned if the disrupted medulla was indeed capable of still having some impact on proliferation of DC, causing functional abnormalities in $Ltbr^{TEC}$ mice. To assess this, BrdU incorporation was used with $Ltbr^{TEC}$ mice and $Foxn1^{Cre}$ control mice injected with BrdU intraperitoneally, before being harvested 18 hours later for thymic analysis of DC populations by flow cytometry. Proportions of BrdU positive DCs remained comparable to one another between $Ltbr^{TEC}$ and $Foxn1^{Cre}$ mice (Figure 3.19 A), but also in addition, proportions were in the same range as

Figure 3.18:
Dendritic Cells In Thymus Are Unaffected In *Ltbr*^{TEC} mice

A) Representative FACs plots illustrating the dendritic cell populations in the thymus in *Foxn1*^{Cre} and *Ltbr*^{TEC} mice. Lineage again includes the exclusion of CD19, CD3 and NK1.1.

B) Analysis of absolute numbers for thymus cellularity and thymic dendritic cell populations in *Foxn1*^{Cre} control mice (black bar) and *Ltbr*^{TEC} mice (white bar). Data is representative of three experiments where n=10.

C) Representative FACs plots of the splenic dendritic cell populations in *Foxn1*^{Cre} and *Ltbr*^{TEC} mice. Similarly lineage excludes CD19, CD3 and NK1.1.

D) Splenic absolute number analysis of total cellularity and dendritic cells. *Foxn1*^{Cre} mice (black bar) and *Ltbr*^{TEC} mice (white bar). Data is representative of three experiments where n=10.

All significance was noted as: *<0.05, **<0.01, ***<0.001, ***<0.0001.

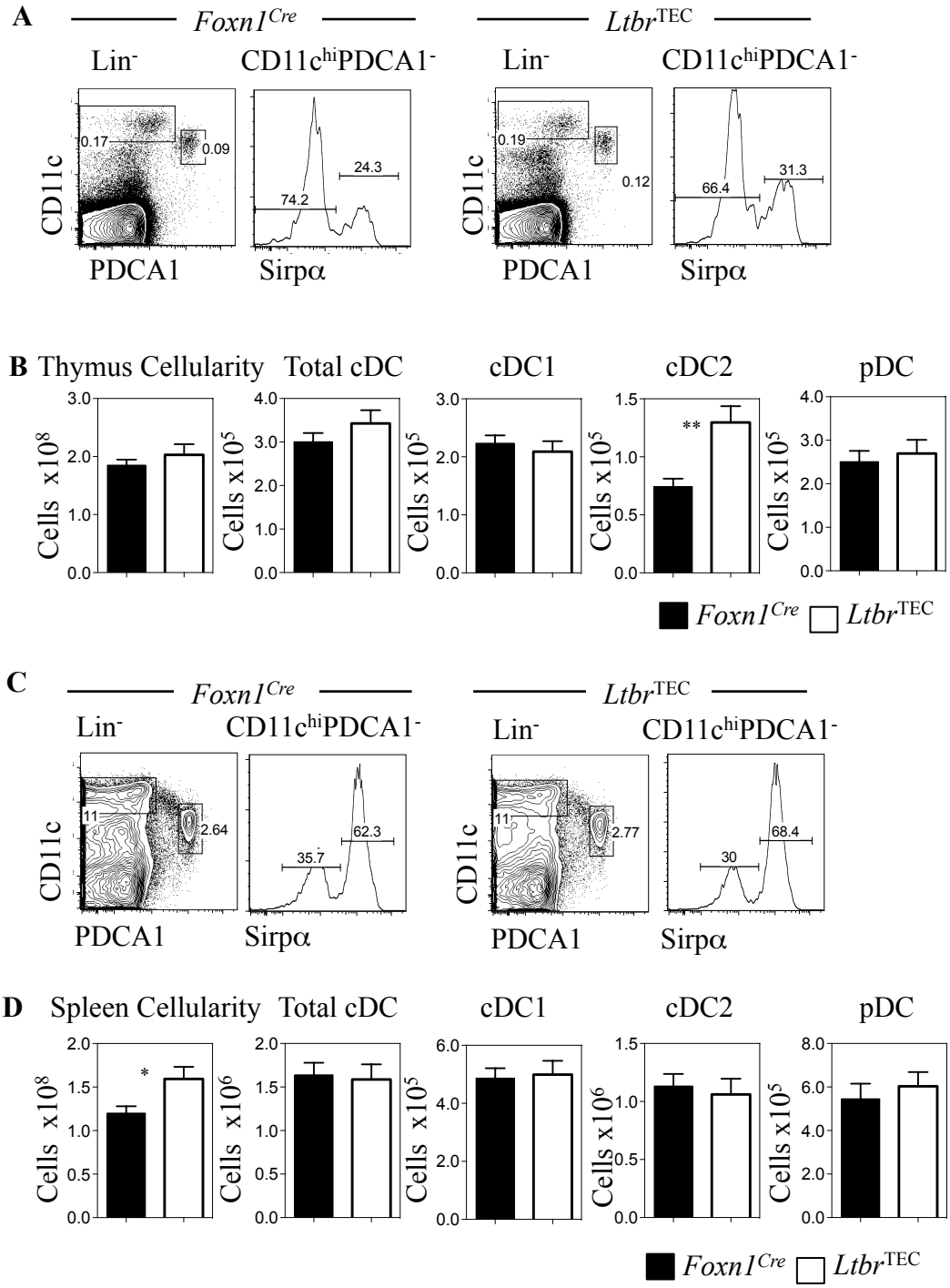
A
Foxn1Cre
LtbrTEC
Lin-
CD11chiPDCA1-
CD11c
PDCA1
Sirpα
0.17
0.09
74.2
24.3
0.19
0.12
66.4
31.3
B Thymus Cellularity
Total cDC
cDC1
cDC2
pDC
Cells x10^8
Cells x10^5
**
Foxn1Cre
LtbrTEC
C
11
2.64
35.7
62.3
2.77
30
68.4
D Spleen Cellularity
Cells x10^6
*

Figure 3.19:

LTβR Absence From Thymic Epithelial Cells Fails To Affect Dendritic Cell Proliferation

A) FACs plots showing the relative proportions of $BrdU^+$ thymic dendritic cell populations in *Foxn1*^{Cre} mice (top panel) compared to *Ltbr*^{TEC} mice (bottom panel).

B) Proportion of dendritic cells and pre-cDC in thymus that were BrdU positive with *Foxn1*^{Cre} mice (black bar) compared to *Ltbr*^{TEC} mice (white bar). Data is from two independent experiments, *Foxn1*^{Cre} mice (n=5) and *Ltbr*^{TEC} mice (n=5).

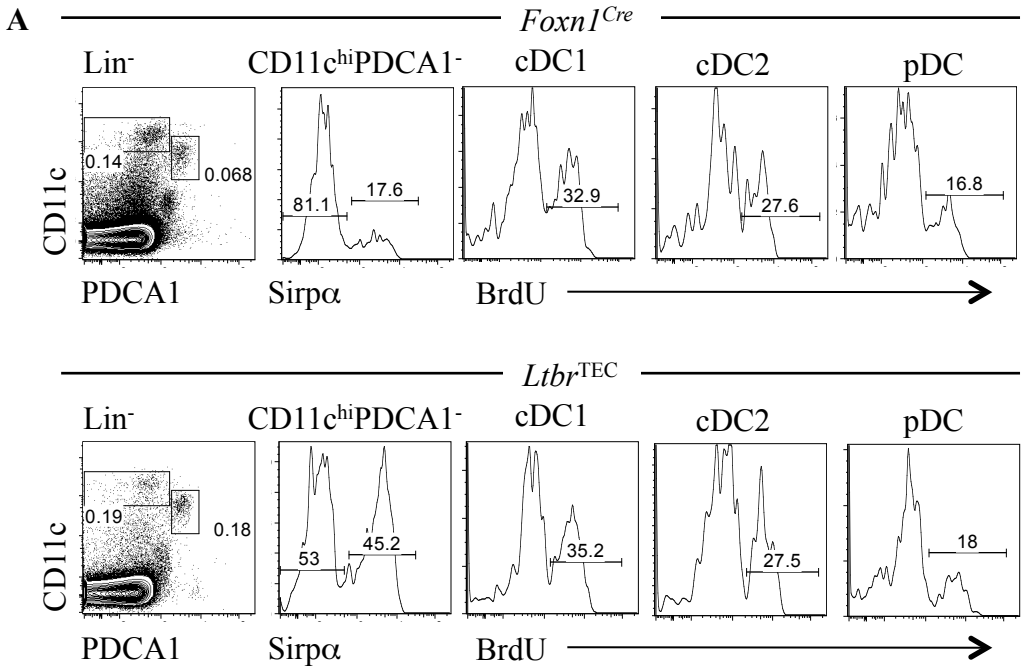
A
Foxn1Cre
Lin-
CD11chiPDCA1-
cDC1
cDC2
pDC
CD11c
0.14
0.068
81.1
17.6
32.9
27.6
16.8
PDCA1
Sirpα
BrdU
Ltbr TEC
Lin-
CD11chiPDCA1-
cDC1
cDC2
pDC
CD11c
0.19
0.18
53
45.2
35.2
27.5
18
PDCA1
Sirpα
BrdU

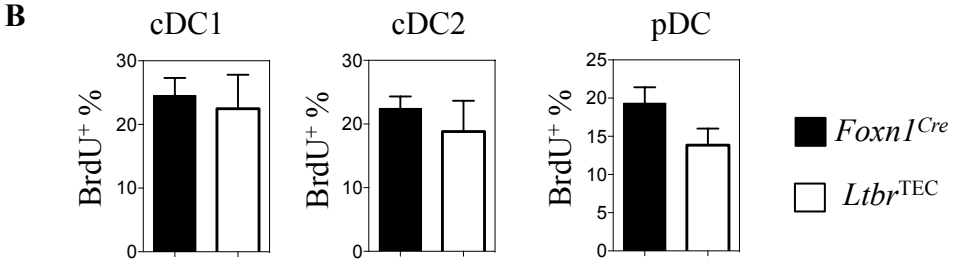
B
cDC1
cDC2
pDC
BrdU+ %
30
20
10
0
30
20
10
0
25
20
15
10
5
0
Foxn1Cre
Ltbr TEC

those seen in WT and *Ltbr*$^{-/-}$ analysis (Figure 3.8). Quantitation confirmed this trend with no significant difference seen in proliferative proportion of DCs in the thymus of *Ltbr*^{TEC} and *Foxn1*^{Cre} mice. As a result, this confirmed absence of LTβR from TEC was unable to disturb functioning of thymic DC.

However, despite the proliferation of DC being shown to be comparable between WT, *Ltbr*$^{-/-}$, *Foxn1*^{Cre} and *Ltbr*^{TEC} mice, the positioning of the DCs in this disrupted medulla was unknown and could correlate to defective activity of DC in negative selection, as this requires medullary positioning. To assess this, confocal quantitation of DCs was conducted on freshly frozen and sectioned thymi which were stained for ERTR5 (green) to highlight medullary areas of the thymus, with absence of ERTR5 staining reflecting cortical areas and CD11c (red) to identify DC positioning (Figure 3.20). Firstly WT and *Ltbr*$^{-/-}$ mice sections were compared and the distribution of thymic DC remained predominately localised to the medulla in the *Ltbr*$^{-/-}$ mice despite smaller medullary areas being found (Figure 3.20 A). This was shown graphically (Figure 3.20 B) from which there was therefore no difference in the proportion of DCs localised to cortex or medulla for the WT compared to *Ltbr*$^{-/-}$ mice. The same analysis was completed in *Ltbr*^{TEC} and *Foxn1*^{Cre} mice with confocal plots (Figure 3.20 C) showing distribution of thymic DCs localised to the medullary areas. Furthermore, quantitation also showed that the localisation of DC within the *Ltbr*^{TEC} and *Foxn1*^{Cre} mice was comparable with no distributional difference (Figure 3.20 D). Therefore disrupted mTEC populations in *Ltbr*^{TEC} and *Ltbr*$^{-/-}$ mice does not alter the localisation of thymic DCs, which still reside in the remaining medulla.

Figure 3.20:

Intrathymic Dendritic Cells Remain Correctly Positioned Despite LTβR Absence

A) Confocal graphs of the position of dendritic cells in the thymus of WT (left panel) compared to LTβR deficient mice (right panel) with ERTR5 (green) defining mTEC and CD11c (red) defining dendritic cells.

B) Quantitation of the proportion of total $CD11c^+$ cells counted in 3-4 sections per thymus per strain. Five images were randomly taken per section for both medullary and cortical areas. The CD11c+ cells within these areas were recorded for both cortex and medulla; WT mice (black bars) or *Ltbr*$^{-/-}$ mice (white bars). Data was obtained from three individual samples per WT/ *Ltbr*$^{-/-}$ mouse.

C) Confocal plots showing the positioning of dendritic cells (CD11c+, red) in the thymus of *Foxn1*^{Cre} and *Ltbr*^{TEC}. ERTR5 defines mTEC populations.

D) Quantitation of the proportion of total dendritic cells within 3-4 thymus sections taken for both *Foxn1*^{Cre} and *Ltbr*^{TEC} mice. Within these sections five randomly selected areas for both the cortex and medulla had $CD11c^+$ cells counted and recorded; *Foxn1*^{Cre} control mice (black bar) and *Ltbr*^{TEC} mice (white bar). Data was from three individual thymus samples for both *Foxn1*^{Cre} and *Ltbr*^{TEC} mice.

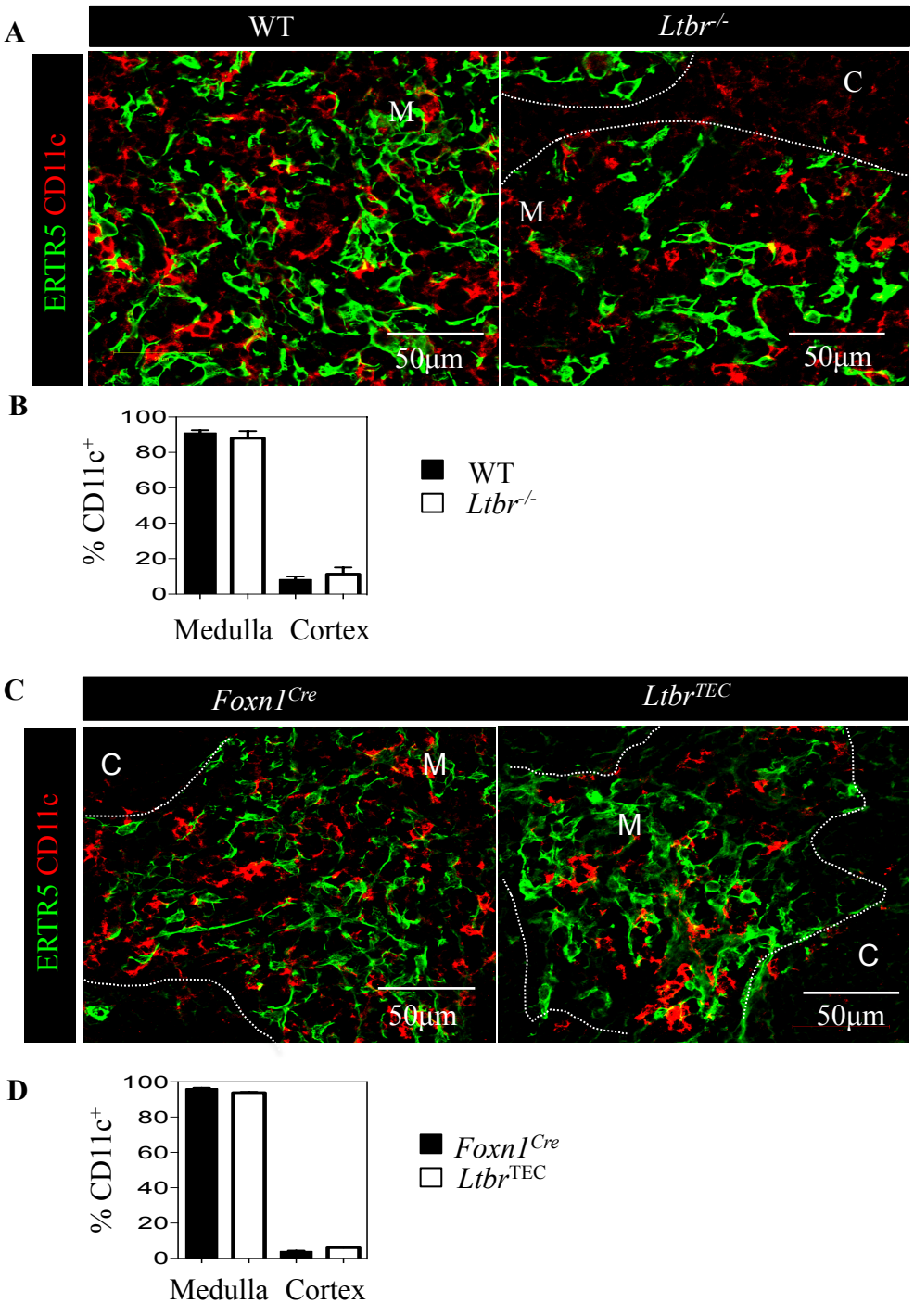
A
WT
Ltbr-/-
ERTR5 CD11c
M
C
M
50µm
50µm
B
% CD11c+
100
80
60
40
20
0
Medulla
Cortex
WT
Ltbr-/-
C
Foxn1Cre
LtbrTEC
ERTR5 CD11c
C
M
M
C
50µm
50µm
D
% CD11c+
100
80
60
40
20
0
Medulla
Cortex
Foxn1Cre
LtbrTEC

The total numerical reduction in DCs in *Ltbr*$^{-/-}$ mice (Figure 3.7) indicates this may be a reason for tolerance breakdown. Yet why reduced DC may result in a break in tolerance in *Ltbr*$^{-/-}$ mice remained unanswered. Given the role of thymic DCs in central tolerance, we examined if reduced DCs were causing altered negative selection. To answer this, expression of Caspase-3 was assessed (Figure 3.21) to identify dead/dying cells which could then be separated into those triggered to undergo death during negative selection ($CD5^+CD69^+$) or rather death by neglect ($CD5^-CD69^-$) (Stritesky et al., 2013). Subsequently all four mouse strains were analysed by flow cytometry for these parameters, with representative FACs shown (Figure 3.21 A). This analysis suggested that WT, *Foxn1*^{Cre} and *Ltbr*^{TEC} mice, all had similar proportions of cell death and negative selection yet the proportion of Caspase-3 positive cells was reduced in *Ltbr*$^{-/-}$ mice compared to controls with a further reduction specifically in cells undergoing negative selection (Figure 3.21 A). Absolute number analysis was conducted to quantify the reduction in negative selection in the absence of LTβR. This analysis highlighted that the total number of Caspase-3 positive cells was significantly reduced in *Ltbr*$^{-/-}$ mice compared to WT control mice, whereas *Ltbr*^{TEC} and *Foxn1*^{Cre} control mice were comparable (Figure 3.21 B). When Caspase-3^+ cells were divided into $CD5^+CD69^+$ negatively selected cells, *Ltbr*$^{-/-}$ mice had reduced number of cells undergoing negative selection compared to WT control mice; with *Ltbr*^{TEC} and *Foxn1*^{Cre} mice remaining comparable. Finally those negatively selected cells that were $CD4^+$ thymocytes ($CD5^+CD69^+CD4^+$) were significantly reduced in the *Ltbr*$^{-/-}$ mice compared to WT with no difference between *Ltbr*^{TEC} and *Foxn1*^{Cre} control mice. Therefore this emphasises that the breakdown in tolerance seen in *Ltbr*$^{-/-}$ mice correlates with reduced negative selection; attributed to defects in DC populations.

Figure 3.21:

Negative Selection Becomes Reduced In Germline LTβR Deficient Mice

A) FACs plots illustrating how cells undergoing death and then subsequently death by neglect or negative selection were identified for analysis with their relative proportions in the thymus of WT, *Ltbr*$^{-/-}$, *Foxn1*^{Cre} and *Ltbr*^{TEC} mice shown.

B) Absolute number analysis of Caspase-3^{+} cells as well as those undergoing negative selection (Caspase^{+}CD5^{+}CD69^{+}) and CD4 SP negatively selected cells (Caspase^{+}CD5^{+}CD69^{+}CD4^{+}). WT mice (black bar), *Ltbr*$^{-/-}$ mice (white bar), *Foxn1*^{Cre} mice (dark grey bar) and *Ltbr*^{TEC} mice (light grey bar). Data was obtained from at least two independent experiments; n=8.

All significance was noted as: *<0.05, **<0.01, ***<0.001, ***<0.0001.

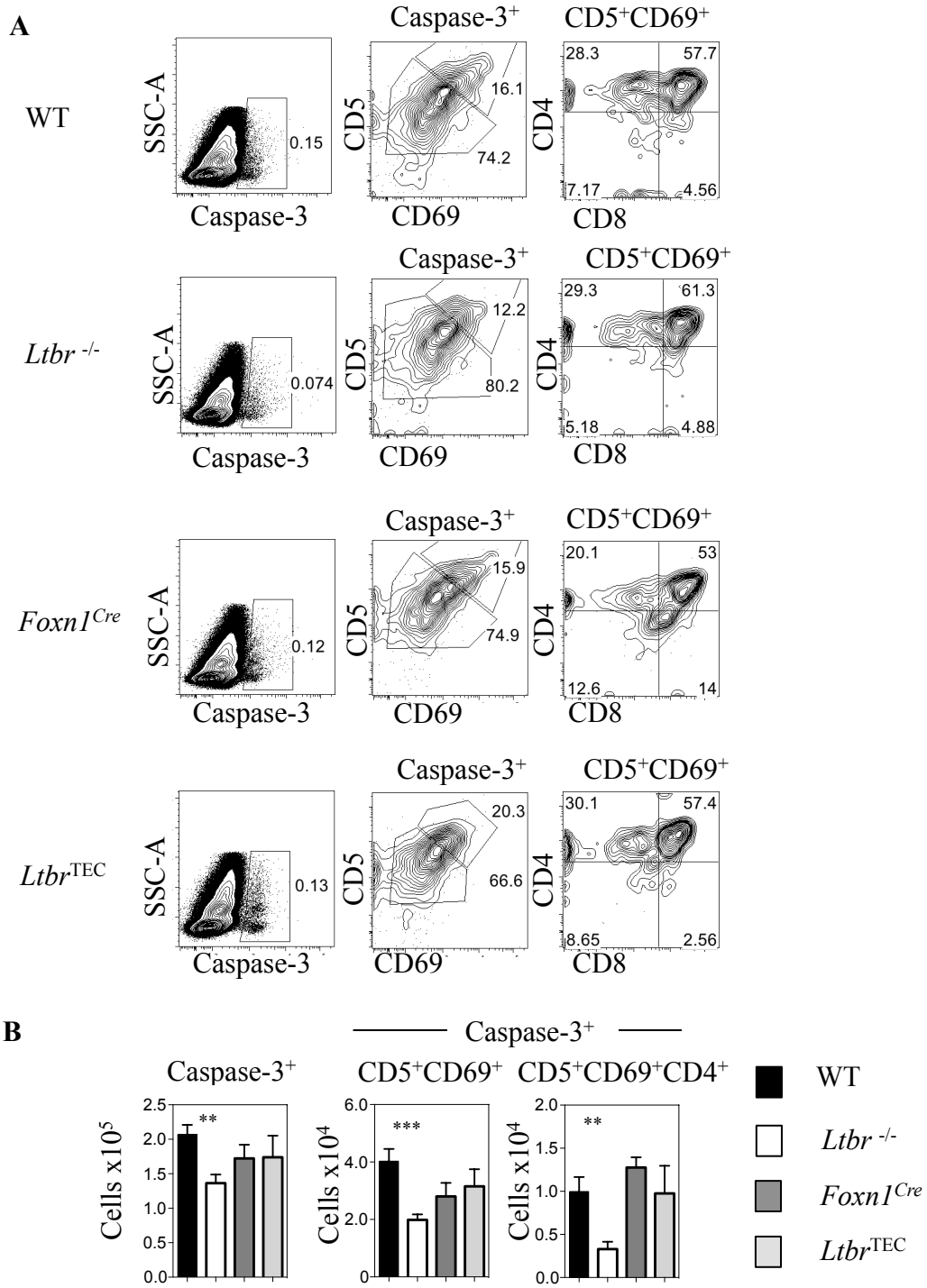
A
WT
Ltbr -/-
Foxn1Cre
LtbrTEC
SSC-A
Caspase-3
0.15
0.074
0.12
0.13
Caspase-3+
CD5
CD69
16.1
74.2
12.2
80.2
15.9
74.9
20.3
66.6
CD5+CD69+
CD4
CD8
28.3
57.7
7.17
4.56
29.3
61.3
5.18
4.88
20.1
53
12.6
14
30.1
57.4
8.65
2.56
B
Caspase-3+
CD5+CD69+
CD5+CD69+CD4+
Cells x10^5
Cells x10^4
**
***
WT
Ltbr -/-
Foxn1Cre
LtbrTEC

3.3 Discussion

3.3.1 Development of Thymic DC Populations

The thymus is known to contain DC populations that are implicated in central tolerance induction. However the ability of the thymus to regulate these populations still requires greater investigation. Ontogeny analysis shows that intrathymic DC populations increase as thymus size increases, indicating that DC are regulated by the thymus directly. This may relate to a larger thymus containing increased thymic niches and therefore being able to support greater numbers of DC. This can be suggested in the spleen also where the same trend was observed. However as well as regulation of DC numbers, the thymus also acts to differentially alter the DC phenotype as it promotes increased activation, which is itself necessary to support DC function in thymocyte interactions and tolerance induction (Proietto et al., 2008b, Li et al., 2009). Furthermore, this increased activation of thymic DC has been linked to CD4 or CD8 single positive thymocytes as analysis of TCR$\alpha^{-/-}$ mice showed that cDC have a less activated phenotype and that this was due to a requirement for CD40L provision by T-cells (Spidale et al., 2014). However in culture experiments using anti-CD40 stimulation, cDC2 activation was selectively increased. Considering this, in our hands, the intrathymic activation of cDC1 and pDC may be governed by factors other than stimulation through CD40. Further analysis of pathways regulating cDC1 and pDC activation in the thymus focused on LTβR stimulation using in vitro cultures. This was of interest, as it was shown in lymph node studies that LTβR signalling on DC through interactions with $LT\alpha_1\beta_2$ on T-cells increased CD86 expression (Summers-DeLuca et al., 2007). This study furthermore proposed that CD40 and LTβR signalling were infact working in combination to support the greatest level of DC maturation. Interestingly, however, our in vitro studies suggested no effect of LTβR stimulation or any cumulative influence with anti-CD40 on thymic DC.

This indicates that DC in the thymus may require different signals to promote their activation from the mechanisms previously reported to drive peripheral DC activation. This leaves the possibility for alternative thymocyte related factors such as RANK to possibly play a role in the process of intrathymic DC activation. The RANK/RANKL pathway is known to be active intrathymically as it is involved in TEC development and further peripherally it has been implicated in the regulation of DC populations (Desanti et al., 2012, Rossi et al., 2007). In lymph nodes, T-cell/DC (RANKL/RANK) interactions have been shown to drive increased B-cell lymphoma XL (Bcl-x_L) and Bcl-2 expression to support survival of DCs, with a similar mechanism utilised also in bone marrow (Josien et al., 2000, Williamson et al., 2002). Additionally, under in vitro blockade of OPG, a decoy receptor for RANKL, free RANKL availability increased and as a consequence was shown to support greater survival of bone marrow derived DC (Chino et al., 2009). As a result, this research on RANK and DC maintenance in various tissues in the periphery brings into question whether this mechanism may be potentially responsible for DC maturation in the thymus and is something that would be interesting to explore in more detail. Furthermore the thymic stromal populations that DC are closely associated to may support DC activation through factors such as thymic stromal lymphopoietin, as this is already known to prime DC for T-regulatory cell induction in thymus (Watanabe et al., 2005, Hanabuchi et al., 2010).

The thymus also appears to regulate the general composition of the DC compartment, with variation occurring with age in turn suggesting that mechanisms regulating DC in the thymus must correspondingly alter with age. This could also be said for splenic regulation of DC populations. Intrathymically, a visible transition in DC proportions took place between 2-5 weeks of age suggesting that this time point marks a switch in factors regulating DC

maintenance or recruitment in early ontogeny, from those seen later in development and throughout adulthood. This 'change over period' saw increased populations such as pDC and cDC2 entering into the thymus, which we hypothesise, may relate to a requirement for an increased repertoire of antigens for greater T-cell selection earlier in development (around 2-5 weeks). This was supported by a recent study, showing that negative selection was inefficient in early ontogeny but efficiency of tolerance induction increased with age, corresponding to increased cDC2 and pDC influxing into the thymus (Kroger et al., 2016). cDC2 in particular were shown to provide greater antigen processing capacity to assist in effective negative selection. As a result, the altered composition in DC populations in the adult thymus therefore appears to occur in order to support the function of the thymus in negative selection and to possibly prevent the reduced T-cell clonality seen through thymic involution later in life.

3.3.2 LTβR and Thymic DC Regulation

Mechanisms regulating intrathymic DC were revealed through analysis of LTβR deficient mice for a similar ontogeny sequence. This suggested that the later phases of ontogeny concerning cDC1 and pDC were dependent on LTβR mediated regulation as there was only comparability between *Ltbr*$^{+/-}$ control and *Ltbr*$^{-/-}$ mice until the transitional phase of 2-5 weeks of age. From which point, these strains diverged with cDC1 and pDC being reduced in *Ltbr*$^{-/-}$ mice. Interestingly, it was apparent through the ontogeny series as well as by adult analysis of DC in *Ltbr*$^{-/-}$ mice compared to WT controls, that cDC2 were developing in the thymus independently of LTβR. This was surprising to find as peripherally it has been shown that cDC2 require LTβR signalling cell intrinsically to support their maintenance in the spleen (Kabashima et al., 2005, Wang et al., 2005). This was confirmed in adult analysis, with reduced splenic cDC2 in *Ltbr*$^{-/-}$ mice compared to WT control mice along with bone marrow

chimera analysis supporting a cell intrinsic signalling requirement for LTβR on splenic cDC2. Therefore, it appears that LTβR mediated regulation of DC subsets differs upon both anatomical localisation and the DC subset being regulated. It is possible that mechanisms regulating the alternative DC subsets vary in order to ensure the maintenance of some DC in the thymus even under conditions of LTβR absence, given the known requirement for DC in tolerance induction (Ohnmacht et al., 2009).

As a result of the above findings, it was decided to focus upon the regulation of thymic cDC1 and pDC by LTβR in the thymus. Consequently regulation of thymic DC was shown to be dependent upon stromal mediated LTβR signals, through bone marrow chimera and kidney capsule graft generation. However, due to LTβR being implicated in thymic medulla formation and DC subsequently localising to these sites, it could be suggested that these disrupted medullary areas may in turn be indirectly modulating DC in thymus (Boehm et al., 2003). Exploration of this was possible through the generation of $Ltbr^{TEC}$ mice in which $Foxn1^{Cre}$ mice were crossed with $Ltbr^{fl/fl}$ mice. This initially revealed that the disruption of the medullary areas within $Ltbr^{-/-}$ and $Ltbr^{TEC}$ mice was due to a cell intrinsic requirement for LTβR signalling on TEC populations to support their persistence in the thymus. This novel finding builds upon previous work and furthermore supports a recent publication using an alternative TEC-specific LTβR deletional model, which confirmed our finding (Boehm et al., 2003, Wu et al., 2017). This disrupted development of the medullary areas was further suggested to occur due to the prevention of LTβR dependent mTEC progenitors (Cld3,4 SSEA-1^{+}) from developing into mTEC, an aspect that we did not investigate in our studies (Wu et al., 2017). Therefore our findings, supported by recent research, suggest LTβR is cell intrinsically required to maintain mTEC in the thymus and that this further may be at the level

of medullary progenitor development. It would therefore be interesting to uncover in future experiments exactly how an absence of LTβR may affect mTEC progenitor populations as LTβR signals from mature T-cells have already been implicated in the later stage terminal development of mTEC (White et al., 2010). This may be investigated through alternative models of disrupted medullary structure such as *Tcrα*$^{-/-}$ mice. Here, it is possible that medullas are disrupted because the absence of single positive thymocytes leaves them unable to supply the LTβR signals that could be necessary for development of mTEC. Therefore the supplementation of LTβR ligands in these models would to be interesting to consider to determine if it is through this axis that medullary development may have become limited. However as smaller medullary areas are still able to form in *Ltbr*$^{-/-}$ mice, it is clear that there are other mechanisms independent of LTβR that support medullary formation to compensate at least partially for this LTβR absence – another area that would be interesting to explore.

Nonetheless, despite the factors regulating mTEC development requiring further research, whether the DC population defect in *Ltbr*$^{-/-}$ mice resulted from these disrupted mTEC populations was unknown. However it is possible this could be responsible for disrupted DC as there is a fundamental requirement for the medulla in the maintenance of thymic DC. Studies using *Relb*$^{-/-}$ mice, or *aly/aly* mice with a natural mutation in the NIK gene, both suffer from almost a total loss of mTEC, and have dysregulated DC populations (Wu et al., 1998, Mouri et al., 2014). Recent analysis showed that absence of RelB specifically from mTEC caused a significant loss of mTEC populations and this correlated directly to the cDC1 and pDC population being reduced in the thymus due to the alterations in mTEC themselves (Riemann et al., 2017, Briseno et al., 2017). This emphasises that the medulla is absolutely required to be present for thymic cDC1 maintenance, however the level of medulla necessary

to support DC was somewhat questioned following our findings. Through analysis of *Ltbr*^{TEC} mice, we found that the medulla itself is not required to be fully formed and further mTEC can be rather quantitatively reduced, whilst still remaining competent at regulating normal DC populations intrathymically. Considering this and the reduced DC seen in total medullary absence, it puts forward the idea of a threshold of mTEC being necessary in thymus to maintain normal DC numbers. Further, considering bone marrow chimeras which suggested stromal mediated regulation of the cDC1 and pDC, this finding of normal DC populations in *Ltbr*^{TEC} mice shows that LTβR mediated regulation of TEC is dispensable for intrathymic DC maintenance and supports that indirect medullary disorganisation is not responsible for the DC defects seen in *Ltbr*$^{-/-}$ mice. Furthermore, it emphasises that the reduced cDC1 and pDC seen in *Ltbr*$^{-/-}$ mice rather relates to an LTβR dependent process that must be occurring on an alternative non-TEC stromal population.

In addition, the inability of the medulla to fully form in *Ltbr*$^{-/-}$ and *Ltbr*^{TEC} mice was shown to further be insufficient to prevent the correct localisation of the thymic DC populations. This shows that the quantitative reduction in the number of Aire expressing mTEC that remained in these mice were still sufficient to be able to produce the Aire-dependent chemokine XCL1 to attract the XCR1^{+} cDC1 which are predominately medullary localised (Lei et al., 2011). However the levels of XCL1 production in these models was not investigated but it would be interesting to determine whether they remained equivalent in the *Ltbr*$^{-/-}$ and *Ltbr*^{TEC} mice. Additionally, the proliferation of these DC populations was unchanged in *Ltbr*$^{-/-}$ and *Ltbr*^{TEC} mice. This was itself surprising as administration of agonistic LTβR antibody in vivo led to increased splenic DC proliferation through cell intrinsic LTβR signals that overrode the inhibitory herpesvirus entry mediator- B and T lymphocyte attenuator (HVEM-BTLA)

pathway normally acting to suppress DC proliferation (De Trez et al., 2008). Yet in the thymus of the *Ltbr*$^{-/-}$ and *Ltbr*^{TEC} mice, DC may utilise alternative mechanisms than LTβR signalling to support their homeostatic proliferation. This also puts forward the idea that reduced mTEC in the thymus in *Ltbr*^{TEC} mice are still sufficient to support medullary function in the thymus for normal DC regulation with regards to positioning and proliferation. As a result it reinforces that the reduced cDC1 and pDC populations seen in *Ltbr*$^{-/-}$ mice rather relate to a requirement for LTβR signalling on non-TEC stroma and that this reduction occurs independently of medullary disorganisation in this model as determined through comparisons to equally disrupted *Ltbr*^{TEC} mice.

3.3.3 LTβR and Central Tolerance

As well as the role of the medulla in DC regulation, it is also absolutely essential for the process of central tolerance as studies of *Relb*$^{-/-}$ mice, with an absence of medullary areas, portray a phenotype of autoimmunity (Wu et al., 1998, Weih et al., 1995). Original studies used this finding in *Relb*$^{-/-}$ mice to suggest that defects in central tolerance in *Ltbr*$^{-/-}$ mice arose from defective medullary areas. It was further previously suggested that these altered medullas in *Ltbr*$^{-/-}$ mice were reduced in their ability to produce CCL19/CCL21 expression, which in turn prevented the migration of CCR7 expressing newly selected single positive cells into the medulla, inhibiting tolerance induction (Zhu et al., 2007). Considering this, analysis of *Ltbr*^{TEC} mice with disrupted mTEC populations that are identical to in *Ltbr*$^{-/-}$ mice, would be expected to have the same mislocalisation of single positive thymocytes and failure to induce negative selection if this theory was true. However the correct induction of central tolerance in the *Ltbr*^{TEC} mice despite reduced CCL21 expressing mTEC numbers and disrupted mTEC, acts to disprove this theory. This therefore highlights that the process of

negative selection that is reported to be altered in *Ltbr*$^{-/-}$ mice does not relate solely to mislocalisation of single positive thymocytes causing an inability of these cells as a result to undergo negative selection. Rather it correlates to alterations in the alternative regulators of central tolerance other than mTEC which are responsible for the tolerance breakdown. In addition, the dysregulation of the medullary areas seen in *Ltbr*$^{-/-}$ mice is itself insufficient to directly drive the break in tolerance reported in these mice.

Importantly from this, analysis of *Ltbr*$^{-/-}$ and *Ltbr*^{TEC} mice further brought into question the regulation of the machinery that is necessary to support TRA expression for thymocyte screening and tolerance induction. Aire expression was expected in *Ltbr*$^{-/-}$ and *Ltbr*^{TEC} mice, as previous research has shown that Aire is regulated by RANK signalling in mTEC and not by LTβR associated mechanisms (Venanzi et al., 2007, Martins et al., 2008). However LTβR had previously been reported to be essential for Fezf2 expression in the thymus – but our findings with confocal microscopy, highlight that there is still a clear presence of Fezf2 in the thymus in *Ltbr*$^{-/-}$ and *Ltbr*^{TEC} mice; thus rather bringing in to question if LTβR is the key regulator of Fezf2 (Takaba et al., 2015). Furthermore the sustained and equivalent presence of this machinery in *Ltbr*$^{-/-}$ and *Ltbr*^{TEC} mice, despite reduced mTEC, suggests that TRA expression alterations is not responsible for the break in tolerance seen in the *Ltbr*$^{-/-}$ mice. Additionally this highlights that LTβR is dispensable for Fezf2 expression and therefore suggests alternative regulators in this process that need to be investigated.

Additionally it seems that the intact medulla is also dispensable for the generation of T-regulatory cells implicated in tolerance, which was surprising as it had previously been shown through kidney capsule transplant experiments of *Relb*$^{-/-}$ thymic lobes that there was a

requirement for an intact medulla for the generation of T-regulatory cells (Cowan et al., 2013). As a result, the normal generation of Treg in the *Ltbr*^{TEC} mice suggests that the medulla is able to provide sufficient TRAs for antigen cross presentation through normal numbers of DC, to support Treg generation. Furthermore and perhaps more interestingly, when the cDC1 and pDC populations were reduced along with mTEC in the *Ltbr*$^{-/-}$ mice, there still remained to be sufficient TRA presentation to not perturb Treg development – despite DC and mTEC being shown to be pivotal regulators of Treg induction (Tai et al., 2013, Perry et al., 2014). The lack of Treg disruption in *Ltbr*$^{-/-}$ mice could relate to cDC2 being normally maintained under LTβR absence, as cDC2 have previously been suggested to be the main DC subset involved in intrathymic Treg induction and so may be supporting Treg generation in these mice (Proietto et al., 2008b). Therefore the maintenance of alternative central tolerance regulators in the *Ltbr*$^{-/-}$ mice in comparable levels to the *Ltbr*^{TEC} mice emphasises that as cDC1 and pDC populations are the only differing factor between these mice, their maintenance in the thymus directly correlates with the correct induction of central tolerance through the process of sustained negative selection (shown in summary Figure 3.22).

Considering this chapter as a whole, it questions how intact the medullary compartment needs to be to effectively carry out its role in central tolerance, with a substantial quantitative loss of mTEC still having no detrimental effect on tolerance induction. Furthermore, the regulation of the medullary compartment by LTβR is distinct from the role of LTβR in the regulation of thymic DC – again segregating the association between the medulla and thymic DC regulation. This chapter further identifies that the breakdown in tolerance previously reported in *Ltbr*$^{-/-}$ mice, is not due to medullary disruption itself or by this disruption directly impacting upon alternative cellular regulators of tolerance. However, it instead correlates to a

Figure 3.22:
Summary Diagram For LTβR Mediated Regulation Of Thymic DC

A) Summary diagram of the regulation of thymic tolerance in the four different mouse models used in this chapter. The thymic structure with regards to medullary architecture is depicted in the left hand panel with relative DC and mTEC proportional populations shown in the central panel and the consequential outcome on tolerance explained in the right hand panel.

A

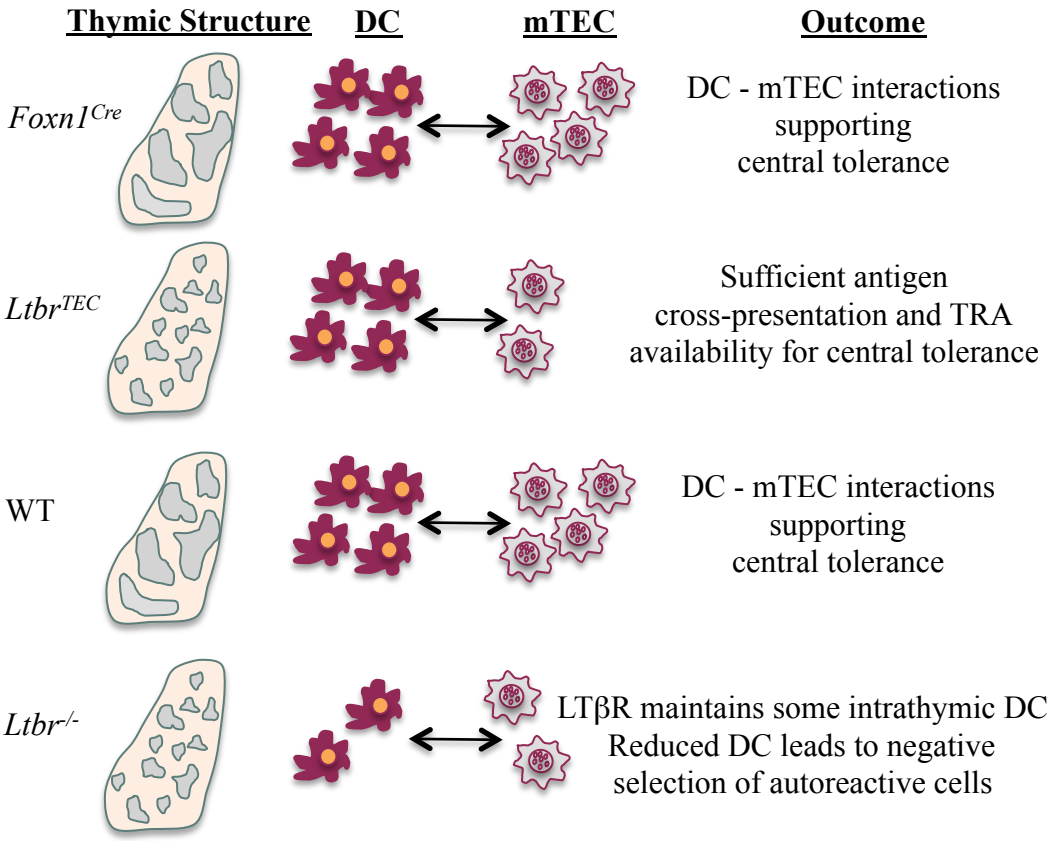

	Ltbr$^{-/-}$	*Ltbr*^{TEC}
mTEC	↓	↓
Tolerance	↓	-
T-Reg	-	-
DC	↓	-

requirement for LTβR-dependent signalling on non-TEC stromal cells to in turn indirectly support the maintenance of cDC1 and pDC that are vital regulation of effective negative selection for the prevention of autoimmune disease. This poses the question as to whether the maintenance of thymic DC is possibly more pivotal for the prevention of autoimmunity than that of mTEC, with potentially only a threshold level of mTEC being necessary to support complete tolerance induction.

CHAPTER FOUR:

PRE-CDC ENTRY INTO THE THYMUS IS REGULATED BY LTβR AND CCR7

4.1 Introduction

Of the three DC populations within the thymus, the conventional DC subset cDC1 are the only subset thought to develop intrathymically from a progenitor (pre-cDC) that is recruited from the bone marrow. Whilst the precursor product relationship during DC development is not yet fully clear, a pre-cDC has been described with a $Lin^{-}MHCII^{-}CD11c^{+}Flt3^{+}Sirp\alpha^{int}$ phenotype in the bone marrow and spleen (Liu et al., 2009). In this study, pre-cDC were shown to be generated in the bone marrow and actively divide before migrating in the blood and into lymphoid tissues. Pre-cDC isolated from the bone marrow and spleen were adoptively transferred into host mice and shown to give rise to both cDC1 and cDC2 populations. In contrast the availability of these cells in thymus has not been assessed, although it is known that cDC2 arise from a peripherally mature population that migrates in to the thymus (Baba et al., 2009, Li et al., 2009). Research in the thymus concerning cDC1 progenitors infact previously determined pre-cDC as $CD8\alpha^{+}CD172\alpha^{-}$ cells, with the suggestion that these progenitors contribute towards the DN1c subset of thymic settling progenitors (Luche et al., 2011). Purified transfers of $CD8\alpha^{+}CD172\alpha^{-}$ pre-cDC cells in this study additionally indicated that this pre-cDC population could be detected in the thymus and ultimately gave rise to cDC1. Therefore it is initially important in this chapter to establish consistent identification of the pre-cDC ($Lin^{-}MHCII^{-}CD11c^{+}Flt3^{+}Sirp\alpha^{int}$) population between both the periphery and the thymus to allow for effective comparisons between these different compartments in the study of pre-cDC.

Following on from this, further investigations will consider the mechanisms that may be affecting the recruitment of pre-cDC into the thymus. This is important as in contrast to the known recruitment of pDC and cDC2 DC subsets via CCR9 and CCR2 expression, the factors

that are regulating pre-cDC remain undetermined (Hadeiba et al., 2012, Baba et al., 2009). Therefore possible regulators of pre-cDC will be considered in this chapter. To begin with, the previous chapter indicated that cDC1 were regulated by LTβR signalling on thymic stromal cells and the cDC1 population is the direct progeny of pre-cDC. This raises the question as to whether pre-cDC recruitment is in turn LTβR dependent. As a result, the correlation of the cDC1 reduction with alterations in thymic pre-cDC will be investigated in this chapter with regards to the potential role of LTβR in the regulation of pre-cDC.

Furthermore if LTβR absence is shown to affect pre-cDC, the mechanisms by which this may be occurring will additionally be considered with the use of different mouse models to dissect this process. For example, a possible role for LTβR in pre-cDC recruitment may involve LTβR mediated chemotaxis. This should be considered as pre-cDC may enter into the thymus via similar mechanisms of recruitment to ETP, for which recruitment is dependent upon exposure to certain chemokines. Indeed, ETP recruitment has been suggested to occur through the chemokines CCR7 and CCR9 as CCR7/CCR9 expressing ETP have been shown to become attracted to CCL19/CCL21 and CCL25, produced within the thymus (Lkhagvasuren et al., 2013, Seach et al., 2008, Ueno et al., 2004, Zhu et al., 2007). As a consequence, mouse models that were *Ccr7*$^{-/-}$ indeed demonstrated a detrimental decline in ETP presence in the thymus (Krueger et al., 2010, Misslitz et al., 2004, Zlotoff et al., 2010). As a result, the potential for the CCR7 axis to be implicated in pre-cDC recruitment will also be examined in this chapter with the study of pre-cDC in various mouse models lacking CCR7 associated factors.

4.2 Results

4.2.1.Regulation of cDC1 Progenitors Through LTβR

To begin to address the role of LTβR in the regulation of pre-cDC, firstly the development of pre-cDC in steady state conditions was assessed. The development of the DC populations themselves is known to depend upon a progressive developmental pattern from upstream progenitor populations, which have a distinct anatomical localisation. Therefore, upstream progenitors were identified to be restricted to the correct sites (Figure 4.1 A). For this, bone marrow was retrieved from hind legs of WT mice (detailed in methods) along with spleen and thymus, which were freshly isolated and disaggregated to obtain cells for flow cytometric analysis. Representative FACs plots show the Macrophage Dendritic Cell Progenitor (MDP) and Common Dendritic Cell Progenitor (CDP) were restricted to the bone marrow and absent from the spleen and thymus (Figure 4.1 A). This could further be seen in quantitation of FACs proportions with MDP and CDP only detected in the bone marrow (BM) samples (Figure 4.1 B). The downstream development of pre-cDC ($Lin^{-}MHCII^{-}CD11c^{+}Flt3^{+}Sirp\alpha^{int}$) was also confirmed to occur in the bone marrow through similar cell preparations, with the identification of progenitors through FACs analysis (Figure 4.1 C). Further quantitation showed that these progenitors could also be seen in the spleen and thymus as they migrate into these tissues for their development (Figure 4.1 C). Quantitation of numbers of pre-cDC show that they can be abundantly found in the bone marrow and then become less frequent in spleen and further in thymus. Therefore the localisation of the DC progenitors in WT adult mice appears to correlate with the previous literature, with MDP and CDP being bone marrow restricted and pre-cDC identifiable in bone marrow, spleen and thymus.

Figure 4.1:
Dendritic Cells and Their Progenitors Are Correctly Localised

A) The gating strategy used to identify the myeloid dendritic progenitors (MDP) and common dendritic cell progenitors (CDP) in bone marrow, spleen and thymus. Prior gating again included lineage discrimination, which excludes all cell expressing CD19, CD3, B220, Ter119, NK1.1.

B) FACs plots of MDP and CDP in bone marrow (BM), spleen and thymus. Data is representative of two independent experiments with n=6.

C) Gating strategy used to identify pre-cDC populations within the bone marrow, thymus and spleen. Lineage dump channel included NK1.1, CD19, CD3, B220, Ter119 with positively stained cells excluded prior to onward gating. Staining is representative of that seen in the bone marrow. Subsequent plots for the final identification of pre-cDC are shown with quantitation of absolute numbers in each tissue. Results were compiled from 3 independent experiments where n=11.

All significance was noted as: *<0.05, **<0.01, ***<0.001, ***<0.0001.

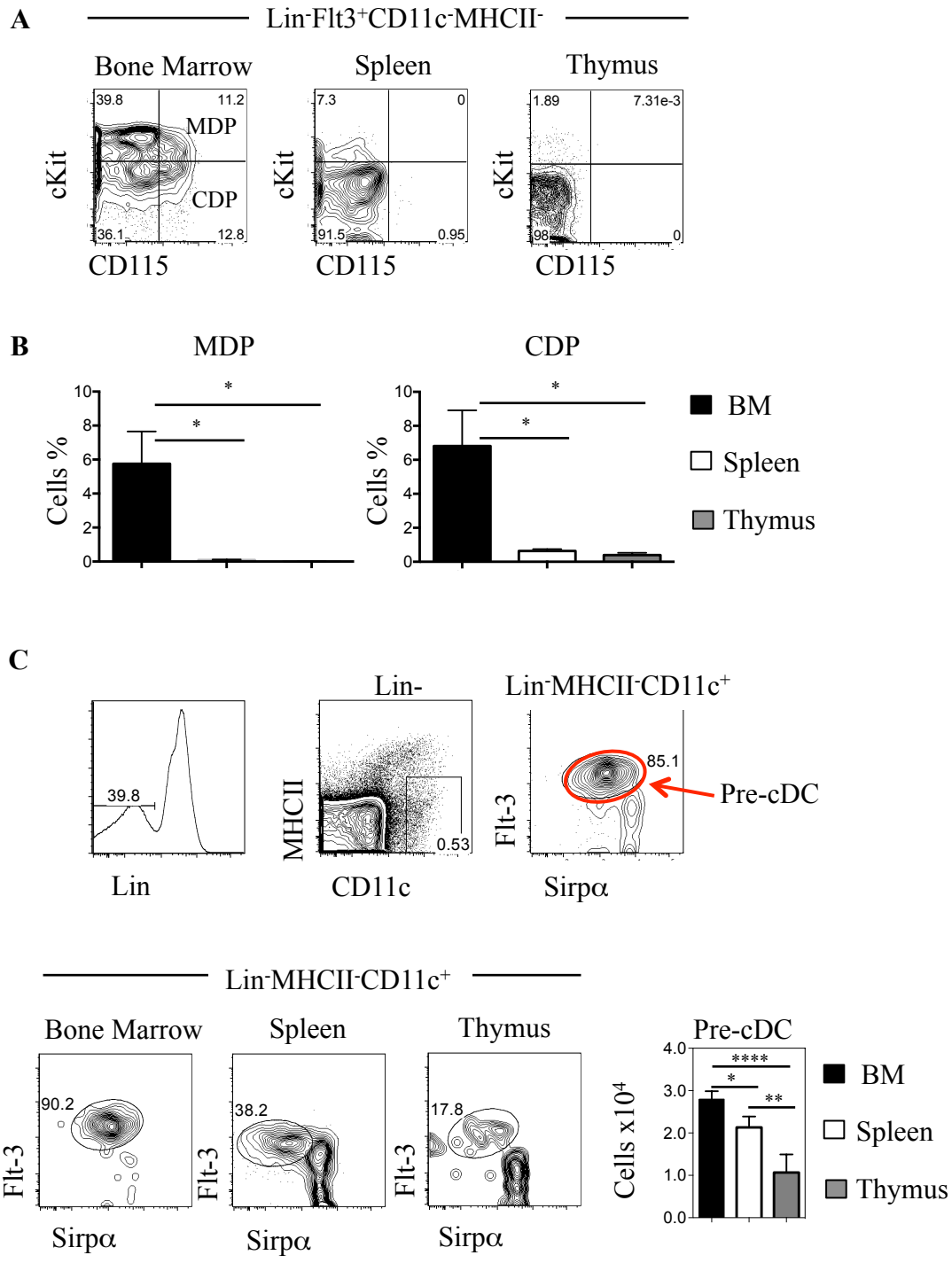
A
Lin-Flt3+CD11c-MHCII-
Bone Marrow
Spleen
Thymus
cKit
CD115
39.8
11.2
MDP
CDP
36.1
12.8
7.3
0
91.5
0.95
1.89
7.31e-3
98
0
B
MDP
CDP
Cells %
BM
Spleen
Thymus
C
Lin-
Lin-MHCII-CD11c+
39.8
Lin
MHCII
CD11c
0.53
Flt-3
Sirpα
85.1
Pre-cDC
Lin-MHCII-CD11c+
Bone Marrow
Spleen
Thymus
90.2
38.2
17.8
Flt-3
Sirpα
Pre-cDC
Cells x10^4
BM
Spleen
Thymus

Pre-cDC can give rise to cDC1 as they undergo recruitment from the bone marrow to the thymus. Considering this and the previous chapter whereby LTβR signalling was shown to regulate the cDC1 population of DC, whether the pre-cDC population was affected under LTβR absence was therefore investigated. As a result, WT, *Ltbr*$^{-/-}$, *Ltbr*^{TEC} and *Foxn1*^{Cre} mouse strains were analysed for pre-cDC populations to determine if there were any alterations in this pre-cDC population. To begin with *Ltbr*$^{-/-}$ mice were analysed for pre-cDC through flow cytometric analysis in the bone marrow, spleen and thymus which were all freshly isolated from adult mice (Figure 4.2 A). The proportions of pre-cDC in WT and *Ltbr*$^{-/-}$ mice were comparable as shown in representative FACs plots for the bone marrow and spleen. However there was a loss of the pre-cDC population in the *Ltbr*$^{-/-}$ thymus compared to WT control mice. This was confirmed by absolute number quantitation with comparable numbers of pre-cDC in the bone marrow and spleen, but a reduction in pre-cDC in thymus of *Ltbr*$^{-/-}$ mice compared to WT control mice (Figure 4.2 A right panel).

This phenotype raised the question of whether this defect in pre-cDC was occurring at the level of LTβR signalling on thymic stromal cells. Therefore, bone marrow chimeras were generated whereby T-cell depleted bone marrow from either *Ltbr*$^{-/-}$ or WT mice was transferred into lethally irradiated WT hosts (pre-cDC would be lacking LTβR) and left for 8 weeks before being sacrificed for pre-cDC absolute number analysis (Figure 4.3 A). When analysed by flow cytometry, results showed that numbers of pre-cDC in the bone marrow, thymus and spleen remained comparable between control WT and *Ltbr*$^{-/-}$ bone marrow transfers; further with no significant difference seen. The reverse chimeras were also generated with lethally irradiated *Ltbr*$^{-/-}$ or WT host mice being reconstituted with WT bone marrow and left for 8 weeks (Figure 4.3 B). Analysis of the pre-cDC in these mice showed

Figure 4.2:
Pre-cDC Are Reduced In Thymus Under LTβR absence

A) Identification of pre-cDC ($Lin^{-}MHCII^{-}CD11c^{+}Flt3^{+}Sirp\alpha^{int}$) with Lin referring to CD19, B220, Ter119, NK1.1 and CD3. These were identified in bone marrow, spleen and thymus of WT and *Ltbr*$^{-/-}$ mice. Absolute number analysis is shown in the right panel with the WT (black bar) and *Ltbr*$^{-/-}$ (white bar). Data is representative of three independent experiments with a sample number of 11 per strain, per tissue.

All significance was noted as: *<0.05, **<0.01, ***<0.001, ***<0.0001.

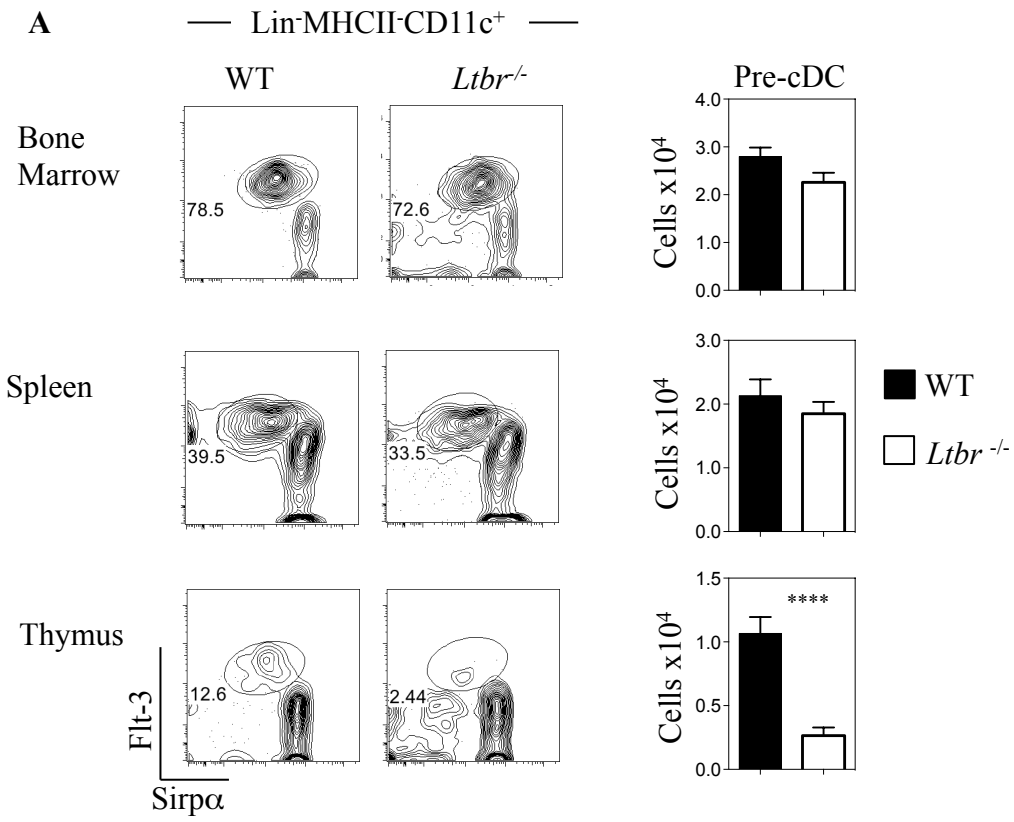
A
Lin-MHCII-CD11c+
WT
Ltbr-/-
Pre-cDC
Bone Marrow
78.5
72.6
Cells x10^4
4.0
3.0
2.0
1.0
0.0
Spleen
39.5
33.5
3.0
2.0
1.0
0.0
WT
Ltbr -/-
Thymus
12.6
2.44
****
1.5
1.0
0.5
0.0
Flt-3
Sirpα

Figure 4.3:

LTβR Absence From Stroma Maps To Pre-cDC Defect But Not Specifically to Thymic Epithelial Cells

Pre-cDC were all identified as $Lin^{-}MHCII^{-}CD11c^{+}Flt3^{+}Sirp\alpha^{int}$ with Lin including the exclusion of CD19, B220, Ter119, NK1.1 and CD3.

A) Generation of bone marrow chimeras with WT bone marrow transferred into a WT host (black bar) or *Ltbr*$^{-/-}$ bone marrow into a WT host (white bar). Mice were analysed 8 weeks post reconstitution for pre-cDC, across three independent experiments where n=10 for both chimeras.

B) Generation of bone marrow chimeras with host thymus analysis following an 8 week period of reconstitution; WT bone marrow into WT host (black bar) and WT bone marrow into *Ltbr*$^{-/-}$ host (white bar). Graphs indicate absolute number analysis of cDC1 progenitors in bone marrow, spleen and thymus. Data represents five independent experiments WT host (15) and *Ltbr*$^{-/-}$ (10).

C) Generation of *Ltbr*^{TEC} mice. Absolute number analysis of pre-cDC in *Foxn1*^{Cre} (black bar) and *Ltbr*^{TEC} (white bar) mice under steady state analysis. Data was obtained across three experiments with n=13 per sample, per strain.

All significance was noted as: *<0.05, **<0.01, ***<0.001, ***<0.0001.

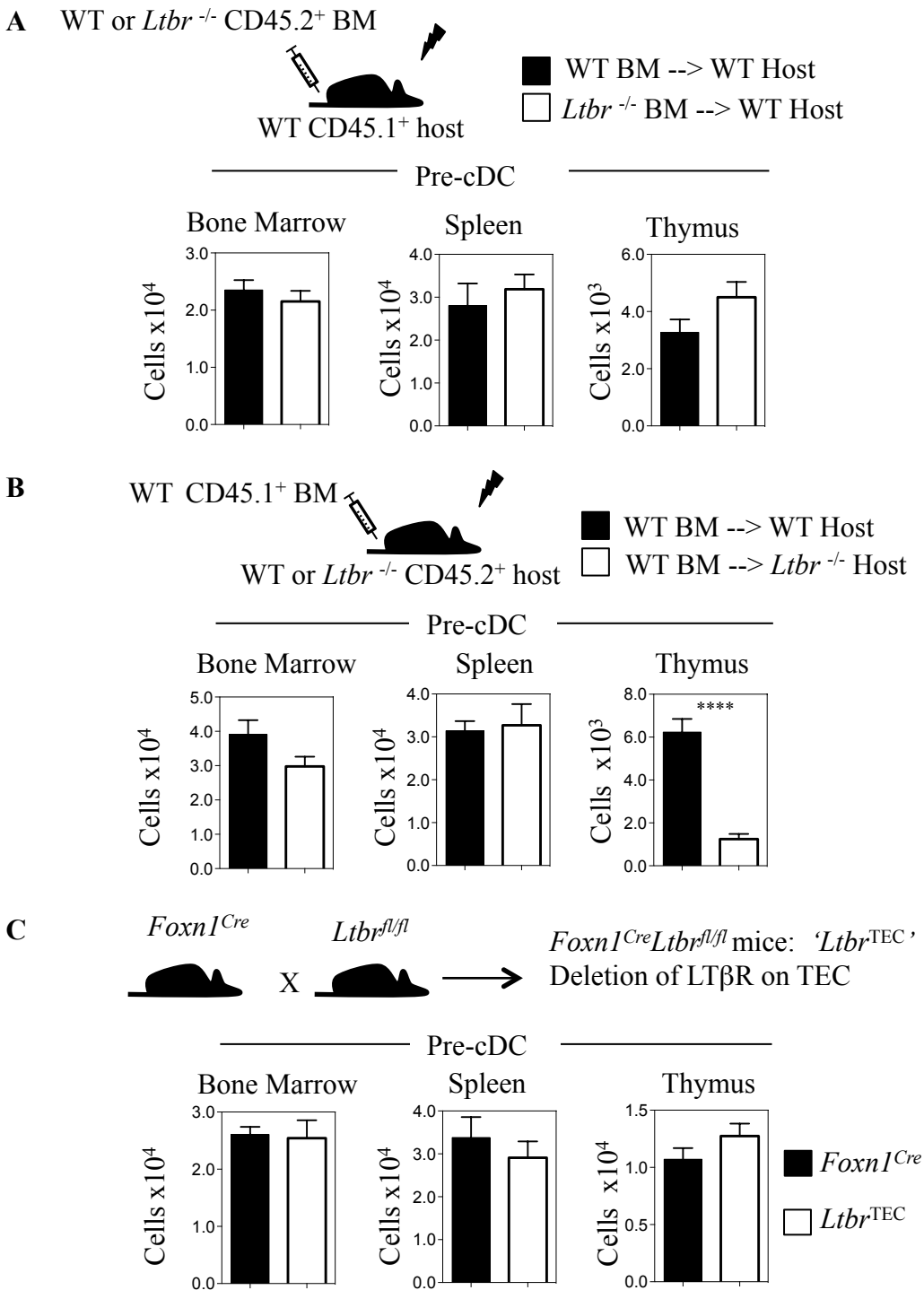
A
WT or Ltbr -/- CD45.2+ BM
WT CD45.1+ host
WT BM --> WT Host
Ltbr -/- BM --> WT Host
Pre-cDC
Bone Marrow
Spleen
Thymus
Cells x10^4
Cells x10^4
Cells x10^3
B
WT CD45.1+ BM
WT or Ltbr -/- CD45.2+ host
WT BM --> WT Host
WT BM --> Ltbr -/- Host
Pre-cDC
Bone Marrow
Spleen
Thymus
****
Cells x10^4
Cells x10^4
Cells x10^3
C
Foxn1Cre
X
Ltbrfl/fl
Foxn1CreLtbrfl/fl mice: 'LtbrTEC'
Deletion of LTβR on TEC
Pre-cDC
Bone Marrow
Spleen
Thymus
Cells x10^4
Cells x10^4
Cells x10^4
Foxn1Cre
LtbrTEC

that absolute numbers were comparable between WT and *Ltbr*$^{-/-}$ hosts in the bone marrow and spleen. However a reduction was seen in pre-cDC in the thymus of WT bone marrow reconstituted *Ltbr*$^{-/-}$ host mice when compared to WT reconstituted controls. Therefore when thymic stroma was deficient in LTβR, cDC1 progenitors became defective within the thymus, but remained unaffected in alternative tissues. Additional analysis then questioned if the requirement for LTβR signalling on thymic stroma for pre-cDC regulation mapped to any difference in *Ltbr*^{TEC} mice compared with *Foxn1*^{Cre} controls (Figure 4.3 C). In this analysis, pre-cDC were unchanged in the bone marrow, spleen and thymus between the *Ltbr*^{TEC} and *Foxn1*^{Cre} mice, with no absolute number difference; suggesting no role for LTβR signalling on TEC in pre-cDC recruitment to the thymus.

From this, we tried to address whether the alternative stromal populations of thymic mesenchyme and endothelial cells were necessary to support pre-cDC recruitment via LTβR signalling, with these populations previously shown to express LTβR (Figure 3.6). Therefore, LTβR deletion on these cells was targeted through the generation of mice in a similar manner to *Ltbr*^{TEC}, using a similar Cre/flox system. To target endothelial cells for LTβR deletion, initially the endothelial marker Tie2 was used, which forms part of the cell surface angiopoietin receptor required to bind angiopoietin. From this, *Tie2*^{Cre} mice (Kisanuki et al., 2001) were crossed with the *Ltbr*$^{fl/fl}$ mice (Wang et al., 2010b), generating *Tie2*^{Cre}*Ltbr*$^{fl/fl}$ mice (Figure 4.4 A). When the thymus of the *Tie2*^{Cre}*Ltbr*$^{fl/fl}$ mice was enzymatically digested following fresh isolation and prepared to examine endothelial cells by flow cytometry, the level of deletion of LTβR from the endothelial cells was incomplete, with the expression pattern spanning both the *Ltbr*$^{-/-}$ and *Tie2*^{Cre} control mice (Figure 4.4 A). The same mice were then analysed for thymic dendritic cell populations, whereby a reduction was seen in pDC

Figure 4.4:
LTβR Deletion From Endothelial Populations Is Incomplete In This Model

A) Generation of endothelial cell specific LTβR deletion model. Analysis in the lower panel indicates level of deletion with isotype for *Ltbr*$^{-/-}$ (grey fill), *Tie2*^{cre} (black solid line) and *Tie2*^{cre}*Ltbr*$^{fl/fl}$ (dashed line).

B) Quantitative analysis of dendritic cell populations in thymus. *Tie2*^{cre} (black bar line) and *Tie2*^{cre}*Ltbr*$^{fl/fl}$ (white bar). Data was obtained from at least two independent experiments (n=6).

C) Pre-cDC analysis of bone marrow, thymus and spleen in *Tie2*^{cre} (black bar line) and *Tie2*^{cre}*Ltbr*$^{fl/fl}$ (white bar). Analysis is representative of n=6 from at least 2 independent experiments.

All data was obtained in collaboration with Kieran James.
All significance was noted as: *<0.05, **<0.01, ***<0.001, ***<0.0001.

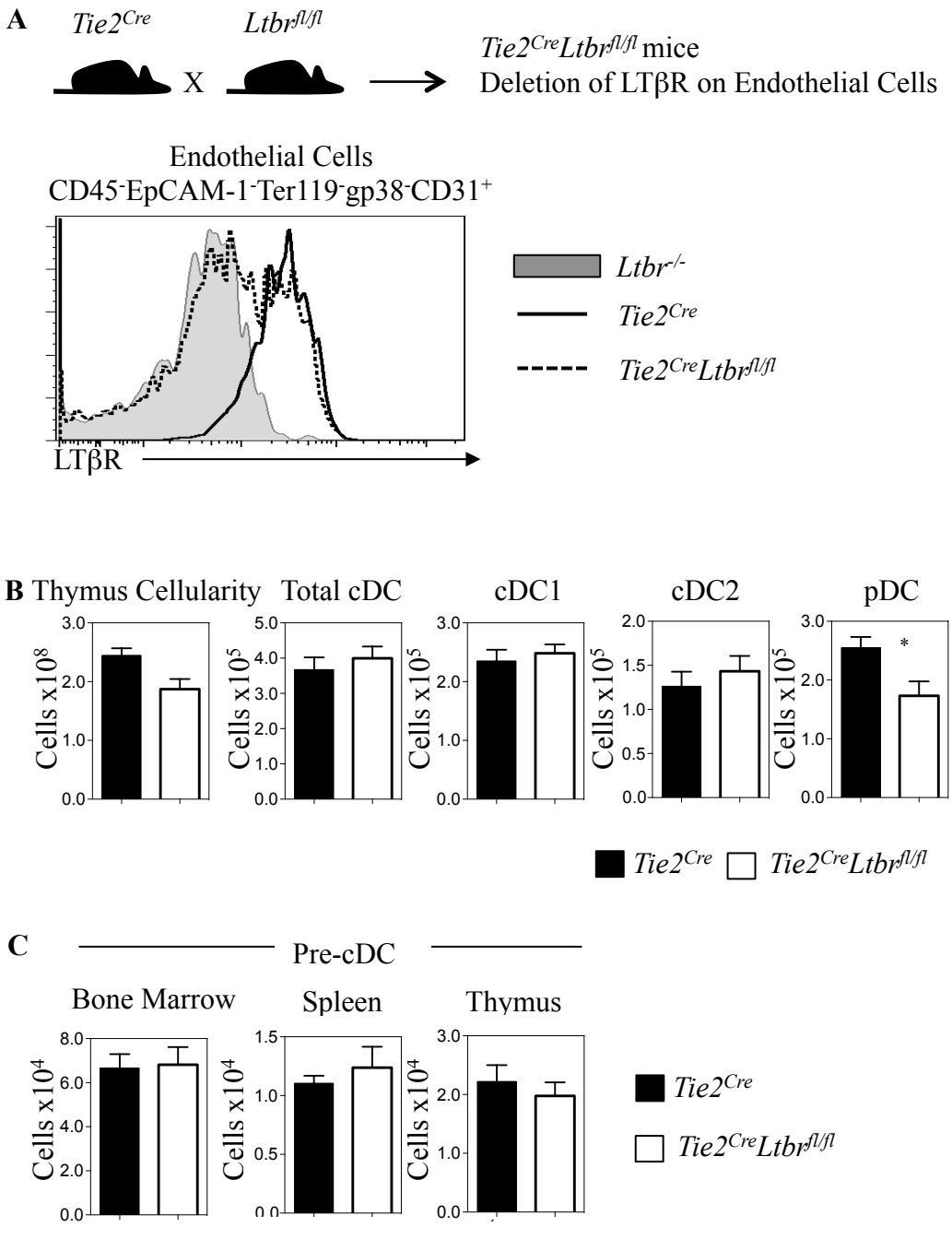
A
Tie2Cre
LtbrfI/fI
X
Tie2CreLtbrfI/fI mice
Deletion of LTβR on Endothelial Cells
Endothelial Cells
CD45-EpCAM-1-Ter119-gp38-CD31+
Ltbr-/-
Tie2Cre
Tie2CreLtbrfI/fI
LTβR
B Thymus Cellularity
Total cDC
cDC1
cDC2
pDC
Cells x10^8
Cells x10^5
*
Tie2Cre
Tie2CreLtbrfI/fI
C
Pre-cDC
Bone Marrow
Spleen
Thymus
Cells x10^4
Tie2Cre
Tie2CreLtbrfI/fI

compared to *Tie2*^{Cre} control mice, but there were no changes in any other dendritic cell subset (Figure 4.4 B). In addition, pre-cDC analysis in isolated bone marrow, spleen and thymus samples from *Tie2*^{Cre}*Ltbr*$^{fl/fl}$ mice, showed no difference compared to controls. Therefore a partial deletion failed to achieve the same phenotype as the germline *Ltbr*$^{-/-}$ mice.

Subsequently, an alternative endothelial marker was selected, with the use of the *Flk1*^{Cre} mouse model (Motoike et al., 2003), with Flk1 being a receptor for Vascular Endothelial Growth Factor (VEGF). These mice were crossed to *Ltbr*$^{fl/fl}$ mice (Wang et al., 2010b) to generate *Flk1*^{Cre}*Ltbr*$^{fl/fl}$ mice (Figure 4.5 A). The deletion of LTβR on these mice was then assessed to check whether there would be due to successful deletion from endothelial cells. This was shown through FACs analysis following preparation of thymus samples with enzymatic digestion, anti-CD45 MACs bead depletion and antibody staining for endothelial cell identification (CD45^{-}EpCAM-1^{-}Ter119^{-}gp38^{-}CD31^{+}) (Figure 4.5 A). Deletional analysis showed that LTβR was successfully deleted from the endothelial cells in the *Flk1*^{Cre}*Ltbr*$^{fl/fl}$ mice with levels of LTβR mapping to the *Ltbr*$^{-/-}$ control mice; positive staining for LTβR expression was only seen on the *Flk1*^{Cre} control mice. Subsequently, FACs analysis was also performed to assess the impact on thymic DCs in *Flk1*^{Cre}*Ltbr*$^{fl/fl}$ mice, with similar thymus digestion upon isolation and antibody staining but for DC identification. This highlighted that cDC were unchanged, and pDC were reduced by half compared to *Flk1*^{Cre} control mice (Figure 4.5 B). Furthermore, this unchanged cDC1 population was supported by no difference in pre-cDC, which were identified by flow cytometry in bone marrow, spleen and thymus of *Flk1*^{Cre} and *Flk1*^{Cre}*Ltbr*$^{fl/fl}$ mice (Figure 4.5 C).

Figure 4.5:
Alternative Model For LTβR deletion From Endothelial Cells Yields Complete Deletion

A) Model of LTβR deletion from endothelial cells. The lower panel highlights the level of deletion in this system with staining for *Ltbr*$^{-/-}$ (grey fill), *Flk1*^{Cre} (black solid line) and *Flk1*^{Cre}*Ltbr*$^{fl/fl}$ (dashed line). Representative of two independent experiments n=6.

B) Absolute number analysis of thymic dendritic cell populations; representative of two independent experiments with *Flk1*^{cre} (black bar) n=6 and *Flk1*^{cre}*Ltbr*$^{fl/fl}$ (white bar) n=4.

C) Pre-cDC absolute number analysis in the bone marrow, spleen and thymus. Pre-cDC are identified as Lin^{-}MHCII^{-}CD11c^{+}Flt3^{+}Sirpα^{int} with Lin referring to the exclusion of CD19, B220, Ter119, NK1.1 and CD3. *Flk1*^{cre}*Ltbr*$^{fl/fl}$ (white bars), *Flk1*^{cre} controls (black bars). Data is representative of two independent experiment with *Flk1*^{cre}n=6 and *Flk1*^{cre}*Ltbr*$^{fl/fl}$ n=4.

All significance was noted as: *<0.05, **<0.01, ***<0.001, ***<0.0001.

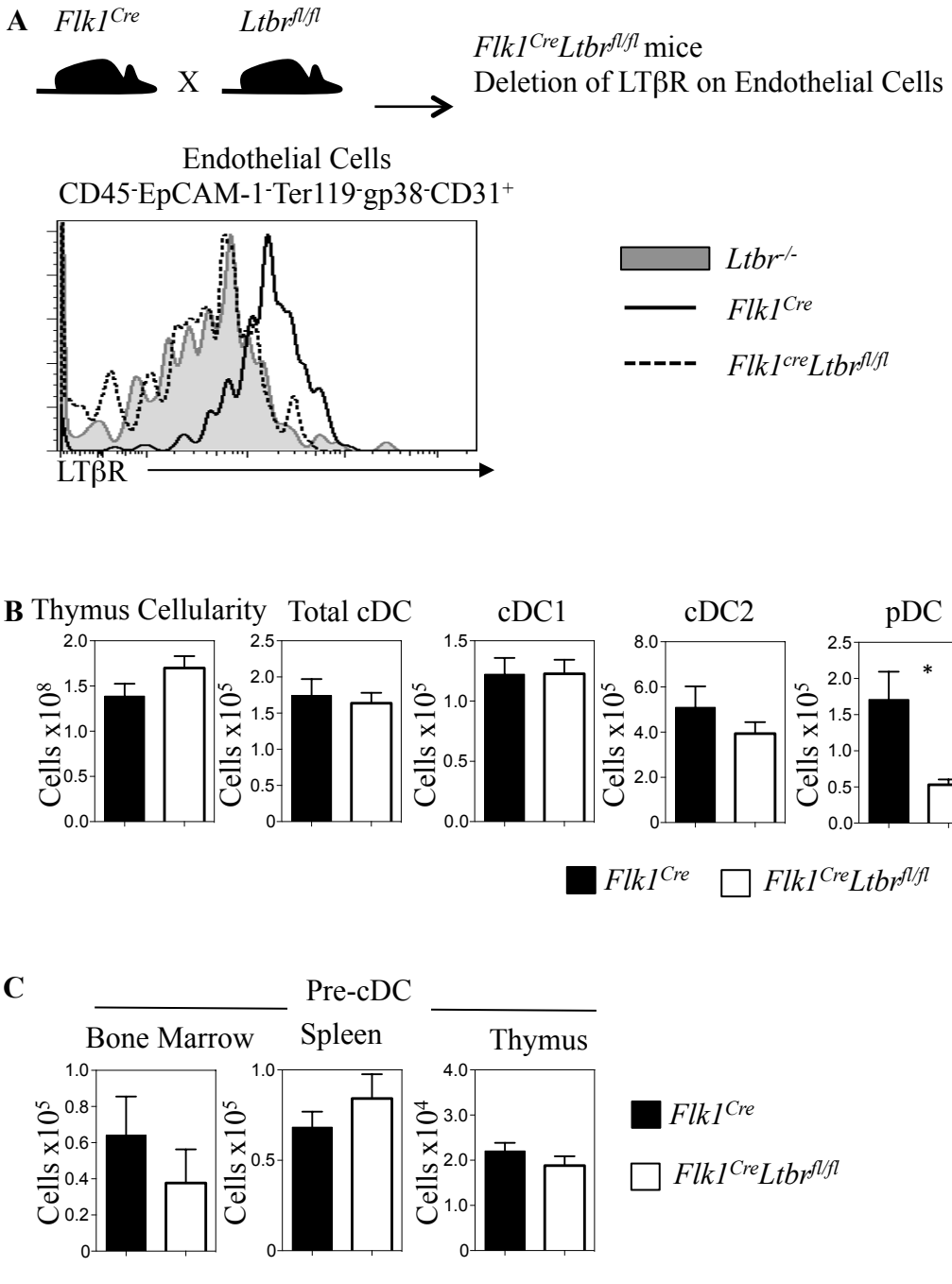
A
Flk1Cre
Ltbrfl/fl
X
Flk1CreLtbrfl/fl mice
Deletion of LTβR on Endothelial Cells
Endothelial Cells
CD45-EpCAM-1-Ter119-gp38-CD31+
LTβR
Ltbr-/-
Flk1Cre
Flk1creLtbrfl/fl
B Thymus Cellularity
Total cDC
cDC1
cDC2
pDC
Cells x10^8
Cells x10^5
Cells x10^5
Cells x10^5
Cells x10^5
*
Flk1Cre
Flk1CreLtbrfl/fl
C
Pre-cDC
Bone Marrow
Spleen
Thymus
Cells x10^5
Cells x10^5
Cells x10^4
Flk1Cre
Flk1CreLtbrfl/fl

Furthermore, mesenchymal cells were then targeted for LTβR deletion, which was initially investigated through *PDGFRβ*^{Cre} mice (Foo et al., 2006) that were crossed with *Ltbr*$^{fl/fl}$ mice (Wang et al., 2010b), generating *PDGFRβ*^{Cre}*Ltbr*$^{fl/fl}$ mice (Figure 4.6 A). Platelet derived growth factor receptor β (PDGFRβ), is expressed by mesenchymal cells and therefore was a good target for mesenchymal deletion of LTβR. However when *PDGFRβ*^{Cre}*Ltbr*$^{fl/fl}$ mice, were analysed for the deletion of LTβR from mesenchymal cells that were retrieved from thymus, there was incomplete deletion with LTβR expression on *PDGFRβ*^{Cre}*Ltbr*$^{fl/fl}$ mice overlapping with *PDGFRβ*^{Cre} mice as a positive staining control (Figure 4.6 A). Therefore this highlighted incomplete deletion once again. However again, DC were analysed to determine if any phenotype may subsequently be achieved with this partial deletion. Yet following this, DC populations in *PDGFRβ*^{Cre}*Ltbr*$^{fl/fl}$ mice were comparable to *PDGFRβ*^{Cre} controls (Figure 4.6 B) and in addition analysis of pre-cDC again highlighted no difference between these mice in bone marrow, spleen or thymus (Figure 4.6 C).

From this, it was decided to try again to generate alternative versions of these mice to obtain deletion of LTβR from mesenchymal cell populations. Therefore *Wnt1*^{Cre} mice (Lewis et al., 2013) were crossed with the *Ltbr*$^{fl/fl}$ mice (Wang et al., 2010b) to generate *Wnt1*^{Cre}*Ltbr*$^{fl/fl}$ mice to drive deletion of LTβR on mesenchymal cells which are of neural crest origin and present within the thymus (Figure 4.7 A) (Foster et al., 2008, Muller et al., 2008). Analysis of the deletion of LTβR from mesenchymal cells in *Wnt1*^{Cre}*Ltbr*$^{fl/fl}$ mice was conducted via flow cytometry. This showed that there was partial deletion, with *Wnt1*^{Cre}*Ltbr*$^{fl/fl}$ mice having a shifted expression of LTβR compared to the *Wnt1*^{Cre} control mice, but failing to completely overlap with the *Ltbr*$^{-/-}$ negative control. Therefore it appears to have some level of successful deletion but again remains incomplete.

Figure 4.6:
LTβR Deletion From Mesenchymal Populations Is Incomplete In This Model

A) Generation of a model for LTβR deletion from mesenchymal cells. Lower panel highlights level of LTβR deletion with *Ltbr*$^{-/-}$ (grey fill), *PDGFRβ*^{Cre} (black solid line) and *PDGFRβ*^{Cre}*Ltbr*$^{fl/fl}$ (dashed line).

B) Quantitative analysis of dendritic cell populations in thymus. *PDGFRβ*^{Cre} (black bar line) and *PDGFRβ*^{Cre}*Ltbr*$^{fl/fl}$ (white bar). Data was obtained from at least two independent experiments (n=5).

C) Pre-cDC absolute number analysis from bone marrow, spleen and thymus of *PDGFRβ*^{Cre} (black bar line) and *PDGFRβ*^{Cre}*Ltbr*$^{fl/fl}$ (white bar) mice. Data was obtained from two independent experiments, n=5.

All data was obtained in collaboration with Kieran James.

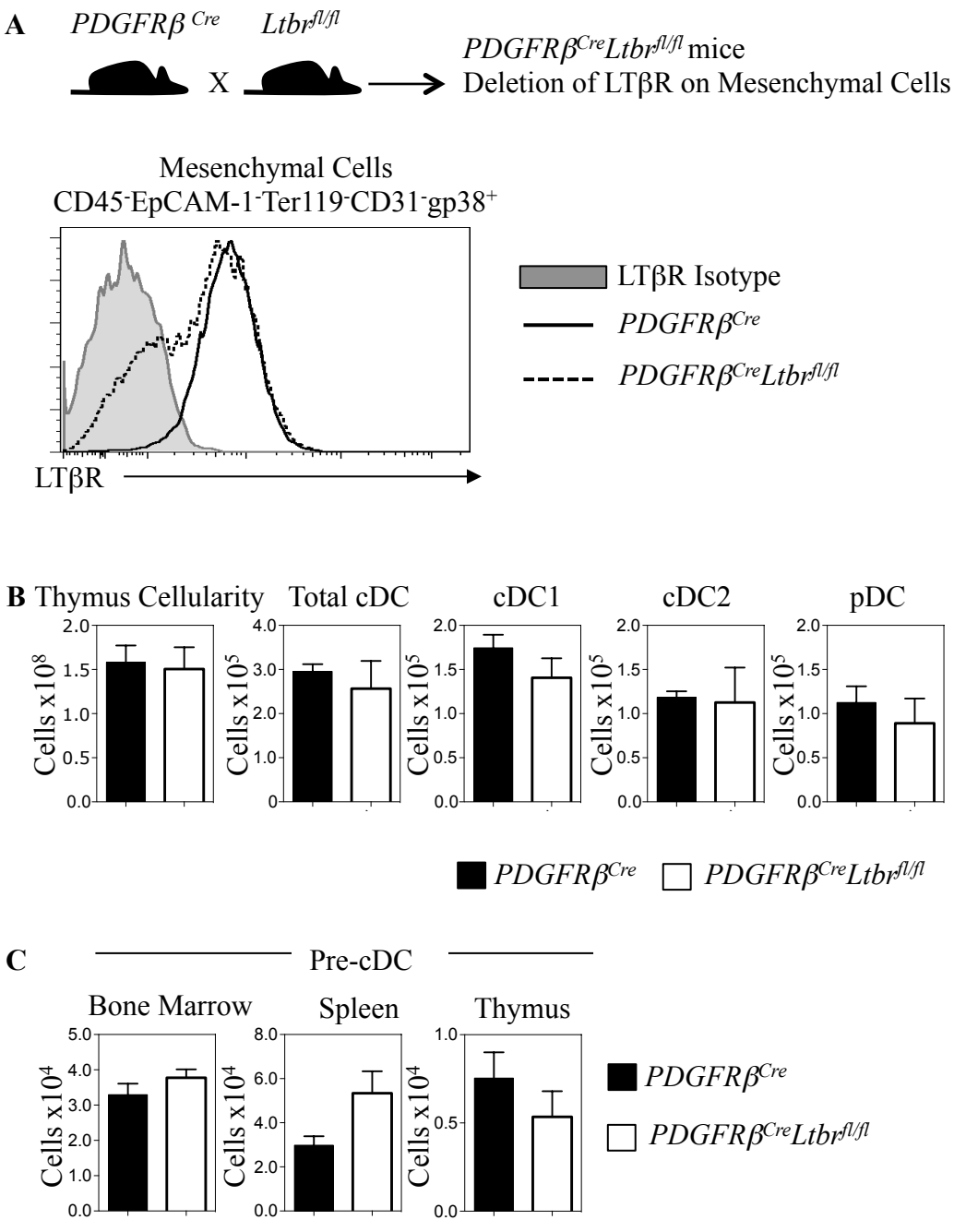
A
PDGFRβ Cre
Ltbr fl/fl
X
PDGFRβCreLtbrfl/fl mice
Deletion of LTβR on Mesenchymal Cells
Mesenchymal Cells
CD45-EpCAM-1-Ter119-CD31-gp38+
LTβR Isotype
PDGFRβCre
PDGFRβCreLtbrfl/fl
LTβR
B Thymus Cellularity
Total cDC
cDC1
cDC2
pDC
Cells x10^8
Cells x10^5
PDGFRβCre
PDGFRβCreLtbrfl/fl
C
Pre-cDC
Bone Marrow
Spleen
Thymus
Cells x10^4
PDGFRβCre
PDGFRβCreLtbrfl/fl

Figure 4.7:

Generation of An Alternative Mesenchymal LTβR Deletional Model Fails To Yield Complete Deletion

A) Mechanism of generation of the *Wnt1*^{Cre}*Ltbr*$^{fl/fl}$ mice. Lower panel shows deletional analysis obtained from LTβR expression analysis on CD45^{-}EpCAM-1^{-}Ter119^{-}CD31^{-}gp38^{+} mesenchymal cells with *Ltbr*$^{-/-}$ (grey fill), *Wnt1*^{Cre} (black solid line) and *Wnt1*^{Cre}*Ltbr*$^{fl/fl}$ (dashed line) mice. This deletion was repeated across three independent experiments where n=8

B) Corresponding absolute number analysis of thymic dendritic cells with *Wnt1*^{Cre} (black bar) and *Wnt1*^{Cre}*Ltbr*$^{fl/fl}$ (white bar) mice obtained from three independent experiments n=7/8 respectively.

C) Analysis of absolute numbers of pre-cDC in the bone marrow, thymus and spleen of *Wnt1*^{Cre}and *Wnt1*^{Cre}*Ltbr*$^{fl/fl}$ mice (black and white bars respectively). Data is again representative of three individual experiments with n=7 for *Wnt1*^{Cre} and n=8 for *Wnt1*^{Cre}*Ltbr*$^{fl/fl}$ mice.

All significance was noted as: *<0.05, **<0.01, ***<0.001, ***<0.0001.

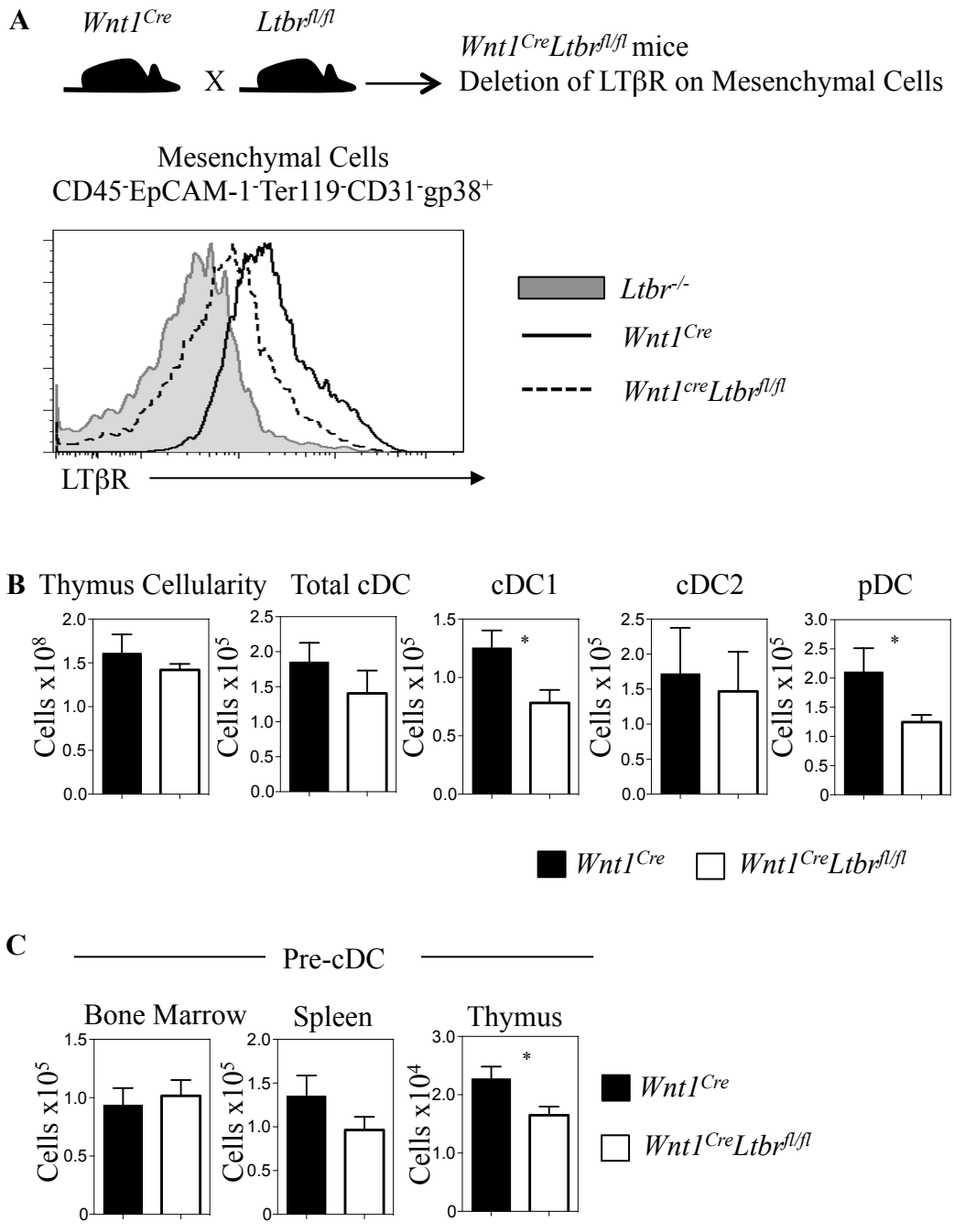
A
Wnt1Cre
Ltbrfl/fl
X
Wnt1CreLtbrfl/fl mice
Deletion of LTβR on Mesenchymal Cells
Mesenchymal Cells
CD45-EpCAM-1-Ter119-CD31-gp38+
LTβR
Ltbr-/-
Wnt1Cre
Wnt1creLtbrfl/fl
B
Thymus Cellularity
Total cDC
cDC1
cDC2
pDC
Cells x10^8
Cells x10^5
Wnt1Cre
Wnt1CreLtbrfl/fl
C
Pre-cDC
Bone Marrow
Spleen
Thymus
Cells x10^5
Cells x10^4
Wnt1Cre
Wnt1CreLtbrfl/fl

Subsequent analysis of these *Wnt1*^{Cre}*Ltbr*$^{fl/fl}$ mice with thymic preparation and intrathymic DC identification by flow cytometry showed that the partial deletion was sufficient to cause a phenotype with regards to thymic DC (Figure 4.7 B). Absolute number quantitation showed that when the *Wnt1*^{Cre} and *Wnt1*^{Cre}*Ltbr*$^{fl/fl}$ mice were compared, total cellularities, total cDC and cDC2 were comparable in the thymus. However, the partial deletion seen in *Wnt1*^{Cre}*Ltbr*$^{fl/fl}$ mice was sufficient to generate a phenotype of cDC1 and pDC reduction compared to *Wnt1*^{Cre} control mice (Figure 4.7 B). Additionally when the bone marrow, spleen and thymus were isolated and analysed for pre-cDC populations, there was no reduction seen in pre-cDC in the bone marrow or spleen but a reduced population in the thymus of *Wnt1*^{Cre}*Ltbr*$^{fl/fl}$ mice compared to control *Wnt1*^{Cre} mice (Figure 4.7 C). As a result, this suggests that the partial deletion seen in these *Wnt1*^{Cre}*Ltbr*$^{fl/fl}$ mice is sufficient to support a pre-cDC reduction in thymus and a corresponding cDC1 reduction most similar to the phenotype reported in the *Ltbr*$^{-/-}$ germline model.

4.2.2 Alternative Mechanisms For Recruitment of cDC1 Progenitors

It was apparent at this stage, that the dissection of the stromal population signalling through LTβR to impact pre-cDC recruitment to the thymus for subsequent cDC1 development was suggestive of a role for thymic mesenchyme. As a result, it was decided to investigate the contribution of possible chemokines to this process of pre-cDC recruitment as they have previously been implicated in recruitment of mature dendritic cell populations (cDC2 and pDC) into the thymus (Baba et al., 2009, Hadeiba et al., 2012). Further due to the association between LTβR and CCR7 ligand production in the thymus, the potential role for CCR7 in the regulation of pre-cDC populations was explored (Lkhagvasuren et al., 2013, Krueger et al., 2010).

As a result, expression of CCR7 by the DC populations was initially assessed (Figure 4.8 A). This was completed with isolation of thymic tissue and enzymatic digestion for DC retrieval. Antibody staining was then completed to identify the DC subpopulations but further whether they expressed CCR7 on their surface as detected by flow cytometry. FACs analysis, using a CCR7 isotype (Figure 5.8 A), showed positive staining on cDC1, pre-cDC and cDC2, but that pDC for the most part, had no CCR7 expression. Considering this positive result for cDC1 it was possible that CCR7 signalling may be implicated in the regulation of the cDC1 population.

From this, there was analysis of *Ccr7*$^{-/-}$ mice to determine if under the absence of CCR7 expression, dendritic cell populations, in particular the cDC1 and their progenitors were defective. However, due to CCR7 ligands being required in development of mTEC populations, it was decided to firstly check that TEC compartments were intact in *Ccr7*$^{-/-}$ mice, so that if any difference was reported in thymic DC analysis, it was not the result of a bystander effect of altered TEC populations. TEC were therefore analysed through enzymatic digestion of freshly isolated adult thymic tissue prior to flow cytometric analysis of WT control and *Ccr7*$^{-/-}$ mice. Representative FACs plots showing WT compared to *Ccr7*$^{-/-}$ thymi for all TEC populations suggested that proportions of TEC populations were unchanged between these mice including Aire expressing and CCL21 expressing mTEC, which remained largely comparable (Figure 4.9 A). Absolute number analysis in the thymus was completed and similarly, TEC populations remained comparable between WT and *Ccr7*$^{-/-}$ mice (Figure 4.9 B) with no significant differences seen.

Figure 4.8:
CCR7 Is Expressed by Some Dendritic Cell Populations

A) Expression of CCR7 on different thymic DC populations. This was determined by FAC with positive staining (blue line) detected against a CCR7 isotype (grey filled). Representative plots are shown from two independent repeats, totaling n=7.

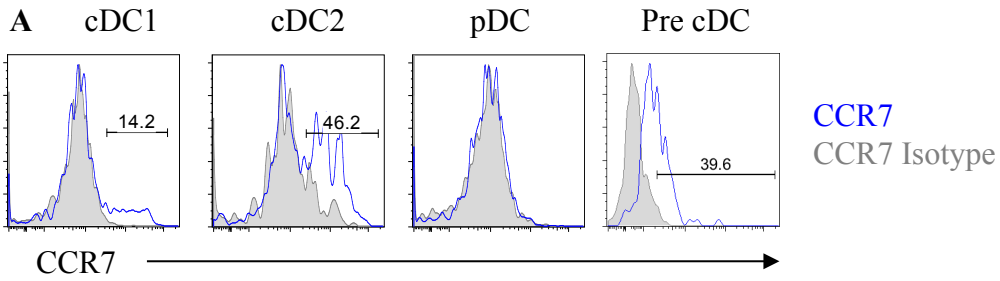
A
cDC1
cDC2
pDC
Pre cDC
14.2
46.2
39.6
CCR7
CCR7
CCR7 Isotype

Figure 4.9:

CCR7 Deficient Mice Have Comparable Thymic Epithelial Cell Analysis to WT Controls

A) FACs plots show the proportional make up of TEC populations within a WT and *Ccr7*$^{-/-}$ thymus. It also clearly highlights the gating strategy used in the identification of these populations.

B) Absolute numbers of TEC populations were calculated in the thymus of WT (black bars) and *Ccr7*$^{-/-}$ (white bars) mice with total thymus cellularity also shown. Data is representative of two independent experiments where n=6.

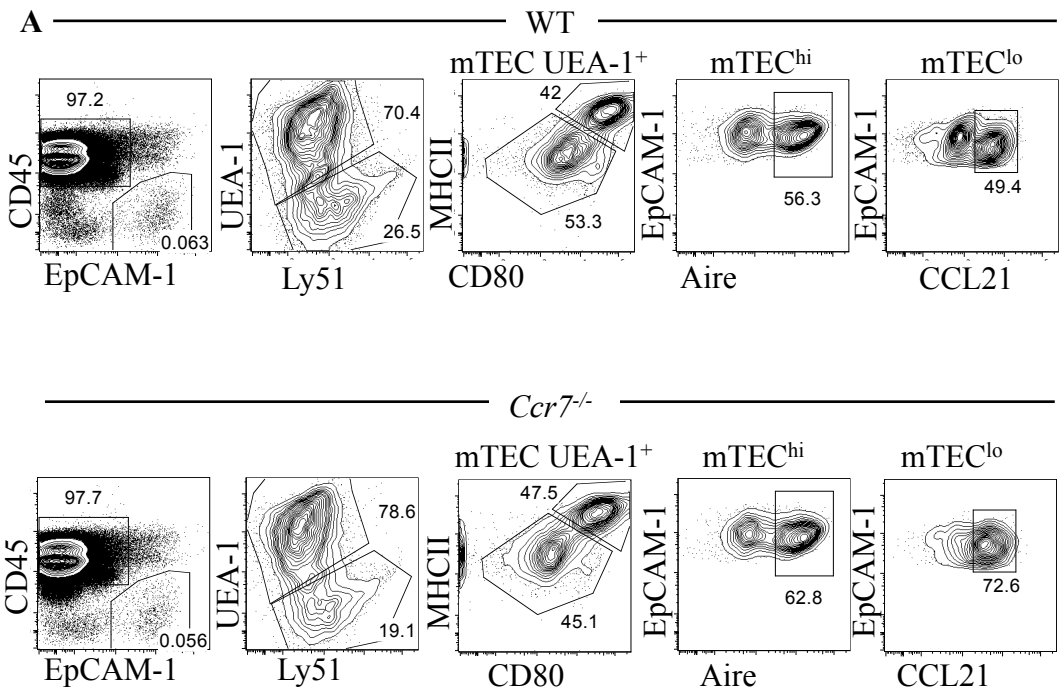
A
WT
mTEC UEA-1+
mTEChi
mTEClo
97.2
0.063
CD45
EpCAM-1
70.4
26.5
UEA-1
Ly51
42
53.3
MHCII
CD80
EpCAM-1
56.3
Aire
EpCAM-1
49.4
CCL21
Ccr7-/-
mTEC UEA-1+
mTEChi
mTEClo
97.7
0.056
CD45
EpCAM-1
78.6
19.1
UEA-1
Ly51
47.5
45.1
MHCII
CD80
EpCAM-1
62.8
Aire
EpCAM-1
72.6
CCL21

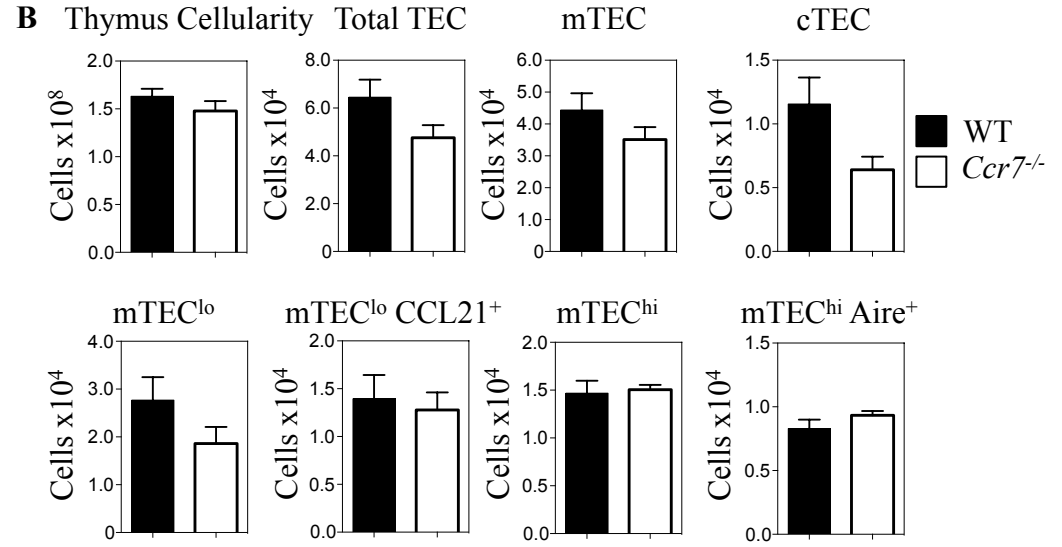
B
Thymus Cellularity
Total TEC
mTEC
cTEC
Cells x10^8
Cells x10^4
Cells x10^4
Cells x10^4
WT
Ccr7-/-
mTEClo
mTEClo CCL21+
mTEChi
mTEChi Aire+
Cells x10^4
Cells x10^4
Cells x10^4
Cells x10^4

Therefore due to these unaltered TEC populations, analysis of the intrathymic DC compartment in WT compared to *Ccr7*$^{-/-}$ mice could be conducted to see if there was a direct effect on these DC populations following CCR7 absence.

Firstly, DCs were identified in the thymus of WT and *Ccr7*$^{-/-}$ mice through flow cytometric analysis and representative plots showed that under the absence of CCR7, proportions of total cDC and cDC1 and pDC were reduced (Figure 4.10 A). Quantitation from this highlighted a significant reduction in total cDC which correlated in particular to reduced cDC1 as cDC2 remained unchanged (Figure 4.10 B). Additionally pDC were reduced to a significant level. Therefore this data is suggestive of a potential requirement for CCR7 to coordinate cDC1 and pDC in the thymus. Splenic analysis was also completed to rule out any peripheral alterations in DC in *Ccr7*$^{-/-}$ mice and data showed no effect compared to WT control mice (Figure 4.10 C). Furthermore pre-cDC were identified by flow cytometry in the bone marrow, spleen and thymus and absolute numbers showed that WT controls were comparable to *Ccr7*$^{-/-}$ mice in the bone marrow however reduced pre-cDC were seen in the spleen and a more significant reduction was seen in the thymus of *Ccr7*$^{-/-}$ mice compared to WT control mice (Figure 4.10 C). Therefore this suggests a possible requirement for CCR7 to be present to support recruitment of pre-cDC and cDC1 development.

Considering this possibility, whether there was a direct requirement for CCR7 signalling on the CCR7 expressing DCs themselves was not shown. This was therefore investigated through the generation of CCR7 mixed bone marrow chimeras. For this, WT mice that had been lethally irradiated were reconstituted with T-cell depleted WT CD45.1^{+} and WT/*Ccr7*$^{-/-}$

Figure 4.10:
***Ccr7*$^{-/-}$ Mice Have Reductions In Dendritic Cell Populations**

A) FACs plots show the distribution of dendritic cells in WT and *Ccr7*$^{-/-}$ mice.

B) The lower panel shows corresponding absolute number analysis generated following FACs with total thymus cellularities and dendritic cell populations highlighted. WT (black bar) is representative of n=14 and *Ccr7*$^{-/-}$ (white bar) n=14 in the thymus obtained from four independent experiments.

C) Absolute number analysis of splenic dendritic cell populations in WT (black bar) is representative of n=14 and *Ccr7*$^{-/-}$ (white bar) n=14 obtained from four independent experiments.

D) Pre-cDC analysis in bone marrow, spleen, thymus in WT (black bar) and *Ccr7*$^{-/-}$ (white bar). Pre-cDC were Lin^{-}MHCII^{-}CD11c^{+}Flt3^{+}Sirpα^{int} with Lin excluding CD19, B220, Ter119, NK1.1 and CD3 positive cells. Data was obtained from three independent experiments where n=10.

All significance was noted as: *<0.05, **<0.01, ***<0.001, ***<0.0001.

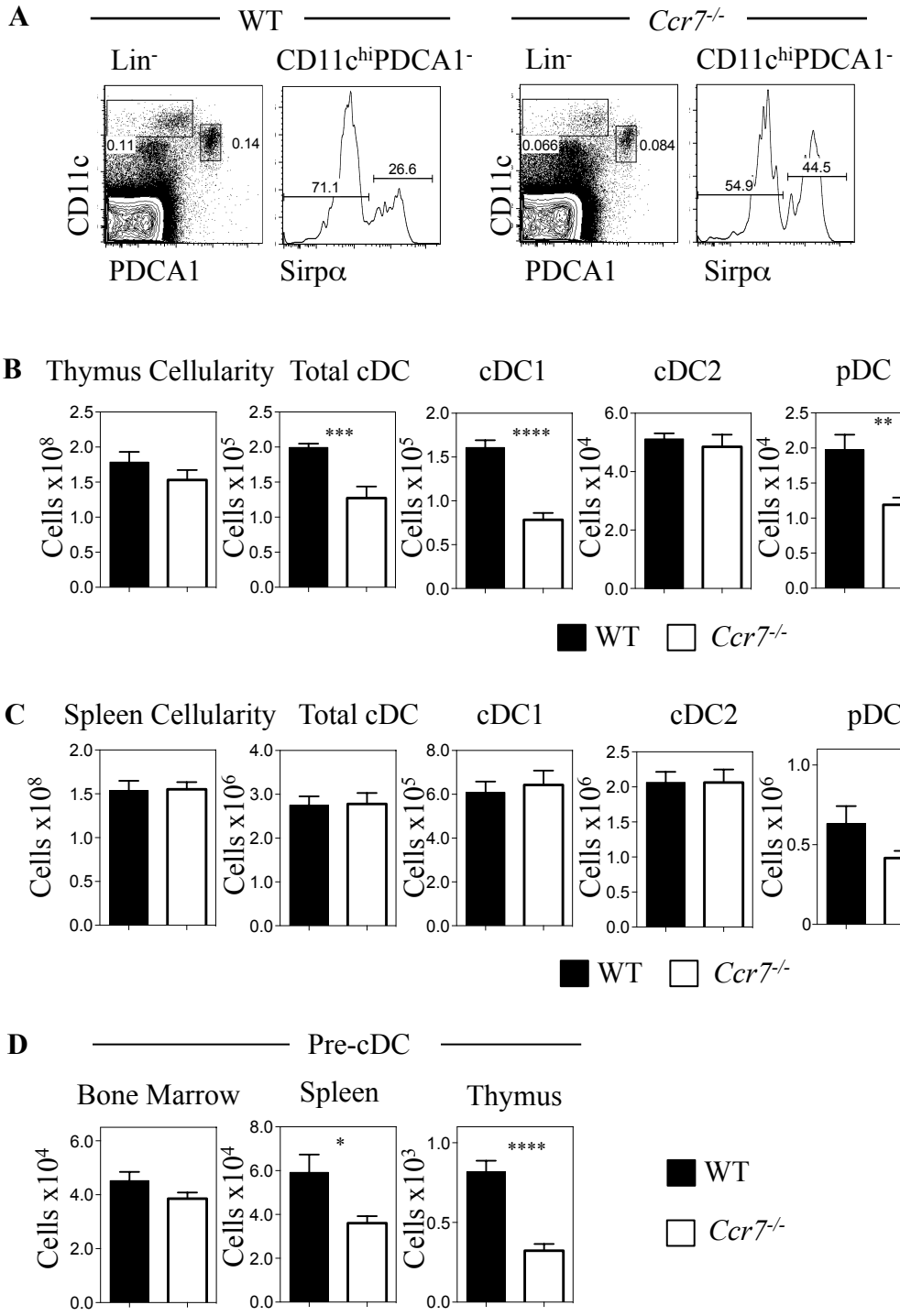
A
WT
Ccr7-/-
Lin-
CD11chiPDCA1-
Lin-
CD11chiPDCA1-
0.11
0.14
71.1
26.6
0.066
0.084
54.9
44.5
CD11c
PDCA1
Sirpα
CD11c
PDCA1
Sirpα
B
Thymus Cellularity
Total cDC
cDC1
cDC2
pDC
Cells x10^8
Cells x10^5
Cells x10^5
Cells x10^4
Cells x10^4
***
****
**
WT
Ccr7-/-
C
Spleen Cellularity
Total cDC
cDC1
cDC2
pDC
Cells x10^8
Cells x10^6
Cells x10^5
Cells x10^6
Cells x10^6
WT
Ccr7-/-
D
Pre-cDC
Bone Marrow
Spleen
Thymus
Cells x10^4
Cells x10^4
Cells x10^3
*
****
WT
Ccr7-/-

CD45.2^{+} bone marrow in equal proportions. Experimental mice contained WT and *Ccr7*$^{-/-}$ bone marrow co-transfers whereas controls contained WT:WT bone marrow. This allowed analysis concerning the ability of CCR7 deficient bone marrow to compete with WT for the development of DCs in the thymus as well as their ability to support pre-cDC (Figure 4.11).

By gating on the DC populations first, the proportion of the DC subsets that were reconstituted by CD45.1 expressing WT or CD45.1 lacking (CD45.2^{+}) *Ccr7*$^{-/-}$ or WT bone marrow could be determined. Proportional analysis appeared to show roughly equivalent reconstitution of CD45.1^{+} or CD45.1^{-} compartments of DC in WT:WT transfers. However WT:*Ccr7*$^{-/-}$ bone marrow transfers had proportional differences, shown in representative FACs plots (Figure 4.11 B) in the cDC1 and pre-cDC populations compared to WT controls.

This was quantitated through proportional analysis for the contribution of CD45.1 or CD45.2 to the DC (Figure 4.11 C). The relative proportions of WT:WT transfers remained reasonably equal in all populations however comparisons between WT:WT and WT:*Ccr7*$^{-/-}$ transfers for the relative CD45.1/2 proportion, identified differences in cDC1. The WT population in the WT:*Ccr7*$^{-/-}$ transfers contributed more to the cDC1 population as it outcompeted the *Ccr7*$^{-/-}$ proportion making up 75% and 25% of the cDC1 population as a whole respectively. This was shown to be particularly skewed when compared to the relative WT:WT controls, which reconstituted at roughly 50%, 50%. Therefore a significant increase could be seen between the WT CD45.1^{+} compartment from WT:*Ccr7*$^{-/-}$ transfers when compared with the WT CD45.1^{+} compartment in WT:WT transfers for cDC1. Also a reduction could be seen for the CD45.2^{+} *Ccr7*$^{-/-}$ proportion from the WT: *Ccr7*$^{-/-}$ transfers when compared to the WT CD45.2^{+} compartment in WT:WT transfers. This exact trend was recapitulated with the pre-cDC

Figure 4.11:
cDC1 Require Cell Intrinsic Signalling Through CCR7 For Thymic Persistence

A) Model used for WT and *Ccr7*$^{-/-}$ bone marrow transfer into WT congenically distinguished hosts. Representative FACs plots show the method used to identify the dendritic cell populations and their make-up with regards to differently labelled reconstituting compartments. Pre-cDC are also shown for the final CD45.1 discrimination rather than population identification. Pre-cDC were Lin^{-}MHCII^{-}CD11c^{+}Flt3^{+}Sirpα^{int} with lineage excluding CD19, CD3, B220, NK1.1 and Ter119.

B) Control chimera generation with WT:WT bone marrow placed equally into an irradiated WT host utilising congenic markers to distinguish each population. The lower panel shows dendritic cell identification from different CD45 compartments. Pre-cDC proportions of CD45.1$^{+/-}$ were included and identified as in A.

C) Analysis of host thymus following bone marrow reconstitution. Analysis is all proportional with the left bar of each graph representing the WT:WT bone marrow reconstituted WT host. Within this, the black part of the bar correlates to WT CD45.1 and the white part being WT CD45.2. The right bar of each graph represents WT:*Ccr7*$^{-/-}$ bone marrow used to reconstitute the WT host with the black section referring to the WT CD45.1 bone marrow derived cells and the white being CD45.2 *Ccr7*$^{-/-}$. Data is obtained across two independent experiments n=8. For pre-cDC data is from two independent experiments n=6.

All significance was noted as: *<0.05, **<0.01, ***<0.001, ***<0.0001.

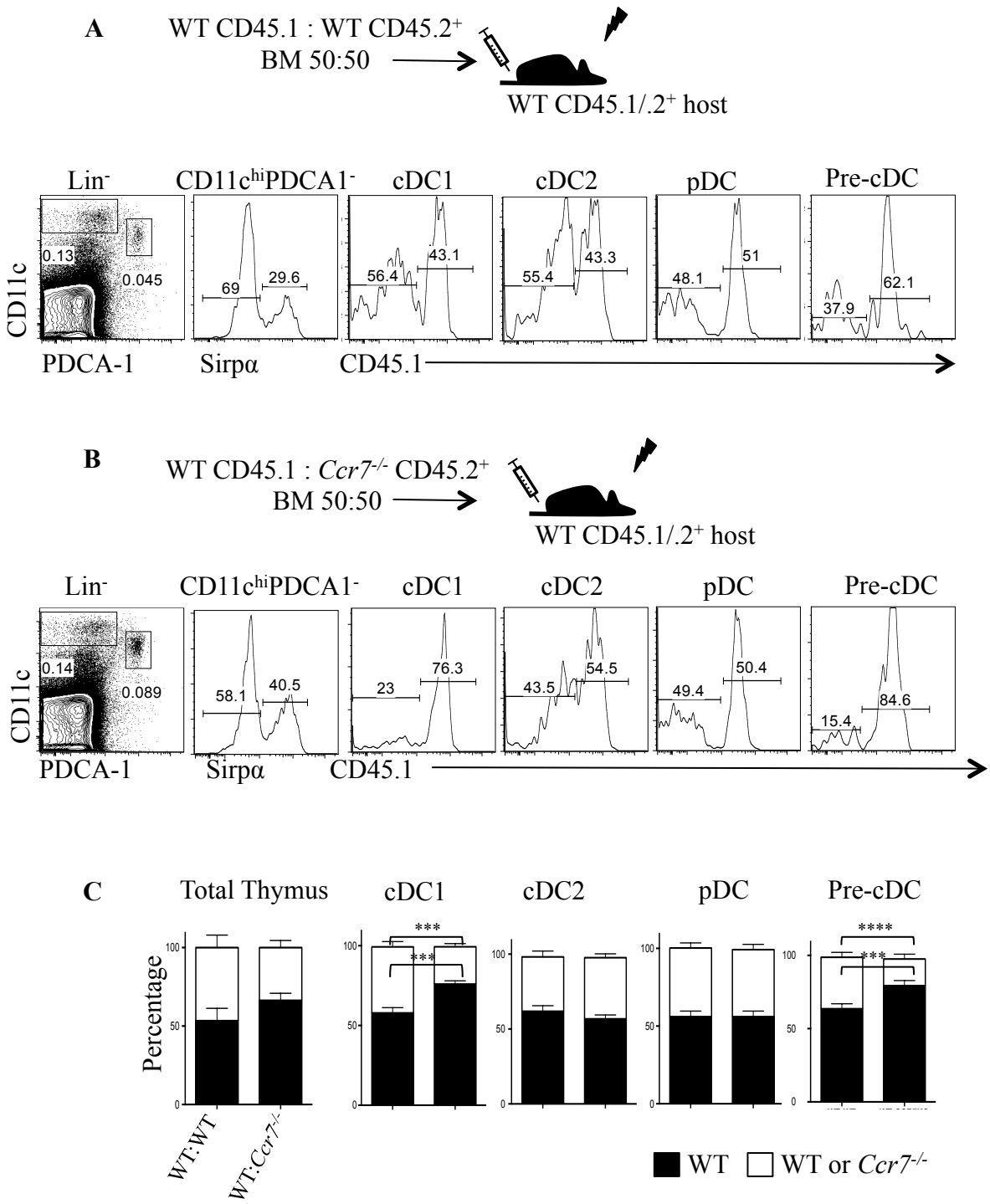
A
WT CD45.1 : WT CD45.2+
BM 50:50
WT CD45.1/.2+ host
Lin-
CD11chiPDCA1-
cDC1
cDC2
pDC
Pre-cDC
CD11c
PDCA-1
Sirpα
CD45.1
0.13
0.045
69
29.6
56.4
43.1
55.4
43.3
48.1
51
37.9
62.1
B
WT CD45.1 : Ccr7-/- CD45.2+
BM 50:50
WT CD45.1/.2+ host
Lin-
CD11chiPDCA1-
cDC1
cDC2
pDC
Pre-cDC
CD11c
PDCA-1
Sirpα
CD45.1
0.14
0.089
58.1
40.5
23
76.3
43.5
54.5
49.4
50.4
15.4
84.6
C
Total Thymus
cDC1
cDC2
pDC
Pre-cDC
Percentage
WT:WT
WT:Ccr7-/-
***
***
***
***
WT
WT or Ccr7-/-

analysis, highlighting reduced ability for *Ccr7*$^{-/-}$ progenitor derived cells to persist against WT control cells. Therefore there is a reduced ability of CCR7 deficient bone marrow derived cDC1 and pre-cDC to compete with WT counterparts; highlighting a requirement cell intrinsically for CCR7 expression on cDC1 and cDC1 progenitors for their thymic maintenance.

Confirming the requirement for CCR7 signalling, it was decided to look at mice deficient for CCR7 ligands – these being *plt/plt* mice, which lack CC19 and CCL21 expression. *plt/plt* mice were examined for DC populations in the thymus and spleen with flow cytometric analysis compared to WT controls. Representative FACs plots following analysis showed a switch in the cDC1/cDC2 proportions in *plt/plt* mice compared to WT mice with a pDC reduction also seen (Figure 4.12 A). When absolute numbers were calculated, there was no total thymus cellularity difference but a reduction in total cDC that specifically mapped to cDC1 and a pDC reduction was also seen in *plt/plt* mice. Splenic analysis showed no difference in cDC but a slight pDC reduction was seen (Figure 4.12 C). Furthermore pre-cDC were analysed following preparations of bone marrow, splenic and thymic cells for flow cytometric analysis and showed that there was a reduction in pre-cDC in the thymus of *plt/plt* mice, but no alteration seen in the bone marrow or the spleen of *plt/plt* mice compared to WT controls (Figure 4.12 D). This data suggests similarly to the *Ccr7*$^{-/-}$ mouse analysis that pre-cDC may require CCR7 and signalling through CCR7 by its ligands in a cell intrinsic manner for maintenance of cDC1 in the thymus.

Which ligand, CCL19 or CCL21 was specifically necessary for the phenotype seen linking *Ccr7*$^{-/-}$ and *plt/plt* mice to the reduction in the cDC1 and pre-cDC population, was then

Figure 4.12:
Mice Lacking CCR7 Ligands Suffer Dendritic Cell Defects

A) FACs plots to illustrate identification of the dendritic cell populations within WT and *plt/plt* mice which lack CCR7 ligands.

B) Absolute number analysis in the thymus for total cellularity and dendritic cell populations is within the lower panel. WT (black bar) and *plt/plt* (white bar). DC data was obtained from four independent experiments WT (n=13) and *plt/plt* (n=14).

C) Splenic absolute number analysis for total cellularity and DC populations within WT (black bars) and *plt/plt* (white bars) is shown graphically, with n=13 and 14 respectively across four independent experiments.

D) Analysis of pre-cDC defined as $Lin^{-}MHCII^{-}CD11c^{+}Flt3^{+}Sirp\alpha^{int}$ with Lin referring to the exclusion of CD19, B220, Ter119, NK1.1 and CD3. Pre-cDC absolute numbers were analysed for bone marrow, thymus and spleen in WT (black bars) and *plt/plt* (white bars) with n=12 and 11 respectively across three independent experiments.

All significance was noted as: *<0.05, **<0.01, ***<0.001, ***<0.0001.

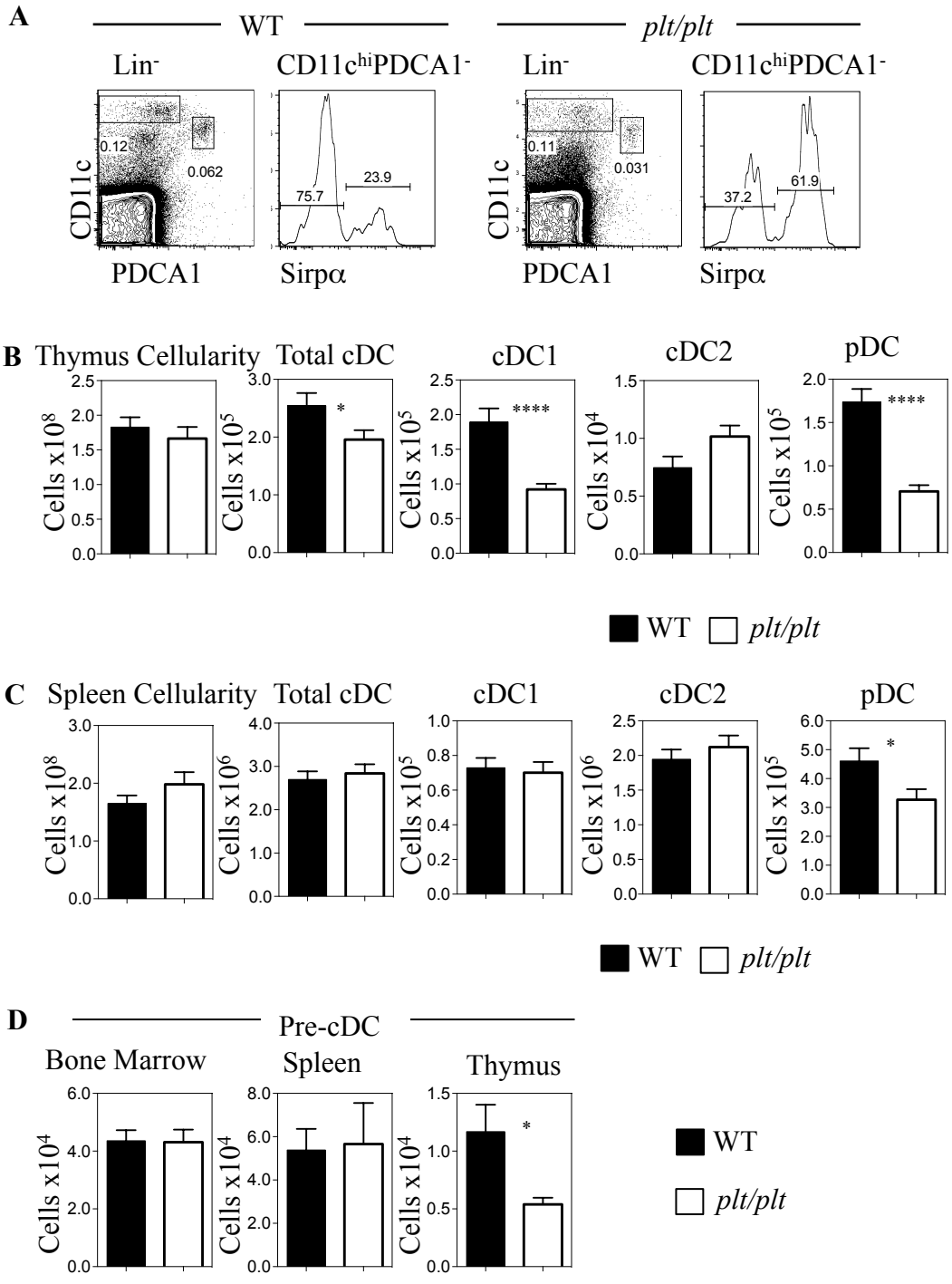
A
WT
plt/plt
Lin-
CD11chiPDCA1-
Lin-
CD11chiPDCA1-
0.12
0.062
75.7
23.9
0.11
0.031
37.2
61.9
CD11c
PDCA1
Sirpα
CD11c
PDCA1
Sirpα
B Thymus Cellularity
Total cDC
cDC1
cDC2
pDC
Cells x10^8
Cells x10^5
Cells x10^5
Cells x10^4
Cells x10^5
*
****
****
WT
plt/plt
C Spleen Cellularity
Total cDC
cDC1
cDC2
pDC
Cells x10^8
Cells x10^6
Cells x10^5
Cells x10^6
Cells x10^5
*
WT
plt/plt
D
Pre-cDC
Bone Marrow
Spleen
Thymus
Cells x10^4
Cells x10^4
Cells x10^4
*
WT
plt/plt

addressed. This was possible through analysis of *Ccl19*$^{-/-}$ or *Ccl21α*$^{-/-}$ mice which were both obtained from collaborators with for *Ccl19*$^{-/-}$ mouse thymus tissue shipped for analysis and *Ccl21*$^{-/-}$ mouse thymic analysis being conducted by the collaborators in Japan. Firstly *Ccl19*$^{-/-}$ mice were analysed for thymic DC populations and showed through representative FACs plots that the proportional distribution of thymic DC populations was maintained between mouse strains (Figure 4.13 A). Further absolute number analysis confirmed this distribution with absolute numbers being comparable for all parameters; total cellularity, total cDC, cDC1, cDC2 and pDC as well as pre-cDC remaining unaffected. Furthermore, this suggests that there may not be a role for CCL19 in the regulation of thymic DC populations. As a result this highlights CCL21 as a possible regulator. This was investigated through thymic preparations of WT and *Ccl21α*$^{-/-}$ mice for flow cytometric analysis of DC populations in thymus and showed that all populations could be identified within the thymus (Figure 3.13 B). Representative plots showing DC proportions appeared to suggest that there was a reduction in the cDC population as a whole which specifically mapped to cDC1, whereas pDC appeared little affected. Additional analysis of absolute numbers showed that under the absence of CCL21, there was a corresponding reduction in total cDC and cDC1 linking directly to a significant loss of pre-cDC that was also seen in the *Ccl21a*$^{-/-}$ thymus, whereas cDC2 and pDC remained unaltered. From this it appears that there is a requirement for CCR7 ligands, in particular CCL21, in the regulation of pre-cDC recruitment to the thymus to allow for the subsequent generation of intrathymic cDC1.

Figure 4.13:

CCL21 Is Responsible For The Pre-cDC Recruitment To Thymus For cDC1 Development

A) FACs plots showing representative distribution of dendritic cell populations in WT and *Ccl19*$^{-/-}$ mice. The lower panel shows the absolute number analysis with total cellularity and dendritic cell populations highlighted as well as the pre-cDC (Lin^{-}MHCII^{-} CD11c^{+}Flt3^{+}Sirpα^{int}) population. The WT is indicated by the black bar and *Ccl19*$^{-/-}$ the white bar. Data is from two independent experiments where WT n=9 and *Ccl19*$^{-/-}$ n=10. Data was obtained in collaboration with Sanjiv Luther (Switzerland).

B) FACs plots to illustrate the dendritic cell populations in *Ccl21*$^{+/-}$ controls and *Ccl21*$^{-/-}$ hosts. The lower panel quantitates the differences between these mice with regards to absolute number analysis. Data was preliminarily obtained from 9 independent experiments n=9. Data was obtained in collaboration with Yousuke Takahama (Japan).

All significance was noted as: *<0.05, **<0.01, ***<0.001, ***<0.0001.

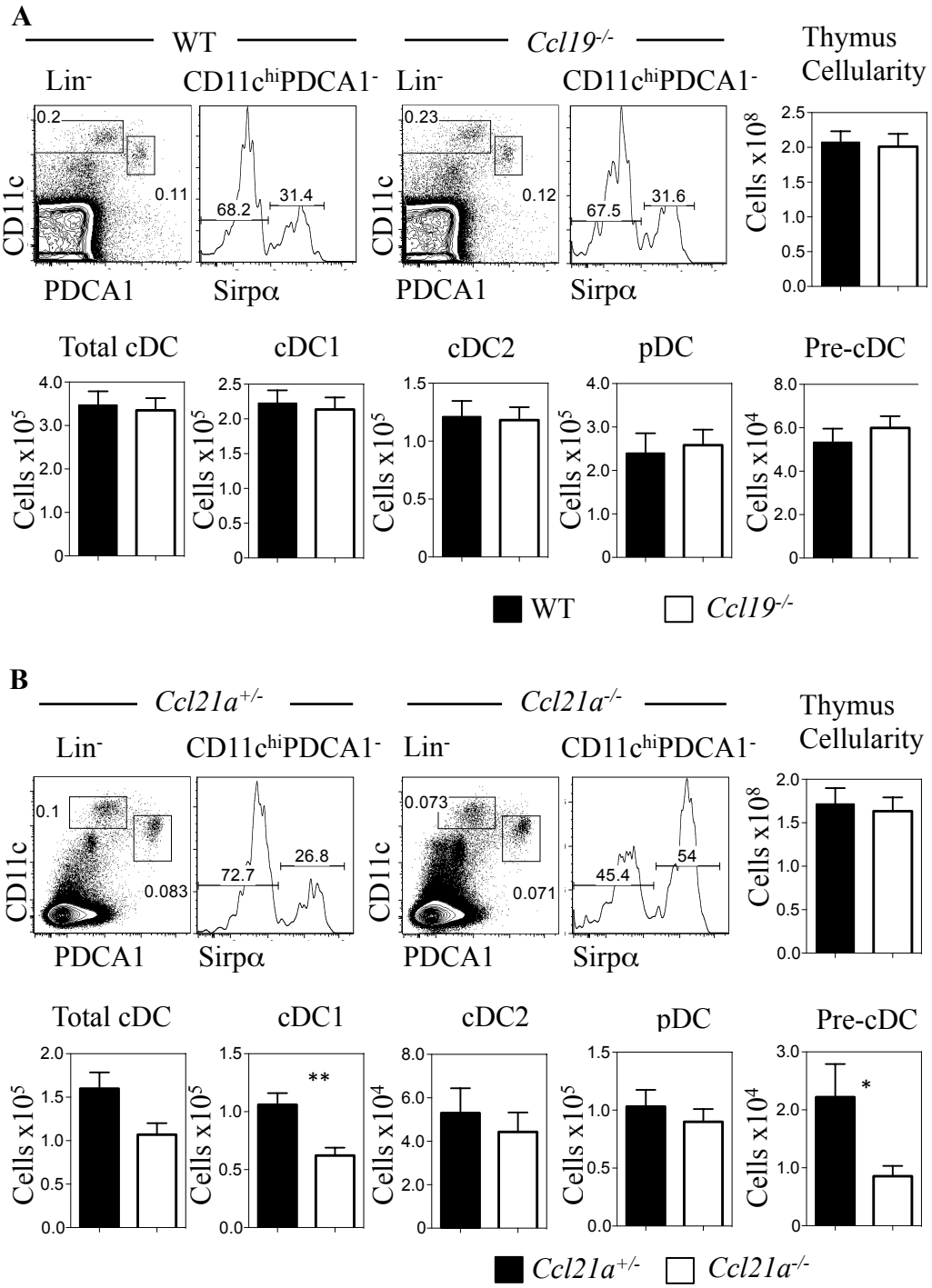
A
WT
Ccl19-/-
Thymus Cellularity
Lin-
CD11chiPDCA1-
Lin-
CD11chiPDCA1-
0.2
0.11
68.2
31.4
0.23
0.12
67.5
31.6
CD11c
PDCA1
Sirpα
Cells x10^8
Total cDC
cDC1
cDC2
pDC
Pre-cDC
Cells x10^5
Cells x10^4
WT
Ccl19-/-
B
Ccl21a+/-
Ccl21a-/-
Thymus Cellularity
0.1
0.083
72.7
26.8
0.073
0.071
45.4
54
**
*
Ccl21a+/-
Ccl21a-/-

4.3 Discussion

4.3.1 LTβR Mediated Regulation of Pre-cDC and pDC Recruitment

The previous chapter revealed that there were thymic reductions in cDC1 in *Ltbr*$^{-/-}$ mice, while BrdU analysis suggested that this was not due to a difference in proliferative status of cDC1. Thus reduced cDC1 in *Ltbr*$^{-/-}$ mice may be due to altered recruitment of cDC1 progenitors to the thymus; a focus of this chapter. Previous research suggested that a CD11c^{+}MHCII^{-}Flt-3^{+}Sirpα^{int} pre-cDC population could give rise to cDC in the periphery. It was also suggested that cDC1 progenitors migrate into the thymus to contribute towards the DN1c subset for intrathymic cDC generation (Luche et al., 2011, Liu and Nussenzweig, 2010). Therefore this peripherally defined pre-cDC population was analysed as a cDC1 progenitor in bone marrow, spleen and thymus. Collectively data suggested that pre-cDC could exit the bone marrow and migrate into the spleen normally, but were reduced in numbers in the thymus of *Ltbr*$^{-/-}$ mice. This indicates that the thymus employs different recruitment mechanisms to those seen in the spleen and further that thymic pre-cDC recruitment depends to some extent upon LTβR. In turn, this was shown to be necessary at the level of the thymic stroma. To break this requirement down further, Cre/flox model systems were used to determine which stromal compartment was mediating pre-cDC regulation and in turn cDC1 maintenance.

The *Flk1*^{Cre}*Ltbr*$^{fl/fl}$ mice, with their successful deletion of LTβR from endothelial cells, appeared to suggest that LTβR signalling on endothelium was dispensable for pre-cDC recruitment. Therefore, when considering that *Ltbr*^{TEC} mice also showed no pre-cDC alteration, it suggests a role for thymic mesenchyme in recruitment of pre-cDC to thymus or further cooperation between multiple cell compartments. Yet the partial deletion in both the

PDGFRβ^{Cre}*Ltbr*$^{fl/fl}$ mice and the *Wnt1*^{Cre}*Ltbr*$^{fl/fl}$ mice makes it a challenge to correlate these ideas. Despite this, the level of deletion appeared to be more effective in the *Wnt1*^{Cre}*Ltbr*$^{fl/fl}$ mice compared to *PDGFRβ*^{Cre}*Ltbr*$^{fl/fl}$ mice and this was associated with a phenotype of reduced pre-cDC. As this partial deletion is sufficient to cause a pre-cDC reduction, it suggests that mesenchymal LTβR signals regulate thymic pre-cDC recruitment. Therefore, mechanistically, LTβR mediated modulation of mesenchymal cells may influence mesenchymal activation that could be necessary for pre-cDC recruitment. Analysis of the phenotype of mesenchymal cells in the various *Ltbr*$^{-/-}$ mouse strains may provide insight into how this population can become defective, in turn identifying factors that may support pre-cDC recruitment.

In addition, analysis of pDC showed a reduction in the *Wnt1*^{Cre}*Ltbr*$^{fl/fl}$ mice which suggests that LTβR signals on thymic mesenchyme may influence pDC recruitment. However in addition, the *Flk1*^{Cre}*Ltbr*$^{fl/fl}$ mice also showed a reduction in pDC to a similar extent to the germline *Ltbr*$^{-/-}$ mice. This was suggestive that pDC are being regulated by LTβR signalling on thymic endothelium potentially more so than signals on mesenchyme – however mesenchyme may be additionally implicated. Considering this, recruitment of pDC to the thymus from the periphery requires a multistep adhesion cascade with a series of tethering, rolling, firm adhesion to allow for subsequent transmigration of pDC into the thymus (Alvarez et al., 2008). Thymic endothelial cells have been shown to express VCAM-1, ICAM-1 and P-selectin which support the recruitment and entry of cells into the thymus (Lepique et al., 2003, Sultana et al., 2012). P-selectin has been suggested to interact with (P-selectin glycoprotein ligand 1) PSGL-1 expressed on migratory DC for rolling on the endothelium, with firm adhesion associated with endothelial VCAM-1 in turn binding to

VLA-4 on DC for entry into the thymus (Bonasio et al., 2006). This questions whether LTβR may regulate these molecules on thymic endothelium to influence pDC entry into the thymus.

From this, RT-PCR analysis of mesenchyme and endothelial cell sorted populations showed that the expression of ICAM-1 and VCAM-1 was regulated by LTβR, with significant reductions in adhesion molecule expression in the absence of LTβR (Lucas et al., 2016). Therefore it would be interesting to further determine if LTβR dependent regulation of ICAM-1 and VCAM-1 expression on endothelium or mesenchyme in the thymus may be responsible for altered pDC recruitment. However, analysis of P-selectin expression failed to show the same trend as ICAM-1, VCAM-1 and P-selectin expression in WT and *Ltbr*$^{-/-}$ mice showed no difference by RT-PCR (Lucas et al., 2016). Yet interestingly, P-selectin may still be involved in pDC recruitment as it was shown that although P-selectin is expressed in *Ltbr*$^{-/-}$ thymus, lack of LTβR led to the loss of a CD31^{+}CD45^{-}EpCAM-1^{+}Ly6C^{-}P-selectin^{+} subset of thymic endothelium (Shi et al., 2016). The lack of this population was shown to abrogate recruitment of T-cell progenitors into the thymus. Therefore, if the homing process of cells into the thymus is relatively conserved, it is possible that loss of the Ly6C^{-}P-selectin^{+} endothelial population could in turn impact upon thymic pDC recruitment. These ideas combine to suggest that LTβR mediated regulation of adhesion molecules on endothelial and or mesenchymal cells may be necessary for successful pDC recruitment and this warrants further investigation. Despite this, pDC were slightly reduced in splenic analysis of *Ltbr*$^{-/-}$ mice, causing additional confirmation that pDC do not require LTβR for their normal development in the bone marrow to be necessary. This would allow direct correlation of reduced pDC in thymus with reduced recruitment, rather than altered production or availability.

4.3.2 CCR7 Mediated Regulation of Pre-cDC and pDC Recruitment

While work from Cre/flox models indicate mesenchyme as the stromal population required to support pre-cDC entry into the thymus via LTβR signals, the persistence of a proportion of pre-cDC in *Ltbr*$^{-/-}$ mice is suggestive of alternative regulatory mechanisms. From this, CCR7 was investigated as an alternative regulator given its implication in thymic progenitor homing (Zlotoff et al., 2010, Krueger et al., 2010). However it was important to confirm that there was no difference in the stromal compartment of the thymus in *Ccr7*$^{-/-}$ mice compared to WT mice in terms of TEC populations, to directly correlate any altered pre-cDC finding to reduced recruitment rather than indirectly to altered TEC. This was particularly relevant, as in the absence of CCR7 mice are known to have smaller medullary areas that are increased in frequency (Misslitz et al., 2004, Ueno et al., 2004). Additionally, using quantitative analysis we showed that the absolute numbers of different TEC compartments were unaltered in WT and *Ccr7*$^{-/-}$ mice, despite this changed organisation.

Therefore, following this, further analysis of *Ccr7*$^{-/-}$ mice with reduced cDC1 and pre-cDC, showed that pre-cDC may be utilising CCR7 mediated migration to enter the thymus and give rise to the cDC1. This was shown through mixed bone marrow chimeras to be necessary at a cell intrinsic level with an absence of CCR7 leading to a reduced ability of pre-cDC and cDC1 to compete with WT counterparts to gain entry into the thymus. Therefore this further rules out a non-cell autonomous requirement for CCR7 expression and suggests that TEC are supporting CCR7 ligand production that is directing these CCR7 expressing pre-cDC into the thymus (Lkhagvasuren et al., 2013). The correlation of *plt/plt* mice with the defect seen in the *Ccr7*$^{-/-}$ mice confirms a requirement for CCR7 ligands in signalling via CCR7 for pre-cDC recruitment and cDC1 maintenance in thymus. Furthermore, it was apparent that this

reduction in the thymus correlated to a tissue specific requirement for CCR7-CCR7L mediated recruitment, as both the bone marrow and the spleen in *plt/plt* mice had equivalent numbers of pre-cDC populations. In addition the requirement for CCR7 ligands in this pre-cDC recruitment process was directly correlated to CCL21 as *Ccl21a*$^{-/-}$ mice suffered reduced pre-cDC, while *Ccl19*$^{-/-}$ mice were not affected.

Interestingly, in analysis of *Ccr7*$^{-/-}$ mice, pDC appeared to also be affected and this is somewhat harder to unravel given our inability to detect CCR7 expression on pDC. Supporting this, despite migration of pDC to the thymus being linked to the CCR9/CCL25 axis, lymph node studies using isolated pDC showed through transwell migration assays that pDC could migrate towards CCR7 ligands, supporting an ability of pDC to be influenced by CCR7 ligands (Hadeiba et al., 2012, Seth et al., 2011). Yet despite this being feasible, further experiments with our mixed bone marrow chimera analysis argue against a requirement for CCR7 expression by pDC for their recruitment to the thymus, as pDC lacking CCR7 expression were able to compete with WT pDC and be represented equally in the thymus. Therefore, the reductions in thymic pDC in *Ccr7*$^{-/-}$ mice and additionally in *plt/plt* mice proposes that CCR7 signalling may be necessary for pDC to be recruited to the thymus but via an indirect intermediate population. There appeared to be a requirement further for both CCL19 and CCL21 in this process as an absence of either of these ligands did not affect pDC, suggesting that these ligands are able to compensate for one another for pDC recruitment to the thymus. Therefore, overall, this suggests CCR7 mediated regulation of an intermediate population, which is perturbed in *Ccr7*$^{-/-}$ mice, is necessary to indirectly regulate the recruitment of pDC into the thymus. It will be interesting to determine which intermediate cell type this may be as many cells in the thymus are dependent upon CCR7 signalling for

their regulation such as thymocytes that require CCR7 signals for cortex to medulla migration (Kurobe et al., 2006, Ueno et al., 2004).

In conclusion, this chapter highlights the requirement for LTβR in the recruitment of pre-cDC and subsequently cDC1 maintenance in the thymus. Despite inefficiency of Cre/flox animal models, $Wnt1^{Cre}xLtbr^{fl/fl}$ mice hint towards a role for mesenchyme in this process. Furthermore this chapter emphasises that CCR7 is also involved in the recruitment of pre-cDC to the thymus, specifically via CCL21 exposure on pre-cDC in a cell intrinsic manner. This suggested process is shown in a summary diagram Figure 4.14. Additionally pDC were considered in this chapter and were shown to be regulated predominately by LTβR signalling on endothelial cells, although mesenchymal cells appeared to also have a role. How this works mechanistically remains unknown but it may be suggested to occur through alterations in adhesion molecules necessary for pDC recruitment.

Considering the two parts of this chapter, CCR7 ligand production in the thymus is indeed known to be due to LTβR signalling on TEC (Lkhagvasuren et al., 2013, Seach et al., 2008). As a result, the possibility for the observation of reduced pre-cDC and cDC1 in $Ltbr^{-/-}$ mice to be linked to reductions in CCR7 ligands is possible. This process further has been suggested, through work in this chapter, to relate to mesenchymal cells. However CCL21 is not produced by mesenchyme, leaving the production of CCL21 by TEC to be required subsequently for presentation by mesenchyme. Furthermore, this is a possibility as mesenchyme has been shown to present CCL21 in the thymus as it binds to podoplanin (Fuertbauer et al., 2013). In addition, studies of mesenchymal cells in lymph nodes showed that their activation was affected under the absence of LTβR with reduced VCAM-1 and ICAM-1 expression and reduced immunocompetency of these cells (Chai et al., 2013). Therefore this information

combines to suggest the possibility of LTβR mediated maturation of mesenchymal cells to support mesenchymal presentation of TEC produced CCL21. This in turn may support the recruitment of pre-cDC and cDC1 into the thymus. This hypothesis requires further confirmation, potentially by proving the ability of mesenchyme in WT mice to present CCL21 and further determine whether *Wnt1*^{Cre}*xLtbr*$^{fl/fl}$ mice have altered mesenchymal activation that would perturb this presentation process.

Figure 4.14:
Summary Diagram For Pre-cDC Regulation By CCL21 In Thymus

A) Model to show the proposed process of pre-cDC recruitment into the thymus. 1) TEC produce CCL21. 2) CCL21 is presented by mesenchyme cells that mature through LTβR signalling. 3) Pre-cDC expressing CCR7 are attracted to the CCL21 presented on mesenchyme in the thymus. 4) Recruited pre-cDC enter into the thymus attracted by CCL21 and give rise to the cDC1 population.

A

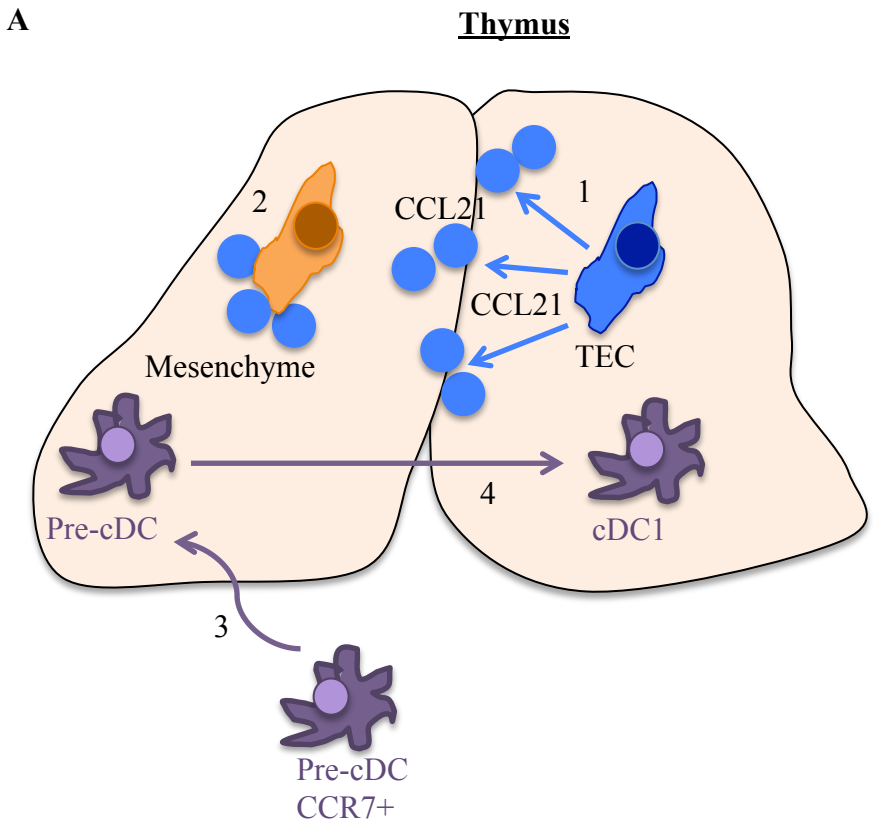
Thymus
2
CCL21
1
CCL21
Mesenchyme
TEC
Pre-cDC
4
cDC1
3
Pre-cDC
CCR7+

CHAPTER FIVE:

EOSINOPHILS MEDIATE RECOVERY OF THE THYMUS POST-DAMAGE

5.1 Introduction

The thymus medulla is classically known as a home for mature SP thymocytes. In addition, as described in previous chapters, the thymus medulla contains important hematopoietic elements, namely DC that play vital roles in thymus function. Interestingly, it has also been reported to contain multiple other hematopoietic cells, whose functions are perhaps less clear. These include cells of the adaptive immune system, such as B-cells as well as a wide range of innate immune cells including iNKT cells, macrophages and eosinophils.

Eosinophils are thought to enter into the thymus through their expression of CCR3, being attracted towards eotaxin (CCL11) which is readily detectable within the thymus and localises eosinophils to the medullary areas (Matthews et al., 1998). Current research suggests a possible role for eosinophils in the thymus for the clearance of apoptotic cells that arise following negative selection and death by neglect processes (Kim et al., 2010). This study suggested that when apoptosis was induced through γ irradiation there was an increase in $TUNEL^+$ cells which coincided with increased infiltration of eosinophils into the thymus and clearance of dying cells. This clearance was less effective under eosinophil absence and therefore eosinophils were suggested to have a role in the thymus in apoptotic cell clearance. Interestingly, other studies suggest that eosinophils potentially contribute towards the process of negative selection itself in the thymus through antigen cross-presentation (Throsby et al., 2000). Despite these studies, the role of eosinophils in thymus function is poorly understood, and further research into the functional role of eosinophils in thymus remains to be fully addressed.

Importantly, and in addition to their influence on immune system function, eosinophils have been shown to support the recovery of multiple tissues following damage. To begin with, upon damage to the liver, it had previously been reported that a rapid type 2 immune response was consistently initiated and originally this was suggested to relate to macrophages that were thought to be responsible for the repair of damaged tissue barriers (Allen and Wynn, 2011, Palm et al., 2012). However through a model of injury using carbon tetrachloride, the role of eosinophils in this regeneration process was uncovered (Goh et al., 2013). Following damage, a huge influx of eosinophils were seen into the liver correlating to an increase in hepatocyte proliferation. Analysis of the eosinophil deficient model, dblGATA mice, illustrated that this repair process was impaired and therefore highlighted a role for eosinophils in the repair of liver tissue (Goh et al., 2013). A similar study was carried out in muscle, showing again that upon muscle damage, large numbers of eosinophils were recruited to the damaged site, which in turn supported muscle regeneration. Again, in the absence of eosinophils, this recovery was hindered (Heredia et al., 2013). Mechanistically, both studies concluded that eosinophils were functioning to repair tissue through their production of IL-4. In hepatocytes, this triggered entry into cell cycle to recover liver cell numbers post damage (Goh et al., 2013), whereas in muscle IL-4 was shown to induce the differentiation and conversion of fibro/adipocyte progenitors into myofibres to support muscle regeneration (Heredia et al., 2013).

Therefore it appears that eosinophils have a vital role in tissue repair. Whether they possess this role in the thymus remains completely uninvestigated. Considering this, regeneration of the thymus has gained extensive interest due to thymic involution which occurs with age as well as following damage such as irradiation therapy; both causing the thymus, in turn, to be immunologically inefficient (Aw et al., 2007, Lynch et al., 2009, Steinmann et al., 1985). As a

result much research has been focused on mechanisms regulating the process of thymus regeneration with an emphasis on regenerating the TEC compartment to support enhanced thymus reconstitution. Current techniques include, administration of Fibroblast growth factor 7 (FGF7) to trigger TEC expansion (Erickson et al., 2002, Dooley et al., 2007) as well as insulin like growth factor and IL-7 administration to enhance T-cell development (Mackall et al., 2001, Bolotin et al., 1996, Chu et al., 2008). An additional study highlighted that there may be a role for intrathymic IL-22 production by lymphoid tissue inducer (LTi) cells following damage in the regeneration of TEC and this is currently being explored in clinical trials (Dudakov et al., 2012). As a result, this chapter will focus on preliminarily addressing whether thymic eosinophils may be capable of supporting recovery of the thymus post damage and if so, then it will begin to hypothesise and address potential mechanisms through which this process of regeneration may be working.

5.2 Results

5.2.1 Phenotypic Analysis Of Thymic Eosinophils

To examine the possibility of eosinophils supporting the process of thymic regeneration, they firstly required further identification and characterisation in the thymus. To identify eosinophils, fresh thymus and splenic tissues were prepared by enzymatic digest. Antibody staining was then performed and eosinophils were identified as $CD45^{+}CD4^{-}CD8^{-}TCR\beta^{-}$ $Ter119^{-}$ cells that co-expressed CD11b and Siglec-F (Figure 5.1 A). The population of eosinophils identified in the thymus and spleen has been shown with representative plots (Figure 5.1 B). Proportions of eosinophils between the thymus and spleen were further compared with increased proportions of eosinophils in thymus. Eosinophil populations were then compared between the thymus and spleen for subsequent phenotypic analysis of mean fluorescent intensity by flow cytometry for Siglec-F and CD11b expression. This was conducted as such markers directly correlate to an activated phenotype, allowing the relative activation status of eosinophils in the thymus to be compared to those in the spleen. A significant difference was noted between thymic and splenic eosinophils upon this analysis, suggesting that eosinophils in the thymus represent an activated population (Figure 5.1 C).

Despite the presence of eosinophils in the thymus, little is known about their emergence during life. Therefore, a developmental ontogeny series looking at the presence of eosinophils in the thymus was generated; with WT mice harvested at specified time points and further timed matings established to look at embryonic stages in development (Figure 5.2). As previously seen in Chapter 3 with regards to DC ontogeny, as mice increased in age, the total thymus cellularity correlated with an initial growth phase from E18 to around three weeks of age with statistically significant increases in size. The thymus size then began to

Figure 5.1:
Eosinophils Are Present In The Thymus and Spleen of WT mice

A) FACs plots to show the gating strategy that was employed to identify eosinophil populations. This was common to thymus and spleen. Final eosinophils were identified as $CD45^{=}CD4^{-}CD8^{-}TCR\beta^{-}Ter119^{-}CD11b^{+}Siglec\text{-}F^{+}$.

B) Representative FACs plots to illustrate the presence of eosinophils identified in thymus and spleen. Quantitation of FACs percentages of eosinophils in the right hand panel for thymus compared to spleen. Thymus (n=10), spleen (n=10).

C) Analysis of Siglec-F and CD11b mean fluorescence intensity (MFI) representative of activation status n=10. Thymus and spleen are compared to one another for these markers with the black bar representing thymic data, and the white bar referring to splenic.

All significance was noted as: *<0.05, **<0.01, ***<0.001, ***<0.0001.

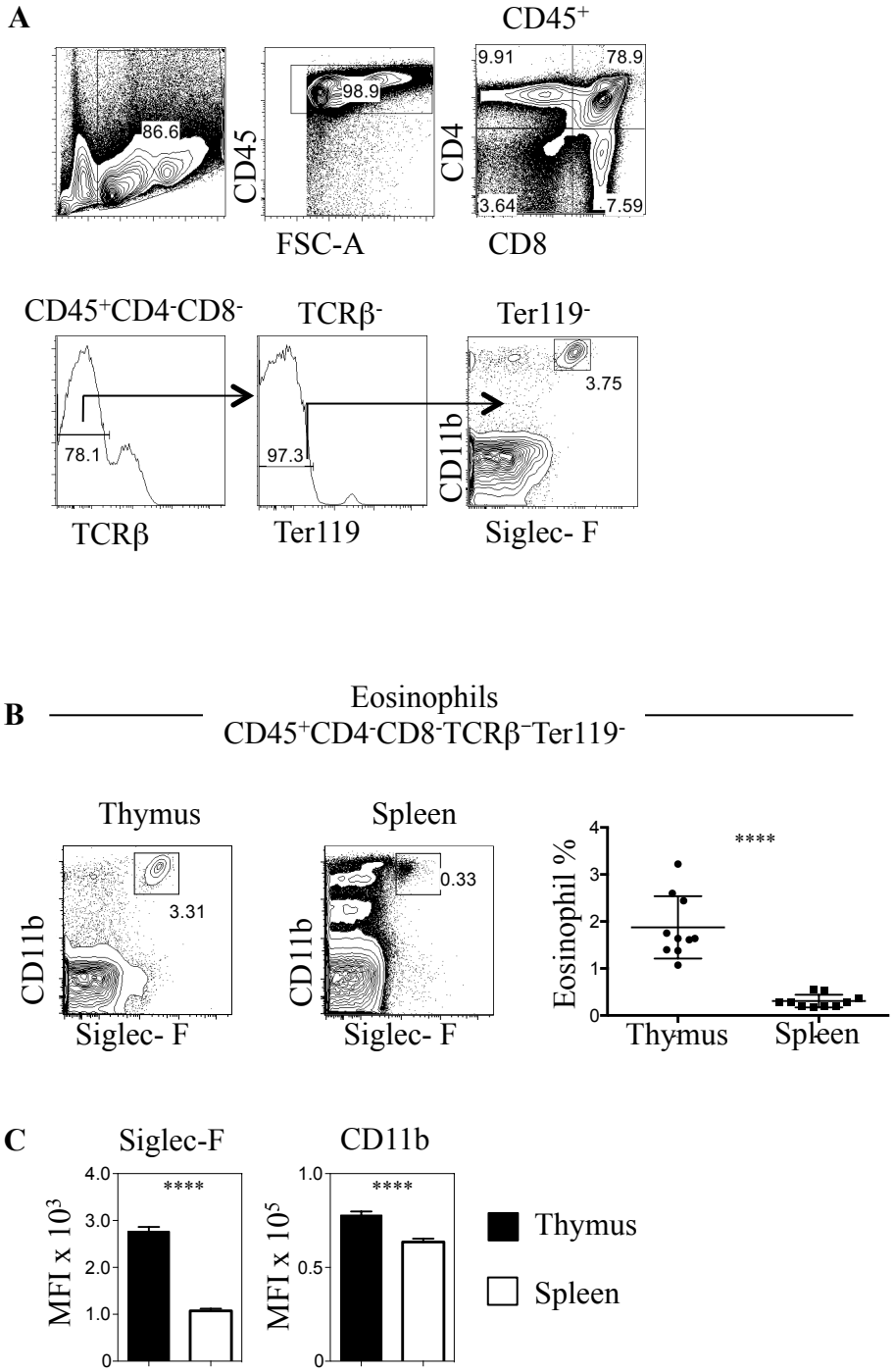
A
CD45+
86.6
98.9
CD45
FSC-A
9.91
78.9
3.64
7.59
CD4
CD8
CD45+CD4-CD8-
78.1
TCRβ
TCRβ-
97.3
Ter119
Ter119-
3.75
CD11b
Siglec- F
B
Eosinophils
CD45+CD4-CD8-TCRβ−Ter119-
Thymus
3.31
CD11b
Siglec- F
Spleen
0.33
CD11b
Siglec- F
****
Eosinophil %
4
3
2
1
0
Thymus
Spleen
C
Siglec-F
****
MFI x 10^3
4.0
3.0
2.0
1.0
0
CD11b
****
MFI x 10^5
1.0
0.5
0
Thymus
Spleen

Figure 5.2:
Eosinophils In Thymus Alter With Ontogeny

Ontogeny series data was representative of the following sample numbers; E18 2x(6 lobes pooled per repeat), 1 week (n=8), 3 weeks (n=9), 5 weeks (n=7), 7 weeks (n=13), 9 weeks (n=8). All samples were analysed freshly upon isolation.

Analysis of total thymus cellularity with development (A) and corresponding numbers of thymic eosinophils (B). Thymic eosinophils (B) are shown on a per mouse basis (left panel) and also a summary plot of total eosinophils seen in the right panel with average values plotted.

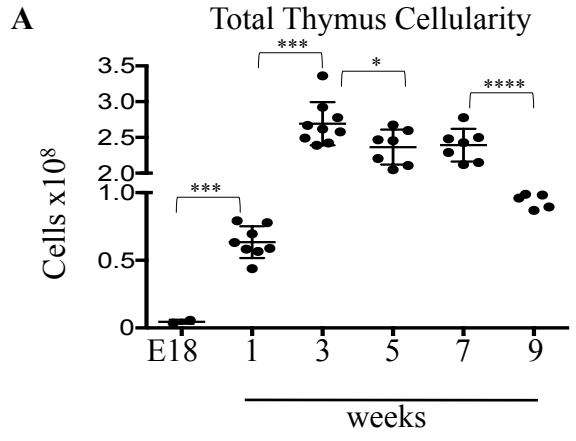
A
Total Thymus Cellularity
Cells x10^8
3.5
3.0
2.5
2.0
1.0
0.5
0
***
***
*
****
E18
1
3
5
7
9
weeks

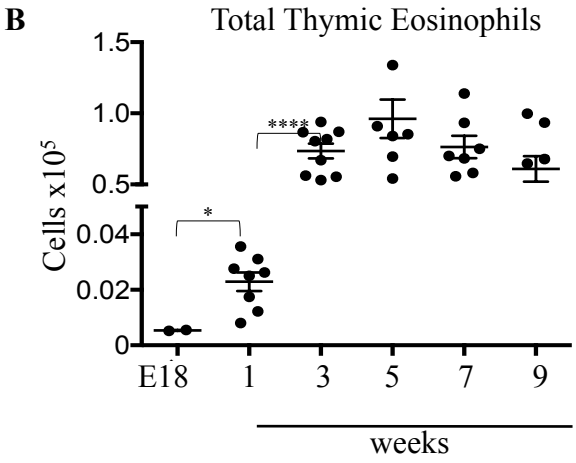
B
Total Thymic Eosinophils
Cells x10^5
1.5
1.0
0.5
0.04
0.02
0
****
*
E18
1
3
5
7
9
weeks

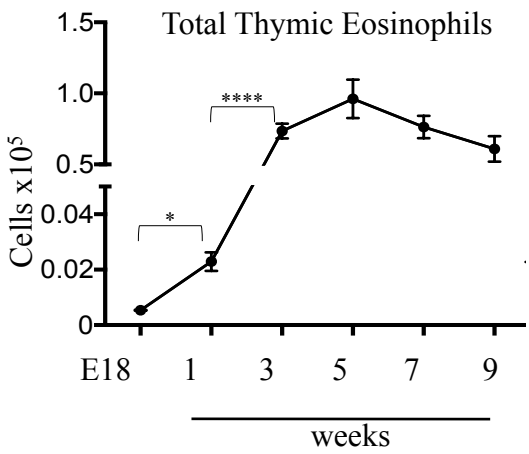
Total Thymic Eosinophils
Cells x10^5
1.5
1.0
0.5
0.04
0.02
0
****
*
E18
1
3
5
7
9
weeks

decline with a significant drop from three to five weeks before continuing to decrease in size with the onset of involution of the thymus through adulthood life, between seven to nine weeks of age (Figure 5.2 A). Following thymus analysis for total size, the presence of eosinophils was examined by flow cytometry and a population of eosinophils was distinguishable from E18 in the thymus of WT Balb/c mice (Figure 5.2 B). The trend in eosinophil numbers mirrored the thymus size, with increases until around five weeks of age from which point numbers began to decline again from five to nine weeks, coordinating with changes in total thymus cellularity. This could be seen on a per mouse basis (Figure 5.2 B top panel) as well as in a summary analysis with average numbers of eosinophils calculated (Figure 5.2 B bottom panel). Therefore this data series shows that thymic eosinophils persist throughout the thymus, independent of thymic age and are very much in synchrony with the thymic size.

As eosinophils are thought to be localised in medullary areas, we questioned if there was a requirement for the medulla to regulate thymic eosinophils (Matthews et al., 1998, Throsby et al., 2000). To address this, the presence of eosinophils in the thymus was initially investigated under circumstances where the thymic medulla and further the thymic architecture was disrupted. For this, *Tcrα*$^{-/-}$ mice, which lack single positive thymocytes and therefore as a result, due to the reciprocal requirement for single positives to promote mTEC development, suffer from disrupted mTEC populations and disorganised medullary structure, were analysed to see if the eosinophil populations were resultantly altered (Figure 5.3)(Desanti et al., 2012, Palmer et al., 1993). Firstly, thymi from *Tcrα*$^{-/-}$ adult mice were digested enzymatically along with WT controls and eosinophils were identified through antibody staining for detection by flow cytometry. Despite comparable overall thymus size (Figure 5.3 B), eosinophils showed a

Figure 5.3:
Eosinophils Are Reduced In Mice Lacking Single Positive Thymocytes

A) FACs plots showing the identification of thymic eosinophils ($CD45^+CD4^-CD8^-$ $TCR\beta^-$ $Ter119^-CD11b^+Siglec\text{-}F^+$) in the left hand plot and eosinophil identification in the right hand plot through $CD45^+CD11b^+Siglec\text{-}F^+$ which separates eosinophils more so based upon activation status for WT and *Tcrα*$^{-/-}$ mice.

B) Quantitation of total thymus cellularity is shown in the left plot, Facs% of eosinophils (middle plot) and eosinophil absolute numbers (right plot) for WT and *Tcrα*$^{-/-}$ mice. Data is representative of three independent experiments (n=10).

C) FACs plots showing eosinophils ($CD45^+CD4^-CD8^-$ $TCR\beta^-Ter119^-CD11b^+Siglec\text{-}F^+$) in the spleen in the left hand plot and eosinophil identification based upon activation in the right hand plot for WT and *Tcrα*$^{-/-}$ mice.

D) Absolute number analysis with total splenic cellularity, eosinophil FACs% and eosinophil absolute numbers in WT and *Tcrα*$^{-/-}$ mice. Data was obtained from three independent experiments with (n=10).

All significance was noted as: *<0.05, **<0.01, ***<0.001, ***<0.0001.

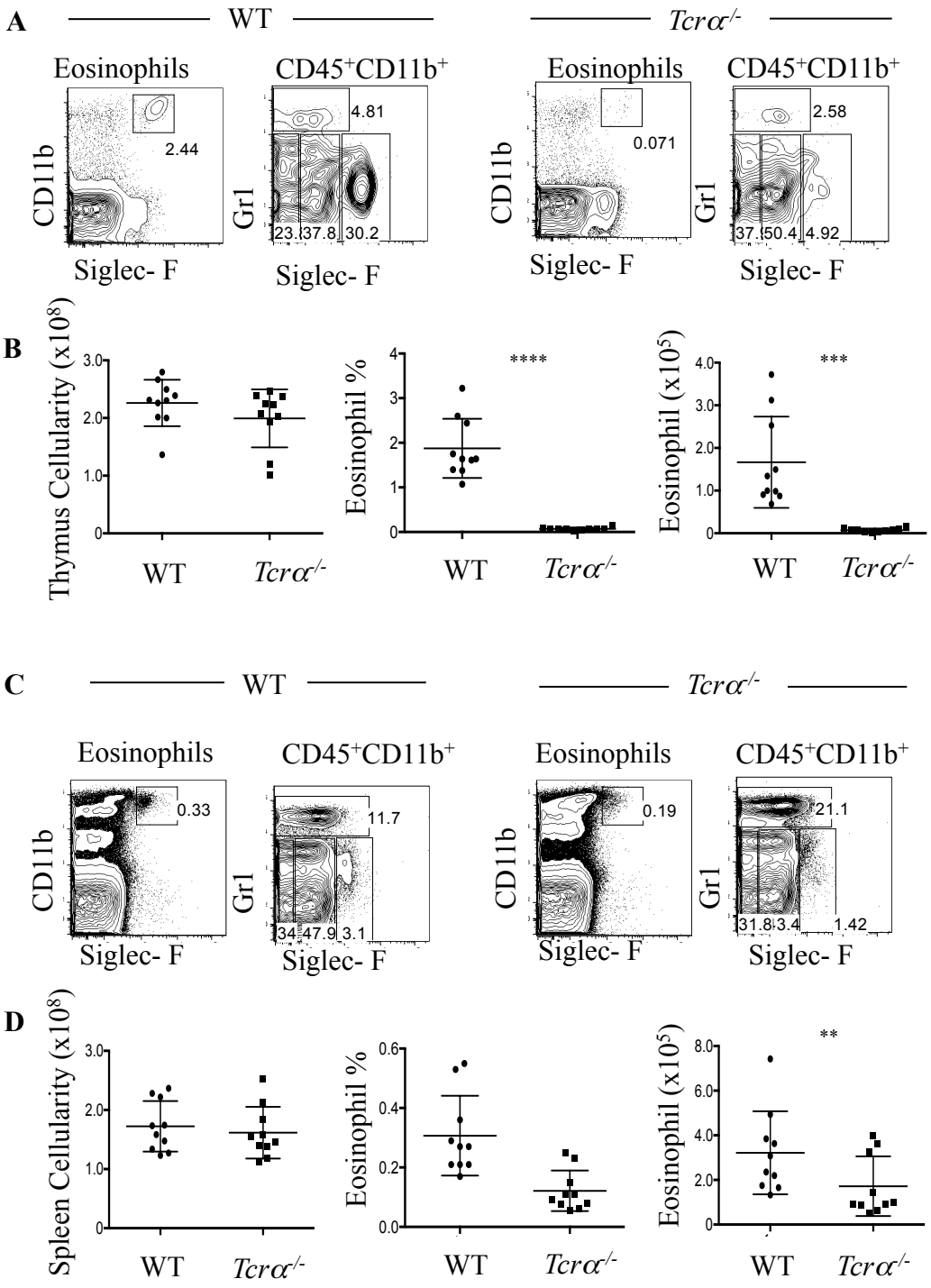
A
WT
Tcrα-/-
Eosinophils
CD45+CD11b+
CD11b
Gr1
Siglec- F
2.44
4.81
23.
37.8
30.2
0.071
2.58
37.
50.4
4.92
B
Thymus Cellularity (x10^8)
Eosinophil %
Eosinophil (x10^5)
****
***
WT
Tcrα-/-
C
0.33
11.7
34.
47.9
3.1
0.19
21.1
31.8
3.4
1.42
D
Spleen Cellularity (x10^8)
**

vast reduction in proportion in *Tcrα*$^{-/-}$ thymus compared to WT control mice (Figure 5.3 A). Furthermore when eosinophils were identified and separated based upon their levels of Siglec-F expression, linked with increased activation; there was downregulation of Siglec-F by eosinophils in the *Tcrα*$^{-/-}$ mice compared to WT mice (Figure 5.3 A). Additional analysis at an absolute number level of the total number of eosinophils showed that they were almost completely absent from *Tcrα*$^{-/-}$ mice (Figure 5.3 B). Therefore this data suggests a requirement for the medulla in the regulation of thymic eosinophils and furthermore a possible requirement for single positive cells in thymic eosinophil maintenance.

Building upon this, splenic eosinophil populations were identified in WT and *Tcrα*$^{-/-}$ mice following isolation and splenic tissue preparation. Upon analysis, proportionally eosinophils appeared to be slightly reduced compared to WT controls (Figure 5.3 C). Activation analysis suggested that eosinophils may also be less activated in the spleen of *Tcrα*$^{-/-}$ mice, with a loss of the highest expressing Siglec-F population when compared to WT mice. Absolute number analysis showed no difference in total splenic cellularity and no significance was seen in proportional eosinophil analysis either, whereas total eosinophil numbers were significantly reduced in the spleen of *Tcrα*$^{-/-}$ mice (Figure 5.3 D). Therefore this data suggests that there could be a peripheral requirement for αβT cells in the maintenance of the splenic eosinophil populations.

5.2.2 Analysis of Eosinophil Deficient dblGATA Mice Under Steady State Conditions

To begin to address the possible thymic role of eosinophils, we utilised a model of eosinophil deficiency: dblGATA mice, on a Balb/c background. These mice have a deletion of the high affinity double Gata binding site in the Gata-1 promoter, which is required to drive the

development of eosinophils and have been shown to lack eosinophils (Yu et al., 2002). Thymuses from 8-12 week old WT and dblGATA mice were digested and stained for eosinophil specific cell markers including Siglec-F and CD11b to define eosinophils. Figure 5.4 A shows that while detectable in the WT thymus, eosinophils were markedly absent from thymus of dblGATA mice. To examine whether eosinophils impact upon steady state thymus formation and/or development, fresh thymi were isolated from WT and dblGATA mice. The physical structure of the thymus as a whole remained unaltered upon isolation with the gross size remaining comparable between WT and dblGATA mice (Figure 5.4 B). Further some of these thymi were snap frozen before being sectioned and stained with antibodies for confocal microscopy. In this analysis, thymocytes were identified through CD4(red) and CD8(blue) with this staining highlighting single positive ($CD4^+$ or $CD8^+$) and double positive ($CD4^+CD8^+$) thymocytes in the thymus. Medullary areas were further highlighted with the staining of ERTR5 (green) as a medullary marker (Figure 5.4 C). Double positive thymocytes were shown to be correctly positioned in the cortex and single positive thymocytes were present in the medullary regions of the dblGATA thymi, with comparable staining to WT controls.

Next, in-depth analysis of TEC was conducted to determine if there was correct development of the thymic stromal structure in the absence of eosinophils. For this, thymus samples were enzymatically digested and FACs analysis was performed. Representative plots have been shown (Figure 5.5 A) of the proportions of TEC populations in the steady state between WT and dblGATA mice. This further highlights the gating strategy used for TEC population identification which as a whole were classified as $CD45^-EpCAM\text{-}1^+$ cells. Subpopulations of TEC could be then identified as $UEA\text{-}1^-Ly51^+$ for cTEC and $UEA\text{-}1^+Ly51^-$ for mTEC with

Figure 5.4:
dblGATA Mice Are A Model Of Successful Eosinophil Absence

A) FACs analysis verifying the model of dblGATA mice by highlighting how the dblGATA mice suffered from an effective loss of eosinophils compared to WT controls. Plots are identifying eosinophils as ($CD45^{+}CD4^{-}CD8^{-}$ $TCR\beta^{-}Ter119^{-}CD11b^{+}Siglec\text{-}F^{+}$). Absolute numbers are also shown. Data is representative of two independent experiments where n=6.

B) Visual representation of thymic size in WT and dblGATA adult mice from age and sex-matched mice.

C) Confocal analysis of the thymus of dblGATA mice showing CD4 staining (red), CD8 staining (blue) and ERTR5 (green).

All significance was noted as: *<0.05, **<0.01, ***<0.001, ***<0.0001.

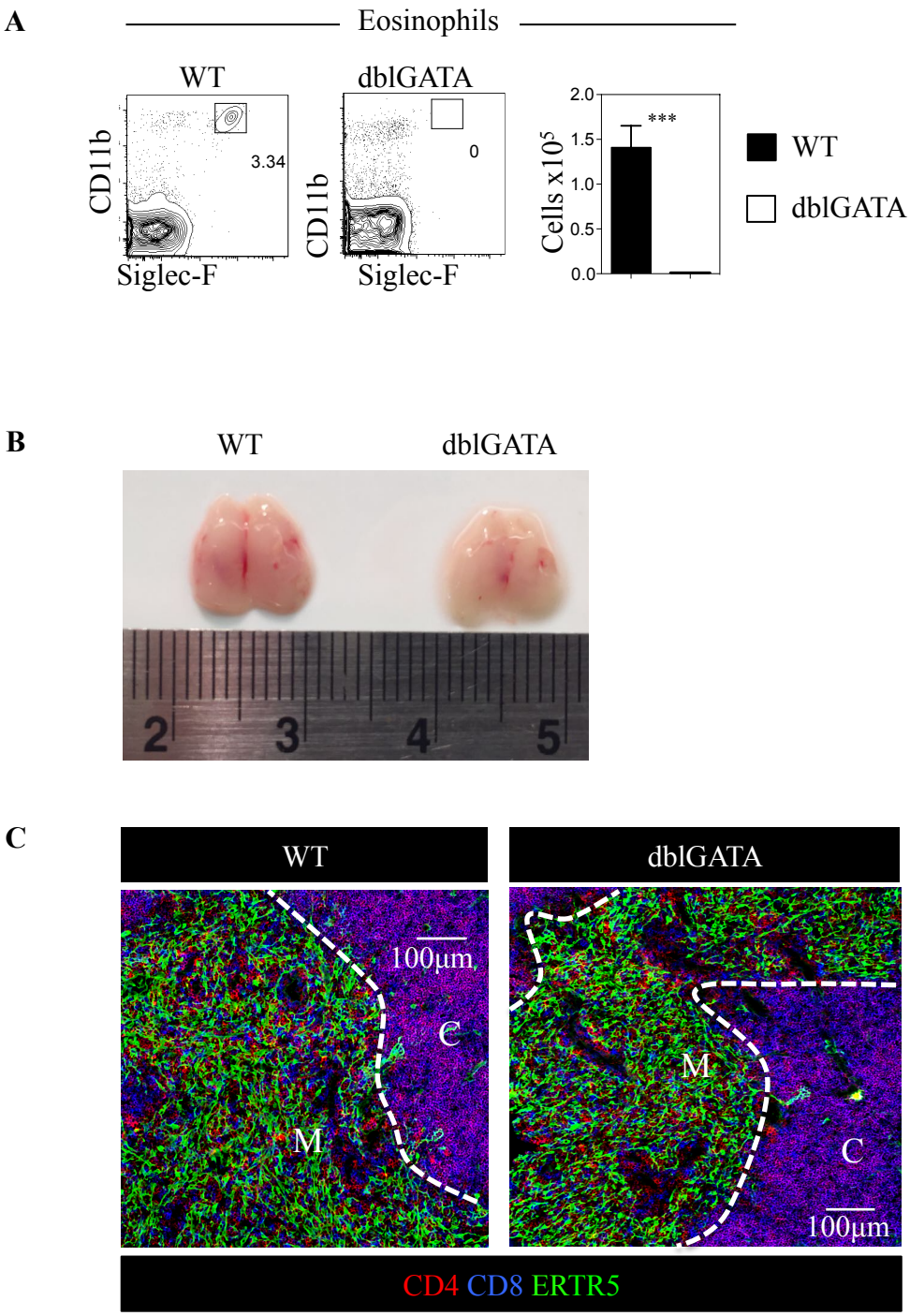
A
Eosinophils
WT
dblGATA
CD11b
Siglec-F
3.34
0
Cells x10^5
2.0
1.5
1.0
0.5
0.0
***
WT
dblGATA
B
WT
dblGATA
2
3
4
5
C
WT
dblGATA
100μm
C
M
M
C
100μm
CD4 CD8 ERTR5

Figure 5.5:

Steady State TEC Development Is Unchanged In Eosinophil Deficient Mice

A) FACs analysis of Thymic Epithelial Cell (TEC) populations between WT and dblGATA including mTEC subpopulations indicating the corresponding gating strategy used for identification such as $mTEC^{hi}$ ($EpCAM\text{-}1^{+}UEA\text{-}1^{+}Ly51^{-}MHCII^{+}CD80^{+}$) and $mTEC^{lo}$ ($EpCAM\text{-}1^{+}UEA\text{-}1^{+}Ly51^{-}MHCII^{-}CD80^{-}$) shown in the top panel.

B) Analysis of weight and total thymus cellularity between WT and dblGATA mice. Data is representative of two independent experiments WT (n=5) dblGATA (n=7) shown by the black and white bars respectively.

C) Corresponding absolute number analysis of TEC populations identified in A, performed from two independent experiments with WT (n=5) dblGATA (n=7), all adult mice. Black bar shows WT data and the white bar relates to dblGATA.

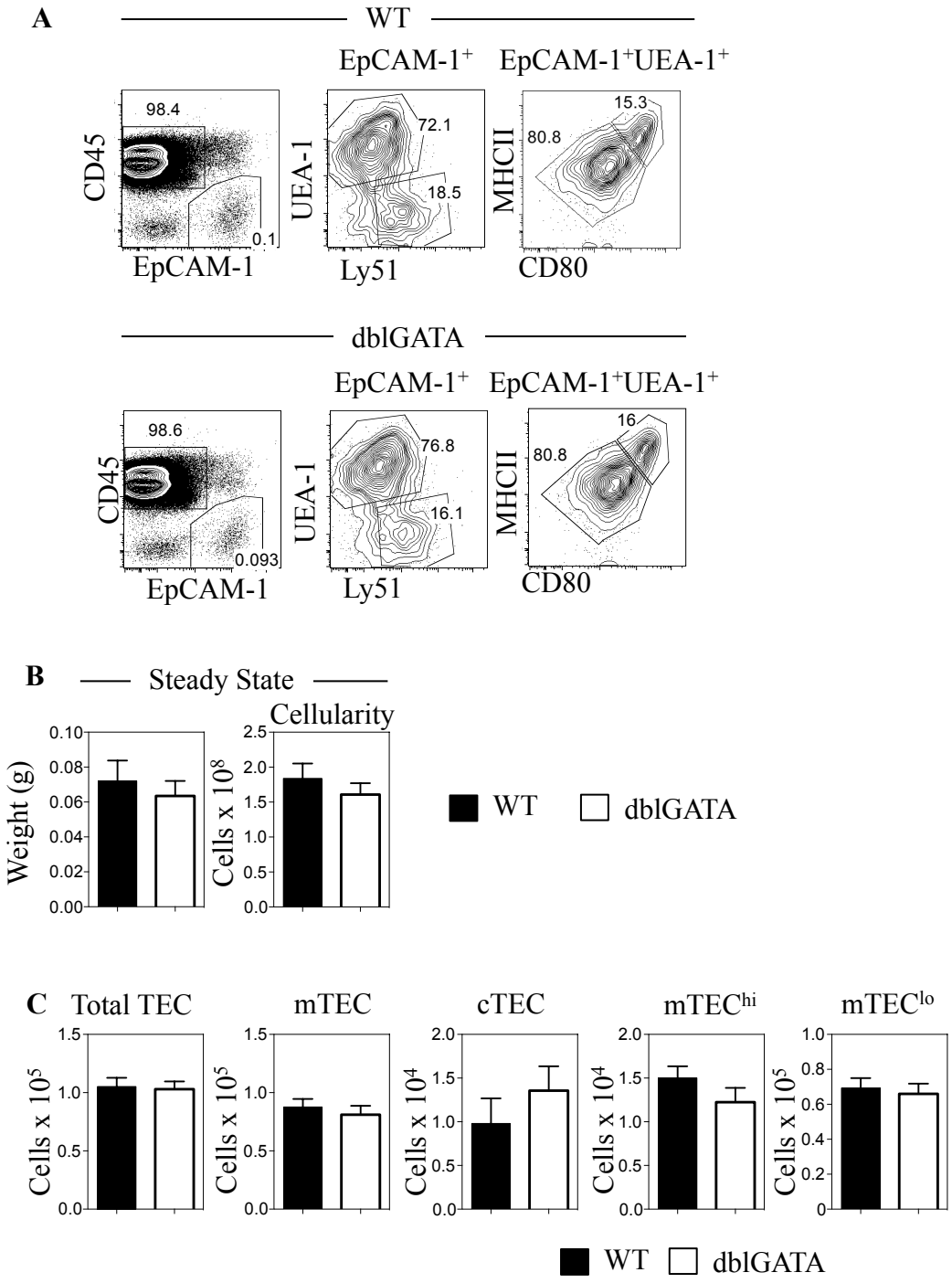
A
WT
EpCAM-1+
EpCAM-1+UEA-1+
98.4
0.1
CD45
EpCAM-1
72.1
18.5
UEA-1
Ly51
15.3
80.8
MHCII
CD80
dblGATA
EpCAM-1+
EpCAM-1+UEA-1+
98.6
0.093
CD45
EpCAM-1
76.8
16.1
UEA-1
Ly51
16
80.8
MHCII
CD80
B
Steady State
Cellularity
Weight (g)
0.10
0.08
0.06
0.04
0.02
0.00
Cells x 10^8
2.5
2.0
1.5
1.0
0.5
0.0
WT
dblGATA
C
Total TEC
mTEC
cTEC
mTEC^hi
mTEC^lo
Cells x 10^5
Cells x 10^4
WT
dblGATA

mTEC then subdivided into MHCII^{+}CD80^{+} mTEC^{hi} and MHCII^{-}CD80^{-} mTEC^{lo} cells. The weight of the thymus was also equivalent between WT and dblGATA mice in steady state conditions, supported by no difference in total thymus cellularity (Figure 5.5 B). Following from this, absolute number analysis reflected the lack of difference in TEC proportions (Figure 5.5 C lower panel). These findings suggest that TEC development is unaffected in dblGATA mice, indicating that eosinophils are not required for TEC development.

T-cell development in steady state WT and dblGATA mice was additionally conducted to determine quantitation of thymocyte populations. Isolated steady state thymi were disaggregated to release thymocytes for identification by flow cytometry. Representative FACs plots of thymocytes are shown in WT and dblGATA mice (Figure 5.6 A) where proportions of CD4^{+} cells appeared comparable, with further gating for mature single positive CD4^{+}TCRβ^{hi} cells also remaining proportionally comparable even at the level of Treg (CD4^{+}TCRβ^{hi}CD25^{+}Foxp3^{+}). Additionally, the maturation status of the CD4^{+}TCRβ^{hi} population was assessed and showed that the most mature CD62L^{+}CD69^{-} population in dblGATA thymi was again similar proportionally to the WT mice. However, interestingly, CD4^{-}CD8^{+} thymocytes were reduced in dblGATA mice, which mapped to reduced populations of the most mature CD62L^{+}CD69^{-} subset. Absolute number analysis supported these representative proportions and concluded that total thymus cellularities, CD4^{+}CD8^{+} double positive and CD4^{+}TCRβ^{hi} populations including T-Regulatory cells were comparable to WT mice (Figure 5.6 B). Furthermore no defect was seen in CD4^{+}TCRβ^{hi} maturation status. However the reduction in thymic CD8^{+} T-cells remained significantly altered. As a

Figure 5.6:
T-cell Development Is Comparable Between WT and dblGATA Mice

A) Representative FACs plots illustrating the gating strategy for T-cell analysis and identification of CD4SP and CD8SP T cell populations as well as their subsequent subsets including T-Regulatory $CD4^{+}TCR\beta^{+}CD25^{+}Foxp3^{+}$ and the splitting of CD4SP upon CD69 and CD62L to highlight the most mature $CD69^{-}CD62L^{+}$ and immature $CD69^{+}CD62L^{-}$ subsets.

B) Absolute number quantitation of T-cell populations in WT Balb/c and adult dblGATA mice. Data is for n=6 across two independent experiments. WT (black bar), dblGATA (white bar). $CD4^{+}$ and $CD8^{+}$ cells have also been subdivided based upon expression of the maturation markers CD69 and CD62L to separate the mature ($CD69^{-}CD62L^{+}$) from the immature ($CD69^{+}CD62L^{-}$).

All significance was noted as: *<0.05, **<0.01, ***<0.001, ***<0.0001.

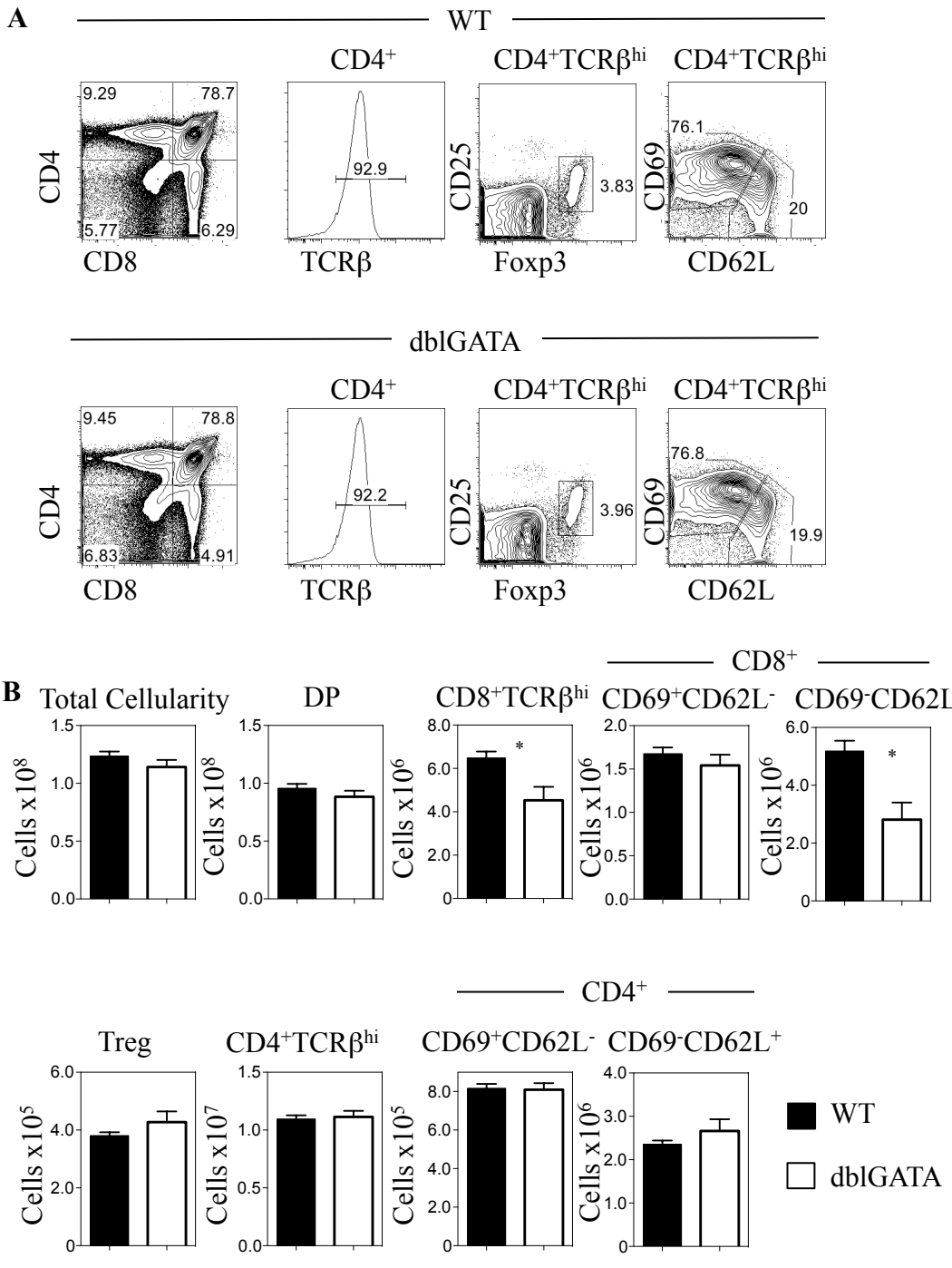
A
WT
CD4+
CD4+TCRβhi
CD4+TCRβhi
9.29
78.7
5.77
6.29
CD4
CD8
92.9
TCRβ
CD25
3.83
Foxp3
CD69
76.1
20
CD62L
dblGATA
9.45
78.8
6.83
4.91
92.2
3.96
76.8
19.9
B
CD8+
Total Cellularity
DP
CD8+TCRβhi
CD69+CD62L-
CD69-CD62L+
Cells x10^8
Cells x10^6
CD4+
Treg
CD4+TCRβhi
CD69+CD62L-
CD69-CD62L+
Cells x10^5
Cells x10^7
WT
dblGATA

result, this steady state analysis highlights that overall T-cell development occurs normally in dblGATA mice with the exception of a slight reduction in $CD8^{+}TCR\beta^{+}$ cells.

5.2.3 Sub-lethal Irradiation Damage of Eosinophil Deficient dblGATA Mice

As thymus development in the steady state of dblGATA mice is comparable to WT mice (all 8-12 weeks old and female only), we next examined if under conditions of thymic damage a potential role for eosinophils could be unveiled. To begin with, we decided to induce thymic damage by employing a model of sub-lethal irradiation (SIR) whereby mice were exposed to a single dose of 425 rad level of irradiation at the day 0 time point. Subsequently the recovery of the thymus from this initial exposure could be addressed upon sacrifice and compared between WT and dblGATA mice. Initially we assessed if following SIR, the extent of thymic damage was similar between WT and dblGATA mice. To do this, we chose an early time point day four (d4) post SIR and compared TEC damage between WT and dblGATA mice (Figure 5.7). Initial analysis of thymus weight showed a slight reduction in dblGATA mice but this was not of significance. However when total cellularity was compared, dblGATA mice had reduced overall cell numbers correlating directly to the reduction seen in $CD45^{+}$ thymocytes (Figure 5.7 A). Further, following isolation of thymi at the d4 timepoint, thymi were digested and alternatively stained with TEC specific antibodies to assess TEC populations by flow cytometry. This showed that TEC populations were comparable between WT and dblGATA mice at d4 post SIR (Figure 5.7 B). Similarly, when absolute numbers of TEC populations were quantified, there was no significant difference seen between WT and dblGATA thymi at this time point (Figure 5.7 C).

Figure 5.7:

dblGATA Mice Have Comparable TEC To WT Controls At d4 Post Sub-lethal Irradiation (SIR)

A) Weights, cellularities and numbers of thymocytes ($CD45^+$) in the thymus of sub-lethally irradiated (SIR) WT were compared to sub-lethally irradiated eosinophil deficient mice at day four following damage. Data is of WT (n=6) and dblGATA (n=7) with black bars and white bars respectively obtained from two independent experiments.

B) Representative FACs plots of Thymic Epithelial Cell (TEC) analysis with mTEC subpopulation gating shown ($EpCAM\text{-}1^+UEA\text{-}1^+$) in WT and dblGATA irradiated mice at d4 post irradiation harvest. Typical proportional plots are shown for the two strains.

C) Quantitation of TEC analysis with further breakdown of TEC subsets for comparison between WT black bars and dblGATA white bars. The mTEC population is subdivided into $mTEC^{hi}$ ($EpCAM\text{-}1^+UEA\text{-}1^+Ly51^-MHCII^+CD80^+$) and $mTEC^{lo}$ ($EpCAM\text{-}1^+UEA\text{-}1^+Ly51^-MHCII^-CD80^-$) for quantitation and comparison. WT (n=6), dblGATA (n=7) across two independent experiments.

All significance was noted as: *<0.05, **<0.01, ***<0.001, ***<0.0001.

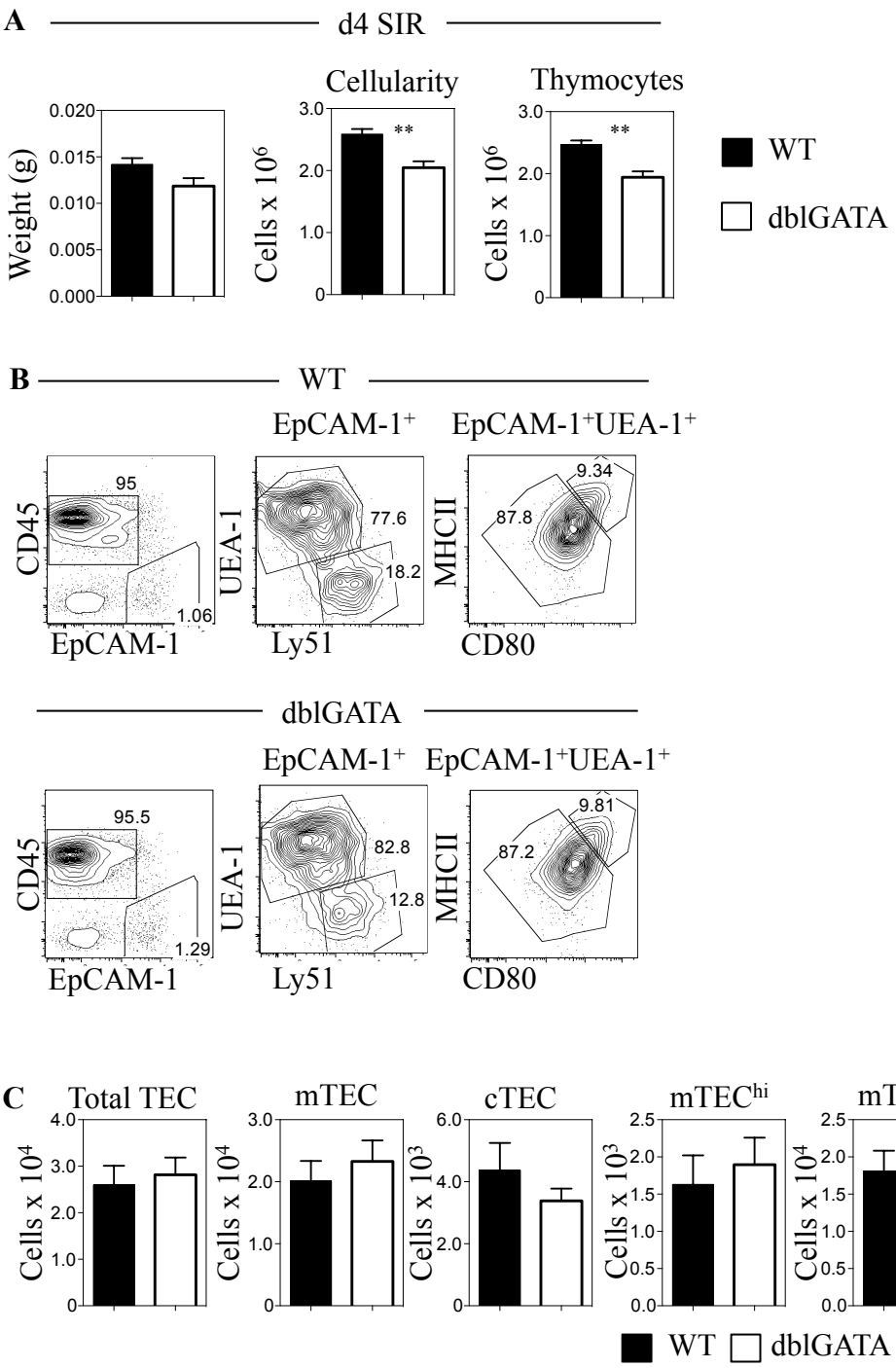
A
d4 SIR
Cellularity
Thymocytes
Weight (g)
Cells x 10^6
Cells x 10^6
0.020
0.015
0.010
0.005
0.000
3.0
2.0
1.0
0
**
**
WT
dblGATA
B
WT
EpCAM-1+
EpCAM-1+UEA-1+
CD45
EpCAM-1
95
1.06
UEA-1
Ly51
77.6
18.2
MHCII
CD80
87.8
9.34
dblGATA
EpCAM-1+
EpCAM-1+UEA-1+
CD45
EpCAM-1
95.5
1.29
UEA-1
Ly51
82.8
12.8
MHCII
CD80
87.2
9.81
C
Total TEC
mTEC
cTEC
mTEChi
mTEClo
Cells x 10^4
Cells x 10^4
Cells x 10^3
Cells x 10^3
Cells x 10^4
4.0
3.0
2.0
1.0
0
6.0
4.0
2.0
2.5
2.0
1.5
1.0
0.5
0.0
WT
dblGATA

Continuing on to a day seven (d7) time point following SIR, thymi between WT and dblGATA mice were examined to assess the ability of the thymus to carry out mechanisms of recovery, as it had previously been shown that the thymus begins recovering from this time point following damage (Figure 5.8) (Dudakov et al., 2012). For this, sub-lethally irradiated thymi from WT and dblGATA mice were similarly prepared with isolation, enzymatic digestion for TEC retrieval and flow cytometric analysis to identify TEC populations. What was apparent to begin with, was that there was a marked reduction in thymus weight in dblGATA mice, supported by reduced cellularity from around $6x10^6$ cells seen in the WT mice down to a reduced $2x10^6$ cells in dblGATA mice (Figure 5.8 A). This coincided with a similar fractional reduction in thymocytes that was further of significance. Interestingly, subsequent analysis of TEC populations demonstrated that all populations were present in WT and dblGATA mice with the proportions of these further being comparable when gated in an identical manner (Figure 5.8 B). However, absolute number analysis saw a large reduction in total TEC in dblGATA mice when compared to WT sub-lethally irradiated control mice (Figure 5.8 C). The reduction in total TEC was due to a significant decrease in all TEC populations, with $mTEC^{hi}$ being the most significantly affected. As a result, this highlights that dblGATA mice have perturbed thymic recovery following SIR.

The experiments described above indicating reduced recovery of dblGATA thymi following sub-lethal irradiation (SIR) were performed using dblGATA ($dblGATA^{-/-}$) mice and WT controls that were not littermate controls. Next littermate controls of $dblGATA^{+/-}$ and $dblGATA^{-/-}$ mice were generated for comparison to confirm if the trend mirrored that seen between the non-littermate WT and $dblGATA^{-/-}$ mice previously assessed. It allowed also for comparison between $dblGATA^{+/-}$ and WT non-littermate controls to determine control

Figure 5.8:

Eosinophil Deficient Mice Fail To Recover To The Level of WT Controls Following Sub-lethal Irradiation at a d7 Timepoint

A) Analysis of weights of thymus, total thymus cellularities and number of thymocytes ($CD45^{+}$) at d7 post sub-lethal irradiation (SIR) of dblGATA mice (white bar) compared to WT controls (black bar). Data was obtained from three experiments with a sample number of 7.

B) FACs plots showing TEC populations in WT compared to dblGATA mice d7 post sub-lethal irradiation. Proportions were representative of the populations and illustrate how the gating was completed.

C) Absolute number analysis of the TEC populations, mTEC being defined as EpCAM-1^{+}UEA-1^{+}Ly51^{-} and cTEC as EpCAM-1^{+}UEA-1^{-}Ly$51^{+,}$ $mTEC^{hi}$ (EpCAM-1^{+}UEA-1^{+}Ly51^{-} $MHCII^{+}CD80^{+}$) and $mTEC^{lo}$ (EpCAM-1^{+}UEA-1^{+}Ly$51^{-}MHCII^{-}CD80^{-}$) seen in (B). Data is from three independent experiments (n=7). Black bar represents WT and white bar is dblGATA analysis.

All significance was noted as: *<0.05, **<0.01, ***<0.001, ***<0.0001.

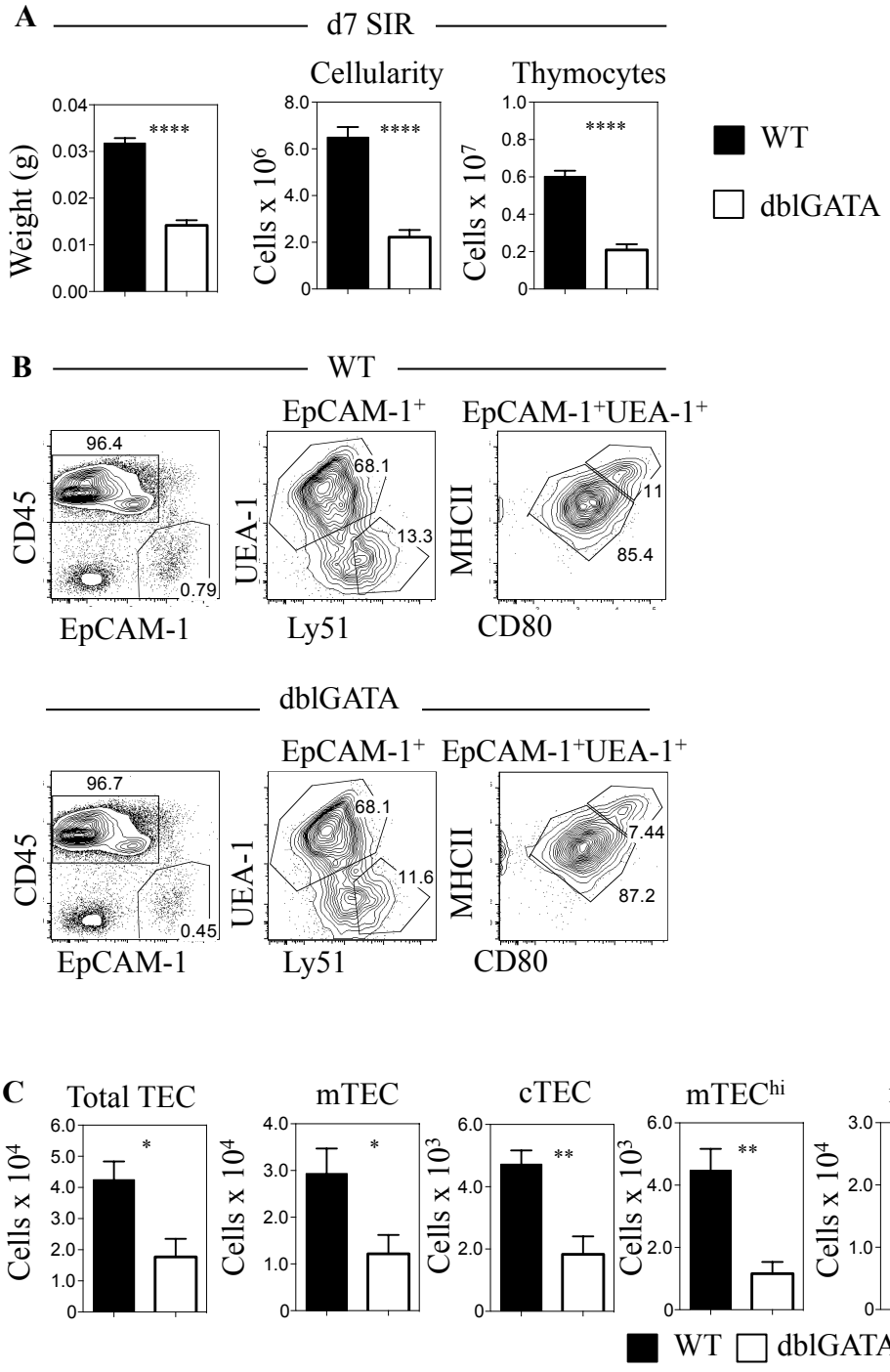
A
d7 SIR
Cellularity
Thymocytes
Weight (g)
Cells x 10^6
Cells x 10^7
****
WT
dblGATA
B
WT
EpCAM-1+
EpCAM-1+UEA-1+
96.4
0.79
68.1
13.3
11
85.4
CD45
EpCAM-1
UEA-1
Ly51
MHCII
CD80
dblGATA
96.7
0.45
68.1
11.6
7.44
87.2
C
Total TEC
mTEC
cTEC
mTEC^hi
mTEC^lo
Cells x 10^4
Cells x 10^3
*
**
WT
dblGATA

comparability. The presence of thymic eosinophils in WT and dblGATA$^{+/-}$ mice along with relative absence from dblGATA$^{-/-}$ mice confirmed the phenotype was correct (Figure 5.9 A). There appeared to be a proportional reduction in eosinophils in the thymus of dblGATA$^{+/-}$ compared with WT controls, and a further reduction between dblGATA$^{+/-}$ and dblGATA$^{-/-}$ mice with dblGATA$^{-/-}$ having a complete absence of eosinophils detectable by FACs. When this was quantitated however, there was no statistical difference between WT and dblGATA$^{+/-}$ mice for eosinophil number. But a significant reduction was seen when dblGATA$^{-/-}$ mice were compared to both WT and dblGATA$^{+/-}$ controls.

Additional analysis was then completed to assess TEC populations (Figure 5.9 B). Thymi were isolated from age-matched mice and digested enzymatically for TEC analysis. There was no difference in the steady state for any of the TEC populations between the littermate control dblGATA$^{+/-}$ and dblGATA$^{-/-}$ mice. Furthermore, the WT non-littermate controls were also equivalent with regards to absolute numbers of TEC to the dblGATA$^{+/-}$ littermate controls. This highlights in the steady state that there is no difference in the development of TEC and that the WT mice remain comparable to dblGATA$^{+/-}$ littermate control mice. Development of T-cell populations was also addressed, with isolated thymus samples being disaggregated to release thymocytes for analysis by flow cytometry. FACs analysis and absolute number quantitation was conducted and showed that total thymus cellularity was comparable between the three mouse strains (Figure 5.9 C). Furthermore all of the T-cell sub-populations were comparable to one another with similar levels of double positive ($CD4^+CD8^+$), $CD4^+TCR\beta^{hi}$ mature single positive CD4 T-cells and T-Regulatory cells. However the $CD8^+TCR\beta^{hi}$ population increased gradually from WT through to

Figure 5.9:

Littermate Heterozygous Controls for dblGATA Mice Are Comparable To WT Mice In Steady State Analysis

A) Eosinophil staining in steady state mice WT, dblGATA heterozygous (Het) and dblGATA knockout (KO) mice with representative plots for the final identification of eosinophils shown as $CD45^{+}CD4^{-}CD8^{-}TCR\beta^{-}Ter119^{-}CD11b^{+}Siglec\text{-}F^{+}$. Absolute numbers of eosinophils is quantified in the right panel graph. Data was obtained from two independent experiments where n=6.

B) Absolute number analysis highlights TEC analysis in the steady state of littermate controls for dblGATA compared to WT. WT (black bar), Het (grey bar), dblGATA KO (white bar). Data was obtained from one independent experiment with n=4.

C) Absolute number analysis in the steady state of T-cell populations within the thymus of littermate controls for dblGATA Het/KO (white bar/ dark grey) and comparison to WT (black bar). Data was obtained from one independent experiment where n=3.

All significance was noted as: *<0.05, **<0.01, ***<0.001, ***<0.0001. Comparisons were made using one-way ANOVA.

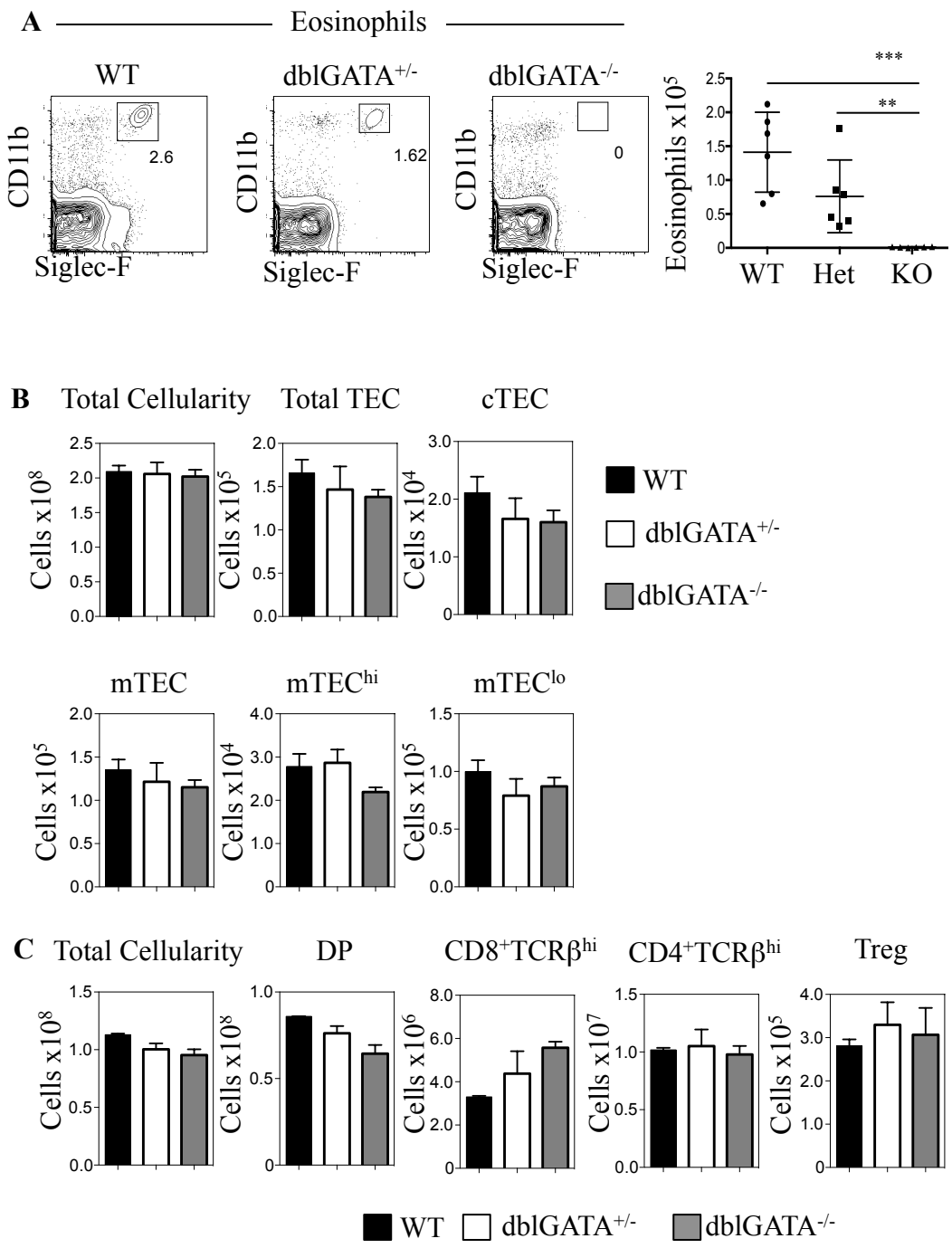
A
Eosinophils
WT
dblGATA+/-
dblGATA-/-
CD11b
Siglec-F
2.6
1.62
0
Eosinophils x10^5
***
**
WT
Het
KO
B
Total Cellularity
Total TEC
cTEC
Cells x10^8
Cells x10^5
Cells x10^4
WT
dblGATA+/-
dblGATA-/-
mTEC
mTEChi
mTEClo
C
Total Cellularity
DP
CD8+TCRβhi
CD4+TCRβhi
Treg
Cells x10^8
Cells x10^6
Cells x10^7

dblGATA$^{+/-}$ and finally dblGATA$^{-/-}$ mice. As a result, there was comparability between WT and dblGATA$^{+/-}$ mice also for T-cell development in the steady state level.

The response of WT and dblGATA$^{+/-}$ mice to SIR at d7 was assessed next. We therefore irradiated the littermate control dblGATA$^{+/-}$ and dblGATA$^{-/-}$ mice along with non-littermate WT mice for comparison, with one dose of 425 rad of irradiation, and harvested the mice seven days following damage induction. TEC analysis was completed with representative FACs plots shown for TEC populations, which were clearly identifiable and comparable (Figure 5.10 A). Additional numerical analysis showed comparability between WT and dblGATA$^{+/-}$ mice at d7 post SIR in total cellularity, total thymocytes and total TEC. But a significant reduction was maintained when WT and dblGATA$^{+/-}$ mice were individually compared to dblGATA$^{-/-}$ mice for all parameters (Figure 5.10 B). Therefore it appears that WT non-littermate controls again behave the same as the dblGATA$^{+/-}$ mice even when under conditions of SIR.

5.2.4 Long Term Recovery of dblGATA Thymus Post SIR

Considering the relative comparability of non littermate WT and dblGATA$^{+/-}$ mice in steady state and irradiation conditions, with the phenotype of reduced recovery in dblGATA$^{-/-}$ (dblGATA) mice previously described (Figure 5.8), we wanted to confirm that the presence and persistence of eosinophils in the thymus was the determining factor encouraging recovery of WT sub-lethally irradiated thymi and hindering it in dblGATA mice. For this, we decided to assess the relative radioresistance of eosinophils in the thymus of WT adult mice. For this, SIR WT mice (one dose of 425rad) were compared to unmanipulated controls for the presence of eosinophils; with relative numbers of eosinophils related to total thymus

Figure 5.10:
dblGATA Littermate Heterozygous Controls Mirror WT Mice At d7 Following Sub-lethal Irradiations

A) Representative FACs plots of TEC analysis in the three mouse strains; WT, dblGATA Heterozygous (Het), dblGATA deficient (KO).

B) Absolute number analysis of total thymus cellularity, thymocytes ($CD45^+$) and total TEC ($CD45^-EpCAM\text{-}1^+$) seen in WT, dblGATA Het or dblGATA KO at d7 following sub-lethal irradiations (SIR). Data was obtained from two independent experiments where WT (n=4), Het (n=5) and KO (n=6).

All significance was noted as: *<0.05, **<0.01, ***<0.001, ***<0.0001. Comparisons were made using one-way ANOVA.

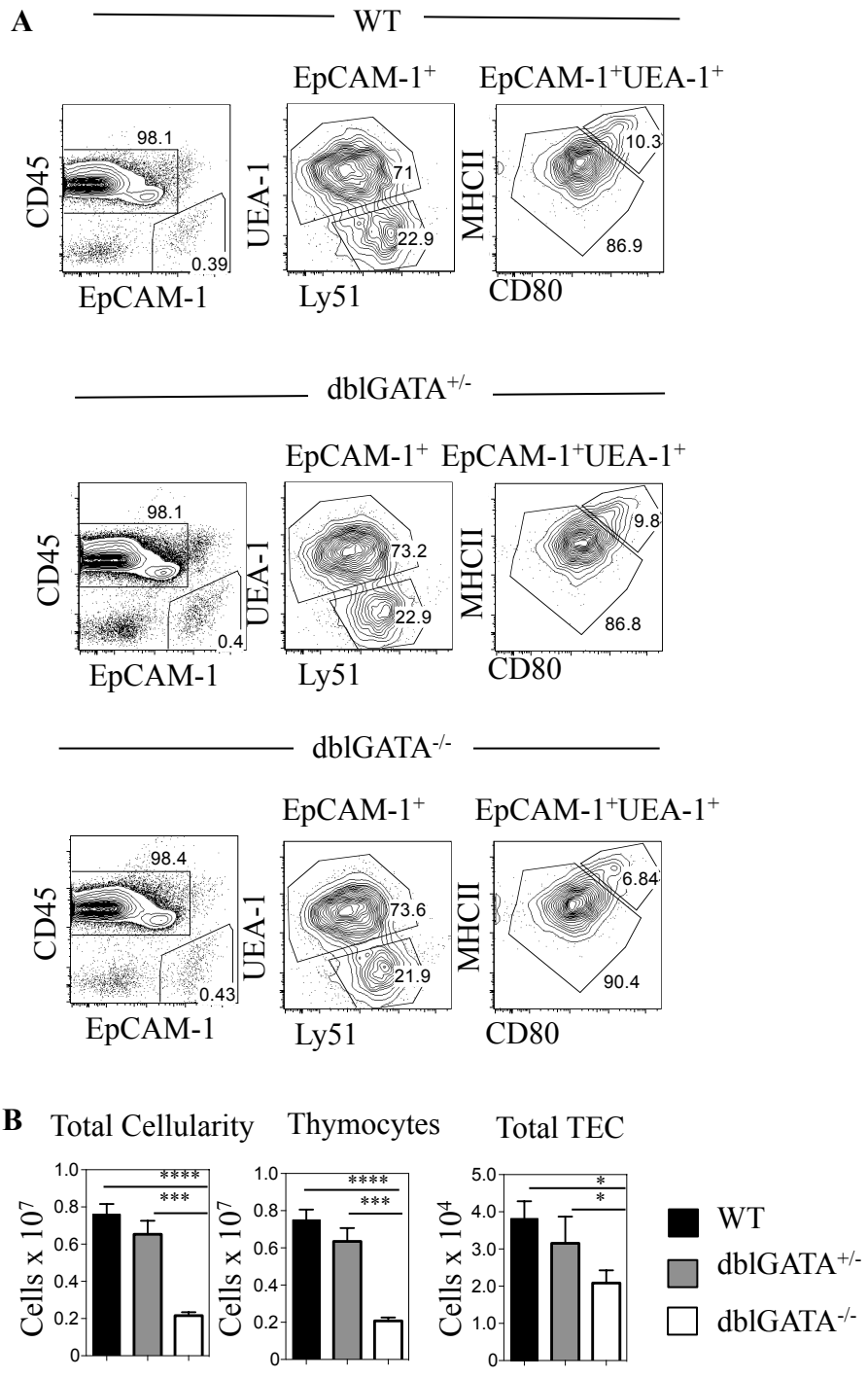
A
WT
EpCAM-1+
EpCAM-1+UEA-1+
98.1
0.39
CD45
EpCAM-1
71
22.9
UEA-1
Ly51
10.3
86.9
MHCII
CD80
dblGATA+/-
EpCAM-1+
EpCAM-1+UEA-1+
98.1
0.4
CD45
EpCAM-1
73.2
22.9
UEA-1
Ly51
9.8
86.8
MHCII
CD80
dblGATA-/-
EpCAM-1+
EpCAM-1+UEA-1+
98.4
0.43
CD45
EpCAM-1
73.6
21.9
UEA-1
Ly51
6.84
90.4
MHCII
CD80
B
Total Cellularity
Thymocytes
Total TEC
Cells x 10^7
Cells x 10^7
Cells x 10^4
1.0
0.8
0.6
0.4
0.2
0
5.0
4.0
3.0
2.0
1.0
****
***
*
*
WT
dblGATA+/-
dblGATA-/-

cellularity calculated (Figure 5.11). Analysis by flow cytometry showed that eosinophils were detectable in the thymus even following damage induction and that the relative proportions of eosinophils were unchanged in FACs analysis (Figure 5.11 A). By then subdividing eosinophils based upon their lack of Gr1 expression but Siglec-F expression, there were a greater proportion of eosinophils positioned within the Siglec-F high fraction following SIR (Figure 5.11 B). However mean fluorescence intensity (MFI) for the expression level of Siglec-F by eosinophils in the thymus failed to be significantly different (Figure 5.11 B). Furthermore, thymus cellularity was reduced in WT SIR mice compared to WT unmanipulated controls from around $1.5x10^8$ cells to $0.5x10^8$ cells (Figure 5.11 C) as would be expected following damage and subsequent thymic involution. However because of this loss of total thymus cellularity, the persistence of eosinophils in the thymus numerically would be reduced as a consequence. Therefore by calculating the number of eosinophils per $1x10^6$ thymus cells to compensate for the loss of thymus cells induced following irradiation, eosinophils present per $1x10^6$ thymus cells in control steady state mice and sub-lethally irradiated WT adult mice were comparable, suggesting that thymic eosinophils may be less susceptible to irradiation (Figure 5.11 C).

Given the potential persistence of eosinophils in WT thymi following damage, we continued investigating the regeneration of the thymus at later time points (d14 and d35) following SIR damage to determine if dblGATA mice recovered eventually to the same level as WT controls or were hindered in their ability to recover (Figure 5.12). Upon thymus isolation and analysis, at d14, thymus recovery of dblGATA mice was reduced. This continued into analysis of total cellularity and also total thymocytes with dblGATA mice having reduced numbers compared to WT control mice (Figure 5.12 A). However, interestingly at d14, there was little difference

Figure 5.11:
Thymic Eosinophils Appear Radioresistant Post Exposure To Sub-lethal Irradiation

Mice were irradiated sub-lethally (SIR) and the thymus was compared to WT non-irradiated steady state Balb/c mice d7 post irradiation to investigate the relative radio-resistance of eosinophils.

A) FACs plots showing identification of the eosinophil population ($(CD45^{+}CD4^{-}CD8^{-}$ $TCR\beta^{-}$ $Ter119^{-}CD11b^{+}Siglec\text{-}F^{+}$) in WT steady state unmanipulated (left panel) and irradiated (right panel) and analysed at d7. Proportional analysis of FACs percentages of eosinophil populations was also quantified on the far right with steady state (black bar, n=2) and SIR d7 WT (white bar, n=7).

B) Representative FACs plots show activation of eosinophils ($CD45^{+}CD11b^{+}Siglec\text{-}F^{+}Gr\text{-}1^{-}$) through relative expression levels of Siglec-F and lack of Gr1 expression comparing WT steady state and WT irradiated examined d7 post sub-lethal exposure. MFI of Siglec-F on eosinophils was shown in far panel comparing these two conditions; black bar (steady state, n=2) and white bar (SIR d7, n=7).

C) Absolute number analysis of thymus cellularity (left panel) in control mice compared to those irradiated sub-lethally with analysis day 7 post irradiation. Number of eosinophils (right panel) were calculated and corrected in relation to the total cellularity due to the reduction seen following irradiation. As a result data shows number of eosinophils per $1x10^{6}$ total thymus cells. Circles represent controls (n=2) and squares represent irradiated mice (n=7). Data was obtained across two independent experiments.

All significance was noted as: *<0.05, **<0.01, ***<0.001, ***<0.0001.

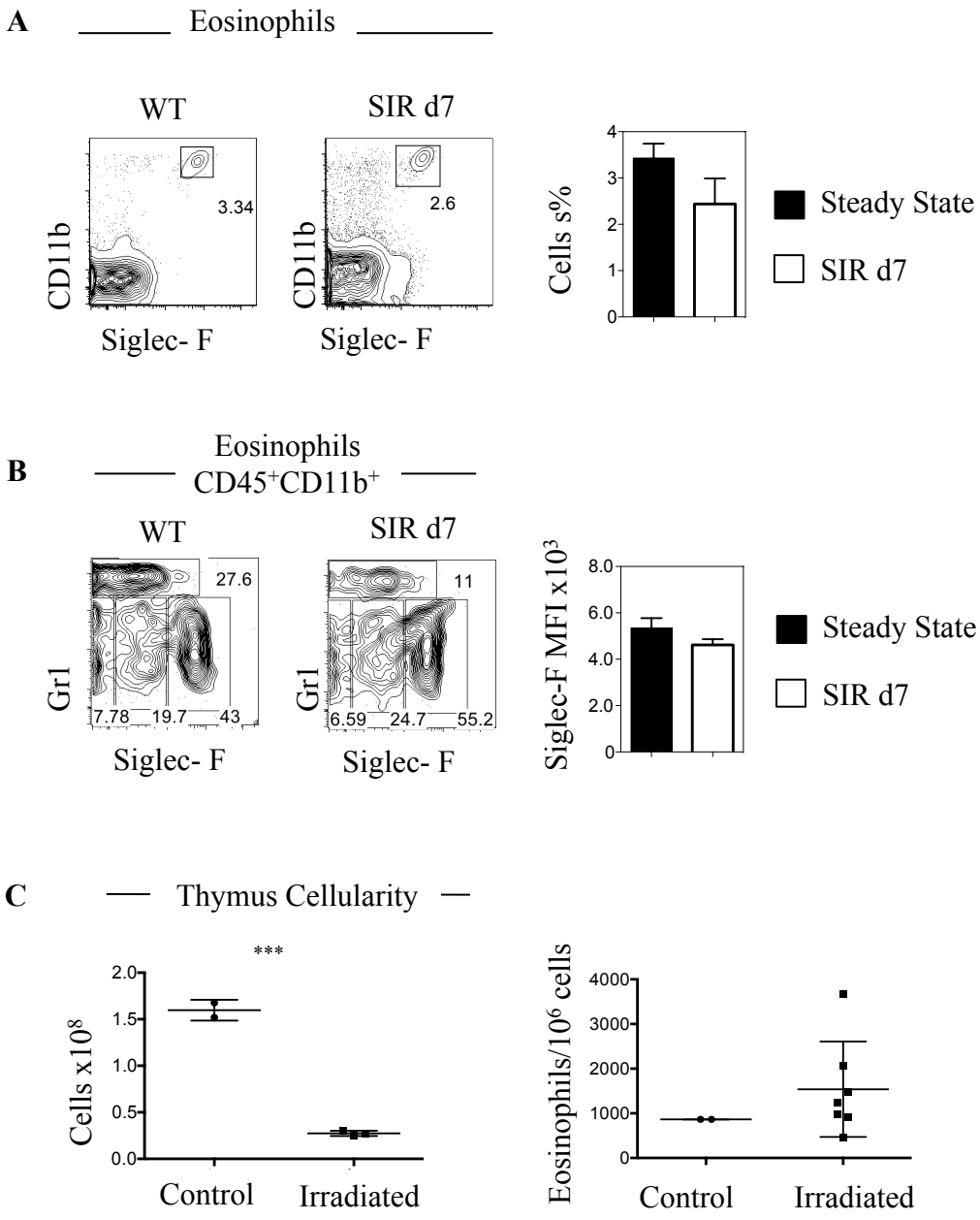
A
Eosinophils
WT
SIR d7
3.34
2.6
CD11b
Siglec- F
Cells s%
Steady State
SIR d7
B
Eosinophils
CD45+CD11b+
WT
SIR d7
27.6
11
Gr1
7.78
19.7
43
6.59
24.7
55.2
Siglec- F
Siglec-F MFI x10^3
Steady State
SIR d7
C
Thymus Cellularity
***
Cells x10^8
Control
Irradiated
Eosinophils/10^6 cells
Control
Irradiated

Figure 5.12:

dblGATA Mice Have Alterations In TEC Recovery At d14 and d35 Timepoints Following Sub-lethal Irradiation

A) d14 timepoint post sub-lethal irradiation (SIR) analysis of thymus weights, cellularity, thymocytes ($CD45^+$) and TEC populations; total TEC ($CD45^-EpCAM\text{-}1^+$) and the corresponding subpopulations. WT (black bar) and dblGATA (white bar). Data was obtained from two independent experiments (n=7).

B) d35 timepoint following sub-lethal irradiation (SIR). Analysis of weights of thymus, cellularity and total thymocytes ($CD45^+$) along with absolute numbers of TEC and subpopulations in WT (black bar) compared to dblGATA (white bar). Data was obtained from one experiment where WT (n=5) and dblGATA (n=6).

All significance was noted as: *<0.05, **<0.01, ***<0.001, ***<0.0001.

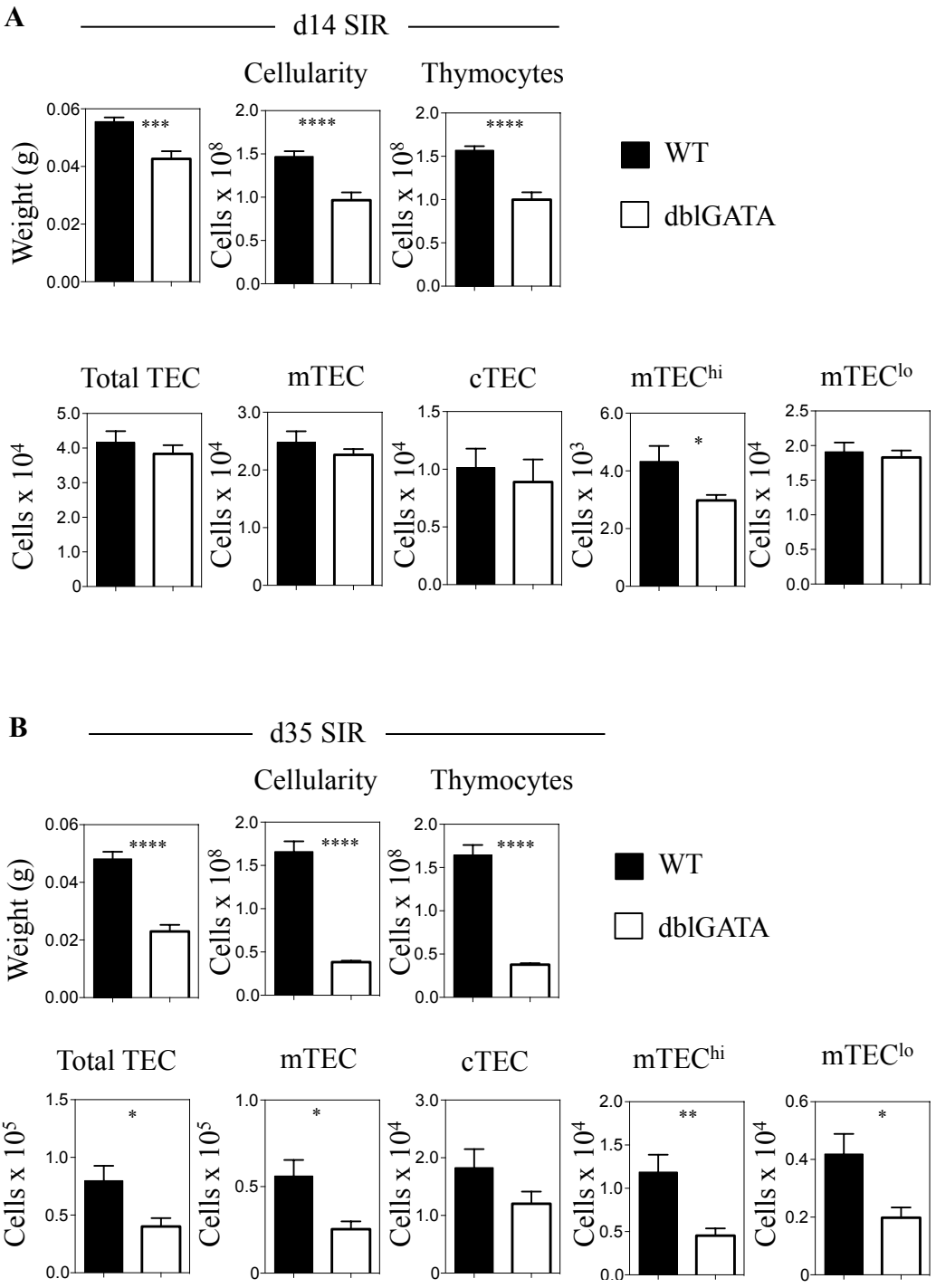
A
d14 SIR
Cellularity
Thymocytes
Weight (g)
Cells x 10^8
Cells x 10^8
***
****
****
WT
dblGATA
Total TEC
mTEC
cTEC
mTEC^hi
mTEC^lo
Cells x 10^4
Cells x 10^4
Cells x 10^4
Cells x 10^3
Cells x 10^4
*
B
d35 SIR
Cellularity
Thymocytes
Weight (g)
Cells x 10^8
Cells x 10^8
****
****
****
WT
dblGATA
Total TEC
mTEC
cTEC
mTEC^hi
mTEC^lo
Cells x 10^5
Cells x 10^5
Cells x 10^4
Cells x 10^4
Cells x 10^4
*
*
**
*

seen statistically within the breakdown of the TEC populations apart from the $mTEC^{hi}$ population that maintained significance.

When an additional d35 time point was analysed for the same parameters, the differences between the WT and dblGATA mice following SIR began to widen once again (Figure 5.12 B). The weight differences of the thymus were more statistically significant and as were the cellularities and total thymocytes – with reductions in dblGATA mice compared to WT controls. Surprisingly there was again a difference in TEC population absolute numbers with total TEC reductions in dblGATA mice and further this was seen in all populations with the $mTEC^{hi}$ cells again being the most significantly affected (Figure 5.12 B). As a result, it appears that there is a failure for long term recovery of dblGATA mice in the thymus with regards to TEC regeneration following injury through SIR.

Based on these observations, a summary time course figure was constructed to highlight the long term differences in the recovery of the dblGATA mice compared to WT controls (Figure 5.13). Firstly, analysis in the steady state of total thymus cellularity highlighted that WT and dblGATA mice were comparable with similar total cell numbers. However, upon injury at day 0, the thymus damage induced following SIR was greater at day 4 in dblGATA mice compared to WT controls with a reduced thymus cellularity seen in dblGATA mice. Further analysis at later time points following SIR damage appeared to show that infact this difference in thymus size continued to widen between WT and dblGATA mice with a potential regression in any apparent recovery that the dblGATA mice may have previously achieved between d14 and d35 (Figure 5.13 A).

Figure 5.13:
dblGATA mice Fail To Recover Their Thymus Cellularity And TEC To The Level of WT Mice Following Sub-lethal Irradiation

For all time points data was obtained from a minimum of two independent experiments with; d0 (WT n=5, dblGATA n=7), d4 (WT n=5, dblGATA n=7), d7 (WT n=7, dblGATA n=7), d10 (WT n=4, dblGATA n=4), d14 (WT n=7, dblGATA n=7), d35 (WT n=5, dblGATA n=5).

A) Total cellularity changes overtime for the thymus following sub-lethal irradiations have been plotted with regards to the mean value obtained from replicate experiments for WT (black line) against dblGATA (blue line).

B) Total TEC ($CD45^{-}EpCAM\text{-}1^{+}$) absolute numbers have been plotted over time following sub-lethal irradiations to allow comparisons between WT (black circles) and dblGATA (blue squares).

All significance was noted as: *<0.05, **<0.01, ***<0.001, ***<0.0001.

A

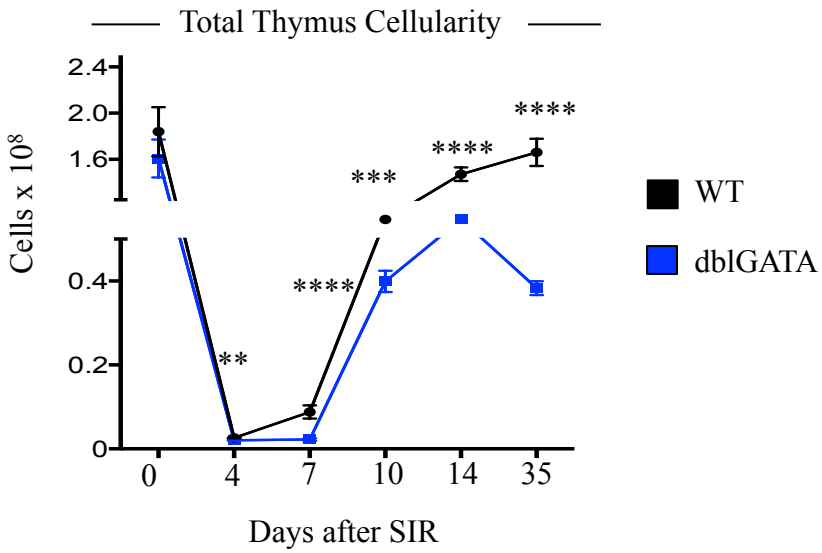
Total Thymus Cellularity
Cells x 10^8
2.4
2.0
1.6
0.4
0.2
0
**
****
***
****
****
0
4
7
10
14
35
Days after SIR
WT
dblGATA

B

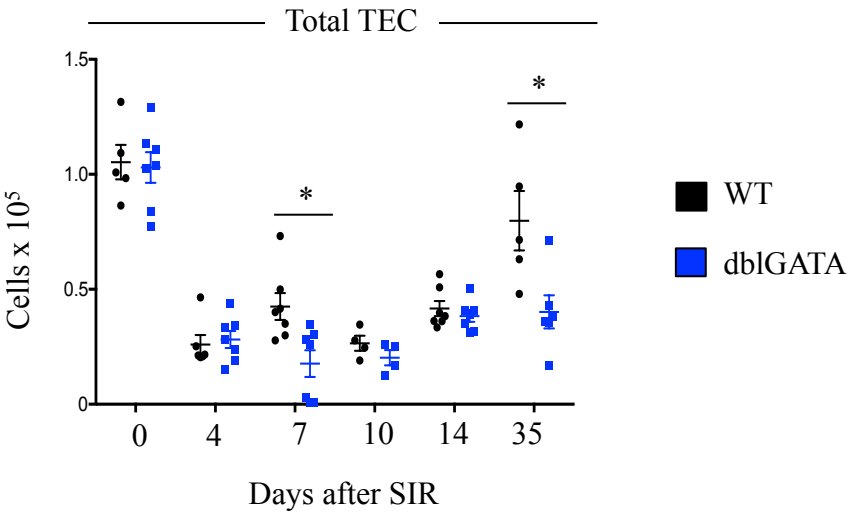
Total TEC
Cells x 10^5
1.5
1.0
0.5
0
*
*
0
4
7
10
14
35
Days after SIR
WT
dblGATA

Total TEC analysis additionally showed a similar trend to that seen in total cellularity, with WT mice recovering post SIR in a U shaped curve, with the later time points having TEC numbers which were approaching those seen prior to damage (Figure 5.13 B). However when the dblGATA TEC recovery was examined, it seemed that despite comparable levels of damage at day 4 with similar TEC numbers, by day 7 a significant difference had been generated between these mice. This partially looked to recover especially at the day 14 time point but then at day 35, TEC populations in dblGATA mice had failed to increase from d14, leaving the graph to generate more of a plateau shape (Figure 5.13 B). This leaves reduced TEC recovery in dblGATA mice suggestive of an inability of the TEC populations to subsequently recover fully in dblGATA mice following damage.

5.2.5 Sub-lethal Irradiation Analysis of T-cell Recovery In dblGATA Mice

Having generated a time series of TEC recovery in dblGATA mice under SIR damage, there was then interest into what was happening to the relative T-cell populations. For this, mice were similarly irradiated sub-lethally (1x425 rad) and at d7 following damage, T-cell analysis through flow cytometry was conducted on harvested thymi.

WT mice showed a profile of T-cell development (CD4vsCD8) that was remarkably different from that seen in dblGATA mice (Figure 5.14 A). Firstly and most strikingly, the proportion of double positive T-cell populations ($CD4^+CD8^+$) was reduced in dblGATA mice at d7 analysis compared to SIR WT control mice. In addition, a large proportion of $CD8^+$ cells were seen in dblGATA mice compared to WT and $CD4^+$ cells also appeared relatively increased. But the division of $CD4^+$ and $CD8^+$ on the expression of TCRβ was relatively similar with regards to proportions of $TCR\beta^{hi}$ cells. Absolute number analysis from this highlighted some

interesting findings (Figure 5.14 B). Total thymus cellularity was again significantly reduced in dblGATA mice compared to WT mice at d7 post SIR as was expected, but interestingly, this appeared when broken down, to be due to the reduction in double positive thymocytes. Interestingly results also suggested that there might be a reduction in total $CD4^+CD8^-$ thymocytes.

To see if the same developmental defects in T-cell development were seen when the total cellularity was at its most different in dblGATA compared to WT mice following SIR; the d35 time point was assessed for T-cell development (Figure 5.15). Interestingly, there was an apparent difference in the developmental profile of thymocytes with greatly reduced proportions of $CD4^+CD8^+$ thymocytes and a consequential increase in the $CD4^+CD8^-$ thymocytes (Figure 5.15 A). In addition, absolute number analysis showed that dblGATA mice had a significant reduction in total cellularity compared to WT controls and because of this there were subsequently reduced absolute numbers in all thymocyte populations (Figure 5.15 B).

5.2.6 Mechanisms of Eosinophil Mediated Thymus Recovery Following Sub-lethal Irradiation Damage

Mechanistically, how eosinophils may be acting to repair the thymus post injury as a process needs to be considered. In other tissues, eosinophils have been linked to the production of IL-13 and IL-4 for their recovery following damage. To examine whether a similar axis may be operating in thymus we used *Il4ra*$^{-/-}$ mice (Goh et al., 2013, Heredia et al., 2013). WT and *Il4ra*$^{-/-}$ mice were sub-lethally irradiated, as conducted in WT and dblGATA mice previously, and analysed seven days after to assess TEC development as a phenotype was previously seen

Figure 5.14:

T-cell Analysis In dblGATA Is Altered Compared To WT Mice d7 Following Sub-lethal Irradiations

A) FACs plots showing the T-cell development in WT mice (top panel) and dblGATA mice (lower panel) d7 following sub-lethal irradiations (SIR). T-cell analysis was obtained through CD4 and CD8 single positive gating and subsequently dividing this population on TCRβ expression. Plots were representative of proportions seen during analysis.

B) Absolute number analysis of T-cell populations in WT (black bar) and dblGATA (white bar) d7 following sub-lethal irradiations. Data was obtained from one experiment where n=3.

All significance was noted as: *<0.05, **<0.01, ***<0.001, ***<0.0001.

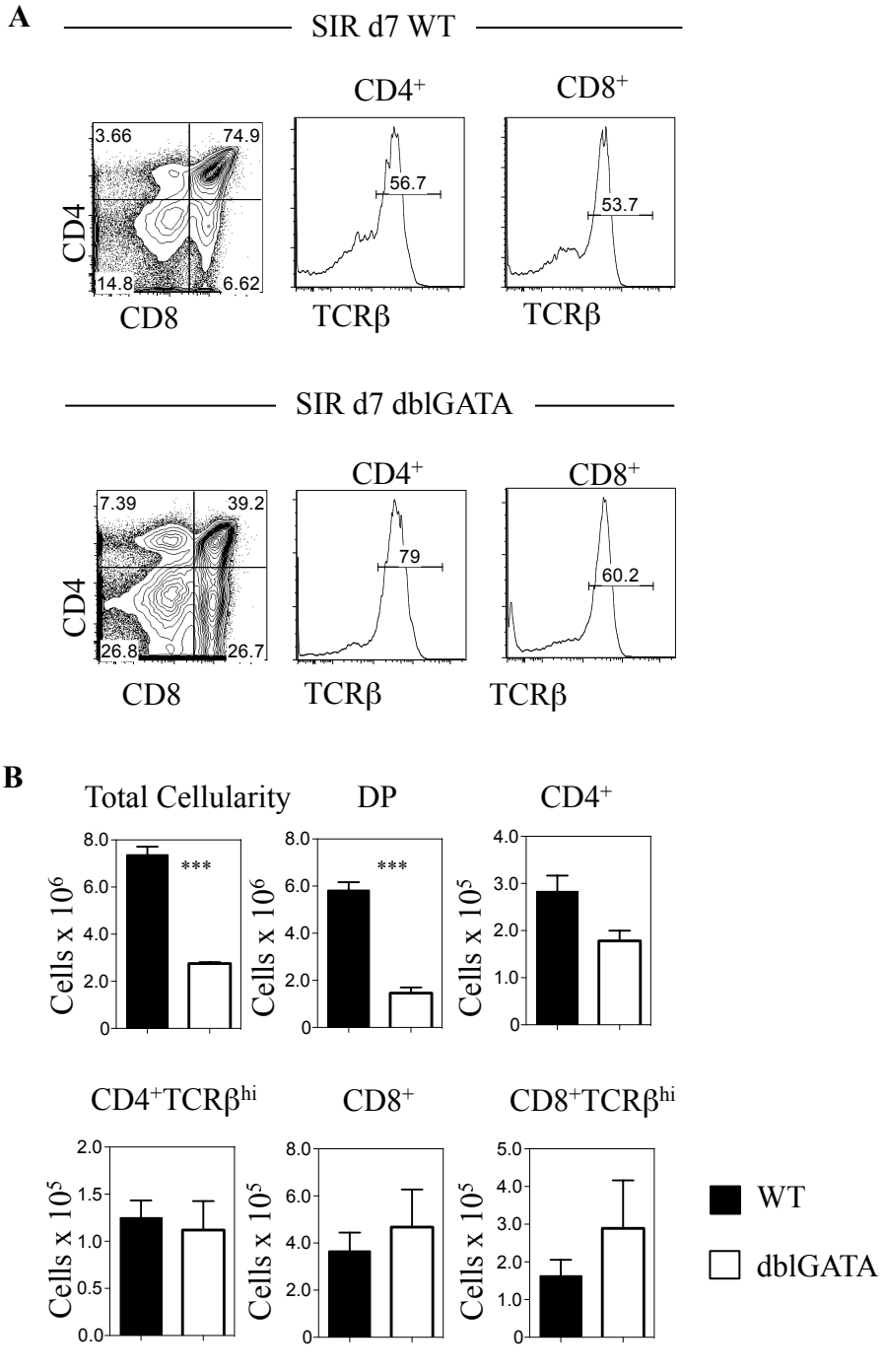
A
SIR d7 WT
CD4+
CD8+
3.66
74.9
14.8
6.62
CD4
CD8
56.7
53.7
TCRβ
TCRβ
SIR d7 dblGATA
CD4+
CD8+
7.39
39.2
26.8
26.7
CD4
CD8
79
60.2
TCRβ
TCRβ
B
Total Cellularity
DP
CD4+
Cells x 10^6
Cells x 10^6
Cells x 10^5
***
***
CD4+TCRβhi
CD8+
CD8+TCRβhi
Cells x 10^5
Cells x 10^5
Cells x 10^5
WT
dblGATA

Figure 5.15:
T-cell Analysis In dblGATA and WT Mice d35 Following Sub-lethal Irradiations

A) FACs plots showing T-cell development in WT mice (top panel) and dblGATA mice (lower panel) d35 following sub-lethal irradiations. T-cells were identified as expressing either CD4 or CD8 and then were divided upon TCRβ expression.

B) Absolute number analysis of T-cell populations in WT (black bar) and dblGATA (white bar) d35 following sub-lethal irradiations. Data was obtained from one experiment n=4 .

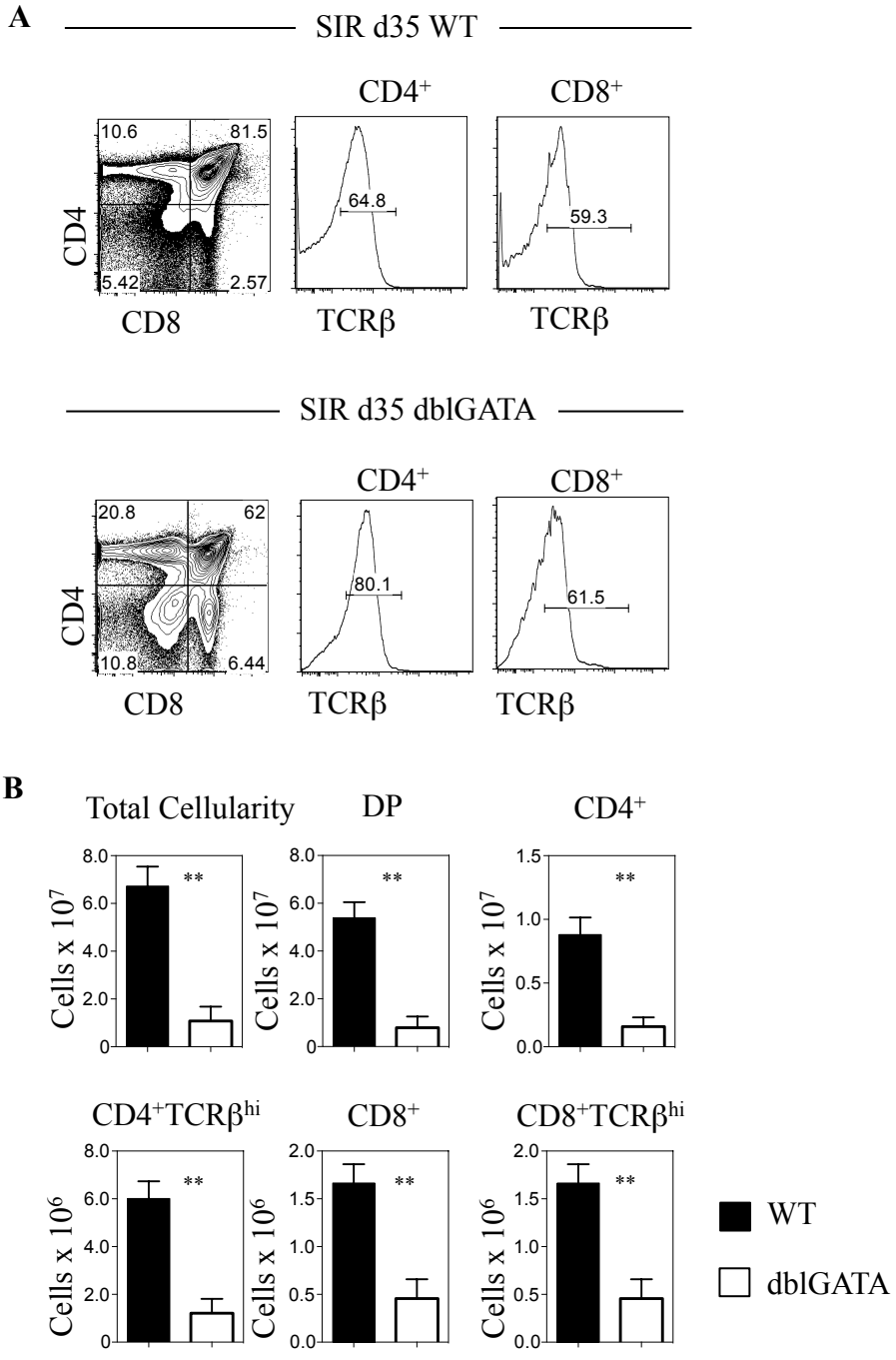
A
SIR d35 WT
CD4+
CD8+
10.6
81.5
5.42
2.57
CD4
CD8
64.8
59.3
TCRβ
TCRβ
SIR d35 dblGATA
CD4+
CD8+
20.8
62
10.8
6.44
CD4
CD8
80.1
61.5
TCRβ
TCRβ
B
Total Cellularity
DP
CD4+
Cells x 10^7
Cells x 10^7
Cells x 10^7
CD4+TCRβhi
CD8+
CD8+TCRβhi
Cells x 10^6
Cells x 10^6
Cells x 10^6
**
WT
dblGATA

in dblGATA mice at this stage (Figure 5.16). Initial analysis following thymus isolation at d7 post SIR for thymus weight, cellularity and total thymocytes, showed that there were no significant differences between WT and *Il4ra*$^{-/-}$ mice (Figure 5.16 A). Interestingly it seemed that there was a trend for increased numbers of total cells and thymocytes in the *Il4ra*$^{-/-}$ mice, but it was insignificant. Further TEC analysis following thymi isolation and digestion prior to antibody cell surface staining, showed that while all of the TEC populations could be identified, total TEC proportions were reduced between WT and *Il4ra*$^{-/-}$ mice. The make up of the TEC compartment however remained comparable with proportions of TEC subpopulations being similar between WT and *Il4ra*$^{-/-}$ mice (Figure 5.16 B). Absolute number analysis showed that although there was a trend towards reduced numbers of TEC in all subpopulations including cTEC, mTEC, mTEC^{hi} and mTEC^{lo}, none of these were statistically significant, but some of the p values shown were close to significance.

However, due to dblGATA mice having significantly altered thymocyte populations following damage and the profound contribution of thymocytes to total thymus cellularity along with their requirement to reciprocally support TEC development, thymocytes in *Il4ra*$^{-/-}$ mice were analysed at d7 following SIR (Figure 5.17 A). Data collected from freshly isolated and prepared thymi from WT and *Il4ra*$^{-/-}$ mice at d7 post SIR showed marked thymocyte alterations by flow cytometry. However there was a loss of the CD8^{+}CD4^{-} thymocytes and their subsequent TCRβ^{hi} subpopulation - a feature of *Il4ra*$^{-/-}$ mice as eosmesodermin CD8 T-cells have been shown to be IL-4 dependent (Jameson et al., 2015). Absolute number analysis supported the lack of proportional changes seen by FACs, with no population except for that of the CD8^{+} cells being significantly altered when *Il4ra*$^{-/-}$ mice were compared to WT control mice following SIR (Figure 5.17 B).

Figure 5.16:
***Il4rα*$^{-/-}$ Deficient Mice Have Reduced TEC At d7 Following Sub-lethal Irradiations**

A) Thymus weight, total thymus cellularity and absolute number of thymocytes ($CD45^{+}$) is shown for WT (black bar) and *Il4rα*$^{-/-}$ mice (white bar) d7 following sub-lethal irradiations. Data was from three independent experiments WT (n=10) and *Il4rα*$^{-/-}$ (n=12).

B) FACs plots for TEC analysis in WT and *Il4rα*$^{-/-}$ mice at d7 following sub-lethal irradiations.

C) Absolute number analysis of total TEC ($CD45^{-}EpCAM\text{-}1^{+}$) and TEC subsets in WT (black bar) and *Il4rα*$^{-/-}$ (white bar) d7 post sub-lethal irradiations. Data was obtained from three independent experiments with WT (n=10) and *Il4rα*$^{-/-}$ (n=12).

All significance was noted as: *<0.05, **<0.01, ***<0.001, ***<0.0001.

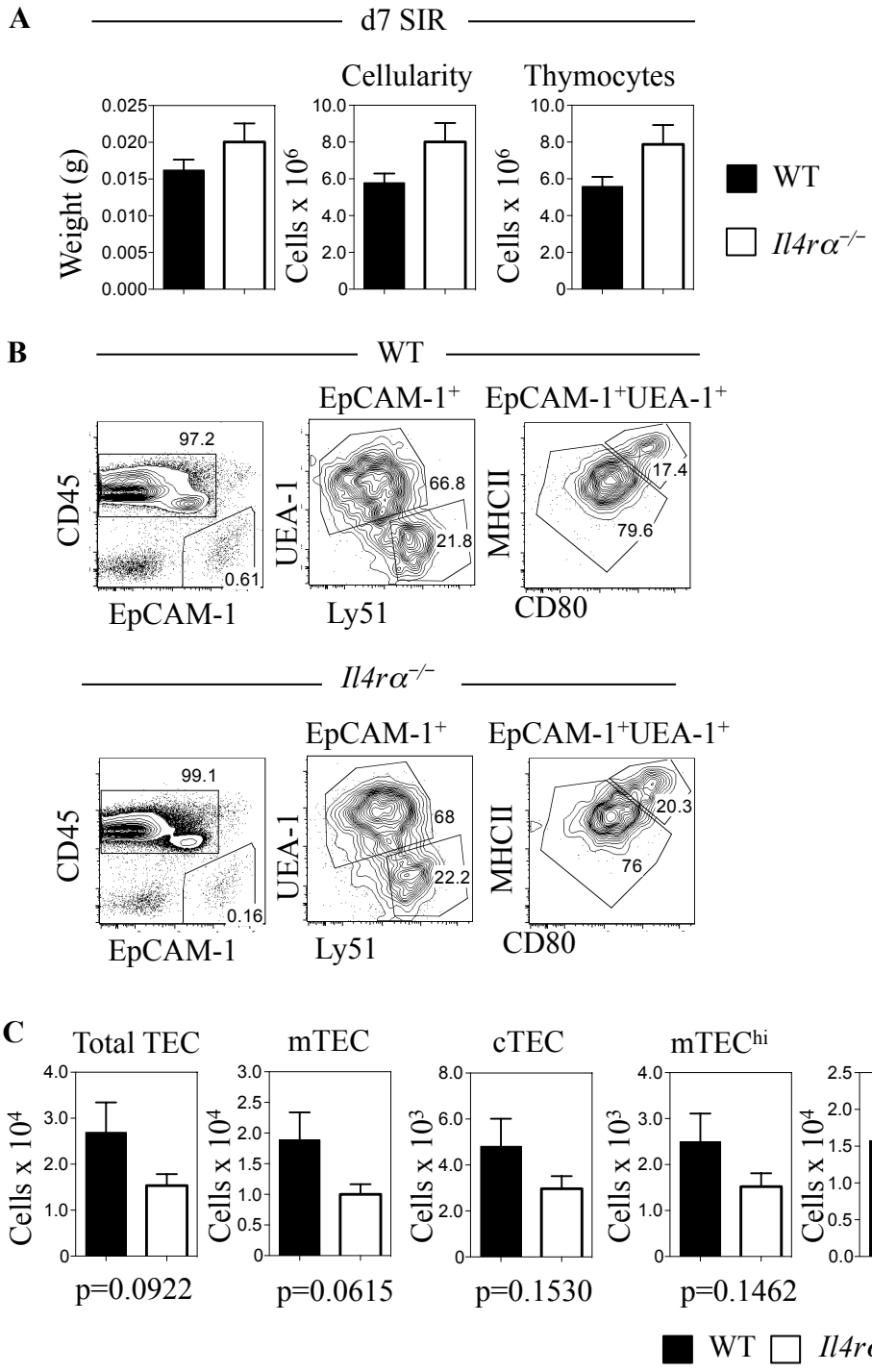
A
d7 SIR
Cellularity
Thymocytes
Weight (g)
Cells x 10^6
Cells x 10^6
WT
Il4rα−/−
B
WT
EpCAM-1+
EpCAM-1+UEA-1+
97.2
0.61
CD45
EpCAM-1
66.8
21.8
UEA-1
Ly51
17.4
79.6
MHCII
CD80
Il4rα−/−
EpCAM-1+
EpCAM-1+UEA-1+
99.1
0.16
CD45
EpCAM-1
68
22.2
UEA-1
Ly51
20.3
76
MHCII
CD80
C
Total TEC
mTEC
cTEC
mTEChi
mTEClo
Cells x 10^4
Cells x 10^4
Cells x 10^3
Cells x 10^3
Cells x 10^4
p=0.0922
p=0.0615
p=0.1530
p=0.1462
p=0.0515
WT
Il4rα−/−

Figure 5.17:

T-cell Analysis Of *Il4rα*$^{-/-}$ Mice Is Unchanged Compared To Controls For d7 Following Sub-lethal Irradiation

A) Representative plots shown for FACs thymic analysis of T-cell development at d7 after sub-lethal irradiation; WT (top panel) and *Il4rα*$^{-/-}$ mice (bottom panel).

B) Absolute number analysis is also shown with total cellularity and thymocyte populations in the lower panel. WT (black bar) *Il4rα*$^{-/-}$ (white bar). Data was obtained from one experiment n=4.

All significance was noted as: *<0.05, **<0.01, ***<0.001, ***<0.0001.

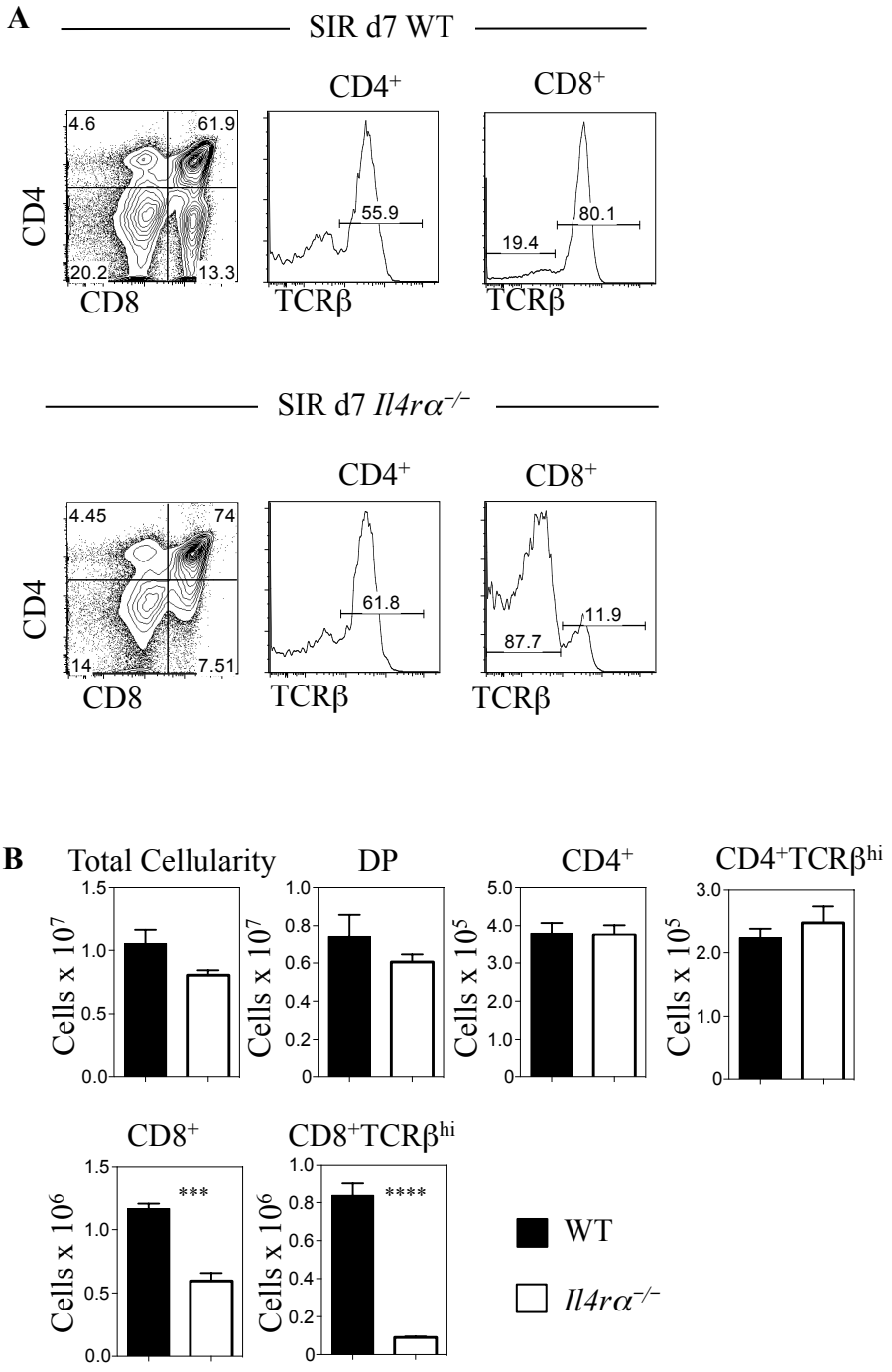
A
SIR d7 WT
CD4+
CD8+
4.6
61.9
20.2
13.3
CD4
CD8
55.9
TCRβ
19.4
80.1
TCRβ
SIR d7 Il4rα−/−
4.45
74
14
7.51
61.8
87.7
11.9
B
Total Cellularity
DP
CD4+
CD4+TCRβhi
CD8+
CD8+TCRβhi
Cells x 10^7
Cells x 10^5
Cells x 10^6
***
****
WT
Il4rα−/−

As dblGATA mice had a great difference in thymus recovery at the d35 timepoint post SIR, we conducted a later timepoint for thymocyte analysis of the *Il4ra*$^{-/-}$ mice at this stage with thymus isolation, disaggregation and antibody staining for flow cytometry (Figure 5.18 B). Representative FACs plots showed that the proportions of all thymocyte populations were comparable between WT and *Il4ra*$^{-/-}$ mice except for the maintained reduction in CD8^{+}CD4^{-} cells. However in absolute number analysis a difference in total cellularity of the thymus and CD4^{+}CD8^{+} (DP), CD4^{+} and CD4^{+}TCRβ^{hi} cells were all reduced in *Il4ra*$^{-/-}$ mice compared to WT control mice following SIR (Figure 5.18 B). This reduction was of significance and highlighted that there may be an issue with recovery of *Il4ra*$^{-/-}$ thymi long term following damage. While this does not fully phenocopy that seen in the dblGATA mice, it may provide an indication that eosinophils and IL-4Rα are both required for thymus recovery.

Figure 5.18:

T-cell Development In *Il4rα*$^{-/-}$ Mice Is Reduced Compared To Controls At d35 Following Sub-lethal Irradiation

A) FACs analysis of thymus for T-cell development, d35 following sub-lethal irradiations; WT in top panel and *Il4rα*$^{-/-}$ mice bottom panel.

B) Absolute number analysis is also shown with WT (black bar) and *Il4rα*$^{-/-}$ (white bar). Data was obtained from one experiment n=4.

All significance was noted as: *<0.05, **<0.01, ***<0.001, ***<0.0001.

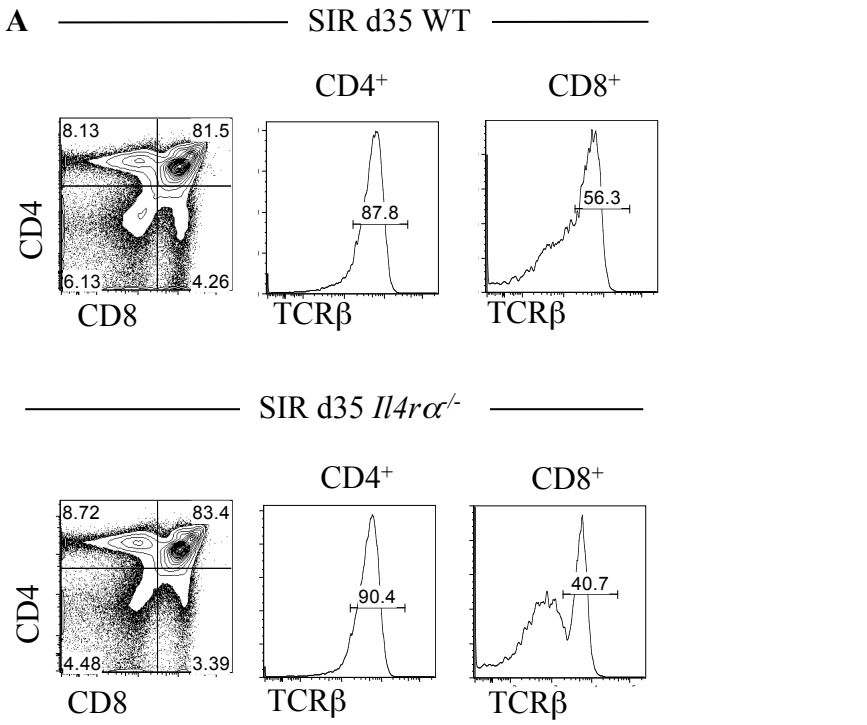
A
SIR d35 WT
CD4+
CD8+
8.13
81.5
6.13
4.26
CD4
CD8
87.8
56.3
TCRβ
TCRβ
SIR d35 Il4rα-/-
CD4+
CD8+
8.72
83.4
4.48
3.39
CD4
CD8
90.4
40.7
TCRβ
TCRβ

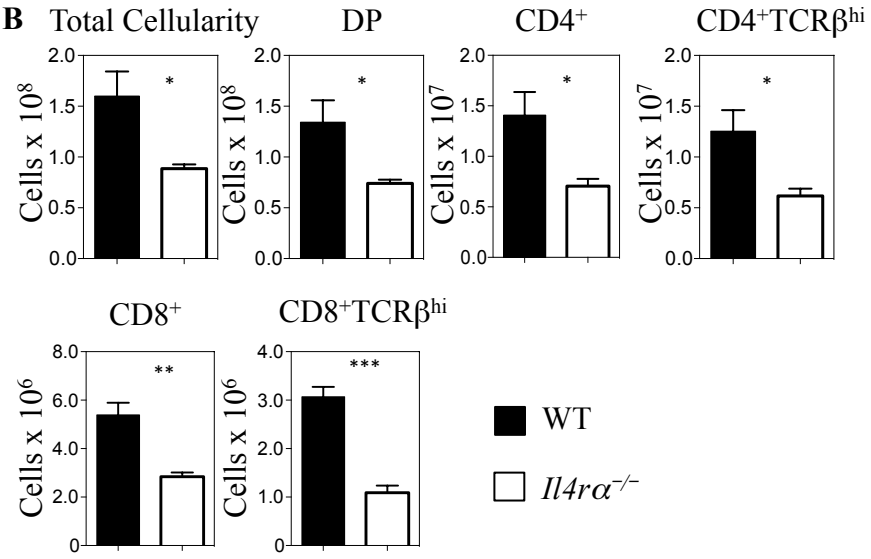
B
Total Cellularity
DP
CD4+
CD4+TCRβhi
Cells x 10^8
Cells x 10^8
Cells x 10^7
Cells x 10^7
CD8+
CD8+TCRβhi
Cells x 10^6
Cells x 10^6
WT
Il4rα-/-

5.3 Discussion

5.3.1 Medullary Regulation of Thymic Eosinophils

The thymus is composed of many different types of accessory cells with distinct roles. Intrathymic dendritic cell subsets are associated with central tolerance induction whereas macrophages have been related to clearance of apoptotic cells and ILC3 cells have been suggested to support thymus regeneration (Gallegos and Bevan, 2004, Dudakov et al., 2012). However eosinophils have also been identified in the thymus and previously were suggested to aid in apoptotic cell clearance and possibly in negative selection (Guerri et al., 2013, Kim et al., 2010). In *Relb*$^{-/-}$ mice that fail to form an intact medulla, a loss of thymic eosinophils has been reported (Throsby et al., 2000). This suggests that thymic microenvironment and the medulla in particular directly regulates the intrathymic eosinophil pool. Similarly in *Tcrα*$^{-/-}$ mice, which also possess a disrupted medulla, we reported a corresponding loss of eosinophils. This therefore further suggests a requirement for the medulla in the support of eosinophils in the thymus. This could relate to the medulla being necessary for the production of eotaxin with reduced mTEC leading to a lower concentration of chemokine to recruit eosinophils, which would be interesting to determine (Matthews et al., 1998). Furthermore the lack of mTEC is likely to also prevent a typical 3D medullary structure being present, which may be necessary to support eosinophils in the thymus via survival factor provision.

Interestingly the reduced eosinophil population in the spleen of *Tcrα*$^{-/-}$ mice implies that there may also be involvement of single positive T-cells in eosinophil maintenance. It is known that IL-5 is necessary for eosinophil development and release from the bone marrow into the periphery, with a study indicating that eosinophil progenitors express IL-5Rα and proliferate following IL-5 exposure which increases circulating eosinophil numbers (Iwasaki et al.,

2005). Considering this, eosinophilia, in infected states such as helminth infections and asthma has also been linked to IL-5, with increased IL-5 seen in disease being associated with Th2 cells (Gause et al., 2003, Behm and Ovington, 2000, Tomaki et al., 2000). Indeed, T-cells are known to home to the bone marrow at naïve, effector or memory stages, allowing the presence of these cells in the bone marrow to potentially influence eosinophil development (Di Rosa and Pabst, 2005, Mazo et al., 2005). In addition, it has been shown that IFN-γ produced by Th1 cells homing to bone marrow during immune activation has the capacity to hinder eosinophil development (de Bruin et al., 2010). In turn this puts forward the possibility of Th2 cells being implicated in eosinophil development, potentially providing the reason behind reduced eosinophils in *Tcrα*$^{-/-}$ mice. This could be assessed by analysis of eosinophil generation in the bone marrow of *Tcrα*$^{-/-}$ mice, which so far has not been determined, but would conclude whether there was a requirement for single positive T-cells in eosinophil development. If this was not the case, it should be considered that T-cells may support tissue eosinophils by modulating the local stromal populations within the thymus and spleen which could be necessary to in turn recruit eosinophils.

The thymus appears to further modulate eosinophils not just in terms of absolute numbers but also their activation status. Indeed compared to peripheral counterparts, eosinophils in the thymus show evidence of upregulated activation, including increased Siglec-F and CD11b expression. Interestingly Siglec-F expression by eosinophils was shown in the small intestine to be important in preventing degranulation and increasing survival, as well as CD11b supporting increased cellular adhesions (Verjan Garcia et al., 2011, Griseri et al., 2015, Mahmudi-Azer et al., 2002). Therefore higher levels of Siglec-F expression by thymic eosinophils may prolong eosinophil survival. This functionally could promote enhanced

interactions of eosinophils with developing thymocytes, assisted by increased CD11b, to support negative selection and T-regulatory cell induction (Throsby et al., 2000, Guerri et al., 2013). Given the reduction in eosinophil activation seen in the thymus of *Tcrα*$^{-/-}$ mice, with almost total loss of Siglec-F^{+} cells; it further proposes a role for mTEC and possibly also single positive thymocytes in the regulation of this activation process. Therefore this suggests that not only is the presence of eosinophils in the thymus medullary dependent but also that the medulla regulates eosinophil activation status to support their thymic function.

5.3.2 Role of Eosinophils In Thymic Recovery Post Damage

Given the role of eosinophils that has been suggested in tissue regeneration post damage, initial exploration through a sub-lethal irradiation (SIR) model suggested that dblGATA mice, with an absence of eosinophils, suffer from an inability to fully regenerate the thymus (Goh et al., 2013, Heredia et al., 2013). Interestingly, initial development of the thymus can occur independently of eosinophils as correct development of both T-cell and TEC compartments is seen in dblGATA mice under steady state conditions. As a result, it appears that upon damage induction through SIR, an eosinophil dependent pathway becomes triggered that is necessary to support thymus recovery. However the mechanisms regulating this pathway for thymic regeneration have not been explored and require further characterisation.

Thymic eosinophils may be triggered to initiate thymus regeneration following damage through the release of the alarmin IL-33 from epithelial surfaces (Oboki et al., 2011). This is an axis that has been shown to be active in asthma models upon lung epithelial inflammation with IL-33 release activating eosinophils to produce factors such as IL-4 and IL-13 for their survival (Willebrand and Voehringer, 2016). However the implication of IL-33 in the process

of thymus regeneration needs to be determined and could be addressed by thymus analysis in IL-33 deficient mice following SIR to identify if these mice also failed to recover. This would support that this axis is both active and necessary in the regeneration of the thymus post damage and if results phenocopied dblGATA mice, it would suggest that this IL-33 pathway of recovery is eosinophil mediated.

Furthermore, for regeneration of the thymus to occur, it is dependent upon the interplay between thymocytes and TEC as the development of one compartment is dependent upon the other for complete thymus formation (Akiyama et al., 2008, Hikosaka et al., 2008, Irla et al., 2008). Eosinophil involvement in regeneration could therefore be either at the level of TEC or T-cells. At d4 the difference in cellularity between WT and dblGATA mice correlated to thymocyte deficiencies with TEC numbers being unaffected, emphasising that eosinophils may be involved in initially targeting thymocytes to regenerate the thymus. Eosinophils could orchestrate this by modulating the survival of thymocytes as damage induced a greater loss of the irradiation sensitive DP thymocytes in dblGATA mice compared to WT controls at d7 post SIR (Li et al., 2012). However, at the same time, $CD4^+$ and $CD8^+$ thymocytes were equivalently maintained in dblGATA mice to WT control mice. This finding is supported by a study on thymus regeneration following SIR that identified a population of intrathymic radioresistant stem cells that are maintained following damage (Zuniga-Pflucker and Kruisbeek, 1990). It can therefore be suggested that the single positive thymocyte populations at d7 post SIR may have developed from this stem cell population, which are unaffected by eosinophil absence. It would be interesting to determine if absence of these stem cells or an inability for them to proliferate, which is thought to be IL-2 mediated, prevents the persistence of these single positive thymocytes following SIR damage, thus supporting the

idea that $CD4^+$ and $CD8^+$ development occurs from these stem cells. This could be addressed by analysis of IL-2Rα deficient mice at the same timepoint post SIR.

However, it should not be discounted that eosinophils alternatively have the capacity to influence TEC after damage and via this axis thymocytes may in turn be regulated for recovery. This potential interaction could occur via production of IL-4 by eosinophils signalling on IL-4Rα expressed by TEC as it has been shown that TEC express IL-4Rα and possess the ability to respond to IL-4 and IL-13 (White et al., 2017). This axis has previously been linked to regeneration of alternative tissues post damage with production of IL-4 by eosinophils in liver damage inducing proliferation of IL-4Rα expressing hepatocytes through Forkhead box protein M1 (FoxM1) – a master regulator of hepatocyte proliferation (Goh et al., 2013) (Davoine and Lacy, 2014). Whether this regulator is induced in TEC following SIR in WT mice would also be of interest to determine, to correlate the potential for an active IL-4/IL-4Rα pathway with thymus regeneration. Considering this, alterations in TEC in *Il4ra*$^{-/-}$ mice following SIR were determined to assess if they mirrored trends in dblGATA mice, which would suggest that this was the mechanism of recovery used by eosinophils to regenerate TEC. To begin with, reduced TEC populations at d7 post SIR in the dblGATA mice failed to be phenocopied in *Il4ra*$^{-/-}$ mice, causing consideration that eosinophils potentially regulate regeneration of the thymus at earlier time points via non-TEC processes. This emphasises that eosinophils may have a role in early stages after thymus damage through the support of thymocyte development. In turn the failure of dblGATA mice to maintain T-cell development at d7 post SIR may prevent T-cells from being available in the thymus to sustain TEC populations, causing the reported reduction in TEC populations at later time points following damage.

Continuing to examine the role of eosinophils at later stages of thymus recovery suggested that they are still involved in this regeneration process as the thymus failed to recover back to that seen in WT mice. The lack of DP thymocytes in dblGATA mice at d7 post SIR was maintained with an inability to develop DP thymocytes at the later time point of d35. The sustained DP reduction emphasises that in the absence of eosinophils, there is a failure to fully recover the T-cell compartment and as a result single positive thymocytes were also reduced at d35 post SIR in dblGATA mice. Considering this, previous thymic analysis suggested that the thymus recruits a new wave of progenitors from the bone marrow which can repopulate the thymus by d28 (Zuniga-Pflucker and Kruisbeek, 1990). The failure of this process in dblGATA mice, with a clear inability to reconstitute the thymus at d35, suggests eosinophil involvement in a recruitment mechanism that supports T-cell progenitors in the thymus post damage. Therefore it would be interesting to determine directly with ETP analysis at this time point as well as the earlier d7 stage post SIR, if there is a failure of dblGATA mice to recover thymic reconstitution.

Failings in thymocyte progenitor recruitment could occur as eosinophils have been shown to produce factors such as Vascular Endothelial Growth Factor (VEGF) production, often reported to be produced by eosinophils in asthma patients (Nishigaki et al., 2003, Asai et al., 2003). This may be implicated in vascular restructuring that could be necessary for efficient entry of thymocyte progenitors. The ability of eosinophils to promote this vascular remodeling has previously been shown in tumour models with eosinophils altering the vasculature to allow CD8 T-cell recruitment into tumours for destruction (Carretero et al., 2015). The ability of eosinophils to perform this process in tumours was correlated to their

activated phenotype which, relating back to initial finding of eosinophils in the thymus being more activated, supports this hypothesis as an idea to pursue in future work.

Despite this, at d35 post SIR, dblGATA mice also failed to support TEC recovery. At this point, whether the TEC reduction is due to the interplay between T-cell and TEC populations for their reciprocal development is difficult to determine, as both remain reduced. Analysis of TEC populations in *Il4ra*$^{-/-}$ mice at d35 for comparison to dblGATA mice would help to determine if eosinophils are acting on the TEC compartment at this late stage of recovery. However, we have so far established that at d35 post SIR, thymocytes are reduced in *Il4ra*$^{-/-}$ mice in addition to reductions in the eomesodermal IL-4Rα dependent CD8^{+} T-cells (Jameson et al., 2015). The lack of a requirement for IL-4Rα signals in either CD4^{+} T-cell development or the recruitment of thymocyte progenitors, along with the observation that both of these populations are reduced in *Il4ra*$^{-/-}$ mice at d35 post SIR, proposes the requirement for indirect IL-4Rα signalling in the maintenance of these T-cell populations.

Collectively this suggests that the reduction in TEC seen in dblGATA mice at d35, may be due to eosinophils being necessary later in thymic recovery to target TEC directly via the IL-4/IL-4Rα axis for regeneration. Confirmation of this hypothesis through IL-4Rα TEC analysis at d35 post SIR would be important to complete. This eosinophil dependent TEC regeneration is likely in turn to be necessary to also influence sustained recruitment of thymocyte progenitors to support T-cell development. Faults in this process, which may occur in dblGATA mice, could lead to limited production of CCL19/CCL21 and CCL25 by thymic stroma, and an inability to effectively attract CCR7^{+}/CCR9^{+} thymocyte precursor populations (Takahama, 2006, Zlotoff et al., 2010). Therefore it would be interesting to determine if

chemokine levels failed to increase in dblGATA mice following SIR compared to WT controls as TEC failed to recover at later stages.

As a result, it is clear that eosinophils are implicated in thymic recovery. However more research is necessary to define the mechanism that thymic eosinophils are employing to support thymic regeneration. From this preliminary work it may suggest that in initial thymic recovery, eosinophils support regeneration via thymocyte modulation. Furthermore, these reduced thymocyte populations in turn may drive the consequential decreases in TEC populations at early stages of thymus recovery. Under the presence of eosinophils in WT mice, this pathway is likely to support recovery of the thymus with T-cell progenitor recruitment and T-cell development assisting TEC regeneration to reciprocally enhance thymus regeneration. However through TEC analysis of dblGATA mice and *Il4rα*$^{-/-}$ mice, it revealed that eosinophils potentially have additional mechanisms in place, signalling through the IL-4/IL-4Rα axis at later time points on TEC to ensure complete thymus recovery post SIR. As a result, this late stage TEC mediated regeneration may be a contingency recovery mechanism utilised by eosinophils if there is a failure to promote thymus recovery, possibly initially via the regulation of T-cell precursor recruitment for the process of T-cell development. However, going forward it will be important to address the relation of this finding to the most recent thymic regeneration proposal. This study found thymus damage triggered ablation of $CD4^{+}CD8^{+}$ thymocytes, activated thymic DCs to produce IL-23, which then caused LTis to produce IL-22 for thymic microenvironment and thymopoiesis regeneration. The implication of eosinophils in this axis or further if eosinophils act independently of this recognised process is somewhat unknown and requires consideration in future work.

CHAPTER SIX:

GENERAL DISCUSSION

6.1 Limitations Of Cre Mouse Models For Cell Type Specific Deletion Of LTβR

A major aim of this thesis was to examine the role of LTβR in thymus biology and to establish mouse knockout models where LTβR is deleted from specific cell types. Initially there was the generation of the $Ltbr^{TEC}$ mice whereby LTβR was exclusively deleted from the TEC population that express the transcription factor FoxN1 through the crossing of $Foxn1^{Cre}$ and $Ltbr^{fl/fl}$ mice. Given the success of the $Ltbr^{TEC}$ mice with complete deletion of LTβR from TEC populations, this system was employed in later experiments to try to delete LTβR from thymic mesenchyme and endothelial cells. However this was met with limited success. From this, two attempts were made to delete LTβR from thymic mesenchyme ($PDGFR\beta^{Cre}xLtbr^{fl/fl}$ and $Wnt1^{Cre}xLtbr^{fl/fl}$) and endothelium ($Tie2^{Cre}xLtbr^{fl/fl}$ and $Flk1^{Cre}xLtbr^{fl/fl}$). Only the $Flk1^{Cre}Ltbr^{fl/fl}$ mice targeting endothelium saw complete LTβR deletion and the $Wnt1^{Cre}xLtbr^{fl/fl}$ was partially successful in the deletion capability. The reasoning behind this varied deletion has been more difficult to determine, but it has highlighted that the use of Cre/flox models needs to be approached with caution especially if the correct checks for functionality of the models are not put in place.

Indeed it is apparent that limitations of incomplete deletion that we faced related to the effectiveness of the Cre mice between the strains being generated, as the same $Ltbr^{fl/fl}$ mice were continuously used in all generations. Issues have been raised concerning the use of Cre recombinase for functional analysis in mice with it previously being reported that there can be unreliable localisation of Cre in cells causing defective deletion (Jeannotte et al., 2011). Considering this, the fidelity of the Cre expression is often assessed by the use of reporter mice with reporter expression indicating successful Cre action. However the literature has previously highlighted that this system does not necessarily relate to the level of

recombination that will be seen in all experimental mice (Schmidt-Supprian and Rajewsky, 2007, Srinivas et al., 2001). This may lead to incorrect mapping of effective deletion of Cre target genes in mouse models, which we also found to be true in additional analysis that we carried out. For this, we crossed all of the Cre only mice to mTmG reporters whereby successful recombination of the Cre with the mTmG caused the cells to change colour from tomato to green which then allowed recombination to be determined by basic flow cytometry. For this, for example, we found that there was successful fate mapping of the *Foxn1*^{Cre}*xmTmG* mice with TEC changing to green only and this Cre action was mirrored with TEC specific LTβR deletion in the *Ltbr*^{TEC} mice. Analysis of the *Tie2*^{Cre}*xmTmG* mice also showed that the Cre action was specific with complete conversion of endothelium (data not shown), yet when *Tie2*^{Cre}*xLtbr*$^{fl/fl}$ mice were analysed for LTβR deletion this was incomplete. As a result, this highlights that results gained from reporter models may not directly correspond to Cre activity in other crosses – leaving further analysis of successful deletion necessary. In addition, issues have been reported with Cre models concerning the activity of Cre recombinase as the introduction of Cre into cells is thought to potentially lead to a detrimental effect on cell viability through Cre-mediated cell toxicity (Carow et al., 2016). But, despite this, reduced thymus cellularities in Cre only mice were not found in our study, with comparability between Cre only controls and WT mice seen in different analyses. Furthermore to consider the possibility of detrimental Cre exposure, in our analysis we used heterozygous Cre only mice as controls for comparisons. Therefore, any alterations that we saw in the Cre/flox system directly correlated to LTβR deletion rather than overt Cre activity.

From this, the main issue and failure of our Cre/flox mice concerned the levels of deletion of LTβR from target cells, rather than any adverse disruption on aspects such as cellularities.

Therefore this ineffective deletion likely relates to the ability of the Cre mice that we selected to undergo successful and complete Cre recombinase activity when crossed with target *Ltbr*$^{fl/fl}$ mice, which was variable in our hands. Therefore a note of caution needs to be employed when using these models or there may be misinterpretation of results if the efficiency of the Cre and the deletion that entails are not checked. Nevertheless, by carefully monitoring and choosing appropriate Cre models, this allowed us to determine that pre-cDC1 recruitment is regulated by LTβR signalling on mesenchymal cells, and further that endothelial mediated LTβR signals may dictate pDC regulation.

6.2 The Balance Between DC and mTEC For Central Tolerance Induction

The main importance of mTEC in T-cell development has been attributed to their involvement in the process of central tolerance induction. mTEC have the capacity to present self-antigens that are essential to support screening of the TCR repertoire on developing thymocytes for correct negative selection (Klein et al., 2009, Klein et al., 2011). This process is supported by DC subsets that can cross present self-antigens from mTEC to increase antigen frequency in the thymus as well as antigen repertoire (Bonasio et al., 2006, Proietto et al., 2008a). As a result, there is strong cooperation between these two compartments for the induction of negative selection and prevention of autoimmunity.

Our studies indicate that the thymus contains various mechanisms to protect its primary role of central tolerance induction, as disorganisation of the medulla in *Ltbr*^{TEC} mice does not alter negative selection. This finding shows that the mTEC compartment can infact compensate for itself with substantial reductions, as seen in our findings with *Ltbr*^{TEC} mice, still allowing for sufficient provision of self-antigens to support Treg induction and efficient negative selection.

This finding alone highlights that due to mTEC being the main compartment necessary for central tolerance, it contains its own buffer that supports its full functioning even under conditions of substantial population loss. Furthermore, the sustained presence of DC populations in these mice allows for sustained negative selection as determined through comparisons between *Ltbr*^{TEC} and *Ltbr*$^{-/-}$ mice. This is maintained in *Ltbr*^{TEC} mice, as sufficient mTEC must remain for the provision of enough TRAs for DC to increase antigen frequency by cross-presentation and enable efficient negative selection. This threshold level of mTEC is important as models that completely lack an intact medulla suffer from autoimmunity due to an inability to provide sufficient TRAs for selection (Weih et al., 1995, Riemann et al., 2017, Wu et al., 1998). mTEC are further necessary to regulate DC themselves, with our work suggesting that DC require some level of mTEC as they are producers of CCL21. This is necessary as through comparison of *plt/plt*, *Ccl19*$^{-/-}$ and *Ccl21*$^{-/-}$ mice, we have shown that CCL21 is indeed required for pre-cDC recruitment, potentially via a mesenchymal intermediate, for cDC1 generation and autoimmunity prevention.

Considering that autoimmunity is prevented in mice with disrupted medullas due to DC presence, it would therefore be interesting to determine what level the DC compartment alone can be reduced before central tolerance is disrupted. This may reveal if thymic DC can similarly be compensated for by an intact medulla and normal numbers of mTEC. This would allow the baseline level of each compartment that is necessary for central tolerance induction to be suggested. Nonetheless, the ability for the DC compartment to compensate for reductions in mTEC in *Ltbr*^{TEC} mice along with the ability for the medulla itself to maintain sufficient provision of TRAs despite population alterations has likely developed as a back-up mechanism to preserve central tolerance.

As a result, the ability for the thymus to function when there are architectural and numerical disruptions brings in to question why the medullary compartment is otherwise maintained at such a large size in comparison to what is necessary for its primary role in tolerance. The size of the medulla could alternatively relate to roles such as those of γδ and NK T-cell development and the requirement for post-selection maturation of developing T-cells (Webb et al., 2016, Xing et al., 2013).

Furthermore, considering the ability of the medulla to function effectively under architectural disruption, a recent publication utilising *Ccl21a*$^{-/-}$ mice suggested that the autoimmune phenotype present in *Ccl21a*$^{-/-}$ mice correlated to a defective ability of single positive thymocytes to enter into the medullary areas, which are further disrupted in these mice (Kozai et al., 2017). However, any potential contribution of altered mTEC populations to the defective negative selection reported in the *Ccl21a*$^{-/-}$ mice is unknown as apart from architectural analysis, mTEC population quantitation was not conducted in this study. As a result, we would put forward an alternative interpretation that although this study clearly highlights through immunofluorescence that there is an alteration in single positive thymocytes in the medullas of *Ccl21a*$^{-/-}$ mice compared to controls, we clearly found DC to also be affected– an aspect that they have not considered. Therefore we would suggest from this that the autoimmunity seen in the *Ccl21a*$^{-/-}$ mice does not solely correspond to architectural disruption of the medullary areas as *Ltbr*^{TEC} mice have disrupted medullary architecture, reduced CCL21 expressing mTEC^{lo} cells but maintain tolerance as DC populations are conserved. Infact, we would suggest that the breakdown in tolerance in *Ccl21a*$^{-/-}$ mice more likely links to the reduced numbers of thymocytes in the medullary areas being unable to undergo correct negative selection due to defective DC populations.

Furthermore the reduced DC populations may hinder any cortical level of negative selection irrespective of medullary disruption; resulting in autoimmunity. As a result, the concept that an altered medulla does not directly correlate with a break in central tolerance is a novel finding that may cause previous medullary centric conclusions to be reassessed, with a new focus on accessory cell involvement over and above any medullary disorganisation previously attributed to tolerance breakdowns.

6.3 Regeneration Strategies For Thymus Recovery

One of the main findings from this study highlights the ability for the thymus to function although the architecture has become altered. Furthermore, if the medulla is not required to be fully formed to support the induction of central tolerance then it begins to bring in to question the current approaches used in thymus regeneration. Following damage or to reverse thymic involution that occurs with age, the research focus appears to be on regenerating or adjusting the TEC compartment for enhanced thymopoiesis (Velardi et al., 2014, Min et al., 2007). A previous study infact showed that forced expression of the transcription factor Foxn1 in the TEC population supported thymus regeneration (Bredenkamp et al., 2014). Furthermore other studies have focused on the administration of substances to promote thymus regeneration by triggering TEC populations to undergo proliferation. For example, it was noted that KGF deficient mice failed to recover post damage compared to WT control mice and therefore KGF administration was used to target TEC to enhance their proliferation and has since been used in trials to promote thymus function following damage (Erickson et al., 2002, Alpdogan et al., 2006).

Such mechanisms that focus on TEC regeneration are important, as it is vital that TEC undergo regeneration to provide an adequate compartment to support thymus functioning. However the amount of regeneration that is necessary is questioned given our findings. Therefore a reduction in thymus function in states of damage or involution may not solely relate to altered TEC compartments, but rather other regulators such as DC should be studied as we found that tolerance was only affected when DC were additionally reduced along with defective TEC populations. Furthermore, future treatments to support regeneration of the thymus following age related involution must consider additional factors as previously it has been suggested that the shrinking of the thymus with age is due to smaller numbers of thymic progenitors proliferating in the bone marrow, leading to fewer progenitors being available to enter into the thymus and give rise to T-cells (Offner et al., 1999, Min et al., 2006). Therefore, increases in thymus size without a concordant increase in thymus settling progenitors may lead to situations such as a leukaemia whereby the availability of fewer progenitors causes those progenitors to proliferate in the many niches of the large regenerating thymus (Boehm and Swann, 2013). As a result, focusing on recovering thymus function without trying to expand thymus size too much may help to prevent the detrimental side effects of large empty thymic niches. Therefore this raises the option for thymic DC to be enhanced to regenerate thymus function.

As a result, once there is establishment of a thymic core structure which may require previously established treatments, the maintenance of DC may suffice to regenerate the necessary level of thymus function. Having uncovered that LTβR signalling in thymic mesenchyme is important for recruitment of pre-cDC to the thymus and that CCR7 ligands are implicated in this process, these could provide options that may enhance thymic DC and

in turn support smaller TEC numbers for the maintenance of thymic function. Furthermore, as DC can be generated in vitro, there is scope for the potential transfer of DC into hosts suffering from thymic damage or malfunction to possibly enhance thymic function (Guo et al., 2016). However guaranteeing transferred DC homed correctly to the thymus may be difficult to regulate. Nevertheless, this provides an alternative angle on the process of thymus regeneration with the thought as to whether it is actually essential for the thymus to be fully maintained with regards to TEC compartment size to be able to carry out its function in central tolerance induction and T-cell generation.

6.3.1 Eosinophil-Mediated Thymus Regeneration

Given the role for thymic DC in the support of central tolerance and the potential for DC mediated therapy to aid the restoration of thymus function following damage, alternative mechanisms that support initial regeneration of the physical structure of the thymus still requires greater insight. Our finding that the absence of thymic eosinophils causes the thymus to be hindered in its ability to recover following damage induction via sub-lethal irradiation, suggests a role in thymus regeneration. The preliminary nature of this finding leaves many unanswered questions, primarily concerning the mechanism by which eosinophils are able to mediate thymus regeneration. Given previous research indicating the potential role of ILC3 in thymus regeneration, along with the recent study showing a new pathway via IL-22 and ILC3 activation for thymic regeneration, the possible involvement of eosinophils in this process would be interesting to dissect (Rossi et al., 2007, Dudakov et al., 2012, Lopes et al., 2017). This may be possible as it was found in the small intestine that eosinophils were necessary to support the maintenance of ILC3 through their production of IL-1β with eosinophil deficient mice having reduced Rorγt expressing ILC3 cells, and this was similarly seen in IL-1β

deficient mice (Jung et al., 2015). Therefore it may be possible that in the thymus, eosinophils support the ILC3 populations already implicated in thymus recovery. Relevant to this, it is unknown whether IL-33 is produced by TEC after thymus damage to stimulate other ILC populations, which itself may provide alternative links to eosinophils and thymus regeneration. ILC2 have infact been associated with eosinophils through their ability to produce high levels of IL-5 and IL-13, with IL-5 stimulating eotaxin production (Nussbaum et al., 2013). Eotaxin is linked to attraction and recruitment of eosinophils while IL-5 and IL-13 are also associated with the production and activation of eosinophils themselves, which may induce them to generate molecules that are necessary for thymus recovery (Rothenberg and Hogan, 2006, Matthews et al., 1998). However eosinophils migrate into the thymus from the bone marrow and whether their role in thymus regeneration correlates with a radioresistant subset in the thymus, or involves eosinophils migrating into the thymus from the periphery is unknown. Therefore greater understanding of how eosinophils may regulate thymus recovery post damage could be used in turn to implement either eosinophils themselves or the factors that they produce as some form of therapy option, regenerating the thymus size.

For all methods so far utilised as a therapy for the regeneration of the thymus size, none yet provide long term protection as withdrawal of treatment leads to regression. It would be ideal to provide a mechanism that following administration appears to kick start the thymus to regenerate itself. The transfer of eosinophils or eosinophil products may trigger TEC to proliferate and obtain a sufficient TEC compartment to support T-cell development again without further treatment being required. This may be possible, as so far our studies have demonstrated that in the steady state, mice that lack eosinophils are able to still maintain the thymus in a manner that is comparable to WT mice. Further it suggests their role in thymus

may simply be in the restarting of the regeneration process to trigger the thymus to maintain itself. Therefore following greater research into eosinophil mechanisms in the regeneration process of the thymus, it would be interesting to determine if this would be transferable to human models in trials for thymus damage and recovery. Furthermore, the possible implication of eosinophils in age-related involution is unknown but again would provide an interesting route to pursue in future work in the hope of uncovering mechanisms to support therapeutics in the future.

6.4 Concluding remarks

Through this thesis we have been able to dissect the regulation of the mTEC compartment from that of thymic DC, conflicting with previous assumptions and concluding that regulation of the medulla is distinct from that of thymic DC. *Ltbr*$^{-/-}$ mice suffer from autoimmunity with the cause of this being independent of medullary disorganisation and instead correlating to alterations in DC populations. This maps specifically to mesenchymal LTβR signalling for recruitment of pre-cDC for cDC1 generation. LTβR signalling in endothelial cells influences pDC migration to the thymus potentially through control of adhesion molecules. In addition pre-cDC require cell-intrinsic CCR7 signalling for cDC1 persistence in the thymus, in turn mapping directly to CCL21. This puts forward the possibility for this CCR7 mediated cDC1 regulation to converge with the alternative LTβR mechanism as LTβR signals on TEC infact control production of CCL21. This leads us to suggest that CCL21 produced by TEC is presented by mesenchyme through an LTβR mediated process to regulate pre-cDC migration into the thymus for cDC1 development. Knowledge of the maintenance of this population and its importance in regulating central tolerance may support future work focusing on sustaining thymus function and regulating autoimmune development.

In addition alternative preliminary work suggests that thymic eosinophils may potentially influence thymic recovery due to the absence of eosinophils in mouse models leading to an impaired ability for the thymus to recover. Mechanisms involved in this process have been more difficult to uncover but may relate to the ability of eosinophils to potentially influence TEC through the IL-4Rα axis and also possibly through their production of factors that may alter thymic vasculature to promote thymocyte precursor recruitment. This is the main aspect from this thesis that will be followed up in future work due to the prospect of it revealing important mechanisms therapeutically.

Papers currently published during this thesis:

Lymphotoxin β Receptor Controls T Cell Progenitor Entry to the Thymus.
Lucas B, James KD, **Cosway EJ**, Parnell SM, Tumanov AV, Ware CF, Jenkinson WE, Anderson G.
J Immunol. 2016 Oct 1;197(7):2665-72.

Control of the thymic medulla and its influence on αβT-cell development.
Lucas B, McCarthy NI, Baik S, **Cosway E**, James KD, Parnell SM, White AJ, Jenkinson WE, Anderson G.
Immunol Rev. 2016 May;271(1):23-37.

The thymus and rheumatology: should we care?
Cosway E, Anderson G, Garside P, Prendergast C.
Curr Opin Rheumatol. 2016 Mar;28(2):189-95.

Recently accepted:

Redefining Thymus Medulla Specialisation For Central Tolerance
Cosway EJ, Lucas B, James KD, Parnell SM, Carvalho-Gaspar M, White AJ, Tumanov AV, Jenkinson WE, Anderson G.
J Exp Med Brief Definitive Reports. Accepted 01.08.17.

REFERENCES:

ABRAMSON, J. & ANDERSON, G. 2017. Thymic Epithelial Cells. *Annu Rev Immunol*.
AKASHI, K., TRAVER, D., MIYAMOTO, T. & WEISSMAN, I. L. 2000. A clonogenic common myeloid progenitor that gives rise to all myeloid lineages. *Nature,* 404**,** 193-7.
AKIRA, S. & TAKEDA, K. 2004. Toll-like receptor signalling. *Nat Rev Immunol,* 4**,** 499-511.
AKIYAMA, N., TAKIZAWA, N., MIYAUCHI, M., YANAI, H., TATEISHI, R., SHINZAWA, M., YOSHINAGA, R., KURIHARA, M., DEMIZU, Y., YASUDA, H., YAGI, S., WU, G., MATSUMOTO, M., SAKAMOTO, R., YOSHIDA, N., PENNINGER, J. M., KOBAYASHI, Y., INOUE, J. & AKIYAMA, T. 2016. Identification of embryonic precursor cells that differentiate into thymic epithelial cells expressing autoimmune regulator. *J Exp Med,* 213**,** 1441-58.
AKIYAMA, T., SHIMO, Y., YANAI, H., QIN, J., OHSHIMA, D., MARUYAMA, Y., ASAUMI, Y., KITAZAWA, J., TAKAYANAGI, H., PENNINGER, J. M., MATSUMOTO, M., NITTA, T., TAKAHAMA, Y. & INOUE, J. 2008. The tumor necrosis factor family receptors RANK and CD40 cooperatively establish the thymic medullary microenvironment and self-tolerance. *Immunity,* 29**,** 423-37.
ALFONSO, C., MCHEYZER-WILLIAMS, M. G. & ROSEN, H. 2006. CD69 down-modulation and inhibition of thymic egress by short- and long-term selective chemical agonism of sphingosine 1-phosphate receptors. *Eur J Immunol,* 36**,** 149-59.
ALIAHMAD, P. & KAYE, J. 2008. Development of all CD4 T lineages requires nuclear factor TOX. *J Exp Med,* 205**,** 245-56.
ALLEN, J. E. & WYNN, T. A. 2011. Evolution of Th2 immunity: a rapid repair response to tissue destructive pathogens. *PLoS Pathog,* 7**,** e1002003.
ALLENDE, M. L., DREIER, J. L., MANDALA, S. & PROIA, R. L. 2004. Expression of the sphingosine 1-phosphate receptor, S1P1, on T-cells controls thymic emigration. *J Biol Chem,* 279**,** 15396-401.
ALLISON, J. P. & HAVRAN, W. L. 1991. The immunobiology of T cells with invariant gamma delta antigen receptors. *Annu Rev Immunol,* 9**,** 679-705.
ALLMAN, D., SAMBANDAM, A., KIM, S., MILLER, J. P., PAGAN, A., WELL, D., MERAZ, A. & BHANDOOLA, A. 2003. Thymopoiesis independent of common lymphoid progenitors. *Nat Immunol,* 4**,** 168-74.
ALPDOGAN, O., HUBBARD, V. M., SMITH, O. M., PATEL, N., LU, S., GOLDBERG, G. L., GRAY, D. H., FEINMAN, J., KOCHMAN, A. A., ENG, J. M., SUH, D., MURIGLAN, S. J., BOYD, R. L. & VAN DEN BRINK, M. R. 2006. Keratinocyte growth factor (KGF) is required for postnatal thymic regeneration. *Blood,* 107**,** 2453-60.
ALUGUPALLI, K. R., LEONG, J. M., WOODLAND, R. T., MURAMATSU, M., HONJO, T. & GERSTEIN, R. M. 2004. B1b lymphocytes confer T cell-independent long-lasting immunity. *Immunity,* 21**,** 379-90.
ALVAREZ, D., VOLLMANN, E. H. & VON ANDRIAN, U. H. 2008. Mechanisms and Consequences of Dendritic Cell Migration. *Immunity,* 29**,** 325.
ALVES, N. L., TAKAHAMA, Y., OHIGASHI, I., RIBEIRO, A. R., BAIK, S., ANDERSON, G. & JENKINSON, W. E. 2014. Serial progression of cortical and medullary thymic epithelial microenvironments. *Eur J Immunol,* 44**,** 16-22.
ANDERSON, M. S., VENANZI, E. S., KLEIN, L., CHEN, Z., BERZINS, S. P., TURLEY, S. J., VON BOEHMER, H., BRONSON, R., DIERICH, A., BENOIST, C. & MATHIS, D. 2002. Projection of an immunological self shadow within the thymus by the aire protein. *Science,* 298**,** 1395-401.
APPELBERG, R. 2007. Neutrophils and intracellular pathogens: beyond phagocytosis and killing. *Trends Microbiol,* 15**,** 87-92.
ARDAVIN, C., WU, L., LI, C. L. & SHORTMAN, K. 1993. Thymic dendritic cells and T cells develop simultaneously in the thymus from a common precursor population. *Nature,* 362**,** 761-3.
ARNETT, K. L., HARRISON, S. C. & WILEY, D. C. 2004. Crystal structure of a human CD3-epsilon/delta dimer in complex with a UCHT1 single-chain antibody fragment. *Proc Natl Acad Sci U S A,* 101**,** 16268-73.
ASAI, K., KANAZAWA, H., KAMOI, H., SHIRAISHI, S., HIRATA, K. & YOSHIKAWA, J. 2003. Increased levels of vascular endothelial growth factor in induced sputum in asthmatic patients. *Clin Exp Allergy,* 33**,** 595-9.
ATIBALENTJA, D. F., BYERSDORFER, C. A. & UNANUE, E. R. 2009. Thymus-blood protein interactions are highly effective in negative selection and regulatory T cell induction. *J Immunol,* 183**,** 7909-18.
ATIBALENTJA, D. F., MURPHY, K. M. & UNANUE, E. R. 2011. Functional redundancy between thymic CD8alpha+ and Sirpalpha+ conventional dendritic cells in presentation of blood-derived lysozyme by MHC class II proteins. *J Immunol,* 186**,** 1421-31.

AU-YEUNG, B. B., DEINDL, S., HSU, L. Y., PALACIOS, E. H., LEVIN, S. E., KURIYAN, J. & WEISS, A. 2009. The structure, regulation, and function of ZAP-70. *Immunol Rev,* 228**,** 41-57.
AW, D., SILVA, A. B. & PALMER, D. B. 2007. Immunosenescence: emerging challenges for an ageing population. *Immunology,* 120**,** 435-46.
BABA, T., NAKAMOTO, Y. & MUKAIDA, N. 2009. Crucial contribution of thymic Sirp alpha+ conventional dendritic cells to central tolerance against blood-borne antigens in a CCR2-dependent manner. *J Immunol,* 183**,** 3053-63.
BAIK, S., JENKINSON, E. J., LANE, P. J., ANDERSON, G. & JENKINSON, W. E. 2013. Generation of both cortical and Aire(+) medullary thymic epithelial compartments from CD205(+) progenitors. *Eur J Immunol,* 43**,** 589-94.
BAIK, S., SEKAI, M., HAMAZAKI, Y., JENKINSON, W. E. & ANDERSON, G. 2016. Relb acts downstream of medullary thymic epithelial stem cells and is essential for the emergence of RANK(+) medullary epithelial progenitors. *Eur J Immunol,* 46**,** 857-62.
BANNARD, O., KRAMAN, M. & FEARON, D. T. 2009. Secondary replicative function of CD8+ T cells that had developed an effector phenotype. *Science,* 323**,** 505-9.
BANSAL, K., YOSHIDA, H., BENOIST, C. & MATHIS, D. 2017. The transcriptional regulator Aire binds to and activates super-enhancers. *Nat Immunol,* 18**,** 263-273.
BARCLAY, A. N. & MAYRHOFER, G. 1981. Bone marrow origin of Ia-positive cells in the medulla rat thymus. *J Exp Med,* 153**,** 1666-71.
BARZAGHI, F., PASSERINI, L. & BACCHETTA, R. 2012. Immune dysregulation, polyendocrinopathy, enteropathy, x-linked syndrome: a paradigm of immunodeficiency with autoimmunity. *Front Immunol,* 3**,** 211.
BASSING, C. H., SWAT, W. & ALT, F. W. 2002. The mechanism and regulation of chromosomal V(D)J recombination. *Cell,* 109 Suppl**,** S45-55.
BEHM, C. A. & OVINGTON, K. S. 2000. The role of eosinophils in parasitic helminth infections: insights from genetically modified mice. *Parasitol Today,* 16**,** 202-9.
BENDELAC, A., MATZINGER, P., SEDER, R. A., PAUL, W. E. & SCHWARTZ, R. H. 1992. Activation events during thymic selection. *J Exp Med,* 175**,** 731-42.
BENZ, C., MARTINS, V. C., RADTKE, F. & BLEUL, C. C. 2008. The stream of precursors that colonizes the thymus proceeds selectively through the early T lineage precursor stage of T cell development. *J Exp Med,* 205**,** 1187-99.
BETTINI, M. L. & KERSH, G. J. 2007. MAP kinase phosphatase activity sets the threshold for thymocyte positive selection. *Proc Natl Acad Sci U S A*.
BEUTLER, B. A. 2009. TLRs and innate immunity. *Blood.* Washington, DC.
BHANDOOLA, A. & SAMBANDAM, A. 2006. From stem cell to T cell: one route or many? *Nat Rev Immunol,* 6**,** 117-26.
BIDULA, S. & SCHELENZ, S. 2016. A Sweet Response to a Sour Situation: The Role of Soluble Pattern Recognition Receptors in the Innate Immune Response to Invasive Aspergillus fumigatus Infections. *In:* HOGAN, D. A. (ed.) *PLoS Pathog.* San Francisco, CA USA.
BIRNBERG, T., BAR-ON, L., SAPOZNIKOV, A., CATON, M. L., CERVANTES-BARRAGAN, L., MAKIA, D., KRAUTHGAMER, R., BRENNER, O., LUDEWIG, B., BROCKSCHNIEDER, D., RIETHMACHER, D., REIZIS, B. & JUNG, S. 2008. Lack of conventional dendritic cells is compatible with normal development and T cell homeostasis, but causes myeloid proliferative syndrome. *Immunity,* 29**,** 986-97.
BLEUL, C. C. & BOEHM, T. 2000. Chemokines define distinct microenvironments in the developing thymus. *Eur J Immunol,* 30**,** 3371-9.
BLEUL, C. C., CORBEAUX, T., REUTER, A., FISCH, P., MONTING, J. S. & BOEHM, T. 2006. Formation of a functional thymus initiated by a postnatal epithelial progenitor cell. *Nature,* 441**,** 992-6.
BLUM, J. S., WEARSCH, P. A. & CRESSWELL, P. 2013. Pathways of antigen processing. *Annu Rev Immunol,* 31**,** 443-73.
BOEHM, T. 2008. Thymus development and function. *Curr Opin Immunol,* 20**,** 178-84.
BOEHM, T., SCHEU, S., PFEFFER, K. & BLEUL, C. C. 2003. Thymic medullary epithelial cell differentiation, thymocyte emigration, and the control of autoimmunity require lympho-epithelial cross talk via LTbetaR. *J Exp Med,* 198**,** 757-69.
BOEHM, T. & SWANN, J. B. 2013. Thymus involution and regeneration: two sides of the same coin? *Nat Rev Immunol,* 13**,** 831-8.
BOLOTIN, E., SMOGORZEWSKA, M., SMITH, S., WIDMER, M. & WEINBERG, K. 1996. Enhancement of thymopoiesis after bone marrow transplant by in vivo interleukin-7. *Blood,* 88**,** 1887-94.

BONASIO, R., SCIMONE, M. L., SCHAERLI, P., GRABIE, N., LICHTMAN, A. H. & VON ANDRIAN, U. H. 2006. Clonal deletion of thymocytes by circulating dendritic cells homing to the thymus. *Nat Immunol,* 7**,** 1092-100.

BOUILLET, P., PURTON, J. F., GODFREY, D. I., ZHANG, L. C., COULTAS, L., PUTHALAKATH, H., PELLEGRINI, M., CORY, S., ADAMS, J. M. & STRASSER, A. 2002. BH3-only Bcl-2 family member Bim is required for apoptosis of autoreactive thymocytes. *Nature,* 415**,** 922-6.

BOURSALIAN, T. E., GOLOB, J., SOPER, D. M., COOPER, C. J. & FINK, P. J. 2004. Continued maturation of thymic emigrants in the periphery. *Nat Immunol,* 5**,** 418-25.

BOUSSO, P., BHAKTA, N. R., LEWIS, R. S. & ROBEY, E. 2002. Dynamics of thymocyte-stromal cell interactions visualized by two-photon microscopy. *Science,* 296**,** 1876-80.

BREDENKAMP, N., NOWELL, C. S. & BLACKBURN, C. C. 2014. Regeneration of the aged thymus by a single transcription factor. *Development,* 141**,** 1627-37.

BRISENO, C. G., GARGARO, M., DURAI, V., DAVIDSON, J. T., THEISEN, D. J., ANDERSON, D. A., 3RD, NOVACK, D. V., MURPHY, T. L. & MURPHY, K. M. 2017. Deficiency of transcription factor RelB perturbs myeloid and DC development by hematopoietic-extrinsic mechanisms. *Proc Natl Acad Sci U S A,* 114**,** 3957-3962.

BRODIN, P. & DAVIS, M. M. 2017. Human immune system variation. *Nat Rev Immunol.* England.

BROWNLIE, R. J. & ZAMOYSKA, R. T cell receptor signalling networks: branched, diversified and bounded.

BRUBAKER, S. W., BONHAM, K. S., ZANONI, I. & KAGAN, J. C. 2015. Innate immune pattern recognition: a cell biological perspective. *Annu Rev Immunol,* 33**,** 257-90.

BRUGNERA, E., BHANDOOLA, A., CIBOTTI, R., YU, Q., GUINTER, T. I., YAMASHITA, Y., SHARROW, S. O. & SINGER, A. 2000. Coreceptor reversal in the thymus: signaled CD4+8+ thymocytes initially terminate CD8 transcription even when differentiating into CD8+ T cells. *Immunity,* 13**,** 59-71.

BRUNKOW, M. E., JEFFERY, E. W., HJERRILD, K. A., PAEPER, B., CLARK, L. B., YASAYKO, S. A., WILKINSON, J. E., GALAS, D., ZIEGLER, S. F. & RAMSDELL, F. 2001. Disruption of a new forkhead/winged-helix protein, scurfin, results in the fatal lymphoproliferative disorder of the scurfy mouse. *Nat Genet,* 27**,** 68-73.

BRYANT, P. & PLOEGH, H. 2004. Class II MHC peptide loading by the professionals. *Curr Opin Immunol,* 16**,** 96-102.

BURNET, F. 1959. Sir. Nashville, Vanderbilt University Press.

CALL, M. E., PYRDOL, J., WIEDMANN, M. & WUCHERPFENNIG, K. W. 2002. The organizing principle in the formation of the T cell receptor-CD3 complex. *Cell,* 111**,** 967-79.

CALL, M. E., SCHNELL, J. R., XU, C., LUTZ, R. A., CHOU, J. J. & WUCHERPFENNIG, K. W. 2006. The structure of the zetazeta transmembrane dimer reveals features essential for its assembly with the T cell receptor. *Cell,* 127**,** 355-68.

CAMOUS, L., ROUMENINA, L., BIGOT, S., BRACHEMI, S., FREMEAUX-BACCHI, V., LESAVRE, P. & HALBWACHS-MECARELLI, L. 2011. Complement alternative pathway acts as a positive feedback amplification of neutrophil activation. *Blood,* 117**,** 1340-9.

CAMPBELL, J. J., PAN, J. & BUTCHER, E. C. 1999. Cutting edge: developmental switches in chemokine responses during T cell maturation. *J Immunol,* 163**,** 2353-7.

CANTRELL, D. A. 2002. T-cell antigen receptor signal transduction. *Immunology,* 105**,** 369-74.

CAROW, B., GAO, Y., COQUET, J., REILLY, M. & ROTTENBERG, M. E. 2016. lck-Driven Cre Expression Alters T Cell Development in the Thymus and the Frequencies and Functions of Peripheral T Cell Subsets. *J Immunol,* 197**,** 2261-8.

CARRETERO, R., SEKTIOGLU, I. M., GARBI, N., SALGADO, O. C., BECKHOVE, P. & HAMMERLING, G. J. 2015. Eosinophils orchestrate cancer rejection by normalizing tumor vessels and enhancing infiltration of CD8(+) T cells. *Nat Immunol,* 16**,** 609-17.

CARROLL, M. C. 2004. The complement system in regulation of adaptive immunity. *Nat Immunol,* 5**,** 981-6.

CHAI, Q., ONDER, L., SCANDELLA, E., GIL-CRUZ, C., PEREZ-SHIBAYAMA, C., CUPOVIC, J., DANUSER, R., SPARWASSER, T., LUTHER, S. A., THIEL, V., RULICKE, T., STEIN, J. V., HEHLGANS, T. & LUDEWIG, B. 2013. Maturation of lymph node fibroblastic reticular cells from myofibroblastic precursors is critical for antiviral immunity. *Immunity,* 38**,** 1013-24.

CHAN, S. H., COSGROVE, D., WALTZINGER, C., BENOIST, C. & MATHIS, D. 1993. Another view of the selective model of thymocyte selection. *Cell,* 73**,** 225-36.

CHEN, W., JIN, W., HARDEGEN, N., LEI, K. J., LI, L., MARINOS, N., MCGRADY, G. & WAHL, S. M. 2003. Conversion of peripheral CD4+CD25- naive T cells to CD4+CD25+ regulatory T cells by TGF-beta induction of transcription factor Foxp3. *J Exp Med,* 198**,** 1875-86.

CHINO, T., DRAVES, K. E. & CLARK, E. A. 2009. Regulation of dendritic cell survival and cytokine production by osteoprotegerin. *J Leukoc Biol,* 86**,** 933-40.
CHU, Y. W., SCHMITZ, S., CHOUDHURY, B., TELFORD, W., KAPOOR, V., GARFIELD, S., HOWE, D. & GRESS, R. E. 2008. Exogenous insulin-like growth factor 1 enhances thymopoiesis predominantly through thymic epithelial cell expansion. *Blood,* 112**,** 2836-46.
CHUPRIN, A., AVIN, A., GOLDFARB, Y., HERZIG, Y., LEVI, B., JACOB, A., SELA, A., KATZ, S., GROSSMAN, M., GUYON, C., RATHAUS, M., COHEN, H. Y., SAGI, I., GIRAUD, M., MCBURNEY, M. W., HUSEBYE, E. S. & ABRAMSON, J. 2015. The deacetylase Sirt1 is an essential regulator of Aire-mediated induction of central immunological tolerance. *Nat Immunol,* 16**,** 737-45.
CIOFANI, M. & ZUNIGA-PFLUCKER, J. C. 2007. The thymus as an inductive site for T lymphopoiesis. *Annu Rev Cell Dev Biol,* 23**,** 463-93.
CORCORAN, L., FERRERO, I., VREMEC, D., LUCAS, K., WAITHMAN, J., O'KEEFFE, M., WU, L., WILSON, A. & SHORTMAN, K. 2003. The lymphoid past of mouse plasmacytoid cells and thymic dendritic cells. *J Immunol,* 170**,** 4926-32.
COWAN, J. E., MCCARTHY, N. I. & ANDERSON, G. 2016. CCR7 Controls Thymus Recirculation, but Not Production and Emigration, of Foxp3(+) T Cells. *Cell Rep,* 14**,** 1041-8.
COWAN, J. E., PARNELL, S. M., NAKAMURA, K., CAAMANO, J. H., LANE, P. J., JENKINSON, E. J., JENKINSON, W. E. & ANDERSON, G. 2013. The thymic medulla is required for Foxp3+ regulatory but not conventional CD4+ thymocyte development. *J Exp Med,* 210**,** 675-81.
CRESSWELL, P. 1996. Invariant chain structure and MHC class II function. *Cell,* 84**,** 505-7.
CYSTER, J. G. 2005. Chemokines, sphingosine-1-phosphate, and cell migration in secondary lymphoid organs. *Annu Rev Immunol,* 23**,** 127-59.
DAKIC, A., SHAO, Q. X., D'AMICO, A., O'KEEFFE, M., CHEN, W. F., SHORTMAN, K. & WU, L. 2004. Development of the dendritic cell system during mouse ontogeny. *J Immunol,* 172**,** 1018-27.
DANIELS, M. A., TEIXEIRO, E., GILL, J., HAUSMANN, B., ROUBATY, D., HOLMBERG, K., WERLEN, G., HOLLANDER, G. A., GASCOIGNE, N. R. & PALMER, E. 2006. Thymic selection threshold defined by compartmentalization of Ras/MAPK signalling. *Nature,* 444**,** 724-9.
DARRASSE-JEZE, G., DEROUBAIX, S., MOUQUET, H., VICTORA, G. D., EISENREICH, T., YAO, K. H., MASILAMANI, R. F., DUSTIN, M. L., RUDENSKY, A., LIU, K. & NUSSENZWEIG, M. C. 2009. Feedback control of regulatory T cell homeostasis by dendritic cells in vivo. *J Exp Med,* 206**,** 1853-62.
DAVIS, C. B., KILLEEN, N., CROOKS, M. E., RAULET, D. & LITTMAN, D. R. 1993. Evidence for a stochastic mechanism in the differentiation of mature subsets of T lymphocytes. *Cell,* 73**,** 237-47.
DAVOINE, F. & LACY, P. 2014. Eosinophil cytokines, chemokines, and growth factors: emerging roles in immunity. *Front Immunol,* 5**,** 570.
DE BRUIN, A. M., BUITENHUIS, M., VAN DER SLUIJS, K. F., VAN GISBERGEN, K. P., BOON, L. & NOLTE, M. A. 2010. Eosinophil differentiation in the bone marrow is inhibited by T cell-derived IFN-gamma. *Blood,* 116**,** 2559-69.
DE TREZ, C. 2012. Lymphotoxin-beta receptor expression and its related signaling pathways govern dendritic cell homeostasis and function. *Immunobiology,* 217**,** 1250-8.
DE TREZ, C., SCHNEIDER, K., POTTER, K., DROIN, N., FULTON, J., NORRIS, P. S., HA, S. W., FU, Y. X., MURPHY, T., MURPHY, K. M., PFEFFER, K., BENEDICT, C. A. & WARE, C. F. 2008. The inhibitory HVEM-BTLA pathway counter regulates lymphotoxin receptor signaling to achieve homeostasis of dendritic cells. *J Immunol,* 180**,** 238-48.
DEAGLIO, S., DWYER, K. M., GAO, W., FRIEDMAN, D., USHEVA, A., ERAT, A., CHEN, J. F., ENJYOJI, K., LINDEN, J., OUKKA, M., KUCHROO, V. K., STROM, T. B. & ROBSON, S. C. 2007. Adenosine generation catalyzed by CD39 and CD73 expressed on regulatory T cells mediates immune suppression. *J Exp Med,* 204**,** 1257-65.
DEINDL, S., KADLECEK, T. A., BRDICKA, T., CAO, X., WEISS, A. & KURIYAN, J. 2007. Structural basis for the inhibition of tyrosine kinase activity of ZAP-70. *Cell,* 129**,** 735-46.
DELVES, P. J. & ROITT, I. M. 2000. The immune system. First of two parts. *N Engl J Med,* 343**,** 37-49.
DENGJEL, J., SCHOOR, O., FISCHER, R., REICH, M., KRAUS, M., MULLER, M., KREYMBORG, K., ALTENBEREND, F., BRANDENBURG, J., KALBACHER, H., BROCK, R., DRIESSEN, C., RAMMENSEE, H. G. & STEVANOVIC, S. 2005. Autophagy promotes MHC class II presentation of peptides from intracellular source proteins. *Proc Natl Acad Sci U S A,* 102**,** 7922-7.
DESANTI, G. E., COWAN, J. E., BAIK, S., PARNELL, S. M., WHITE, A. J., PENNINGER, J. M., LANE, P. J., JENKINSON, E. J., JENKINSON, W. E. & ANDERSON, G. 2012. Developmentally regulated availability of RANKL and CD40 ligand reveals distinct mechanisms of fetal and adult cross-talk in the thymus medulla. *J Immunol,* 189**,** 5519-26.

DI ROSA, F. & PABST, R. 2005. The bone marrow: a nest for migratory memory T cells. *Trends Immunol,* 26**,** 360-6.
DI SANTO, J. P., RADTKE, F. & RODEWALD, H. R. 2000. To be or not to be a pro-T? *Curr Opin Immunol,* 12**,** 159-65.
DIELI, F., TROYE-BLOMBERG, M., IVANYI, J., FOURNIE, J. J., KRENSKY, A. M., BONNEVILLE, M., PEYRAT, M. A., CACCAMO, N., SIRECI, G. & SALERNO, A. 2001. Granulysin-dependent killing of intracellular and extracellular Mycobacterium tuberculosis by Vgamma9/Vdelta2 T lymphocytes. *J Infect Dis,* 184**,** 1082-5.
DONSKOY, E. & GOLDSCHNEIDER, I. 2003. Two developmentally distinct populations of dendritic cells inhabit the adult mouse thymus: demonstration by differential importation of hematogenous precursors under steady state conditions. *J Immunol,* 170**,** 3514-21.
DOOLEY, J., ERICKSON, M., LAROCHELLE, W. J., GILLARD, G. O. & FARR, A. G. 2007. FGFR2IIIb signaling regulates thymic epithelial differentiation. *Dev Dyn,* 236**,** 3459-71.
DUDAKOV, J. A., HANASH, A. M., JENQ, R. R., YOUNG, L. F., GHOSH, A., SINGER, N. V., WEST, M. L., SMITH, O. M., HOLLAND, A. M., TSAI, J. J., BOYD, R. L. & VAN DEN BRINK, M. R. 2012. Interleukin-22 drives endogenous thymic regeneration in mice. *Science,* 336**,** 91-5.
DUDAL, S., TURRIERE, C., BESSOLES, S., FONTES, P., SANCHEZ, F., LIAUTARD, J., LIAUTARD, J. P. & LAFONT, V. 2006. Release of LL-37 by activated human Vgamma9Vdelta2 T cells: a microbicidal weapon against Brucella suis. *J Immunol,* 177**,** 5533-9.
DUDLEY, E. C., PETRIE, H. T., SHAH, L. M., OWEN, M. J. & HAYDAY, A. C. 1994. T cell receptor beta chain gene rearrangement and selection during thymocyte development in adult mice. *Immunity,* 1**,** 83-93.
DURSUN, E., ENDELE, M., MUSUMECI, A., FAILMEZGER, H., WANG, S. H., TRESCH, A., SCHROEDER, T. & KRUG, A. B. 2016. Continuous single cell imaging reveals sequential steps of plasmacytoid dendritic cell development from common dendritic cell progenitors. *Sci Rep,* 6**,** 37462.
DZHAGALOV, I. & PHEE, H. 2012. How to find your way through the thymus: a practical guide for aspiring T cells. *Cell Mol Life Sci,* 69**,** 663-82.
DZHAGALOV, I. L., CHEN, K. G., HERZMARK, P. & ROBEY, E. A. 2013. Elimination of self-reactive T cells in the thymus: a timeline for negative selection. *PLoS Biol,* 11**,** e1001566.
EGERTON, M., SCOLLAY, R. & SHORTMAN, K. 1990. Kinetics of mature T-cell development in the thymus. *Proc Natl Acad Sci U S A,* 87**,** 2579-82.
ENDERS, A., BOUILLET, P., PUTHALAKATH, H., XU, Y., TARLINTON, D. M. & STRASSER, A. 2003. Loss of the pro-apoptotic BH3-only Bcl-2 family member Bim inhibits BCR stimulation-induced apoptosis and deletion of autoreactive B cells. *J Exp Med,* 198**,** 1119-26.
ERICKSON, M., MORKOWSKI, S., LEHAR, S., GILLARD, G., BEERS, C., DOOLEY, J., RUBIN, J. S., RUDENSKY, A. & FARR, A. G. 2002. Regulation of thymic epithelium by keratinocyte growth factor. *Blood,* 100**,** 3269-78.
FARLEY, A. M., MORRIS, L. X., VROEGINDEWEIJ, E., DEPRETER, M. L., VAIDYA, H., STENHOUSE, F. H., TOMLINSON, S. R., ANDERSON, R. A., CUPEDO, T., CORNELISSEN, J. J. & BLACKBURN, C. C. 2013. Dynamics of thymus organogenesis and colonization in early human development. *Development,* 140**,** 2015-26.
FOO, S. S., TURNER, C. J., ADAMS, S., COMPAGNI, A., AUBYN, D., KOGATA, N., LINDBLOM, P., SHANI, M., ZICHA, D. & ADAMS, R. H. 2006. Ephrin-B2 controls cell motility and adhesion during blood-vessel-wall assembly. *Cell,* 124**,** 161-73.
FOSTER, K., SHERIDAN, J., VEIGA-FERNANDES, H., RODERICK, K., PACHNIS, V., ADAMS, R., BLACKBURN, C., KIOUSSIS, D. & COLES, M. 2008. Contribution of neural crest-derived cells in the embryonic and adult thymus. *J Immunol.* United States.
FUERTBAUER, E., ZAUJEC, J., UHRIN, P., RAAB, I., WEBER, M., SCHACHNER, H., BAUER, M., SCHUTZ, G. J., BINDER, B. R., SIXT, M., KERJASCHKI, D. & STOCKINGER, H. 2013. Thymic medullar conduits-associated podoplanin promotes natural regulatory T cells. *Immunol Lett,* 154**,** 31-41.
FUJIMOTO, Y., TU, L., MILLER, A. S., BOCK, C., FUJIMOTO, M., DOYLE, C., STEEBER, D. A. & TEDDER, T. F. 2002. CD83 expression influences CD4+ T cell development in the thymus. *Cell,* 108**,** 755-67.
FUTTERER, A., MINK, K., LUZ, A., KOSCO-VILBOIS, M. H. & PFEFFER, K. 1998. The lymphotoxin beta receptor controls organogenesis and affinity maturation in peripheral lymphoid tissues. *Immunity,* 9**,** 59-70.
GALLEGOS, A. M. & BEVAN, M. J. 2004. Central tolerance to tissue-specific antigens mediated by direct and indirect antigen presentation. *J Exp Med.* United States.

GALLI, S. J., BORREGAARD, N. & WYNN, T. A. 2011. Phenotypic and functional plasticity of cells of innate immunity: macrophages, mast cells and neutrophils. *Nat Immunol,* 12**,** 1035-44.
GANGULY, D., HAAK, S., SISIRAK, V. & REIZIS, B. 2013. The role of dendritic cells in autoimmunity. *Nat Rev Immunol,* 13**,** 566-77.
GASTEIGER, G. & RUDENSKY, A. Y. 2014. Interactions between innate and adaptive lymphocytes. *Nat Rev Immunol.* England.
GAUSE, W. C., URBAN, J. F., JR. & STADECKER, M. J. 2003. The immune response to parasitic helminths: insights from murine models. *Trends Immunol,* 24**,** 269-77.
GEISSMANN, F., MANZ, M. G., JUNG, S., SIEWEKE, M. H., MERAD, M. & LEY, K. 2010. Development of monocytes, macrophages, and dendritic cells. *Science,* 327**,** 656-61.
GOH, Y. P., HENDERSON, N. C., HEREDIA, J. E., RED EAGLE, A., ODEGAARD, J. I., LEHWALD, N., NGUYEN, K. D., SHEPPARD, D., MUKUNDAN, L., LOCKSLEY, R. M. & CHAWLA, A. 2013. Eosinophils secrete IL-4 to facilitate liver regeneration. *Proc Natl Acad Sci U S A,* 110**,** 9914-9.
GOLDMAN, K. P., PARK, C. S., KIM, M., MATZINGER, P. & ANDERSON, C. C. 2005. Thymic cortical epithelium induces self tolerance. *Eur J Immunol,* 35**,** 709-17.
GOLDRATH, A. W. & BEVAN, M. J. 1999. Selecting and maintaining a diverse T-cell repertoire. *Nature,* 402**,** 255-62.
GOMMEAUX, J., GREGOIRE, C., NGUESSAN, P., RICHELME, M., MALISSEN, M., GUERDER, S., MALISSEN, B. & CARRIER, A. 2009. Thymus-specific serine protease regulates positive selection of a subset of CD4+ thymocytes. *Eur J Immunol,* 39**,** 956-64.
GOODNOW, C. C., SPRENT, J., DE ST GROTH, B. F. & VINUESA, C. G. 2005
Cellular and genetic mechanisms of self tolerance and autoimmunity. *Nature***,** 590-597.
GORDON, J. & MANLEY, N. R. 2011. Mechanisms of thymus organogenesis and morphogenesis. *Development,* 138**,** 3865-78.
GORDON, J., WILSON, V. A., BLAIR, N. F., SHERIDAN, J., FARLEY, A., WILSON, L., MANLEY, N. R. & BLACKBURN, C. C. 2004. Functional evidence for a single endodermal origin for the thymic epithelium. *Nat Immunol,* 5**,** 546-53.
GORDON, J., XIAO, S., HUGHES, B., 3RD, SU, D. M., NAVARRE, S. P., CONDIE, B. G. & MANLEY, N. R. 2007. Specific expression of lacZ and cre recombinase in fetal thymic epithelial cells by multiplex gene targeting at the Foxn1 locus. *BMC Dev Biol,* 7**,** 69.
GOSSENS, K., NAUS, S., CORBEL, S. Y., LIN, S., ROSSI, F. M., KAST, J. & ZILTENER, H. J. 2009. Thymic progenitor homing and lymphocyte homeostasis are linked via S1P-controlled expression of thymic P-selectin/CCL25. *J Exp Med,* 206**,** 761-78.
GRAY, D. H., KUPRESANIN, F., BERZINS, S. P., HEROLD, M. J., O'REILLY, L. A., BOUILLET, P. & STRASSER, A. 2012. The BH3-only proteins Bim and Puma cooperate to impose deletional tolerance of organ-specific antigens. *Immunity,* 37**,** 451-62.
GRISERI, T., ARNOLD, I. C., PEARSON, C., KRAUSGRUBER, T., SCHIERING, C., FRANCHINI, F., SCHULTHESS, J., MCKENZIE, B. S., CROCKER, P. R. & POWRIE, F. 2015. Granulocyte Macrophage Colony-Stimulating Factor-Activated Eosinophils Promote Interleukin-23 Driven Chronic Colitis. *Immunity,* 43**,** 187-99.
GRUETER, B., PETTER, M., EGAWA, T., LAULE-KILIAN, K., ALDRIAN, C. J., WUERCH, A., LUDWIG, Y., FUKUYAMA, H., WARDEMANN, H., WALDSCHUETZ, R., MOROY, T., TANIUCHI, I., STEIMLE, V., LITTMAN, D. R. & EHLERS, M. 2005. Runx3 regulates integrin alpha E/CD103 and CD4 expression during development of CD4-/CD8+ T cells. *J Immunol,* 175**,** 1694-705.
GUERRI, L., PEGUILLET, I., GERALDO, Y., NABTI, S., PREMEL, V. & LANTZ, O. 2013. Analysis of APC types involved in CD4 tolerance and regulatory T cell generation using reaggregated thymic organ cultures. *J Immunol,* 190**,** 2102-10.
GUO, X., ZHOU, Y., WU, T., ZHU, X., LAI, W. & WU, L. 2016. Generation of mouse and human dendritic cells in vitro. *J Immunol Methods,* 432**,** 24-9.
HAAS, W., PEREIRA, P. & TONEGAWA, S. 1993. Gamma/delta cells. *Annu Rev Immunol,* 11**,** 637-85.
HADEIBA, H., LAHL, K., EDALATI, A., ODERUP, C., HABTEZION, A., PACHYNSKI, R., NGUYEN, L., GHODSI, A., ADLER, S. & BUTCHER, E. C. 2012. Plasmacytoid dendritic cells transport peripheral antigens to the thymus to promote central tolerance. *Immunity,* 36**,** 438-50.
HAMAZAKI, Y. 2015. Adult thymic epithelial cell (TEC) progenitors and TEC stem cells: Models and mechanisms for TEC development and maintenance. *Eur J Immunol,* 45**,** 2985-93.
HAMAZAKI, Y., FUJITA, H., KOBAYASHI, T., CHOI, Y., SCOTT, H. S., MATSUMOTO, M. & MINATO, N. 2007. Medullary thymic epithelial cells expressing Aire represent a unique lineage derived from cells expressing claudin. *Nat Immunol,* 8**,** 304-11.

HANABUCHI, S., ITO, T., PARK, W. R., WATANABE, N., SHAW, J. L., ROMAN, E., ARIMA, K., WANG, Y. H., VOO, K. S., CAO, W. & LIU, Y. J. 2010. Thymic stromal lymphopoietin-activated plasmacytoid dendritic cells induce the generation of FOXP3+ regulatory T cells in human thymus. *J Immunol,* 184**,** 2999-3007.

HARE, K. J., JENKINSON, E. J. & ANDERSON, G. 2000. An essential role for the IL-7 receptor during intrathymic expansion of the positively selected neonatal T cell repertoire. *J Immunol,* 165**,** 2410-4.

HARRINGTON, L. E., HATTON, R. D., MANGAN, P. R., TURNER, H., MURPHY, T. L., MURPHY, K. M. & WEAVER, C. T. 2005. Interleukin 17-producing CD4+ effector T cells develop via a lineage distinct from the T helper type 1 and 2 lineages. *Nat Immunol,* 6**,** 1123-32.

HAYDAY, A. C. 2000. [gamma][delta] cells: a right time and a right place for a conserved third way of protection. *Annu Rev Immunol,* 18**,** 975-1026.

HE, X., DAVE, V. P., ZHANG, Y., HUA, X., NICOLAS, E., XU, W., ROE, B. A. & KAPPES, D. J. 2005. The zinc finger transcription factor Th-POK regulates CD4 versus CD8 T-cell lineage commitment. *Nature,* 433**,** 826-33.

HENDRIKS, R. W., NAWIJN, M. C., ENGEL, J. D., VAN DOORNINCK, H., GROSVELD, F. & KARIS, A. 1999. Expression of the transcription factor GATA-3 is required for the development of the earliest T cell progenitors and correlates with stages of cellular proliferation in the thymus. *Eur J Immunol,* 29**,** 1912-8.

HERBIN, O., BONITO, A. J., JEONG, S., WEINSTEIN, E. G., RAHMAN, A. H., XIONG, H., MERAD, M. & ALEXANDROPOULOS, K. 2016. Medullary thymic epithelial cells and CD8alpha+ dendritic cells coordinately regulate central tolerance but CD8alpha+ cells are dispensable for thymic regulatory T cell production. *J Autoimmun,* 75**,** 141-149.

HEREDIA, J. E., MUKUNDAN, L., CHEN, F. M., MUELLER, A. A., DEO, R. C., LOCKSLEY, R. M., RANDO, T. A. & CHAWLA, A. 2013. Type 2 innate signals stimulate fibro/adipogenic progenitors to facilitate muscle regeneration. *Cell,* 153**,** 376-88.

HERNANDEZ, J. B., NEWTON, R. H. & WALSH, C. M. 2010. Life and death in the thymus – cell death signaling during T cell development. *Curr Opin Cell Biol,* 22**,** 865-71.

HERNANDEZ-HOYOS, G., SOHN, S. J., ROTHENBERG, E. V. & ALBEROLA-ILA, J. 2000. Lck activity controls CD4/CD8 T cell lineage commitment. *Immunity,* 12**,** 313-22.

HIKOSAKA, Y., NITTA, T., OHIGASHI, I., YANO, K., ISHIMARU, N., HAYASHI, Y., MATSUMOTO, M., MATSUO, K., PENNINGER, J. M., TAKAYANAGI, H., YOKOTA, Y., YAMADA, H., YOSHIKAI, Y., INOUE, J., AKIYAMA, T. & TAKAHAMA, Y. 2008. The cytokine RANKL produced by positively selected thymocytes fosters medullary thymic epithelial cells that express autoimmune regulator. *Immunity,* 29**,** 438-50.

HOLLANDER, G., GILL, J., ZUKLYS, S., IWANAMI, N., LIU, C. & TAKAHAMA, Y. 2006. Cellular and molecular events during early thymus development. *Immunol Rev,* 209**,** 28-46.

HONEY, K., NAKAGAWA, T., PETERS, C. & RUDENSKY, A. 2002. Cathepsin L regulates CD4+ T cell selection independently of its effect on invariant chain: a role in the generation of positively selecting peptide ligands. *J Exp Med,* 195**,** 1349-58.

HSIEH, C. S., LEE, H. M. & LIO, C. W. 2012. Selection of regulatory T cells in the thymus. *Nat Rev Immunol,* 12**,** 157-67.

HUBERT, F. X., KINKEL, S. A., WEBSTER, K. E., CANNON, P., CREWTHER, P. E., PROEITTO, A. I., WU, L., HEATH, W. R. & SCOTT, H. S. 2008. A specific anti-Aire antibody reveals aire expression is restricted to medullary thymic epithelial cells and not expressed in periphery. *J Immunol,* 180**,** 3824-32.

HUSEBYE, E. S., PERHEENTUPA, J., RAUTEMAA, R. & KAMPE, O. 2009. Clinical manifestations and management of patients with autoimmune polyendocrine syndrome type I. *J Intern Med,* 265**,** 514-29.

IRLA, M., HUGUES, S., GILL, J., NITTA, T., HIKOSAKA, Y., WILLIAMS, I. R., HUBERT, F. X., SCOTT, H. S., TAKAHAMA, Y., HOLLANDER, G. A. & REITH, W. 2008. Autoantigen-specific interactions with CD4+ thymocytes control mature medullary thymic epithelial cell cellularity. *Immunity,* 29**,** 451-63.

IVANOV, II, MCKENZIE, B. S., ZHOU, L., TADOKORO, C. E., LEPELLEY, A., LAFAILLE, J. J., CUA, D. J. & LITTMAN, D. R. 2006. The orphan nuclear receptor RORgammat directs the differentiation program of proinflammatory IL-17+ T helper cells. *Cell,* 126**,** 1121-33.

IWASAKI, H., MIZUNO, S., MAYFIELD, R., SHIGEMATSU, H., ARINOBU, Y., SEED, B., GURISH, M. F., TAKATSU, K. & AKASHI, K. 2005. Identification of eosinophil lineage–committed progenitors in the murine bone marrow. *J Exp Med.*

JAMESON, S. C., LEE, Y. J. & HOGQUIST, K. A. 2015. Innate memory T cells. *Adv Immunol,* 126**,** 173-213.

JANAS, M. L., VARANO, G., GUDMUNDSSON, K., NODA, M., NAGASAWA, T. & TURNER, M. 2010. Thymic development beyond beta-selection requires phosphatidylinositol 3-kinase activation by CXCR4. *J Exp Med,* 207**,** 247-61.

JANEWAY, C. A., JR. & MEDZHITOV, R. 2002. Innate immune recognition. *Annu Rev Immunol,* 20**,** 197-216.

JEANNOTTE, L., AUBIN, J., BOURQUE, S., LEMIEUX, M., MONTARON, S. & PROVENCHER ST-PIERRE, A. 2011. Unsuspected effects of a lung-specific Cre deleter mouse line. *Genesis,* 49**,** 152-9.

JOSIEN, R., LI, H. L., INGULLI, E., SARMA, S., WONG, B. R., VOLOGODSKAIA, M., STEINMAN, R. M. & CHOI, Y. 2000. TRANCE, a tumor necrosis factor family member, enhances the longevity and adjuvant properties of dendritic cells in vivo. *J Exp Med,* 191**,** 495-502.

JUNG, D. & ALT, F. W. 2004. Unraveling V(D)J recombination; insights into gene regulation. *Cell,* 116**,** 299-311.

JUNG, Y., WEN, T., MINGLER, M. K., CALDWELL, J. M., WANG, Y. H., CHAPLIN, D. D., LEE, E. H., JANG, M. H., WOO, S. Y., SEOH, J. Y., MIYASAKA, M. & ROTHENBERG, M. E. 2015. IL-1beta in eosinophil-mediated small intestinal homeostasis and IgA production. *Mucosal Immunol,* 8**,** 930-42.

KABASHIMA, K., BANKS, T. A., ANSEL, K. M., LU, T. T., WARE, C. F. & CYSTER, J. G. 2005. Intrinsic lymphotoxin-beta receptor requirement for homeostasis of lymphoid tissue dendritic cells. *Immunity,* 22**,** 439-50.

KAIKO, G. E., HORVAT, J. C., BEAGLEY, K. W. & HANSBRO, P. M. 2008. Immunological decision-making: how does the immune system decide to mount a helper T-cell response? *Immunology,* 123**,** 326-38.

KAWAI, T. & AKIRA, S. 2011. Toll-like receptors and their crosstalk with other innate receptors in infection and immunity. *Immunity,* 34**,** 637-50.

KEEFE, R., DAVE, V., ALLMAN, D., WIEST, D. & KAPPES, D. J. 1999. Regulation of lineage commitment distinct from positive selection. *Science,* 286**,** 1149-53.

KIM, C. H., PELUS, L. M., WHITE, J. R. & BROXMEYER, H. E. 1998. Differential chemotactic behavior of developing T cells in response to thymic chemokines. *Blood,* 91**,** 4434-43.

KIM, H. J., ALONZO, E. S., DOROTHEE, G., POLLARD, J. W. & SANT'ANGELO, D. B. 2010. Selective depletion of eosinophils or neutrophils in mice impacts the efficiency of apoptotic cell clearance in the thymus. *PLoS One,* 5**,** e11439.

KINCAID, E. Z., MURATA, S., TANAKA, K. & ROCK, K. L. 2016. Specialized proteasome subunits have an essential role in the thymic selection of CD8(+) T cells. *Nat Immunol,* 17**,** 938-45.

KISANUKI, Y. Y., HAMMER, R. E., MIYAZAKI, J., WILLIAMS, S. C., RICHARDSON, J. A. & YANAGISAWA, M. 2001. Tie2-Cre transgenic mice: a new model for endothelial cell-lineage analysis in vivo. *Dev Biol,* 230**,** 230-42.

KISHIMOTO, H. & SPRENT, J. 1997. Negative selection in the thymus includes semimature T cells. *J Exp Med,* 185**,** 263-71.

KLEIN, L., HINTERBERGER, M., VON ROHRSCHEIDT, J. & AICHINGER, M. 2011. Autonomous versus dendritic cell-dependent contributions of medullary thymic epithelial cells to central tolerance. *Trends in Immunology,* 32**,** 188-193.

KLEIN, L., HINTERBERGER, M., WIRNSBERGER, G. & KYEWSKI, B. 2009. Antigen presentation in the thymus for positive selection and central tolerance induction. *Nat Rev Immunol,* 9**,** 833-44.

KLEIN, L., KYEWSKI, B., ALLEN, P. M. & HOGQUIST, K. A. 2014. Positive and negative selection of the T cell repertoire: what thymocytes see and don't see. *Nat Rev Immunol,* 14**,** 377-91.

KLEIN, L., ROETTINGER, B. & KYEWSKI, B. 2001. Sampling of complementing self-antigen pools by thymic stromal cells maximizes the scope of central T cell tolerance. *Eur J Immunol,* 31**,** 2476-86.

KOHU, K., SATO, T., OHNO, S., HAYASHI, K., UCHINO, R., ABE, N., NAKAZATO, M., YOSHIDA, N., KIKUCHI, T., IWAKURA, Y., INOUE, Y., WATANABE, T., HABU, S. & SATAKE, M. 2005. Overexpression of the Runx3 transcription factor increases the proportion of mature thymocytes of the CD8 single-positive lineage. *J Immunol,* 174**,** 2627-36.

KONDO, M. 2010. Lymphoid and myeloid lineage commitment in multipotent hematopoietic progenitors. *Immunol Rev,* 238**,** 37-46.

KONDO, M., SCHERER, D. C., MIYAMOTO, T., KING, A. G., AKASHI, K., SUGAMURA, K. & WEISSMAN, I. L. 2000. Cell-fate conversion of lymphoid-committed progenitors by instructive actions of cytokines. *Nature,* 407**,** 383-6.

KOPF, M., BAUMANN, H., FREER, G., FREUDENBERG, M., LAMERS, M., KISHIMOTO, T., ZINKERNAGEL, R., BLUETHMANN, H. & KOHLER, G. 1994. Impaired immune and acute-phase responses in interleukin-6-deficient mice. *Nature,* 368**,** 339-42.

KOZAI, M., KUBO, Y., KATAKAI, T., KONDO, H., KIYONARI, H., SCHAEUBLE, K., LUTHER, S. A., ISHIMARU, N., OHIGASHI, I. & TAKAHAMA, Y. 2017. Essential role of CCL21 in establishment of central self-tolerance in T cells. *J Exp Med,* 214**,** 1925-1935.

KRANICH, J. & KRAUTLER, N. J. 2016. How Follicular Dendritic Cells Shape the B-Cell Antigenome. *Front Immunol,* 7.

KROGER, C. J., SPIDALE, N. A., WANG, B. & TISCH, R. 2017. Thymic Dendritic Cell Subsets Display Distinct Efficiencies and Mechanisms of Intercellular MHC Transfer. *J Immunol,* 198**,** 249-256.

KROGER, C. J., WANG, B. & TISCH, R. 2016. Temporal increase in thymocyte negative selection parallels enhanced thymic SIRPalpha+ DC function. *Eur J Immunol,* 46**,** 2352-2362.

KRUEGER, A., WILLENZON, S., LYSZKIEWICZ, M., KREMMER, E. & FORSTER, R. 2010. CC chemokine receptor 7 and 9 double-deficient hematopoietic progenitors are severely impaired in seeding the adult thymus. *Blood,* 115**,** 1906-12.

KUMAR, H., KAWAI, T. & AKIRA, S. 2009. Pathogen recognition in the innate immune response. *Biochem J,* 420**,** 1-16.

KUROBE, H., LIU, C., UENO, T., SAITO, F., OHIGASHI, I., SEACH, N., ARAKAKI, R., HAYASHI, Y., KITAGAWA, T., LIPP, M., BOYD, R. L. & TAKAHAMA, Y. 2006. CCR7-dependent cortex-to-medulla migration of positively selected thymocytes is essential for establishing central tolerance. *Immunity,* 24**,** 165-77.

KWAN, J. & KILLEEN, N. 2004. CCR7 directs the migration of thymocytes into the thymic medulla. *J Immunol,* 172**,** 3999-4007.

KYEWSKI, B. & FEUERER, M. 2014. Love is in the Aire: mTECs share their assets. *Immunity,* 41**,** 343-5.

LAHOUD, M. H., PROIETTO, A. I., GARTLAN, K. H., KITSOULIS, S., CURTIS, J., WETTENHALL, J., SOFI, M., DAUNT, C., O'KEEFFE, M., CAMINSCHI, I., SATTERLEY, K., RIZZITELLI, A., SCHNORRER, P., HINOHARA, A., YAMAGUCHI, Y., WU, L., SMYTH, G., HANDMAN, E., SHORTMAN, K. & WRIGHT, M. D. 2006. Signal regulatory protein molecules are differentially expressed by CD8- dendritic cells. *J Immunol,* 177**,** 372-82.

LEBIEN, T. W. & TEDDER, T. F. 2008. B lymphocytes: how they develop and function. *Blood,* 112**,** 1570-80.

LEI, Y., RIPEN, A. M., ISHIMARU, N., OHIGASHI, I., NAGASAWA, T., JEKER, L. T., BOSL, M. R., HOLLANDER, G. A., HAYASHI, Y., MALEFYT RDE, W., NITTA, T. & TAKAHAMA, Y. 2011. Aire-dependent production of XCL1 mediates medullary accumulation of thymic dendritic cells and contributes to regulatory T cell development. *J Exp Med,* 208**,** 383-94.

LEPIQUE, A. P., PALENCIA, S., IRJALA, H. & PETRIE, H. T. 2003. Characterization of vascular adhesion molecules that may facilitate progenitor homing in the post-natal mouse thymus. *Clin Dev Immunol,* 10**,** 27-33.

LEVINE, B. & KLIONSKY, D. J. 2004. Development by self-digestion: molecular mechanisms and biological functions of autophagy. *Dev Cell,* 6**,** 463-77.

LEWIS, A. E., VASUDEVAN, H. N., O'NEILL, A. K., SORIANO, P. & BUSH, J. O. 2013. The widely used Wnt1-Cre transgene causes developmental phenotypes by ectopic activation of Wnt signaling. *Dev Biol,* 379**,** 229-34.

LI, A., LIU, X., DUAN, B. & MA, J. 2005. Thymic nurse cells support CD4-CD8+ thymocytes to differentiate into CD4+CD8+ cells. *Cell Mol Immunol,* 2**,** 301-5.

LI, J., CAI, H., JIN, J., WANG, Q. & MIAO, D. 2012. X-ray irradiation selectively kills thymocytes of different stages and impairs the maturation of donor-derived CD4(+)CD8(+) thymocytes in recipient thymus. *J Biomed Res,* 26**,** 355-64.

LI, J., PARK, J., FOSS, D. & GOLDSCHNEIDER, I. 2009. Thymus-homing peripheral dendritic cells constitute two of the three major subsets of dendritic cells in the steady-state thymus. *Journal of Experimental Medicine,* 206**,** 607-622.

LIEBERMAN, J. 2003. The ABCs of granule-mediated cytotoxicity: new weapons in the arsenal. *Nat Rev Immunol,* 3**,** 361-70.

LIENENKLAUS, S., CORNITESCU, M., ZIETARA, N., LYSZKIEWICZ, M., GEKARA, N., JABLONSKA, J., EDENHOFER, F., RAJEWSKY, K., BRUDER, D., HAFNER, M., STAEHELI, P. & WEISS, S. 2009. Novel reporter mouse reveals constitutive and inflammatory expression of IFN-beta in vivo. *J Immunol,* 183**,** 3229-36.

LINK, A., VOGT, T. K., FAVRE, S., BRITSCHGI, M. R., ACHA-ORBEA, H., HINZ, B., CYSTER, J. G. & LUTHER, S. A. 2007. Fibroblastic reticular cells in lymph nodes regulate the homeostasis of naive T cells. *Nat Immunol,* 8**,** 1255-65.

LIO, C. W. & HSIEH, C. S. 2008. A two-step process for thymic regulatory T cell development. *Immunity,* 28**,** 100-11.

LIU, C., SAITO, F., LIU, Z., LEI, Y., UEHARA, S., LOVE, P., LIPP, M., KONDO, S., MANLEY, N. & TAKAHAMA, Y. 2006. Coordination between CCR7- and CCR9-mediated chemokine signals in prevascular fetal thymus colonization. *Blood,* 108**,** 2531-9.
LIU, H., JAIN, R., GUAN, J., VUONG, V., ISHIDO, S., LA GRUTA, N. L., GRAY, D. H., VILLADANGOS, J. A. & MINTERN, J. D. 2016. Ubiquitin ligase MARCH 8 cooperates with CD83 to control surface MHC II expression in thymic epithelium and CD4 T cell selection. *J Exp Med,* 213**,** 1695-703.
LIU, K. & NUSSENZWEIG, M. C. 2010. Origin and development of dendritic cells. *Immunol Rev,* 234**,** 45-54.
LIU, K., VICTORA, G. D., SCHWICKERT, T. A., GUERMONPREZ, P., MEREDITH, M. M., YAO, K., CHU, F. F., RANDOLPH, G. J., RUDENSKY, A. Y. & NUSSENZWEIG, M. 2009. In vivo analysis of dendritic cell development and homeostasis. *Science,* 324**,** 392-7.
LIU, Y. J., JOSHUA, D. E., WILLIAMS, G. T., SMITH, C. A., GORDON, J. & MACLENNAN, I. C. 1989. Mechanism of antigen-driven selection in germinal centres. *Nature,* 342**,** 929-31.
LIU, Y. J., ZHANG, J., LANE, P. J., CHAN, E. Y. & MACLENNAN, I. C. 1991. Sites of specific B cell activation in primary and secondary responses to T cell-dependent and T cell-independent antigens. *Eur J Immunol,* 21**,** 2951-62.
LIU, Z., YU, S. & MANLEY, N. R. 2007. Gcm2 is required for the differentiation and survival of parathyroid precursor cells in the parathyroid/thymus primordia. *Dev Biol,* 305**,** 333-46.
LKHAGVASUREN, E., SAKATA, M., OHIGASHI, I. & TAKAHAMA, Y. 2013. Lymphotoxin beta receptor regulates the development of CCL21-expressing subset of postnatal medullary thymic epithelial cells. *J Immunol,* 190**,** 5110-7.
LODER, F., MUTSCHLER, B., RAY, R. J., PAIGE, C. J., SIDERAS, P., TORRES, R., LAMERS, M. C. & CARSETTI, R. 1999. B cell development in the spleen takes place in discrete steps and is determined by the quality of B cell receptor-derived signals. *J Exp Med,* 190**,** 75-89.
LOO, Y. M. & GALE, M., JR. 2011. Immune signaling by RIG-I-like receptors. *Immunity,* 34**,** 680-92.
LOPES, N., VACHON, H., MARIE, J. & IRLA, M. 2017. Administration of RANKL boosts thymic regeneration upon bone marrow transplantation. *EMBO Mol Med,* 9**,** 835-851.
LUCAS, B., JAMES, K. D., COSWAY, E. J., PARNELL, S. M., TUMANOV, A. V., WARE, C. F., JENKINSON, W. E. & ANDERSON, G. 2016. Lymphotoxin beta Receptor Controls T Cell Progenitor Entry to the Thymus. *J Immunol,* 197**,** 2665-72.
LUCHE, H., ARDOUIN, L., TEO, P., SEE, P., HENRI, S., MERAD, M., GINHOUX, F. & MALISSEN, B. 2011. The earliest intrathymic precursors of CD8alpha(+) thymic dendritic cells correspond to myeloid-type double-negative 1c cells. *Eur J Immunol,* 41**,** 2165-75.
LYNCH, H. E., GOLDBERG, G. L., CHIDGEY, A., VAN DEN BRINK, M. R., BOYD, R. & SEMPOWSKI, G. D. 2009. Thymic involution and immune reconstitution. *Trends Immunol,* 30**,** 366-73.
LYSZKIEWICZ, M., ZIETARA, N., FOHSE, L., PUCHALKA, J., DIESTELHORST, J., WITZLAU, K., PRINZ, I., SCHAMBACH, A. & KRUEGER, A. 2015. Limited niche availability suppresses murine intrathymic dendritic-cell development from noncommitted progenitors. *Blood.* United States: 2015 by The American Society of Hematology.
MACDONALD, H. R., BUDD, R. C. & HOWE, R. C. 1988. A CD3- subset of CD4-8+ thymocytes: a rapidly cycling intermediate in the generation of CD4+8+ cells. *Eur J Immunol,* 18**,** 519-23.
MACKALL, C. L., FRY, T. J., BARE, C., MORGAN, P., GALBRAITH, A. & GRESS, R. E. 2001. IL-7 increases both thymic-dependent and thymic-independent T-cell regeneration after bone marrow transplantation. *Blood,* 97**,** 1491-7.
MACLEOD, M. K. L., KAPPLER, J. W. & MARRACK, P. 2010. Memory CD4 T cells: generation, reactivation and re-assignment. *Immunology,* 130**,** 10-5.
MAEDA, Y., YAGI, H., TAKEMOTO, K., UTSUMI, H., FUKUNARI, A., SUGAHARA, K., MASUKO, T. & CHIBA, K. 2014. S1P lyase in thymic perivascular spaces promotes egress of mature thymocytes via up-regulation of S1P receptor 1. *Int Immunol,* 26**,** 245-55.
MAHMUDI-AZER, S., DOWNEY, G. P. & MOQBEL, R. 2002. Translocation of the tetraspanin CD63 in association with human eosinophil mediator release. *Blood,* 99**,** 4039-47.
MARSHALL, D., SINCLAIR, C., TUNG, S. & SEDDON, B. 2014. Differential requirement for IL-2 and IL-15 during bifurcated development of thymic regulatory T cells. *J Immunol,* 193**,** 5525-33.
MARTINS, V. C., BOEHM, T. & BLEUL, C. C. 2008. Ltbetar signaling does not regulate Aire-dependent transcripts in medullary thymic epithelial cells. *J Immunol,* 181**,** 400-7.
MASUDA, K., ITOI, M., AMAGAI, T., MINATO, N., KATSURA, Y. & KAWAMOTO, H. 2005. Thymic anlage is colonized by progenitors restricted to T, NK, and dendritic cell lineages. *J Immunol,* 174**,** 2525-32.
MATHIS, D. & BENOIST, C. 2009. Aire. *Annu Rev Immunol,* 27**,** 287-312.

MATLOUBIAN, M., LO, C. G., CINAMON, G., LESNESKI, M. J., XU, Y., BRINKMANN, V., ALLENDE, M. L., PROIA, R. L. & CYSTER, J. G. 2004. Lymphocyte egress from thymus and peripheral lymphoid organs is dependent on S1P receptor 1. *Nature,* 427**,** 355-60.

MATTHEWS, A. N., FRIEND, D. S., ZIMMERMANN, N., SARAFI, M. N., LUSTER, A. D., PEARLMAN, E., WERT, S. E. & ROTHENBERG, M. E. 1998. Eotaxin is required for the baseline level of tissue eosinophils. *Proc Natl Acad Sci U S A,* 95**,** 6273-8.

MAYER, C. E., ZUKLYS, S., ZHANYBEKOVA, S., OHIGASHI, I., TEH, H. Y., SANSOM, S. N., SHIKAMA-DORN, N., HAFEN, K., MACAULAY, I. C., DEADMAN, M. E., PONTING, C. P., TAKAHAMA, Y. & HOLLANDER, G. A. 2016. Dynamic spatio-temporal contribution of single beta5t+ cortical epithelial precursors to the thymus medulla. *Eur J Immunol,* 46**,** 846-56.

MAZO, I. B., HONCZARENKO, M., LEUNG, H., CAVANAGH, L. L., BONASIO, R., WENINGER, W., ENGELKE, K., XIA, L., MCEVER, R. P., KONI, P. A., SILBERSTEIN, L. E. & VON ANDRIAN, U. H. 2005. Bone marrow is a major reservoir and site of recruitment for central memory CD8+ T cells. *Immunity,* 22**,** 259-70.

MCCARTHY, N. I., COWAN, J. E., NAKAMURA, K., BACON, A., BAIK, S., WHITE, A. J., PARNELL, S. M., JENKINSON, E. J., JENKINSON, W. E. & ANDERSON, G. 2015. Osteoprotegerin-Mediated Homeostasis of Rank+ Thymic Epithelial Cells Does Not Limit Foxp3+ Regulatory T Cell Development. *J Immunol,* 195**,** 2675-82.

MCCAUGHTRY, T. M., BALDWIN, T. A., WILKEN, M. S. & HOGQUIST, K. A. 2008. Clonal deletion of thymocytes can occur in the cortex with no involvement of the medulla. *J Exp Med,* 205**,** 2575-84.

MCCAUGHTRY, T. M., WILKEN, M. S. & HOGQUIST, K. A. 2007. Thymic emigration revisited. *J Exp Med,* 204**,** 2513-20.

MEIRELES, C., RIBEIRO, A. R., PINTO, R. D., LEITAO, C., RODRIGUES, P. M. & ALVES, N. L. 2017. Thymic crosstalk restrains the pool of cortical thymic epithelial cells with progenitor properties. *Eur J Immunol*.

MELCHERS, F. 2005. The pre-B-cell receptor: selector of fitting immunoglobulin heavy chains for the B-cell repertoire. *Nat Rev Immunol,* 5**,** 578-84.

MIN, D., PANOSKALTSIS-MORTARI, A., KURO, O. M., HOLLANDER, G. A., BLAZAR, B. R. & WEINBERG, K. I. 2007. Sustained thymopoiesis and improvement in functional immunity induced by exogenous KGF administration in murine models of aging. *Blood,* 109**,** 2529-37.

MIN, H., MONTECINO-RODRIGUEZ, E. & DORSHKIND, K. 2006. Reassessing the role of growth hormone and sex steroids in thymic involution. *Clin Immunol,* 118**,** 117-23.

MISSLITZ, A., PABST, O., HINTZEN, G., OHL, L., KREMMER, E., PETRIE, H. T. & FORSTER, R. 2004. Thymic T cell development and progenitor localization depend on CCR7. *J Exp Med,* 200**,** 481-91.

MOHRS, M., LEDERMANN, B., KOHLER, G., DORFMULLER, A., GESSNER, A. & BROMBACHER, F. 1999. Differences between IL-4- and IL-4 receptor alpha-deficient mice in chronic leishmaniasis reveal a protective role for IL-13 receptor signaling. *J Immunol,* 162**,** 7302-8.

MOMBAERTS, P. 1995. Lymphocyte development and function in T-cell receptor and RAG-1 mutant mice. *Int Rev Immunol,* 13**,** 43-63.

MORAN, A. E., HOLZAPFEL, K. L., XING, Y., CUNNINGHAM, N. R., MALTZMAN, J. S., PUNT, J. & HOGQUIST, K. A. 2011. T cell receptor signal strength in Treg and iNKT cell development demonstrated by a novel fluorescent reporter mouse. *J Exp Med,* 208**,** 1279-89.

MORRIS, G. P. & ALLEN, P. M. 2012. How the TCR balances sensitivity and specificity for the recognition of self and pathogens. *Nat Immunol,* 13**,** 121-8.

MORRISON, S. J., WANDYCZ, A. M., HEMMATI, H. D., WRIGHT, D. E. & WEISSMAN, I. L. 1997. Identification of a lineage of multipotent hematopoietic progenitors. *Development,* 124**,** 1929-39.

MOTOIKE, T., MARKHAM, D. W., ROSSANT, J. & SATO, T. N. 2003. Evidence for novel fate of Flk1+ progenitor: contribution to muscle lineage. *Genesis,* 35**,** 153-9.

MOURI, Y., NISHIJIMA, H., KAWANO, H., HIROTA, F., SAKAGUCHI, N., MORIMOTO, J. & MATSUMOTO, M. 2014. NF-kappaB-inducing kinase in thymic stroma establishes central tolerance by orchestrating cross-talk with not only thymocytes but also dendritic cells. *J Immunol,* 193**,** 4356-67.

MOURI, Y., YANO, M., SHINZAWA, M., SHIMO, Y., HIROTA, F., NISHIKAWA, Y., NII, T., KIYONARI, H., ABE, T., UEHARA, H., IZUMI, K., TAMADA, K., CHEN, L., PENNINGER, J. M., INOUE, J., AKIYAMA, T. & MATSUMOTO, M. 2011. Lymphotoxin signal promotes thymic organogenesis by eliciting RANK expression in the embryonic thymic stroma. *J Immunol,* 186**,** 5047-57.

MULLER, S. M., STOLT, C. C., TERSZOWSKI, G., BLUM, C., AMAGAI, T., KESSARIS, N., IANNARELLI, P., RICHARDSON, W. D., WEGNER, M. & RODEWALD, H. R. 2008. Neural crest origin of perivascular mesenchyme in the adult thymus. *J Immunol,* 180**,** 5344-51.

MURATA, S., SASAKI, K., KISHIMOTO, T., NIWA, S., HAYASHI, H., TAKAHAMA, Y. & TANAKA, K. 2007. Regulation of CD8+ T cell development by thymus-specific proteasomes. *Science,* 316**,** 1349-53.
NAKAGAWA, T., ROTH, W., WONG, P., NELSON, A., FARR, A., DEUSSING, J., VILLADANGOS, J. A., PLOEGH, H., PETERS, C. & RUDENSKY, A. Y. 1998. Cathepsin L: critical role in Ii degradation and CD4 T cell selection in the thymus. *Science,* 280**,** 450-3.
NAKAGAWA, Y., OHIGASHI, I., NITTA, T., SAKATA, M., TANAKA, K., MURATA, S., KANAGAWA, O. & TAKAHAMA, Y. 2012. Thymic nurse cells provide microenvironment for secondary T cell receptor alpha rearrangement in cortical thymocytes. *Proc Natl Acad Sci U S A,* 109**,** 20572-7.
NEDJIC, J., AICHINGER, M., EMMERICH, J., MIZUSHIMA, N. & KLEIN, L. 2008. Autophagy in thymic epithelium shapes the T-cell repertoire and is essential for tolerance. *Nature,* 455**,** 396-400.
NEEFJES, J., JONGSMA, M. L., PAUL, P. & BAKKE, O. 2011. Towards a systems understanding of MHC class I and MHC class II antigen presentation. *Nat Rev Immunol,* 11**,** 823-36.
NEHLS, M., KYEWSKI, B., MESSERLE, M., WALDSCHUTZ, R., SCHUDDEKOPF, K., SMITH, A. J. & BOEHM, T. 1996. Two genetically separable steps in the differentiation of thymic epithelium. *Science,* 272**,** 886-9.
NEHLS, M., PFEIFER, D., SCHORPP, M., HEDRICH, H. & BOEHM, T. 1994. New member of the winged-helix protein family disrupted in mouse and rat nude mutations. *Nature,* 372**,** 103-7.
NEMAZEE, D. 2000. Receptor Selection in B and T Lymphocytes. *Annu Rev Immunol,* 18.
NEMAZEE, D. & HOGQUIST, K. A. 2003. Antigen receptor selection by editing or downregulation of V(D)J recombination. *Curr Opin Immunol,* 15**,** 182-9.
NEWTON, K., HARRIS, A. W., BATH, M. L., SMITH, K. G. & STRASSER, A. 1998. A dominant interfering mutant of FADD/MORT1 enhances deletion of autoreactive thymocytes and inhibits proliferation of mature T lymphocytes. *Embo j,* 17**,** 706-18.
NIKOLICH-ZUGICH, J., SLIFKA, M. K. & MESSAOUDI, I. 2004. The many important facets of T-cell repertoire diversity. *Nat Rev Immunol,* 4**,** 123-32.
NISHIGAKI, Y., FUJIUCHI, S., YAMAZAKI, Y., MATSUMOTO, H., TAKEDA, A., FUJITA, Y., OKAMOTO, K., FUJIKANE, T., SHIMIZU, T. & KIKUCHI, K. 2003. Increased vascular endothelial growth factor in acute eosinophilic pneumonia. *Eur Respir J,* 21**,** 774-8.
NITTA, T., MURATA, S., SASAKI, K., FUJII, H., RIPEN, A. M., ISHIMARU, N., KOYASU, S., TANAKA, K. & TAKAHAMA, Y. 2010. Thymoproteasome shapes immunocompetent repertoire of CD8+ T cells. *Immunity,* 32**,** 29-40.
NORIS, M. & REMUZZI, G. 2013. Overview of Complement Activation and Regulation. *Semin Nephrol.*
NUSSBAUM, J. C., VAN DYKEN, S. J., VON MOLTKE, J., CHENG, L. E., MOHAPATRA, A., MOLOFSKY, A. B., THORNTON, E. E., KRUMMEL, M. F., CHAWLA, A., LIANG, H. E. & LOCKSLEY, R. M. 2013. Type 2 innate lymphoid cells control eosinophil homeostasis. *Nature,* 502**,** 245-8.
O'NEILL, L. A., GOLENBOCK, D. & BOWIE, A. G. 2013. The history of Toll-like receptors - redefining innate immunity. *Nat Rev Immunol.* England.
OBAR, J. J. & LEFRANÇOIS, L. 2010. Memory CD8(+) T cell differentiation. *Ann N Y Acad Sci,* 1183**,** 251-66.
OBOKI, K., NAKAE, S., MATSUMOTO, K. & SAITO, H. 2011. IL-33 and Airway Inflammation. *Allergy Asthma Immunol Res,* 3**,** 81-8.
OBUKHANYCH, T. V. & NUSSENZWEIG, M. C. 2006. T-independent type II immune responses generate memory B cells. *J Exp Med.*
OETTINGER, M. A., SCHATZ, D. G., GORKA, C. & BALTIMORE, D. 1990. RAG-1 and RAG-2, adjacent genes that synergistically activate V(D)J recombination. *Science,* 248**,** 1517-23.
OFFNER, F., KERRE, T., DE SMEDT, M. & PLUM, J. 1999. Bone marrow CD34 cells generate fewer T cells in vitro with increasing age and following chemotherapy. *Br J Haematol,* 104**,** 801-8.
OFTEDAL, B. E., HELLESEN, A., ERICHSEN, M. M., BRATLAND, E., VARDI, A., PERHEENTUPA, J., KEMP, E. H., FISKERSTRAND, T., VIKEN, M. K., WEETMAN, A. P., FLEISHMAN, S. J., BANKA, S., NEWMAN, W. G., SEWELL, W. A., SOZAEVA, L. S., ZAYATS, T., HAUGARVOLL, K., ORLOVA, E. M., HAAVIK, J., JOHANSSON, S., KNAPPSKOG, P. M., LOVAS, K., WOLFF, A. S., ABRAMSON, J. & HUSEBYE, E. S. 2015. Dominant Mutations in the Autoimmune Regulator AIRE Are Associated with Common Organ-Specific Autoimmune Diseases. *Immunity,* 42**,** 1185-96.
OH, J. & SHIN, J. S. 2015. The Role of Dendritic Cells in Central Tolerance. *Immune Netw,* 15**,** 111-20.
OHIGASHI, I., KOZAI, M. & TAKAHAMA, Y. 2016. Development and developmental potential of cortical thymic epithelial cells. *Immunol Rev,* 271**,** 10-22.

OHIGASHI, I., ZUKLYS, S., SAKATA, M., MAYER, C. E., HAMAZAKI, Y., MINATO, N., HOLLANDER, G. A. & TAKAHAMA, Y. 2015. Adult Thymic Medullary Epithelium Is Maintained and Regenerated by Lineage-Restricted Cells Rather Than Bipotent Progenitors. *Cell Rep,* 13**,** 1432-43.

OHNMACHT, C., PULLNER, A., KING, S. B., DREXLER, I., MEIER, S., BROCKER, T. & VOEHRINGER, D. 2009. Constitutive ablation of dendritic cells breaks self-tolerance of CD4 T cells and results in spontaneous fatal autoimmunity. *J Exp Med,* 206**,** 549-59.

ORG, T., REBANE, A., KISAND, K., LAAN, M., HALJASORG, U., ANDRESON, R. & PETERSON, P. 2009. AIRE activated tissue specific genes have histone modifications associated with inactive chromatin. *Hum Mol Genet,* 18**,** 4699-710.

OTERO, D. C., BAKER, D. P. & DAVID, M. 2013. IRF7-dependent IFN-beta production in response to RANKL promotes medullary thymic epithelial cell development. *J Immunol,* 190**,** 3289-98.

PAI, S. Y., TRUITT, M. L., TING, C. N., LEIDEN, J. M., GLIMCHER, L. H. & HO, I. C. 2003. Critical roles for transcription factor GATA-3 in thymocyte development. *Immunity,* 19**,** 863-75.

PALM, N. W., ROSENSTEIN, R. K. & MEDZHITOV, R. 2012. Allergic host defences. *Nature,* 484**,** 465-72.

PALMER, D. B., VINEY, J. L., RITTER, M. A., HAYDAY, A. C. & OWEN, M. J. 1993. Expression of the alpha beta T-cell receptor is necessary for the generation of the thymic medulla. *Dev Immunol,* 3**,** 175-9.

PALMER, E. 2003. Negative selection--clearing out the bad apples from the T-cell repertoire. *Nat Rev Immunol,* 3**,** 383-91.

PAPPU, R., SCHWAB, S. R., CORNELISSEN, I., PEREIRA, J. P., REGARD, J. B., XU, Y., CAMERER, E., ZHENG, Y. W., HUANG, Y., CYSTER, J. G. & COUGHLIN, S. R. 2007. Promotion of lymphocyte egress into blood and lymph by distinct sources of sphingosine-1-phosphate. *Science,* 316**,** 295-8.

PARKIN, J. & COHEN, B. 2001. An overview of the immune system. *Lancet,* 357**,** 1777-89.

PERRY, J. S., LIO, C. W., KAU, A. L., NUTSCH, K., YANG, Z., GORDON, J. I., MURPHY, K. M. & HSIEH, C. S. 2014. Distinct contributions of Aire and antigen-presenting-cell subsets to the generation of self-tolerance in the thymus. *Immunity,* 41**,** 414-26.

PETRILLI, V., DOSTERT, C., MURUVE, D. A. & TSCHOPP, J. 2007. The inflammasome: a danger sensing complex triggering innate immunity. *Curr Opin Immunol,* 19**,** 615-22.

PIEPER, K., GRIMBACHER, B. & EIBEL, H. 2013. B-cell biology and development. *J Allergy Clin Immunol,* 131**,** 959-71.

PLOTKIN, J., PROCKOP, S. E., LEPIQUE, A. & PETRIE, H. T. 2003. Critical role for CXCR4 signaling in progenitor localization and T cell differentiation in the postnatal thymus. *J Immunol,* 171**,** 4521-7.

PORRITT, H. E., GORDON, K. & PETRIE, H. T. 2003. Kinetics of steady-state differentiation and mapping of intrathymic-signaling environments by stem cell transplantation in nonirradiated mice. *J Exp Med,* 198**,** 957-62.

PORRITT, H. E., RUMFELT, L. L., TABRIZIFARD, S., SCHMITT, T. M., CARLOS, J., ZUNIGA-PFLUCKER, J. C. & PETRIE, H. T. 2004. Heterogeneity among DN1 prothymocytes reveals multiple progenitors with different capacities to generate T cell and non-T cell lineages. *Immunity,* 20**,** 735-745.

PRINZ, I., SANSONI, A., KISSENPFENNIG, A., ARDOUIN, L., MALISSEN, M. & MALISSEN, B. 2006. Visualization of the earliest steps of gammadelta T cell development in the adult thymus. *Nat Immunol,* 7**,** 995-1003.

PROIETTO, A. I., LAHOUD, M. H. & WU, L. 2008a. Distinct functional capacities of mouse thymic and splenic dendritic cell populations. *Immunol Cell Biol,* 86**,** 700-8.

PROIETTO, A. I., VAN DOMMELEN, S., ZHOU, P., RIZZITELLI, A., D'AMICO, A., STEPTOE, R. J., NAIK, S. H., LAHOUD, M. H., LIU, Y., ZHENG, P., SHORTMAN, K. & WU, L. 2008b. Dendritic cells in the thymus contribute to T-regulatory cell induction. *Proc Natl Acad Sci U S A,* 105**,** 19869-74.

QURESHI, O. S., ZHENG, Y., NAKAMURA, K., ATTRIDGE, K., MANZOTTI, C., SCHMIDT, E. M., BAKER, J., JEFFERY, L. E., KAUR, S., BRIGGS, Z., HOU, T. Z., FUTTER, C. E., ANDERSON, G., WALKER, L. S. K. & SANSOM, D. M. 2011. Trans-Endocytosis of CD80 and CD86: A Molecular Basis for the Cell-Extrinsic Function of CTLA-4. *Science,* 332**,** 600-603.

RADTKE, F., FASNACHT, N. & MACDONALD, H. R. 2010. Notch signaling in the immune system. *Immunity,* 32**,** 14-27.

RADTKE, F., MACDONALD, H. R. & TACCHINI-COTTIER, F. 2013. Regulation of innate and adaptive immunity by Notch. *Nat Rev Immunol,* 13**,** 427-37.

RAMOND, C., BANDEIRA, A., BERTHAULT, C., PEREIRA, P., CUMANO, A. & BURLEN-DEFRANOUX, O. 2015. Characterization of Thymic Settling Progenitors in the Mouse Embryo Using In Vivo and In Vitro Assays. *J Vis Exp***,** e52795.

RAMSDELL, F., JENKINS, M., DINH, Q. & FOWLKES, B. J. 1991. The majority of CD4+8- thymocytes are functionally immature. *J Immunol,* 147**,** 1779-85.

REICHERT, R. A., WEISSMAN, I. L. & BUTCHER, E. C. 1986. Phenotypic analysis of thymocytes that express homing receptors for peripheral lymph nodes. *J Immunol,* 136**,** 3521-8.
RIBEIRO, A. R., MEIRELES, C., RODRIGUES, P. M. & ALVES, N. L. 2014. Intermediate expression of CCRL1 reveals novel subpopulations of medullary thymic epithelial cells that emerge in the postnatal thymus. *Eur J Immunol,* 44**,** 2918-24.
RIECK, M., KREMSER, C., JOBIN, K., METTKE, E., KURTS, C., GRALER, M., WILLECKE, K. & KOLANUS, W. 2017. Ceramide synthase 2 facilitates S1P-dependent egress of thymocytes into the circulation in mice. *Eur J Immunol,* 47**,** 677-684.
RIEMANN, M., ANDREAS, N., FEDOSEEVA, M., MEIER, E., WEIH, D., FREYTAG, H., SCHMIDT-ULLRICH, R., KLEIN, U., WANG, Z. Q. & WEIH, F. 2017. Central immune tolerance depends on crosstalk between the classical and alternative NF-kappaB pathways in medullary thymic epithelial cells. *J Autoimmun,* 81**,** 56-67.
ROBEY, E., ITANO, A., FANSLOW, W. C. & FOWLKES, B. J. 1994. Constitutive CD8 expression allows inefficient maturation of CD4+ helper T cells in class II major histocompatibility complex mutant mice. *J Exp Med,* 179**,** 1997-2004.
ROCHE, P. A. & FURUTA, K. 2015. The ins and outs of MHC class II-mediated antigen processing and presentation. *Nat Rev Immunol,* 15**,** 203-16.
RODEWALD, H. R. 2008. Thymus organogenesis. *Annu Rev Immunol,* 26**,** 355-88.
ROSSI, F. M., CORBEL, S. Y., MERZABAN, J. S., CARLOW, D. A., GOSSENS, K., DUENAS, J., SO, L., YI, L. & ZILTENER, H. J. 2005. Recruitment of adult thymic progenitors is regulated by P-selectin and its ligand PSGL-1. *Nat Immunol,* 6**,** 626-34.
ROSSI, S. W., JENKINSON, W. E., ANDERSON, G. & JENKINSON, E. J. 2006. Clonal analysis reveals a common progenitor for thymic cortical and medullary epithelium. *Nature,* 441**,** 988-91.
ROSSI, S. W., KIM, M. Y., LEIBBRANDT, A., PARNELL, S. M., JENKINSON, W. E., GLANVILLE, S. H., MCCONNELL, F. M., SCOTT, H. S., PENNINGER, J. M., JENKINSON, E. J., LANE, P. J. & ANDERSON, G. 2007. RANK signals from CD4(+)3(-) inducer cells regulate development of Aire-expressing epithelial cells in the thymic medulla. *J Exp Med.* United States.
ROTHENBERG, M. E. & HOGAN, S. P. 2006. The eosinophil. *Annu Rev Immunol,* 24**,** 147-74.
SAMBANDAM, A., MAILLARD, I., ZEDIAK, V. P., XU, L., GERSTEIN, R. M., ASTER, J. C., PEAR, W. S. & BHANDOOLA, A. 2005. Notch signaling controls the generation and differentiation of early T lineage progenitors. *Nat Immunol,* 6**,** 663-70.
SAMELSON, L. E. 2002. Signal transduction mediated by the T cell antigen receptor: the role of adapter proteins. *Annu Rev Immunol,* 20**,** 371-94.
SANCHO, D., GOMEZ, M. & SANCHEZ-MADRID, F. 2005. CD69 is an immunoregulatory molecule induced following activation. *Trends Immunol,* 26**,** 136-40.
SARMA, J. V. & WARD, P. A. 2011. The Complement System. *Cell Tissue Res,* 343**,** 227-35.
SASAKI, K., TAKADA, K., OHTE, Y., KONDO, H., SORIMACHI, H., TANAKA, K., TAKAHAMA, Y. & MURATA, S. 2015. Thymoproteasomes produce unique peptide motifs for positive selection of CD8(+) T cells. *Nat Commun,* 6**,** 7484.
SCHLENNER, S. M., MADAN, V., BUSCH, K., TIETZ, A., LAUFLE, C., COSTA, C., BLUM, C., FEHLING, H. J. & RODEWALD, H. R. 2010. Fate mapping reveals separate origins of T cells and myeloid lineages in the thymus. *Immunity,* 32**,** 426-36.
SCHLITZER, A., SIVAKAMASUNDARI, V., CHEN, J., SUMATOH, H. R., SCHREUDER, J., LUM, J., MALLERET, B., ZHANG, S., LARBI, A., ZOLEZZI, F., RENIA, L., POIDINGER, M., NAIK, S., NEWELL, E. W., ROBSON, P. & GINHOUX, F. 2015. Identification of cDC1- and cDC2-committed DC progenitors reveals early lineage priming at the common DC progenitor stage in the bone marrow. *Nat Immunol,* 16**,** 718-28.
SCHMIDT-SUPPRIAN, M. & RAJEWSKY, K. 2007. Vagaries of conditional gene targeting. *Nat Immunol,* 8**,** 665-8.
SCHMITT, T. M., CIOFANI, M., PETRIE, H. T. & ZUNIGA-PFLUCKER, J. C. 2004. Maintenance of T cell specification and differentiation requires recurrent notch receptor-ligand interactions. *J Exp Med,* 200**,** 469-79.
SCHWAB, S. R., PEREIRA, J. P., MATLOUBIAN, M., XU, Y., HUANG, Y. & CYSTER, J. G. 2005. Lymphocyte sequestration through S1P lyase inhibition and disruption of S1P gradients. *Science,* 309**,** 1735-9.
SCHWARZ, B. A. & BHANDOOLA, A. 2004. Circulating hematopoietic progenitors with T lineage potential. *Nat Immunol,* 5**,** 953-60.

SCHWARZ, B. A. & BHANDOOLA, A. 2006. Trafficking from the bone marrow to the thymus: a prerequisite for thymopoiesis. *Immunol Rev,* 209**,** 47-57.
SCIMONE, M. L., AIFANTIS, I., APOSTOLOU, I., VON BOEHMER, H. & VON ANDRIAN, U. H. 2006. A multistep adhesion cascade for lymphoid progenitor cell homing to the thymus. *Proc Natl Acad Sci U S A*.
SCOTT, C. L., SOEN, B., MARTENS, L., SKRYPEK, N., SAELENS, W., TAMINAU, J., BLANCKE, G., VAN ISTERDAEL, G., HUYLEBROECK, D., HAIGH, J., SAEYS, Y., GUILLIAMS, M., LAMBRECHT, B. N. & BERX, G. 2016. The transcription factor Zeb2 regulates development of conventional and plasmacytoid DCs by repressing Id2. *J Exp Med,* 213**,** 897-911.
SEACH, N., UENO, T., FLETCHER, A. L., LOWEN, T., MATTESICH, M., ENGWERDA, C. R., SCOTT, H. S., WARE, C. F., CHIDGEY, A. P., GRAY, D. H. & BOYD, R. L. 2008. The lymphotoxin pathway regulates Aire-independent expression of ectopic genes and chemokines in thymic stromal cells. *J Immunol,* 180**,** 5384-92.
SEKAI, M., HAMAZAKI, Y. & MINATO, N. 2014. Medullary thymic epithelial stem cells maintain a functional thymus to ensure lifelong central T cell tolerance. *Immunity,* 41**,** 753-61.
SETH, S., OBERDORFER, L., HYDE, R., HOFF, K., THIES, V., WORBS, T., SCHMITZ, S. & FORSTER, R. 2011. CCR7 essentially contributes to the homing of plasmacytoid dendritic cells to lymph nodes under steady-state as well as inflammatory conditions. *J Immunol,* 186**,** 3364-72.
SHAH, D. K. & ZUNIGA-PFLUCKER, J. C. 2014. An overview of the intrathymic intricacies of T cell development. *J Immunol,* 192**,** 4017-23.
SHI, Y., WU, W., CHAI, Q., LI, Q., HOU, Y., XIA, H., REN, B., XU, H., GUO, X., JIN, C., LV, M., WANG, Z., FU, Y. X. & ZHU, M. 2016. LTbetaR controls thymic portal endothelial cells for haematopoietic progenitor cell homing and T-cell regeneration. *Nat Commun,* 7**,** 12369.
SHIOW, L. R., ROSEN, D. B., BRDICKOVA, N., XU, Y., AN, J., LANIER, L. L., CYSTER, J. G. & MATLOUBIAN, M. 2006. CD69 acts downstream of interferon-alpha/beta to inhibit S1P1 and lymphocyte egress from lymphoid organs. *Nature,* 440**,** 540-4.
SHORTMAN, K., SCOLLAY, R., ANDREWS, P. & BOYD, R. 1986. Development of T lymphocytes within the thymus and within thymic nurse cells. *Curr Top Microbiol Immunol,* 126**,** 5-18.
SILVA, A., CORNISH, G., LEY, S. C. & SEDDON, B. 2014. NF-kappaB signaling mediates homeostatic maturation of new T cells. *Proc Natl Acad Sci U S A,* 111**,** E846-55.
SINCLAIR, C., ONO, M. & SEDDON, B. 2015. A Zap70-dependent feedback circuit is essential for efficient selection of CD4 lineage thymocytes. *Immunol Cell Biol,* 93**,** 406-16.
SINGER, A. 2002. New perspectives on a developmental dilemma: the kinetic signaling model and the importance of signal duration for the CD4/CD8 lineage decision. *Curr Opin Immunol,* 14**,** 207-15.
SINGER, A., ADORO, S. & PARK, J. H. 2008. Lineage fate and intense debate: myths, models and mechanisms of CD4- versus CD8-lineage choice. *Nat Rev Immunol.* England.
SINGER, A. & BOSSELUT, R. 2004. CD4/CD8 coreceptors in thymocyte development, selection, and lineage commitment: analysis of the CD4/CD8 lineage decision. *Adv Immunol,* 83**,** 91-131.
SITKOVSKY, M., LUKASHEV, D., DEAGLIO, S., DWYER, K., ROBSON, S. C. & OHTA, A. 2008. Adenosine A2A receptor antagonists: blockade of adenosinergic effects and T regulatory cells. *Br J Pharmacol,* 153 Suppl 1**,** S457-64.
SITNICKA, E., BRYDER, D., THEILGAARD-MONCH, K., BUZA-VIDAS, N., ADOLFSSON, J. & JACOBSEN, S. E. 2002. Key role of flt3 ligand in regulation of the common lymphoid progenitor but not in maintenance of the hematopoietic stem cell pool. *Immunity,* 17**,** 463-72.
SOHN, S. J., FORBUSH, K. A., PAN, X. C. & PERLMUTTER, R. M. 2001. Activated p56lck directs maturation of both CD4 and CD8 single-positive thymocytes. *J Immunol,* 166**,** 2209-17.
SOZA-RIED, C., BLEUL, C. C., SCHORPP, M. & BOEHM, T. 2008. Maintenance of thymic epithelial phenotype requires extrinsic signals in mouse and zebrafish. *J Immunol,* 181**,** 5272-7.
SPIDALE, N. A., WANG, B. & TISCH, R. 2014. Cutting edge: Antigen-specific thymocyte feedback regulates homeostatic thymic conventional dendritic cell maturation. *J Immunol,* 193**,** 21-5.
SRINIVAS, S., WATANABE, T., LIN, C. S., WILLIAM, C. M., TANABE, Y., JESSELL, T. M. & COSTANTINI, F. 2001. Cre reporter strains produced by targeted insertion of EYFP and ECFP into the ROSA26 locus. *BMC Dev Biol,* 1**,** 4.
STARR, T. K., JAMESON, S. C. & HOGQUIST, K. A. 2003. Positive and negative selection of T cells. *Annual Review of Immunology,* 21**,** 139-176.
STEINMANN, G. G., KLAUS, B. & MULLER-HERMELINK, H. K. 1985. The involution of the ageing human thymic epithelium is independent of puberty. A morphometric study. *Scand J Immunol,* 22**,** 563-75.
STRASSER, A. 2005. The role of BH3-only proteins in the immune system. *Nat Rev Immunol,* 5**,** 189-200.

STRASSER, A., CORY, S. & ADAMS, J. M. 2011. Deciphering the rules of programmed cell death to improve therapy of cancer and other diseases. *Embo j,* 30**,** 3667-83.
STRITESKY, G. L., XING, Y., ERICKSON, J. R., KALEKAR, L. A., WANG, X., MUELLER, D. L., JAMESON, S. C. & HOGQUIST, K. A. 2013. Murine thymic selection quantified using a unique method to capture deleted T cells. *Proc Natl Acad Sci U S A,* 110**,** 4679-84.
SULTANA, D. A., ZHANG, S. L., TODD, S. P. & BHANDOOLA, A. 2012. Expression of functional P-selectin glycoprotein ligand 1 on hematopoietic progenitors is developmentally regulated. *J Immunol,* 188**,** 4385-93.
SUMMERS-DELUCA, L. E., MCCARTHY, D. D., COSOVIC, B., WARD, L. A., LO, C. C., SCHEU, S., PFEFFER, K. & GOMMERMAN, J. L. 2007. Expression of lymphotoxin-alphabeta on antigen-specific T cells is required for DC function. *J Exp Med,* 204**,** 1071-81.
SUN, G., LIU, X., MERCADO, P., JENKINSON, S. R., KYPRIOTOU, M., FEIGENBAUM, L., GALERA, P. & BOSSELUT, R. 2005. The zinc finger protein cKrox directs CD4 lineage differentiation during intrathymic T cell positive selection. *Nat Immunol,* 6**,** 373-81.
SUN, Z. J., KIM, K. S., WAGNER, G. & REINHERZ, E. L. 2001. Mechanisms contributing to T cell receptor signaling and assembly revealed by the solution structure of an ectodomain fragment of the CD3 epsilon gamma heterodimer. *Cell,* 105**,** 913-23.
SZABO, S. J., KIM, S. T., COSTA, G. L., ZHANG, X., FATHMAN, C. G. & GLIMCHER, L. H. 2000. A novel transcription factor, T-bet, directs Th1 lineage commitment. *Cell,* 100**,** 655-69.
TAI, X., ERMAN, B., ALAG, A., MU, J., KIMURA, M., KATZ, G., GUINTER, T., MCCAUGHTRY, T., ETZENSPERGER, R., FEIGENBAUM, L., SINGER, D. S. & SINGER, A. 2013. Foxp3 transcription factor is proapoptotic and lethal to developing regulatory T cells unless counterbalanced by cytokine survival signals. *Immunity,* 38**,** 1116-28.
TAKABA, H., MORISHITA, Y., TOMOFUJI, Y., DANKS, L., NITTA, T., KOMATSU, N., KODAMA, T. & TAKAYANAGI, H. 2015. Fezf2 Orchestrates a Thymic Program of Self-Antigen Expression for Immune Tolerance. *Cell,* 163**,** 975-87.
TAKADA, K., KONDO, K. & TAKAHAMA, Y. 2017. Generation of Peptides That Promote Positive Selection in the Thymus. *J Immunol,* 198**,** 2215-2222.
TAKADA, K., VAN LAETHEM, F., XING, Y., AKANE, K., SUZUKI, H., MURATA, S., TANAKA, K., JAMESON, S. C., SINGER, A. & TAKAHAMA, Y. 2015. TCR affinity for thymoproteasome-dependent positively selecting peptides conditions antigen responsiveness in CD8(+) T cells. *Nat Immunol,* 16**,** 1069-76.
TAKAHAMA, Y. 2006. Journey through the thymus: stromal guides for T-cell development and selection. *Nat Rev Immunol.* England.
TAKAHAMA, Y., OHIGASHI, I., BAIK, S. & ANDERSON, G. 2017. Generation of diversity in thymic epithelial cells. *Nat Rev Immunol*.
TAKEDA, A., HOSSAIN, M. S., RANTAKARI, P., SIMMONS, S., SASAKI, N., SALMI, M., JALKANEN, S. & MIYASAKA, M. 2016. Thymocytes in Lyve1-CRE/S1pr1f/f Mice Accumulate in the Thymus due to Cell-Intrinsic Loss of Sphingosine-1-Phosphate Receptor Expression. *Front Immunol,* 7**,** 489.
TAN, J. B., VISAN, I., YUAN, J. S. & GUIDOS, C. J. 2005. Requirement for Notch1 signals at sequential early stages of intrathymic T cell development. *Nat Immunol,* 6**,** 671-9.
TANIUCHI, I., OSATO, M., EGAWA, T., SUNSHINE, M. J., BAE, S. C., KOMORI, T., ITO, Y. & LITTMAN, D. R. 2002. Differential requirements for Runx proteins in CD4 repression and epigenetic silencing during T lymphocyte development. *Cell,* 111**,** 621-33.
THROSBY, M., HERBELIN, A., PLEAU, J. M. & DARDENNE, M. 2000. CD11c+ eosinophils in the murine thymus: developmental regulation and recruitment upon MHC class I-restricted thymocyte deletion. *J Immunol,* 165**,** 1965-75.
TOMAKI, M., ZHAO, L. L., LUNDAHL, J., SJOSTRAND, M., JORDANA, M., LINDEN, A., O'BYRNE, P. & LOTVALL, J. 2000. Eosinophilopoiesis in a murine model of allergic airway eosinophilia: involvement of bone marrow IL-5 and IL-5 receptor alpha. *J Immunol,* 165**,** 4040-50.
TONEGAWA, S. 1983. Somatic generation of antibody diversity. *Nature,* 302**,** 575-81.
TRAMPONT, P. C., TOSELLO-TRAMPONT, A. C., SHEN, Y., DULEY, A. K., SUTHERLAND, A. E., BENDER, T. P., LITTMAN, D. R. & RAVICHANDRAN, K. S. 2010. CXCR4 acts as a costimulator during thymic beta-selection. *Nat Immunol,* 11**,** 162-70.
TURVEY, S. E. & BROIDE, D. H. 2010. Chapter 2: Innate Immunity. *J Allergy Clin Immunol,* 125**,** S24-32.
TZE, L. E., HORIKAWA, K., DOMASCHENZ, H., HOWARD, D. R., ROOTS, C. M., RIGBY, R. J., WAY, D. A., OHMURA-HOSHINO, M., ISHIDO, S., ANDONIOU, C. E., DEGLI-ESPOSTI, M. A. &

GOODNOW, C. C. 2011. CD83 increases MHC II and CD86 on dendritic cells by opposing IL-10-driven MARCH1-mediated ubiquitination and degradation. *J Exp Med,* 208**,** 149-65.
UCAR, A., UCAR, O., KLUG, P., MATT, S., BRUNK, F., HOFMANN, T. G. & KYEWSKI, B. 2014. Adult thymus contains FoxN1(-) epithelial stem cells that are bipotent for medullary and cortical thymic epithelial lineages. *Immunity,* 41**,** 257-69.
UCAR, O., LI, K., DVORNIKOV, D., KREUTZ, C., TIMMER, J., MATT, S., BRENNER, L., SMEDLEY, C., TRAVIS, M. A., HOFMANN, T. G., KLINGMULLER, U. & KYEWSKI, B. 2016. A Thymic Epithelial Stem Cell Pool Persists throughout Ontogeny and Is Modulated by TGF-beta. *Cell Rep,* 17**,** 448-457.
UENO, T., HARA, K., WILLIS, M. S., MALIN, M. A., HOPKEN, U. E., GRAY, D. H., MATSUSHIMA, K., LIPP, M., SPRINGER, T. A., BOYD, R. L., YOSHIE, O. & TAKAHAMA, Y. 2002. Role for CCR7 ligands in the emigration of newly generated T lymphocytes from the neonatal thymus. *Immunity,* 16**,** 205-18.
UENO, T., SAITO, F., GRAY, D. H., KUSE, S., HIESHIMA, K., NAKANO, H., KAKIUCHI, T., LIPP, M., BOYD, R. L. & TAKAHAMA, Y. 2004. CCR7 signals are essential for cortex-medulla migration of developing thymocytes. *J Exp Med,* 200**,** 493-505.
ULYANCHENKO, S., O'NEILL, K. E., MEDLEY, T., FARLEY, A. M., VAIDYA, H. J., COOK, A. M., BLAIR, N. F. & BLACKBURN, C. C. 2016. Identification of a Bipotent Epithelial Progenitor Population in the Adult Thymus. *Cell Rep,* 14**,** 2819-32.
VAIDYA, H. J., BRIONES LEON, A. & BLACKBURN, C. C. 2016. FOXN1 in thymus organogenesis and development. *Eur J Immunol.* Hoboken.
VANTOUROUT, P. & HAYDAY, A. 2013. Six-of-the-best: unique contributions of gammadelta T cells to immunology. *Nat Rev Immunol,* 13**,** 88-100.
VELARDI, E., TSAI, J. J., HOLLAND, A. M., WERTHEIMER, T., YU, V. W., ZAKRZEWSKI, J. L., TUCKETT, A. Z., SINGER, N. V., WEST, M. L., SMITH, O. M., YOUNG, L. F., KREINES, F. M., LEVY, E. R., BOYD, R. L., SCADDEN, D. T., DUDAKOV, J. A. & VAN DEN BRINK, M. R. 2014. Sex steroid blockade enhances thymopoiesis by modulating Notch signaling. *J Exp Med,* 211**,** 2341-9.
VENANZI, E. S., GRAY, D. H., BENOIST, C. & MATHIS, D. 2007. Lymphotoxin pathway and Aire influences on thymic medullary epithelial cells are unconnected. *J Immunol,* 179**,** 5693-700.
VERJAN GARCIA, N., UMEMOTO, E., SAITO, Y., YAMASAKI, M., HATA, E., MATOZAKI, T., MURAKAMI, M., JUNG, Y. J., WOO, S. Y., SEOH, J. Y., JANG, M. H., AOZASA, K. & MIYASAKA, M. 2011. SIRPalpha/CD172a regulates eosinophil homeostasis. *J Immunol,* 187**,** 2268-77.
VIGNALI, D. A., COLLISON, L. W. & WORKMAN, C. J. 2008. How regulatory T cells work. *Nat Rev Immunol,* 8**,** 523-32.
VILLUNGER, A., MARSDEN, V. S., ZHAN, Y., ERLACHER, M., LEW, A. M., BOUILLET, P., BERZINS, S., GODFREY, D. I., HEATH, W. R. & STRASSER, A. 2004. Negative selection of semimature CD4(+)8(-)HSA+ thymocytes requires the BH3-only protein Bim but is independent of death receptor signaling. *Proc Natl Acad Sci U S A,* 101**,** 7052-7.
VIRET, C., BARLOW, A. K. & JANEWAY, C. A., JR. 1999. On the intrathymic intercellular transfer of self-determinants. *Immunol Today,* 20**,** 8-10.
VIRET, C., LAMARE, C., GUIRAUD, M., FAZILLEAU, N., BOUR, A., MALISSEN, B., CARRIER, A. & GUERDER, S. 2011. Thymus-specific serine protease contributes to the diversification of the functional endogenous CD4 T cell receptor repertoire. *J Exp Med,* 208**,** 3-11.
VON BOEHMER, H. & FEHLING, H. J. 1997. Structure and function of the pre-T cell receptor. *Annu Rev Immunol,* 15**,** 433-52.
VON ROHRSCHEIDT, J., PETROZZIELLO, E., NEDJIC, J., FEDERLE, C., KRZYZAK, L., PLOEGH, H. L., ISHIDO, S., STEINKASSERER, A. & KLEIN, L. 2016. Thymic CD4 T cell selection requires attenuation of March8-mediated MHCII turnover in cortical epithelial cells through CD83. *J Exp Med.*
VYAS, J. M., VAN DER VEEN, A. G. & PLOEGH, H. L. 2008. The known unknowns of antigen processing and presentation. *Nat Rev Immunol,* 8**,** 607-18.
WALUNAS, T. L., SPERLING, A. I., KHATTRI, R., THOMPSON, C. B. & BLUESTONE, J. A. 1996. CD28 expression is not essential for positive and negative selection of thymocytes or peripheral T cell tolerance. *J Immunol,* 156**,** 1006-13.
WANG, H., KADLECEK, T. A., AU-YEUNG, B. B., GOODFELLOW, H. E. S., HSU, L. Y., FREEDMAN, T. S. & WEISS, A. 2010a. ZAP-70: An Essential Kinase in T-cell Signaling. *Cold Spring Harb Perspect Biol.*

WANG, Y., KOROLEVA, E. P., KRUGLOV, A. A., KUPRASH, D. V., NEDOSPASOV, S. A., FU, Y. X. & TUMANOV, A. V. 2010b. Lymphotoxin beta receptor signaling in intestinal epithelial cells orchestrates innate immune responses against mucosal bacterial infection. *Immunity,* 32**,** 403-13.
WANG, Y. G., KIM, K. D., WANG, J., YU, P. & FU, Y. X. 2005. Stimulating lymphotoxin beta receptor on the dendritic cells is critical for their homeostasis and expansion. *J Immunol,* 175**,** 6997-7002.
WATANABE, N., WANG, Y. H., LEE, H. K., ITO, T., CAO, W. & LIU, Y. J. 2005. Hassall's corpuscles instruct dendritic cells to induce CD4+CD25+ regulatory T cells in human thymus. *Nature,* 436**,** 1181-5.
WEAVER, C. T., HARRINGTON, L. E., MANGAN, P. R., GAVRIELI, M. & MURPHY, K. M. 2006. Th17: an effector CD4 T cell lineage with regulatory T cell ties. *Immunity,* 24**,** 677-88.
WEBB, L. V., LEY, S. C. & SEDDON, B. 2016. TNF activation of NF-kappaB is essential for development of single-positive thymocytes. *J Exp Med,* 213**,** 1399-407.
WEIH, F., CARRASCO, D., DURHAM, S. K., BARTON, D. S., RIZZO, C. A., RYSECK, R. P., LIRA, S. A. & BRAVO, R. 1995. Multiorgan inflammation and hematopoietic abnormalities in mice with a targeted disruption of RelB, a member of the NF-kappa B/Rel family. *Cell,* 80**,** 331-40.
WEISS, A. 1993. T cell antigen receptor signal transduction: a tale of tails and cytoplasmic protein-tyrosine kinases. *Cell,* 73**,** 209-12.
WERLEN, G., HAUSMANN, B., NAEHER, D. & PALMER, E. 2003. Signaling life and death in the thymus: timing is everything. *Science,* 299**,** 1859-63.
WHITE, A. J., BAIK, S., PARNELL, S. M., HOLLAND, A. M., BROMBACHER, F., JENKINSON, W. E. & ANDERSON, G. 2017. A type 2 cytokine axis for thymus emigration. *J Exp Med*.
WHITE, A. J., NAKAMURA, K., JENKINSON, W. E., SAINI, M., SINCLAIR, C., SEDDON, B., NARENDRAN, P., PFEFFER, K., NITTA, T., TAKAHAMA, Y., CAAMANO, J. H., LANE, P. J., JENKINSON, E. J. & ANDERSON, G. 2010. Lymphotoxin signals from positively selected thymocytes regulate the terminal differentiation of medullary thymic epithelial cells. *J Immunol,* 185**,** 4769-76.
WICK, G., RIEKER, T. & PENNINGER, J. 1991. Thymic nurse cells: a site for positive selection and differentiation of T cells. *Curr Top Microbiol Immunol,* 173**,** 99-105.
WILLEBRAND, R. & VOEHRINGER, D. 2016. IL-33-Induced Cytokine Secretion and Survival of Mouse Eosinophils Is Promoted by Autocrine GM-CSF. *PLoS One,* 11**,** e0163751.
WILLIAMSON, E., BILSBOROUGH, J. M. & VINEY, J. L. 2002. Regulation of mucosal dendritic cell function by receptor activator of NF-kappa B (RANK)/RANK ligand interactions: impact on tolerance induction. *J Immunol,* 169**,** 3606-12.
WITT, C. M., RAYCHAUDHURI, S., SCHAEFER, B., CHAKRABORTY, A. K. & ROBEY, E. A. 2005. Directed migration of positively selected thymocytes visualized in real time. *PLoS Biol,* 3**,** e160.
WONG, K., LISTER, N. L., BARSANTI, M., LIM, J. M., HAMMETT, M. V., KHONG, D. M., SIATSKAS, C., GRAY, D. H., BOYD, R. L. & CHIDGEY, A. P. 2014. Multilineage potential and self-renewal define an epithelial progenitor cell population in the adult thymus. *Cell Rep,* 8**,** 1198-209.
WU, L., D'AMICO, A., WINKEL, K. D., SUTER, M., LO, D. & SHORTMAN, K. 1998. RelB is essential for the development of myeloid-related CD8alpha- dendritic cells but not of lymphoid-related CD8alpha+ dendritic cells. *Immunity,* 9**,** 839-47.
WU, L., LI, C. L. & SHORTMAN, K. 1996. Thymic dendritic cell precursors: relationship to the T lymphocyte lineage and phenotype of the dendritic cell progeny. *J Exp Med,* 184**,** 903-11.
WU, L. & SHORTMAN, K. 2005. Heterogeneity of thymic dendritic cells. *Semin Immunol,* 17**,** 304-12.
WU, W., SHI, Y., XIA, H., CHAI, Q., JIN, C., REN, B. & ZHU, M. 2017. Epithelial LTbetaR signaling controls the population size of the progenitors of medullary thymic epithelial cells in neonatal mice. *Sci Rep,* 7**,** 44481.
XING, Y., JAMESON, S. C. & HOGQUIST, K. A. 2013. Thymoproteasome subunit-beta5T generates peptide-MHC complexes specialized for positive selection. *Proc Natl Acad Sci U S A,* 110**,** 6979-84.
XING, Y., WANG, X., JAMESON, S. C. & HOGQUIST, K. A. 2016. Late stages of T cell maturation in the thymus involve NF-kappaB and tonic type I interferon signaling. *Nat Immunol,* 17**,** 565-73.
XIONG, N. & RAULET, D. H. 2007. Development and selection of gammadelta T cells. *Immunol Rev,* 215**,** 15-31.
YAGI, H., KAMBA, R., CHIBA, K., SOGA, H., YAGUCHI, K., NAKAMURA, M. & ITOH, T. 2000. Immunosuppressant FTY720 inhibits thymocyte emigration. *Eur J Immunol,* 30**,** 1435-44.
YAMASAKI, S., ISHIKAWA, E., SAKUMA, M., OGATA, K., SAKATA-SOGAWA, K., HIROSHIMA, M., WIEST, D. L., TOKUNAGA, M. & SAITO, T. 2006. Mechanistic basis of pre-T cell receptor-mediated autonomous signaling critical for thymocyte development. *Nat Immunol,* 7**,** 67-75.

YASUTOMO, K., DOYLE, C., MIELE, L., FUCHS, C. & GERMAIN, R. N. 2000. The duration of antigen receptor signalling determines CD4+ versus CD8+ T-cell lineage fate. *Nature,* 404**,** 506-10.
YU, C., CANTOR, A. B., YANG, H., BROWNE, C., WELLS, R. A., FUJIWARA, Y. & ORKIN, S. H. 2002. Targeted deletion of a high-affinity GATA-binding site in the GATA-1 promoter leads to selective loss of the eosinophil lineage in vivo. *J Exp Med,* 195**,** 1387-95.
YU, W., NAGAOKA, H., JANKOVIC, M., MISULOVIN, Z., SUH, H., ROLINK, A., MELCHERS, F., MEFFRE, E. & NUSSENZWEIG, M. C. 1999. Continued RAG expression in late stages of B cell development and no apparent re-induction after immunization. *Nature,* 400**,** 682-7.
YUAN, J. S., KOUSIS, P. C., SULIMAN, S., VISAN, I. & GUIDOS, C. J. 2010. Functions of notch signaling in the immune system: consensus and controversies. *Annu Rev Immunol,* 28**,** 343-65.
ZACHARIAH, M. A. & CYSTER, J. G. 2010. Neural crest-derived pericytes promote egress of mature thymocytes at the corticomedullary junction. *Science,* 328**,** 1129-35.
ZAMORA-PINEDA, J., KUMAR, A., SUH, J. H., ZHANG, M. & SABA, J. D. 2016. Dendritic cell sphingosine-1-phosphate lyase regulates thymic egress. *J Exp Med,* 213**,** 2773-2791.
ZHANG, Y., GARCIA‐IBANEZ, L. & TOELLNER K‐, M. 2016. Regulation of germinal center B‐cell differentiation. *Immunol Rev.* Hoboken.
ZHAO, D. M., THORNTON, A. M., DIPAOLO, R. J. & SHEVACH, E. M. 2006. Activated CD4+CD25+ T cells selectively kill B lymphocytes. *Blood,* 107**,** 3925-32.
ZHENG, W. & FLAVELL, R. A. 1997. The transcription factor GATA-3 is necessary and sufficient for Th2 cytokine gene expression in CD4 T cells. *Cell,* 89**,** 587-96.
ZHU, J. & PAUL, W. E. 2008. CD4 T cells: fates, functions, and faults. *Blood,* 112**,** 1557-69.
ZHU, J. & PAUL, W. E. 2010. Peripheral CD4 T cell differentiation regulated by networks of cytokines and transcription factors. *Immunol Rev,* 238**,** 247-62.
ZHU, M., CHIN, R. K., TUMANOV, A. V., LIU, X. & FU, Y. X. 2007. Lymphotoxin beta receptor is required for the migration and selection of autoreactive T cells in thymic medulla. *J Immunol,* 179**,** 8069-75.
ZLOTOFF, D. A., SAMBANDAM, A., LOGAN, T. D., BELL, J. J., SCHWARZ, B. A. & BHANDOOLA, A. 2010. CCR7 and CCR9 together recruit hematopoietic progenitors to the adult thymus. *Blood,* 115**,** 1897-905.
ZONG, W. X., LINDSTEN, T., ROSS, A. J., MACGREGOR, G. R. & THOMPSON, C. B. 2001. BH3-only proteins that bind pro-survival Bcl-2 family members fail to induce apoptosis in the absence of Bax and Bak. *Genes Dev,* 15**,** 1481-6.
ZUNIGA-PFLUCKER, J. C. & KRUISBEEK, A. M. 1990. Intrathymic radioresistant stem cells follow an IL-2/IL-2R pathway during thymic regeneration after sublethal irradiation. *J Immunol,* 144**,** 3736-40.